

**NOT JUST A PASSIVE ADAPTOR, THE PERIPLASMIC COMPONENT  
CUSB OF *ESCHERICHIA COLI*'S CUSCFBA COPPER EFFLUX SYSTEM  
HAS AN ACTIVE FUNCTIONAL ROLE**

**by**

**Ireena Bagai**

---

A Dissertation Submitted to the Faculty of the  
DEPARTMENT OF BIOCHEMISTRY AND MOLECULAR BIOPHYSICS

In Partial Fulfillment of the Requirements  
For the Degree of

DOCTOR OF PHILOSOPHY  
WITH A MAJOR IN BIOCHEMISTRY

In the Graduate College

THE UNIVERSITY OF ARIZONA

2008

THE UNIVERSITY OF ARIZONA  
GRADUATE COLLEGE

As members of the Dissertation Committee, we certify that we have read the dissertation  
prepared by IREENA BAGAI

entitled **Not just a passive adaptor, the periplasmic component CusB of *Escherichia coli*'s CusCFBA copper efflux system has an active functional role**

and recommend that it be accepted as fulfilling the dissertation requirement for the  
Degree of Doctor of Philosophy.

\_\_\_\_\_  
Dr. Megan M. McEvoy Date: April 18, 2008

\_\_\_\_\_  
Dr. Matthew Cordes Date: April 18, 2008

\_\_\_\_\_  
Dr. William R. Montfort Date: April 18, 2008

\_\_\_\_\_  
Dr. Christopher Rensing Date: April 18, 2008

\_\_\_\_\_  
Dr. Gordon Tollin Date: April 18, 2008

\_\_\_\_\_  
Dr. John H. Enemark Date: April 18, 2008

Final approval and acceptance of this dissertation is contingent upon the candidate's  
submission of the final copies of the dissertation to the Graduate College.

I hereby certify that I have read this dissertation prepared under my direction and  
recommend that it be accepted as fulfilling the dissertation requirement.

\_\_\_\_\_  
Dissertation Director: Dr. Megan M. McEvoy Date: April 18, 2008

### **STATEMENT BY AUTHOR**

This dissertation has been submitted in partial fulfillment of requirements for an advanced degree at the University of Arizona and is deposited in the University Library to be made available to borrowers under rules of the library.

Brief quotations from this dissertation are allowable without special permission, provided that accurate acknowledgement of source is made. Requests for permission for extended quotation from or reproduction of this manuscript in whole or in part may be granted by the Head of the Major Department or the Dean of the Graduate College when in his or her judgment the proposed use of the materials is in the interests of scholarship. In all other instances, however, permission must be obtained from the author.

SIGNED: IREENA BAGAI

## ACKNOWLEDGEMENTS

First, I would like to extend my gratitude to my advisor **Megan M. McEvoy** for giving me the opportunity to work on this project and be a part of her lab. Her unshaking optimism, constant encouragement and sympathetic attitude were important ingredients that kept me going. I must thank **Drs. Xristo Zarate** and **Sylvia Franke**, Post-Docs in our lab, whose valuable suggestions on molecular biology and protein purification techniques were very fruitful during early years of the project. I couldn't thank less the undergraduates who had worked with me. Teaching them was a great learning experience, not only with respect to Biochemistry but also with respect to managing people. **Wenbo Liu** and **Craig Sheedy** are two people, who I would especially like to mention for their contributions.

Many thanks to **John Fitch**, **Drs. Matthew Cordes**, **Andrew Hausrath** and **Christopher Rensing** for the fruitful discussions from time-to-time over various aspects of the project. I owe special thanks to all the people in the department whose equipment and resources were used for different experiments. Thanks to my **Committee** for their time and valuable suggestions. My heartfelt thanks go to **Ninian Blackburn**, our collaborator at Oregon Health and Science University, for being kind enough to teach me EXAFS at Stanford Synchrotron Radiation Labs. I also would like to thank **Neil Jacobsen**, our NMR facility manager for his patience and timely assistance on the instrument. He is the best NMR teacher and I loved his classes.

I must thank my friends **Jacquie Brailey**, **Xiaohui Hu**, **Gary Martinez**, **Steve Fernandez**, **Minal Mallik** for all the moral support and good wishes.

Thanks are due to **Olivia Mendoza** and **Maragaret Gomez** for an ever-ready attitude to help with the administrative tasks. Having one thing less to think about gets a big load off. Last but not the least, lots n' lots n' lots of thanks to my **Angels** – the most loving and caring **Parents**, a darling **Brother** and my **Aunt** for everything; for listening to my unending whining, for consistent encouragement, for love and support, for patience, for just being there always whenever I needed a shoulder to cry on. I couldn't have done this without them.

**DEDICATION**

This dissertation is dedicated to my family, my Mommy, Dr. Reeta Bagai, Papa, Mr.

Maharaj Krishan Bagai and Brother, Mr. Ichhit Bagai

## TABLE OF CONTENTS

<b>LIST OF TABLES.....</b>	<b>10</b>
<b>LIST OF FIGURES.....</b>	<b>11</b>
<b>ABSTRACT.....</b>	<b>13</b>
 <b>CHAPTER 1. INTRODUCTION</b>	
1.1 Metals in Biochemistry.....	15
1.2 Copper in Life.....	18
1.2.1 Copper coordination and catalysis.....	19
1.2.2 Copper toxicity.....	22
1.3 Copper Homeostasis in Eukaryotes.....	29
1.4 Copper Homeostasis in Prokaryotes.....	34
1.4.1 Plasmid-encoded copper resistance in <i>E. coli</i> .....	35
1.4.2 Chromosomally-encoded copper resistance in <i>E. coli</i> .....	37
1.4.3 The CusCFBA system of <i>E. coli</i> .....	38
1.5 Significance: From metal-transport systems to multi-drug exporters.	40
1.6 Dissertation Outline.....	41
 <b>CHAPTER 2. SUBSTRATE-LINKED CONFORMATIONAL CHANGE IN THE PERIPLASMIC COMPONENT OF A CU(I)/AG(I) EFFLUX SYSTEM</b>	
2.1 ABSTRACT.....	43
2.2 INTRODUCTION.....	45
2.3 MATERIALS AND METHODS.....	48
2.3.1 Protein expression and purification.....	48
2.3.2 Isothermal titration calorimetry.....	49
2.3.3.1 X-ray absorption spectroscopy.....	50
2.3.3.2 Collection and analysis of XAS data.....	51
2.3.4 Site-directed mutagenesis and growth inhibition studies.....	52
2.3.5 Analytical ultracentrifugation.....	53
2.3.6 Size exclusion chromatography.....	54

## TABLE OF CONTENTS – *Continued*

2.4	RESULTS.....	55
2.4.1	<i>Calorimetric titration indicates Ag(I) binding by CusB.....</i>	55
2.4.2	<i>EXAFS spectroscopy of CusB-Cu(I).....</i>	57
2.4.3	<i>Assignment of the metal-chelating ligands.....</i>	58
2.4.4	<i>Ag(I) affinity of conserved methionine mutants in vitro.....</i>	59
2.4.5	<i>Conserved methionines are crucial for metal resistance.....</i>	62
2.4.6	<i>CusB is monomeric in solution.....</i>	63
2.4.7	<i>Ag(I) binding causes a conformational change.....</i>	66
2.5	DISCUSSION.....	68

### CHAPTER 3. DIRECT METAL TRANSFER BETWEEN THE PERIPLASMIC COMPONENTS OF THE CUSCFBA CU(I)/AG(I) EFFLUX SYSTEM ESTABLISHES A ROLE FOR CUSF AS A METALLOCHAPERONE

3.1	ABSTRACT.....	71
3.2	INTRODUCTION.....	73
3.3	MATERIALS AND METHODS.....	77
3.3.1	<i>Protein expression and purification.....</i>	77
3.3.2	<i>Isothermal titration calorimetry.....</i>	77
3.3.3.1	<i>Extended X-ray absorption fine structure spectroscopy.....</i>	78
3.3.3.2	<i>EXAFS data collection and analysis.....</i>	79
3.4	RESULTS.....	81
3.4.1	<i>CusF and CusB interact only in the presence of metals.....</i>	81
3.4.2	<i>EXAFS analysis of Selenomethionine labeled CusF.....</i>	83
3.4.3	<i>Transfer of Cu(I) from CusF to CusB measured by EXAFS.....</i>	85
3.4.4	<i>Kinetics of transfer measured by EXAFS.....</i>	91
3.4.5	<i>Metal transfer is reversible.....</i>	94
3.4.6	<i>Metal transfer occurs directly between proteins of the Cus system.....</i>	94
3.4.7	<i>CusF and CusB found as a single polypeptide in the putative efflux systems.....</i>	95
3.5	DISCUSSION.....	98

## TABLE OF CONTENTS – *Continued*

### CHAPTER 4. THE CUSB BINDING INTERFACE ON CUSF OVERLAPS WITH THE METAL SITE

4.1	INTRODUCTION.....	104
4.2	MATERIALS AND METHODS.....	106
4.2.1	<i>Protein expression and purification.....</i>	106
4.2.2	<i>NMR spectroscopy.....</i>	107
4.3	RESULTS.....	109
4.3.1	<i>Chemical shift changes reveal metal-dependent interactions between CusF and CusB.....</i>	109
4.3.2	<i>Identification of the CusF residues involved in interaction with CusB.....</i>	118
4.4	DISCUSSION.....	123

### CHAPTER 5. BIOCHEMICAL CHARACTERIZATION OF FULL-LENGTH AND TRUNCATED CUSB CONSTRUCTS

5.1	INTRODUCTION.....	126
5.2	MATERIALS AND METHODS.....	129
5.2.1	<i>CusB crystallization and NMR sample preparation.....</i>	129
5.2.2	<i>Full-length cusB (residues 1-379) cloning in pET22b (CusB- His) and protein expression.....</i>	130
5.2.3	<i>CusB N-terminal domain (residues 11-260) (CusB-NTD) cloning in pET28b and protein purification.....</i>	131
5.2.4	<i>CusB C-terminal domain (residues 260-379) (CusB-His-CTD- Strep) cloning in pET28b, protein purification and CD structure characterization.....</i>	133
5.2.5	<i>CusB CTD (residues 260-379) cloning in pET29a (CusB-CTD- Strep), protein purification and NMR characterization.....</i>	135
5.2.6	<i>CusB (residues 1-260) cloned in pASK3.....</i>	136

## TABLE OF CONTENTS – *Continued*

<b>5.3</b>	<b>RESULTS.....</b>	<b>137</b>
5.3.1	<i>CusB</i> crystallization and NMR sample preparation.....	137
5.3.2	Expression of full-length <i>CusB</i> (residues 1-379) cloned in <i>pET22b</i> ( <i>CusB</i> -His).....	140
5.3.3	<i>CusB</i> N-terminal domain (residues 11-260) ( <i>CusB</i> -NTD) in <i>pET28b</i> , protein purification and characterization.....	144
5.3.4	<i>CusB</i> C-terminal domain (residues 260-379) ( <i>CusB</i> -His-CTD-Strep) cloning in <i>pET28b</i> , protein purification and CD structure characterization.....	147
5.3.5	<i>CusB</i> CTD (residues 260-379) cloning in <i>pET29a</i> , <i>CusB</i> -CTD-Strep purification and NMR characterization.....	149
5.3.6	<i>CusB</i> (residues 1-260) expression in <i>pASK3</i> .....	149
<b>5.4</b>	<b>SUMMARY.....</b>	<b>151</b>
<b>CHAPTER 6. GENERAL CONCLUSIONS AND FUTURE DIRECTIONS.....</b>		<b>152</b>
<b>APPENDIX A: ABBREVIATIONS.....</b>		<b>157</b>
<b>APPENDIX B: ClustalW sequence alignment of the mature, processed form of <i>CusB</i> and homologous proteins identified from a BLAST search of the non-redundant protein database using <i>CusB</i> from <i>E. coli</i> as the query sequence.....</b>		<b>158</b>
<b>APPENDIX C: ClustalW sequence alignment of <i>CusF</i> and homologous proteins identified from a BLAST search of the non-redundant protein database using <i>CusF</i> from <i>E. coli</i> as the query sequence. Only sequences that are membrane fusion proteins are selected for alignment and generate a representative set.....</b>		<b>175</b>
<b>APPENDIX D: HNCA assignments of Ag(I)-<i>CusF</i>/apo-<i>CusB</i> spectra.....</b>		<b>179</b>
<b>REFERENCES.....</b>		<b>181</b>

## LIST OF TABLES

<b>TABLE 1.1</b> Representative copper proteins classified by copper center type, class and biological function.....	25
<b>TABLE 2.1</b> Growth behavior of CusB wild-type and variants on agar plates containing various concentrations of CuCl <sub>2</sub> .....	64
<b>TABLE 3.1</b> Fits obtained to the EXAFS of CusF by curve-fitting using the program EXCURVE 9.2.....	89

## LIST OF FIGURES

<b>FIGURE 1.1</b>	Periodic representation of the elements.....	17
<b>FIGURE 1.2</b>	Schematic of the CusCFBA copper efflux system of <i>Escherichia coli</i> ....	38
<b>FIGURE 2.1</b>	ITC data for titration of 22 $\mu\text{M}$ CusB with 300 $\mu\text{M}$ $\text{AgNO}_3$ at 25 $^\circ\text{C}$ .....	56
<b>FIGURE 2.2</b>	EXAFS data for CusB-Cu(I).....	60
<b>FIGURE 2.3</b>	ITC data for titration of CusB variants with $\text{AgNO}_3$ .....	61
<b>FIGURE 2.4</b>	Sedimentation equilibrium analysis of apo-CusB and CusB-Ag(I).....	65
<b>FIGURE 2.5</b>	Analytical gel filtration on a Superdex 200 10/300GL analytical column of apo- and Ag(I)-bound CusB in 50 mM sodium phosphate, pH 7.0.....	67
<b>FIGURE 3.1</b>	ITC data for titration of (A) 375 $\mu\text{M}$ Ag(I)-CusF into 24 $\mu\text{M}$ apo-CusB; (B) 142 $\mu\text{M}$ Ag(I)-CusB into 17 $\mu\text{M}$ apo-CusF; (C) 375 $\mu\text{M}$ apo-CusF into 20 $\mu\text{M}$ apo-CusB; (D) 375 $\mu\text{M}$ Ag(I)-CusF into 23 $\mu\text{M}$ Ag(I)-CusB in 50 mM cacodylate, pH 7.0....	82
<b>FIGURE 3.2(A)</b>	Se EXAFS of apo-SeM-CusF; (B) Se EXAFS of Cu(I)-loaded SeM-CusF; (C) Cu EXAFS of Cu(I)-loaded SeM-CusF.....	87
<b>FIGURE 3.3(A)</b>	Cu EXAFS of Cu(I)-SeM-CusF mixed with apo-CusB and frozen after 34 minutes; (B) Se EXAFS of Cu(I)-SeM-CusF mixed with apo-CusB and frozen after 34 minutes; (C) Comparison of Se edge FT of SeM-CusF.....	88
<b>FIGURE 3.4</b>	Cu (LEFT) and Se (RIGHT) EXAFS of Cu(I)-loaded SeM-CusF mixed with apo-CusB and, (A) frozen after 14 minutes; (B) frozen after 4 minutes; (C) Comparison of transfer data from Cu(I)-SeM-CusF to apo-CusB at 4 (black), 14 (red), and 34 minute (blue) time points.....	92
<b>FIGURE 3.5</b>	Reverse transfer from Cu(I)-CusB to apo-SeM-CusF measured at the Se edge.....	96
<b>FIGURE 3.6</b>	ITC data for titration of (A) 36 $\mu\text{M}$ apo-SilF with 300 $\mu\text{M}$ $\text{AgNO}_3$ ; (B) 21 $\mu\text{M}$ apo-CusB with 170 $\mu\text{M}$ Ag(I)-SilF; (C) 29 $\mu\text{M}$ apo-CusF with 170 $\mu\text{M}$ Ag(I)-SilF; (D) 30 $\mu\text{M}$ apo-SilF with 275 $\mu\text{M}$ Ag(I)-CusF in 50 mM cacodylate, pH 7.0.....	97
<b>FIGURE 3.7</b>	Model for Cu(I) exchange between CusF and CusB.....	103

# LIST OF FIGURES - *Continued*

<b>FIGURE 4.1</b> $^1\text{H}$ - $^{15}\text{N}$ HSQC spectral overlays (A) Apo-CusF (black) and apo-CusF mixed 1:1 with apo-CusB (red); (B) Apo-CusF (black) and apo-CusF mixed 1:1 with Ag(I)-CusB (red); (C) Ag(I)-CusF (black) and Ag(I)-CusF mixed 1:1 with apo-CusB (red); (D) Apo-CusF mixed 1:1 with Ag(I)-CusB (black) and Ag(I)-CusF mixed 1:1 with apo-CusB (red); (E) expansions; (F) Apo-CusF (black) and apo-CusF mixed with apo-CueO and Ag(I) at a ratio of 1:1:2 (red); (G) Apo-CusF (black) and apo-CusF mixed with apo-BSA and Ag(I) at a ratio of 1:1:2 (red).....	111
<b>FIGURE 4.2</b> Combined $^1\text{H}^{\text{N}}$ and $^{15}\text{N}$ chemical shifts in parts per million between Ag(I)/CusF/CusB and Ag(I)-CusF as a function of CusF residue number.....	120
<b>FIGURE 4.3</b> Cartoon representation of CusF, showing (A) residues (orange) that were broadened beyond detection and; (B) residues (blue) that showed significant chemical shift variations, in Ag(I)/CusF/CusB $^1\text{H}$ - $^{15}\text{N}$ HSQC spectrum; (C) both effects combined.....	121
<b>FIGURE 5.1</b> (A) Crystal screening results; (TOP) 100 mM $\text{NaH}_2\text{PO}_4 \cdot \text{H}_2\text{O}$ , 100 mM CAPS, pH 10.0, 20% (v/v) PEG 400 and; (BOTTOM) 100 mM $\text{Mg}(\text{NO}_3)_2 \cdot 6\text{H}_2\text{O}$ , 100 mM TAPS, pH 9.0, 40% (v/v) PEG 400; (B) CusB drops from crystallization plates ran on SDS-PAGE after 1 week of setting up the plate in condition (i).....	138
<b>FIGURE 5.2</b> $^1\text{H}$ - $^{15}\text{N}$ HSQC collected at 600 MHz for 200 $\mu\text{M}$ full-length CusB in 50 mM phosphate, pH 7.0.....	141
<b>FIGURE 5.3</b> Schematic of various CusB constructs.....	142
<b>FIGURE 5.4</b> SDS-PAGE for CusB-His expressed from <i>cusB</i> -pET22b construct.....	143
<b>FIGURE 5.5</b> Disordered regions in processed full-length CusB as predicted by PONDR.....	145
<b>FIGURE 5.6</b> Far UV-CD spectra for 60 $\mu\text{M}$ CusB-His-CTD-Strep.....	148
<b>FIGURE 5.7</b> $^1\text{H}$ - $^{15}\text{N}$ HSQC of 400 $\mu\text{M}$ CusB-CTD-Strep in 50 mM MOPS, pH 7.0...	150

## ABSTRACT

Increased emergence of antibiotic resistance in bacterial pathogens has posed a serious threat to human health. Due to similar structural and functional characteristics of metal and antibiotic resistance systems in gram-negative bacteria, there is a growing concern that metal contamination functions as a selective agent in the proliferation of antibiotic resistance. The CusCFBA copper/silver resistance system of *Escherichia coli* forms a protein complex that spans the inner and outer membranes and functions in the efflux of metal from the periplasm to the extracellular space. In order to understand the molecular details of metal resistance by the Cus system and more specifically, to define the role of the periplasmic components in CBA type metal transporters, I characterized CusB and probed its interactions with CusF using various structural and biochemical tools. CusB was previously thought to play a relatively passive role as an adaptor protein that stabilized the association of the inner and outer membrane proteins. Through isothermal titration calorimetry (ITC), X-ray absorption spectroscopy (XAS), and mutagenesis, I have shown that CusB binds Cu(I)/Ag(I) with high affinity using three conserved methionines. Gel filtration chromatography experiments showed that upon binding Ag(I), CusB undergoes a substantial conformational change. Importantly, functional metal binding by CusB is essential for cell survival in environments with elevated copper concentrations. The small periplasmic metal binding protein CusF is a unique component of monovalent metal resistance systems serving an unknown function. To determine the nature and specificity of interaction between CusF and CusB, ITC and

NMR were used to show that the interaction between CusF and CusB is metal-dependent and specific for the components of Cus system. From NMR chemical shift perturbations, the CusB interaction face on CusF was determined to overlap with the metal binding site. XAS experiments demonstrate metal transfer between CusB and CusF, which supports the role of CusF as a metallochaperone. In summary, these findings demonstrate an active role for CusB in metal resistance, and suggest that the plausible role for CusF is that of a metallochaperone for CusB.

## CHAPTER 1

### INTRODUCTION

*“If you think that biochemistry is the organic chemistry of living systems; then you are misled, biochemistry is the coordination chemistry of living systems (Wood, Naturaissen Schafter, 1975, 68, 357)”*

#### 1.1 Metals in Biochemistry

Like all eukaryotes and other prokaryotic cells, 97% of *Escherichia coli*'s dry weight is comprised of the elements C, H, O, N, S and P (Wackett et al., 2004). In addition to the 6 non-metals and chlorine, 11 metals are essential components of all microbial cells. These include 4 main group elements consisting of  $\text{Na}^+$ ,  $\text{K}^+$  (alkali metal ions),  $\text{Mg}^{2+}$  and  $\text{Ca}^{2+}$  (alkaline earth metals), 6 transition metals consisting of Fe, Cu, Mo, Mn, Co and Ni in the decreasing order of their prevalence and  $\text{Zn}^{2+}$  (Ellis et al., 2003; Wackett et al., 2004). While  $\text{Zn}^{2+}$  and transition metals constitute only 1-2% of the mass of a microbial cell (Wackett et al., 2004), cell functioning depends on them far more than the figure suggests (Ainscough and Brodie, 1976). Figure 1.1 depicts elements essential for life. The main group elements mostly serve as counter-ions for anions like nucleotides or carbohydrates of aspartate and glutamate residues in proteins (Wong et al., 2004). Transition metal ions, on the other hand, due to their ability to accept and donate electrons, participate in numerous metabolic junctions in every living cell (Nelson, 1999). While the ionic interactions of main group metals are relatively weak, transition metal ions form strong bonds with functional groups such as thiolates and imidazolium

nitrogens in proteins (Wong et al., 2004). Since the discovery of the first metalloenzyme, carbonic anhydrase in 1939 (Keilin and Mann, 1939), several hundreds of other metalloenzymes have been found (Kobayashi and Ponnampersuma, 1985). Notably, both the first globular protein structure (Perutz, 1962) and the first membrane protein structure (Deisenhofer and Michel, 1992) to be solved by X-ray crystallography were metalloproteins. Today, approximately one-third of all known proteins have been found to require metal cofactors for function (Rosenzweig, 2002).

As important as transition metals are, their presence in excess of the required concentrations is toxic for the cells. Since they cannot be degraded or modified like toxic organic compounds, metal concentration is regulated by other mechanisms. First, cations, mostly the sulfur lovers, may be sequestered by thiol-containing molecules. Second, the accumulation of the toxic metal ion can be diminished by active extrusion or efflux from the cell. Third, some metal ions may be reduced to a less toxic oxidation state, e.g. Hg(II) to Hg(0) (Nies, 1999). Fourth, metal exclusion may be mediated by alterations of the cell wall (Bruins et al., 2000). Finally, metal homeostasis may involve a combination of one or more of the mentioned mechanisms (Nies, 1999). This dissertation is an investigation of the efflux mode of copper regulation inside *Escherichia coli*.

Group	1	2	3	4	5	6	7	8	9	10	11	12	13	14	15	16	17	18
Period																		
1	1 H																	2 He
2	3 Li	4 Be											5 B	6 C	7 N	8 O	9 F	10 Ne
3	11 Na	12 Mg											13 Al	14 Si	15 P	16 S	17 Cl	18 Ar
4	19 K	20 Ca	21 Sc	22 Ti	23 V	24 Cr	25 Mn	26 Fe	27 Co	28 Ni	29 Cu	30 Zn	31 Ga	32 Ge	33 As	34 Se	35 Br	36 Kr
5	37 Rb	38 Sr	39 Y	40 Zr	41 Nb	42 Mo	43 Tc	44 Ru	45 Rh	46 Pd	47 Ag	48 Cd	49 In	50 Sn	51 Sb	52 Te	53 I	54 Xe
6	55 Cs	56 Ba	57 Lu	58 Hf	59 Ta	60 W	61 Re	62 Os	63 Ir	64 Pt	65 Au	66 Hg	67 Tl	68 Pb	69 Bi	70 Po	71 At	72 Rn

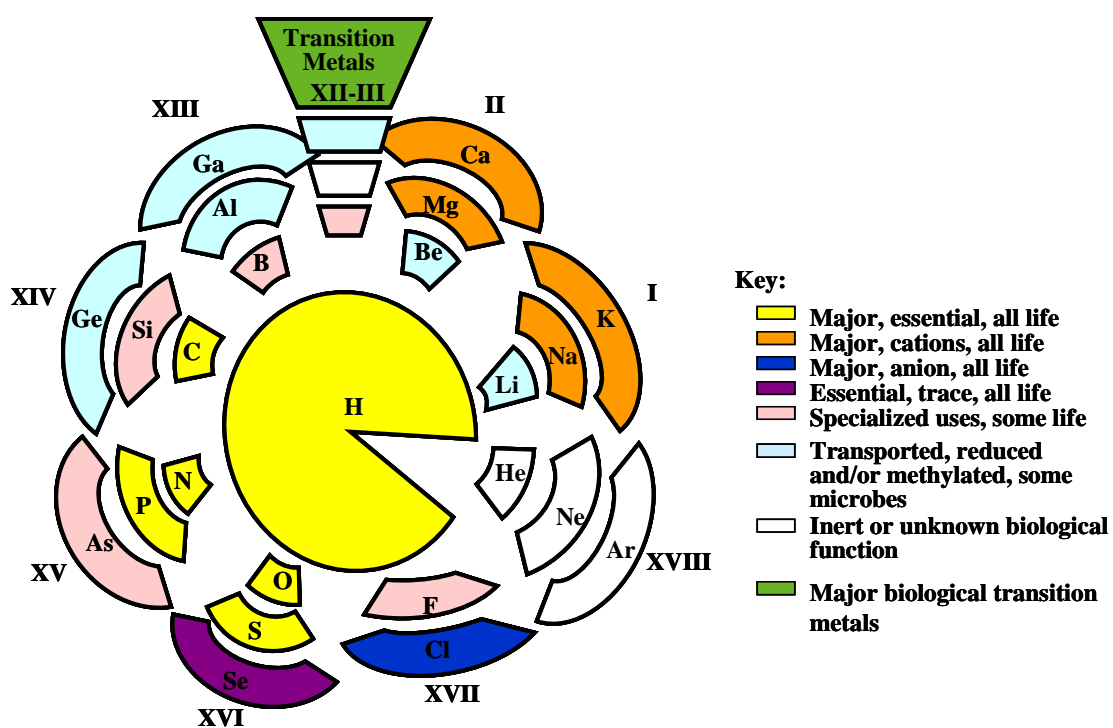


**FIGURE 1.1** Periodic representation of the elements. (A) Conventional table with linear columns and rows; (B) Spiral representation of the elements, which clusters elements that are prominent in biological systems (Adapted from Wackett et al., 2004).

## 1.2 Copper in Life

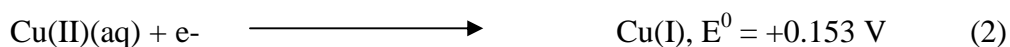
Copper, the second most abundant transition metal in living systems, exists as a cofactor in a large number of metalloproteins. Due to its redox properties, it has an indispensable role in some of the fundamental biochemical processes such as respiration and photosynthesis. Of approximately 13,000 metalloproteins in the Metalloprotein database in March 2007 (<http://metallo.scripps.edu/>), about 530 contained copper. The evolution of biological systems that utilize copper can be traced back to the period in which the earth's atmosphere became oxygenated (Singleton and Le Brun, 2007). Life arose in a reducing medium about 4.0 billion years ago. The primordial oceans were estimated to have high  $\text{H}_2\text{S}$  concentrations amounting to approximately 1 mM (da Silva and Williams, 1991). The reducing atmosphere, by locking copper in the Cu(I) form from which it precipitated as insoluble  $\text{Cu}_2\text{S}$ , resulted in the biological non-availability of copper (Williams and Abolmaali, 1998). The oxygenation of the atmosphere, brought about by cyanobacteria about 1.0-2.0 billion years ago, increased the stability of the oxidized form of transition metal ions (Williams and Abolmaali, 1998). Due to the high potential necessary for oxidation to the Cu(II) state, significant oxidation of insoluble Cu(I) to soluble biologically available Cu(II), however, occurred only after massive oxidation equivalents were produced upon arrival of multicellular photosynthetic organisms. The high potential required for oxidation of Cu(I) to Cu(II) is ideally suited for catalysis of typically inhibited reactions of  $\text{O}_2$  (Kaim and Rall, 1996).

### 1.2.1 Copper coordination and catalysis

Copper is a first row transition metal, which principally has 2 oxidation states, Cu(I) and Cu(II) (Koch et al., 1997), although some Cu(III) complexes are also known (Conry, 2006). The Cu(II)/Cu(I) redox reaction is widely used in biology to activate substrates via redox transformations or to carry out an electron transfer event (Halcrow et al., 2001). In the Cu(I) oxidation state, copper ion is a closed shell, spherically symmetric  $d^{10}$  ion that prefers a coordination number of 2, 3 or 4 with linear, trigonal or tetrahedral geometries, respectively (Conry, 2006). In terms of hard and soft acid-base theory proposed by Pearson (Pearson, 1963), Cu(I) is a soft Lewis acid and prefers soft Lewis base ligands like thiolates or the sulfur of thioether moieties (Koch et al., 1997). When Cu(I) is bound to polypeptides, ligands are usually provided by the amino acids cysteine or methionine (Koch et al., 1997). In the Cu(II) oxidation state, copper is a  $d^9$  ion, which contains one unpaired electron. The metal-ligand interactions in the Cu(II) complexes are usually stabilized through Jahn-Teller distortions (Kaim and Rall, 1996), which lifts the degeneracy of the octahedral  $d^9 e_g$  orbital subset (Housecroft and Sharpe, 2001), resulting in four short equatorial and another one or two longer axial bonds (Conry, 2006). Different extents of axial elongation of the octahedron thus produce tetragonally distorted octahedral, pyramidal and square planar geometries corresponding to the coordination numbers of 6, 5 and 4, respectively (Kaim and Rall, 1996). Cu(II) is an intermediate Lewis acid according to the hard and soft acid-base theory and thus its range of polypeptide ligands is increased to include the imidazole nitrogen atoms of

histidine, carboxylate moieties of aspartate and glutamate, peptide backbone nitrogen and carbonyl groups, and the sulfur atoms of cysteine or methionine (Koch et al., 1997). Cu(I) and Cu(II) have very different coordination preferences and ionic radii (0.96 and 0.72 Å, respectively), which necessitates large geometrical changes in the course of the redox reaction. In contrast, the other metals used for biological redox applications, (e.g. Mn, Fe, Co, Ni, Mo, W, and V), all undergo small to minimal changes in molecular structure for one-electron reactions (Halcrow et al., 2001). The large structural reorganizations associated with copper redox are, however, favorable for catalysis in that they facilitate the oxidative substrate binding reactions found in copper/dioxygen chemistry (da Silva and Williams, 1991). The large reorganization energy is disadvantageous for processes requiring rapid electron transfer. According to the Franck-Condon Principle, the active site geometry of a redox metalloenzyme must approach that of the appropriate transition state for rapid transfer of electrons (Roat-Malone, 2002). An ingenious evolutionary solution to this problem is seen in proteins that contain a type of copper center called type I. Different copper proteins/enzymes have been classified based on the type of copper center present in them as illustrated in Table 1.1. The structure of type I copper site is a compromise between the stereochemical and electronic requirements of Cu(I) and Cu(II). Type I copper sites require minimal reorganization energy to switch between the oxidized and reduced states, since their geometries are essentially identical (Halcrow et al., 2001). The redox potential for the Cu(II)/Cu(I) couple, which lies around 0 V is in a similar range to the potentials of the biologically important redox couples  $O_2/O_2^{\cdot-}/O_2^{2-}$ ,  $NO^+/NO\cdot/NO^-$ , phenoxyl/phenolate or o-quinone/o-semiquinone/catecholate (Kaim,

2003). Half reactions and standard redox potentials (versus NHE) of the Cu(I)/Cu(0) and Cu(II)/Cu(I) couples in aqueous solutions are shown in equations 1 and 2.



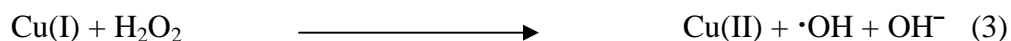
Since the potential for  $\text{O}_2/\text{H}_2\text{O}$  couple is +0.81 V at neutral pH, it is clear that Cu(0) can be readily oxidized to Cu(I) and subsequently to Cu(II) (Singleton and Le Brun, 2007). Numerical values for the above equations change as copper ions contained in enzymes are surrounded not by water but by a variety of biological ligands. These ligands alter the electromotive force of copper ions, making the system more or less easily oxidized or reduced (Roat-Malone, 2002).

As shown in Table 1.1, six different types of copper binding centers have evolved for catalyzing various biochemical reactions. Thus, the role of copper in fundamental biological processes in different life forms cannot be overstated. A condition in humans called Menkes disease is caused due to the disturbed distribution of dietary copper from the site of absorption in intestines to other parts in the body (Singleton and Le Brun, 2007). The resulting copper deficiency causes neurological, skeletal and pigmental abnormalities and death by the age of 3 years (Lutsenko and Petris, 2003; Singleton and Le Brun, 2007).

### 1.2.2 Copper toxicity

The properties of copper that make it an essential cofactor for several enzymes also make it commensurably toxic. Because of its specific electronic state of one unpaired electron in the 4s orbital in Cu(I) and in either  $d_{x^2-y^2}$  or  $d_{z^2}$  orbital in Cu(II), copper has a character comparable to radicals and can thus easily interact with other radicals, best with molecular oxygen (Nies, 1999). A free radical is defined as a species that has one or more unpaired electrons. An  $O_2$  molecule, due to its 2 unpaired electrons, each located in a different  $\pi^*$  orbital, behaves like a radical (Halliwell and Gutteridge, 1984).

Cu(I) readily reacts with super oxide radicals ( $O_2^-$ ) and hydrogen peroxide ( $H_2O_2$ ) (by-products of normal metabolic processes) in Fenton-like reactions (Equation 3) to generate extremely toxic hydroxyl radicals ( $\bullet OH$ ). The resulting Cu(II) is re-reduced by  $O_2^-$  in a Haber-Weiss-like cycle (Equations 4 and 5) (Singleton and Le Brun, 2007). At low steady-state concentrations of  $O_2^-$  and  $H_2O_2$  normally present *in vivo*, the rate constant for the Haber-Weiss (HW) reaction has been shown to be virtually zero. Transition metal ions in an unbound form in the intracellular medium act as catalysts for the HW cycle as they cause an increased formation of hydroxyl radicals (Halliwell and Gutteridge, 1984). Addition of equations 3 and 4 gives the net reaction shown in equation 5. In fact, the conversion of  $O_2^-$  and  $H_2O_2$  to the highly cytotoxic  $\bullet OH$  can only take place when catalytic concentrations of transition metals are present.

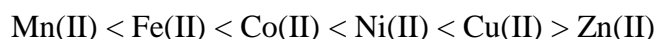




The hydroxyl radicals, once generated, react rapidly (Halliwell and Gutteridge, 1984) with almost every type of molecule found in living cells (Gaetke and Chow, 2003), including sugars, amino acids, phospholipids, DNA and organic acids, resulting in lipid peroxidation, DNA cleavage, and protein damage.

Copper toxicity also likely results from the high affinity of Cu(I) and Cu(II) for different groups in proteins, causing the displacement of the native metal ion from active sites (da Silva and Williams, 1991). The interaction of metal cation with complex ligands depends on its charge/radius ratio or polarizing power. The more polarizable the atomic structure is, the “softer” is the metal ion and stronger are its interactions with ligands (Hobman et al., 2007). On moving from left to right across the periodic table in the first row transition metal series, the ionic radius of free metal ion in the gaseous phase shows a gradual decrease due to the incomplete screening of the additional positive charge. In the case of high spin octahedral complexes however, Ni(II) should be the smallest ion because the additional electron in Cu(II) will go to the  $e_g$  orbital subset, as concluded from the crystal field stabilization energies. Since  $e_g$  orbitals are directed towards the incoming ligand, the additional electron would experience more repulsion and thus a slight increase in the ionic radius of Cu(II). However, since Cu(II) complexes are not truly octahedral due to Jahn-Teller distortions, Cu(II) turns out to be the smallest in size with the highest polarizing power (Housecroft and Sharpe, 2001; Hughes and Poole, 1989). The general stability of high spin octahedral metal complexes for the replacement

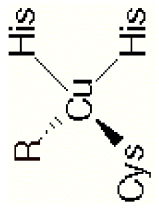
of water by other ligands was presented by the Irving-William series (da Silva and Williams, 1991), as follows:

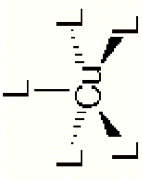


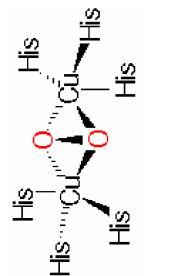
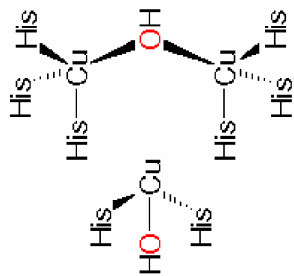
Thus, Cu(II) preferentially binds to ligand sites over other divalent metals (Brown et al., 1994) and if all metal ions were equally available to proteins in a cell, with affinity being the sole criterion for binding, all metallo-proteins would become copper proteins (Tottey et al., 2007). Likewise, other metals that are soft Lewis acids with large and polarizable atomic structure are also mostly toxic (Pearson, 1963). These include Ag(I), Au(I), Cd(II), Hg(II) and Pb(II), which can form stable complexes with soft Lewis bases that possess polarizable donor atoms such as S and N groups (Hobman et al., 2007).

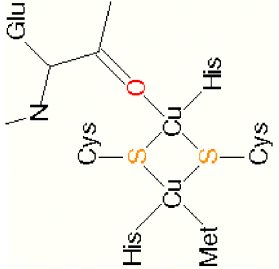
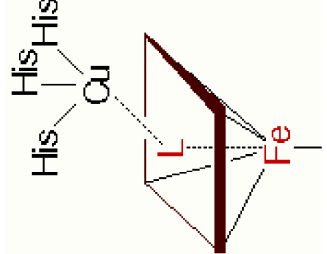
In a normal yeast cell, the concentration of free copper ion has been reported to be extremely low (approximately  $10^{-18}$  M) (Rae et al., 1999). The accumulation of copper in excess of required concentrations is implicated in several neurological pathologies including Alzheimer's, Parkinson's, Amyotrophic Lateral Sclerosis and Prion diseases (Gaggelli et al., 2006). An autosomal recessive genetic disorder called Wilson's disease is caused by a defect in the enzyme responsible for biliary excretion of excess copper resulting in the copper accumulation in liver and death due to liver failure (Brewer, 2000). Several homeostasis systems for regulation of copper concentrations are thus present in all organisms.

**TABLE 1.1** Representative copper proteins classified by copper center type, class and biological function (Falconi and Desideri, 2002; Kaim and Schwederski, 1994; Roat-Malone, 2002).

Copper Center	Protein Class/Family	Occurrence/ Reactivity	Biological Function
<b>Type I</b> 	<b>✓ Small Blue Proteins</b>  Azurin  Plastocyanin	Bacterial photosynthesis  Plant photosynthesis	Reversible Electron Transfer  $\text{Cu(I)} \leftrightarrow \text{Cu(II)} + \text{e}^-$
	<b>✓ Blue Oxidases</b>  Ascorbate oxidase	Oxidation of ascorbate to dehydroascorbate in plants	Catalysis  $\text{O}_2 \rightarrow 2\text{H}_2\text{O}$
	Laccase  Ceruloplasmin	Oxidation of polyphenols and polyamines in plants  Cu transport and storage, Fe mobilization and oxidation , oxidase and antioxygenation function in human and animal serum	

<p><b>Type II</b></p>  <p><math>\text{Cu}(\text{N}^{\delta}\text{His})_m\text{R}_n</math></p> <p>L = N, O or S ligands;  R = O or S ligands  <math>m = 1</math> to <math>4</math>; <math>n = 0</math> to <math>3</math>;  <math>m+n = 4</math> or <math>5</math></p>	<p>✓ <b>Monooxygenases</b></p> <p>Dopamine <math>\beta</math>-monooxygenase</p>	<p>Side chain oxidation of dopamine to nor epinephrine in adrenal cortex in humans.</p>	<p>Catalysis</p> $\text{O}_2 \rightarrow \text{H}_2\text{O} + \text{Substrate-O}$
	<p>✓ <b>Non-blue oxidases</b></p> <p>Galactose oxidase</p> <p>Amine oxidase</p>	<p>Alcohol oxidation in fungi</p> <p>Degradation of amines to carbonyl compounds</p>	$\text{O}_2 \rightarrow \text{H}_2\text{O}_2$
	<p>✓ <b>“Normal” Copper enzymes</b></p> <p>Cu, Zn Superoxide dismutase</p>	<p>Superoxide ion detoxification e.g. in erythrocytes</p>	$2\text{O}_2 + 2\text{H}^+ \rightarrow \text{H}_2\text{O}_2 + \text{O}_2$

<div>Type III</div> <div> <math>\mu\text{O}_2(\text{Cu}(\text{N}^{\epsilon}_{\text{His}})_3)_2</math></div>	<div>✓ Dioxygen transport</div> <div>Hemocyanins</div>	Oxygen transport in mollusks and arthropods	O <sub>2</sub> transport
	<div>✓ Copper oxygenases</div> <div>Tyrosinases</div>	Ortho-hydroxylation of phenols and subsequent oxidation to o-quinones in skin of mammals and fungi.	<div>Tyrosine oxidation</div> <div><math>\text{O}_2 + 2\text{H}^+ + \text{monophenol} \rightarrow o\text{-diphenol} + \text{H}_2\text{O}</math></div> <div><math>\text{O}_2 + 2o\text{-diphenol} \rightarrow 2o\text{-quinone} + 2\text{H}_2\text{O}</math></div>
<div>Trinuclear center (TypeII + TypeIII)</div> <div> <math>\text{Cu}(\text{N}^{\epsilon}_{\text{His}})_2\text{OH}\cdot\mu\text{-OH}(\text{Cu}(\text{N}^{\epsilon}_{\text{His}})_3)_2</math></div>	<div>✓ “Blue” (multicopper) oxidases</div> <div>Ascorbate oxidase</div> <div>Laccase</div> <div>Ceruloplasmin</div>	<div>Oxidation of ascorbate to dehydroascorbate in plants</div> <div>Oxidation of polyphenols and polyamines in fungi and plants</div> <div>Cu transport and storage, Fe mobilization and oxidation in human and animal serum</div>	<div>Catalysis</div> <div><math>\text{O}_2 \rightarrow 2\text{H}_2\text{O}</math></div>

<p><b>Cu<sub>A</sub></b></p>  <p><math>\text{Cu}_2(\text{N}_{\text{His}}^{\delta})_2\text{O}_{\text{Glu}}^{\alpha}\text{S}_{\text{Cys}}^{\delta}</math> Met(<math>\mu\text{S}_{\text{Cys}}^{\delta}</math>)<sub>2</sub></p>	<p>Cytochrome c oxidase</p> <p>Nitrite reductase</p>	<p>End point of the respiratory chain</p> <p>Denitrifying bacteria</p>	<p>Electron transfer</p> <p><math>\text{O}_2 \rightarrow 2\text{H}_2\text{O}</math></p> <p>Reduction of <math>\text{N}_2\text{O}</math> to <math>\text{N}_2</math></p>
<p><b>Cu<sub>B</sub></b></p>  <p><math>\text{CuN}_{\text{His}}^{\delta}(\text{N}_{\text{His}}^{\epsilon})_2\text{L}</math> L = bridging ligand between Cu<sub>B</sub> and Fe of haem <i>a</i><sub>3</sub></p>	<p>Cytochrome c oxidase</p> <p>Ubiquinone oxidase</p>	<p>End point of the respiratory chain</p> <p>Proton pump</p>	<p>Electron transfer</p> <p><math>\text{O}_2 \rightarrow 2\text{H}_2\text{O}</math></p> <p>Reduction of <math>\text{O}_2</math> to <math>\text{H}_2\text{O}</math></p>

### 1.3 Copper Homeostasis in Eukaryotes

The essential yet toxic nature of copper requires an elaborate system for copper sequestration and delivery to various essential enzymes within the cell while preventing accumulation of copper in a free toxic form (Poulos, 1999). The yeast *Saccharomyces cerevisiae* has served as a valuable model to study copper metabolism in eukaryotic cells (Wong et al., 2004). There are 3 known biological processes that require copper in yeast, (i) mitochondrial oxidative phosphorylation, (ii) superoxide anion detoxification and (iii) iron metabolism (Lee et al., 2006). Initial studies on copper uptake in yeast identified the high affinity copper transporter 1 (Ctr1) (Dancis et al., 1994) and two low affinity transporters, Ctr2 (Kampfenkel et al., 1995) and Ctr3 (Knight et al., 1996). Since Ctrs do not possess an ATPase domain, the driving force for the Ctr mediated copper transport is not known (Lee et al., 2006). Ctr1 endocytosis has been speculated to be one mechanism for transport.  $\text{Cu}^+/\text{2K}^+$  antiport was suggested as another mechanism after electrochemical measurements revealed that copper ion uptake is coupled with  $\text{K}^+$  efflux in 1:2 stoichiometry (Derome and Gadd, 1987). Extracellular copper, usually Cu(II), is reduced to Cu(I) by plasma membrane reductases encoded by Fre1 and Fre2 before being imported by Ctrs (Hassett and Kosman, 1995; Rees and Thiele, 2004). Transcription of Fre1 is regulated by intracellular copper through the action of copper-dependent transcription factor Mac1p (Georgatsou and Alexandraki, 1999).

The use of Cu(I) rather than Cu(II) by copper transporters appears thermodynamically favorable. The lower valence states of transition metals are generally more exchange labile, e.g. the water exchange rate for Fe(II) is three orders of magnitude

faster than for Fe(III) ( $10^6 \text{ s}^{-1}$  for Fe(II) compared to  $10^3 \text{ s}^{-1}$  for Fe(III)). In extracellular fluid, the reduction of Cu(II) complexed to organic molecules would favor displacement of the ligand to which the metal ion is bound, thus providing a source of bio-available copper upon reduction (Magnani and Solioz, 2007). Additionally, since Cu(I) has fewer potential chemical ligands than Cu(II), the transport of reduced copper could be an important step in determining the specificity of the process (Labbe and Thiele, 1999).

Once copper crosses the plasma membrane, it needs to be immediately sequestered to prevent its reaction with reactive oxygen species such as  $\text{O}_2^-$  and  $\text{H}_2\text{O}_2$  (Labbe and Thiele, 1999). The cytoplasmic condition of cells is reducing. The tripeptide glutathione (GSH) is present at high concentrations (3-5 mM) and is probably the major reducing agent inside the cytoplasm of all living cells (Tietze, 1969). It is known that copper is immediately complexed by GSH upon entering the cell (Freedman et al., 1989). GSH depletion was shown to potentiate metal toxicity in rats (Fukino et al., 1986), mice (Singhal et al., 1987) and cultured cells (Kang and Enger, 1988; Ochi et al., 1988). Under conditions of high copper concentration in the surrounding environment, a group of small cysteine-rich polypeptides with repeated C-X-X-C or C-X-C sequence motifs, called metallothioneins (MT) are produced in eukaryotic cells. It was shown *in vitro* that Cu(I)-GSH could mediate Cu(I) transfer into metal depleted MT (Ferreira et al., 1993). MTs are effective in copper ion detoxification due to remarkable metal binding properties resulting from a high (30% of the amino acids) cysteine content (Stillman, 1995). By forming polymetallic thiolate bond clusters, MTs shield the metal ion from the cytoplasm and thus prevent it from performing Fenton-type reactions (Elam et al., 2002). Two MTs,

Cup1 (Fogel and Welch, 1982) and Crs5 (Culotta et al., 1994) have been identified in *S. cerevisiae*. Induction of the *cup1* and *crs5* genes is mediated through the copper-binding transcription factor Ace1 (Thiele, 1988). Studies have shown that MTs have no direct role in copper uptake but they are important for storage of metal and for protection against copper toxicity (Lin and Kosman, 1990) .

With this apparent vacuum of free copper, how do copper requiring enzymes obtain their essential cofactor (Field et al., 2002)? The discovery of Menkes (Davies, 1993; Hamer, 1993) and Wilson's (Bull and Cox, 1994; Solioz and Vulpe, 1996) diseases about 15 years ago added a new dimension to the study of intracellular copper metabolism. The molecular details of intracellular trafficking began to emerge with the discovery of copper handling accessory proteins, called copper chaperones (Culotta et al., 1997; Pufahl et al., 1997) or metallochaperones (Rosenzweig, 2001). Copper chaperones are defined as proteins that escort the metal to specific copper-requiring targets in the cell (Culotta et al., 1997), thus ensuring efficient delivery. Not only do they protect the metal ion from the housekeeping scavenging molecules (GSH and MTs), but also protect the environment from the reactive nature of the metal ion (Elam et al., 2002).

In this regard, three small copper-binding proteins, Atx1 (Lin et al., 1997), Cox17 (Glerum et al., 1996) and CCS (Culotta et al., 1997) have been identified as being involved in copper mobilization to the desired destinations in *S. cerevisiae*. By serving as copper chaperones, they deliver copper to the late secretory compartments, mitochondria, and cytosolic Cu,Zn-Superoxide dismutase respectively, providing the required cofactor for three biological processes as discussed above (Labbe and Thiele, 1999). It is

unknown how the chaperones are themselves loaded with copper, or how different chaperones are selected by their partner proteins (Moller and Horn, 2002). Atx1 was shown to interact with the soluble domain of Ctr1 *in vitro* and copper transfer from the importer to the metallochaperone appeared thermodynamically favorable (Xiao et al., 2004).

Atx1 (antioxidant 1) was the first member to be identified (Lin and Culotta, 1995) and was so named because it was first identified as a suppressor of oxidative damage in yeast SOD null mutants. Atx1 is an 8.2 kDa cytosolic protein, which contains a single amino terminal MTCXXC copper-binding motif. Thiols of the two cysteines act as ligands to bind one Cu(I) atom per polypeptide (Pufahl et al., 1997). Cu(I)-Atx1 interacts with the N-terminal MTCXXC residues of the P-type ATPase Ccc2 present in the trans-golgi network and is shown to transfer Cu(I) to Ccc2 via series of bridged Cu(I) intermediates (Pufahl et al., 1997). In an ATP-dependent manner, Cu(I) is then incorporated into Fet3 multicopper oxidase in a post-golgi compartment (Lin et al., 1997; Yuan et al., 1995). Fet3 is located in the cell membrane and is required for the high affinity iron uptake into the yeast cell (Askwith et al., 1994). Atx1 deletion mutants could not grow in iron-limiting conditions, but could be rescued by copper supplementation (Lin et al., 1997). Additionally, Ccc2 overexpression could correct the poor growth phenotype observed in limited iron conditions in  $\Delta$ Atx1 yeast. This corroborated the model where Atx1 delivers Cu(I) to Ccc2, which in turn transfers it to Fet3 (Lin et al., 1997). Ccc2 is a functional and structural homolog of the mammalian WND and MNK P-type ATPase copper transporters, which are impaired in Wilson and

Menkes diseases, respectively. The human homolog of Atx1 is Atox1 which delivers copper to MNK (ATP7A) and WND (ATP7B) ATPases, respectively (Walker et al., 2002). While ATP7A directs copper within the TGN to several cuproenzymes, ATP7B directs copper incorporation into ceruloplasmin, a serum ferroxidase that contains more than 95% of the copper found in blood (Balamurugan and Schaffner, 2006; Hellman and Gitlin, 2002). Both WND and MNK can complement a Ccc2 null mutation in heterologous yeast systems (Hung et al., 1997; Lee et al., 2006; Payne and Gitlin, 1998).

Superoxide Dismutase1 (SOD1) is largely a cytosolic enzyme that employs a copper cofactor to catalytically disproportionate  $O_2^-$  to  $H_2O_2$  and  $O_2$  (McCord and Fridovich, 1969). The chaperone which delivers Cu(I) to SOD1 is CCS (Copper Chaperone for SOD1). The copper chaperone function for CCS first became evident from studies on deletion mutants of *lys7* (gene that encodes CCS). These mutants were devoid of SOD1 activity despite normal expression of SOD1 (Culotta et al., 1997). SOD1 function could be restored by copper supplementation, supporting that its inactivity is the result of inadequate copper incorporation (Culotta et al., 1997). That CCS activates SOD1 by directly inserting the copper cofactor became apparent when copper loaded CCS was found to activate apo-SOD1 in the presence of copper chelating agent (Rae et al., 1999).

The third chaperone identified is Cox17 which facilitates the assembly of copper sites in cytochrome c oxidase (COX). COX is a terminal enzyme of the electron transport chain located in the inner mitochondrial membrane, which catalyzes the oxidation of reduced cytochrome c, coupled to the reduction of oxygen to two molecules

of water. Cox17 was first identified by genetic screening of yeast for respiratory deficient mutants (Glerum et al., 1996). Cox17 is a cysteine rich polypeptide of 69 amino acids that resides partially in the cytosol (40%) and partially in the mitochondrial inter-membrane space (60%) (Beers et al., 1997). Cox17 delivers Cu(I) to Sco1, an accessory protein present in the intermembrane space (Horng et al., 2004), which in turn is involved in the assembly of dinuclear Cu<sub>A</sub> site in COX (Abajian and Rosenzweig, 2006).

#### **1.4 Copper Homeostasis in Prokaryotes**

The best understood copper homeostasis system in prokaryotes is that of the gram-positive bacterium, *Enterococcus hirae* and gram-negative bacterium *Escherichia coli*. Besides copper sensors, neither *E. hirae* nor *E. coli* has any known copper-requiring proteins present in the cytosol. In *E. coli*, known cuproenzymes like cytochrome c oxidase, superoxide dismutase, NADH dehydrogenase2 (NDH-2), aromatic amine oxidase (MaoA) and 3-oxy-D-arabino-heptulosonate-7-phosphate-synthase are all present in the periplasm (Magnani and Solioz, 2007; Rensing and Grass, 2003). In gram-positive bacteria, which are devoid of periplasm, the copper requiring proteins are located outside of the cytoplasm. For example, another gram-positive bacterium *Bacillus subtilis* has a caa3-type cytochrome oxidase in which an externally located cytochrome c is covalently fused to subunit II of the oxidase (Tottey et al., 2005). The only known system that suggests the need for cytoplasmic copper in bacteria is the biosynthesis of molybdenum cofactor (Kuper et al., 2004; Schwarz and Mendel, 2006).

How copper enters the cell is not clear. In *E. coli*, copper has been shown to cross its first barrier, the outer membrane, through porins (Lutkenhaus, 1977). For transport across the cytoplasmic membrane, Ctr1-like systems like those in eukaryotes have not been discovered in bacteria (Magnani and Solioz, 2007). Thus, the mechanism by which copper makes it to the cytosol in bacteria remains unknown. Cu(I) equilibration across the cytoplasmic membrane seems to be the most plausible scenario presently (Outten et al., 2001).

Unlike eukaryotes, metallothioneins involved in copper sequestration in the cytosol are not known to exist in any class of bacteria except cyanobacteria (Turner and Robinson, 1995). In a recent study on identification of proteins expressed by bacterial community in a waste water treatment bioreactor upon exposure to high levels of cadmium, no metallothioneins were detected in the culture (Lacerda et al., 2007). Apparently, the energetic cost of metal complexation is higher than metal efflux (Nies, 1999). Elaborate mechanisms for copper efflux have been recognized (Rensing and Grass, 2003). The participating proteins are found to be either plasmid (e.g. Pco system (Lee et al., 2002)) or chromosomally encoded.

#### **1.4.1 Plasmid-encoded copper resistance in *E. coli***

The plasmid-borne *cop* gene cluster *copABCDRS*, encoding proteins responsible for copper resistance in *Pseudomonas syringae*, was the first copper resistance system to be described in detail. It was discovered in bacteria isolates responsible for causing

speck disease (Bender and Cooksey, 1987) in tomato cultures in Southern California that had been sprayed with copper sulfate for fungal and bacterial disease control (Mellano and Cooksey, 1988b). The *cop* gene products are closely related to the products of the *pcoABCDRS* operon from *E. coli* with amino acids identities of 76%, 55%, 60%, 38%, 61% and 30%, respectively (Silver and Phung, 1996). The Pco system responsible for copper resistance in *E. coli* was first isolated from a strain present in the gut flora of pigs fed on a copper-enriched diet (Brown et al., 1995; Tetaz and Luke, 1983). Copper sulfate was widely used in pig feeds due to its growth promoting capacity (Barber et al., 1955). Copper resistance manifested by the *E. coli pco* (and *P. syringae cop*) operons is copper inducible (Mellano and Cooksey, 1988a; Rouch et al., 1985). The two-component regulatory system, *pcoRS*, induces transcription of the *pcoABCD* operon. PcoS is a periplasmic histidine kinase, which senses copper and autophosphorylates. PcoR, upon phosphorylation by PcoS, binds to DNA and acts as a transcription activator (Mills et al., 1994). Unlike the *cop* operon of *P. syringae*, however, an additional gene called *pcoE* is present in *E. coli*'s *pco* system. *pcoE* is also under the control of PcoRS but it is transcribed from a separate promoter (Rouch and Brown, 1997). PcoA is a multicopper oxidase present in the periplasm (Huffman et al., 2002). PcoB is likely present in the outer membrane (Lee et al., 2002). PcoA, in concert with PcoB confers higher copper resistance. PcoC is also a periplasmic protein (Huffman et al., 2002) that has been shown to bind both Cu(I) and Cu(II) in structural studies (Zhang et al., 2006). PcoC has been proposed to dock with PcoA after acquiring Cu(I) in the periplasm, to effect its oxidation to the less toxic Cu(II) form (Huffman et al., 2002). PcoD is a cytoplasmic membrane

protein with eight predicted transmembrane helices (Lee et al., 2002). PcoE, which is transcribed from its own promoter, is a small periplasmic protein that is required for full copper resistance. It likely functions as a periplasmic copper chaperone (Magnani and Solioz, 2007; Rensing and Grass, 2003). Since toxic transition metals have been abundant on this earth from the beginning of life, it is hypothesized that metal efflux systems arose shortly after prokaryotic life started (Silver, 1996; Silver and Phung le, 2005) and that they are mostly found on plasmids due to their ease of transfer from one to another bacterium.

#### **1.4.2 Chromosomally-encoded copper resistance in *E. coli***

Although the plasmid-encoded copper resistance determinant in *E. coli* has long been known, copper resistance factors encoded by the chromosome were described only recently (Nies, 2003). The two most well studied chromosomally encoded systems found to catalyze the removal of excess copper from the cell are Cue (copper efflux) and Cus (copper sensing) respectively. The Cue system consists of a copper responsive metalloregulatory protein, CueR, that upregulates the expression of 2 proteins, CopA (a P-type ATPase having significant homology to eukaryotic copper transporters), and CueO (a multicopper oxidase, similar to fet3 in yeast and ceruloplasmin in humans). The Cus system, like the Pco system, is regulated by a two component signal transduction system encoded by *cusR* and *cusS*. *cusRS* activates the expression of *cusCFBA*, which

acts to protect the cell under anaerobic conditions when CueO becomes non-functional (Franke et al., 2003; Outten et al., 2001) (Figure 1.2).

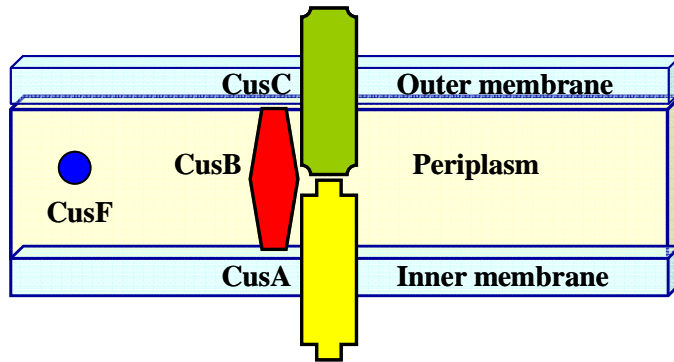


**FIGURE 1.2** Schematic of the CusCFBA copper efflux system of *Escherichia coli*.

The evolution of this sophisticated efflux system (CusCFBA) may be regarded as an adaptive measure to cope with the various metal stress conditions. *E. coli*'s natural habitat is the digestive tract of warm-blooded animals. Here the conditions prevalent are usually anaerobic with possibly high concentrations of copper. Thus, CusCFBA may have been an adaptation to *E. coli*'s specific ecological niche (Rensing and Grass, 2003).

#### 1.4.3 The CusCFBA system of *E. coli*

CusCFBA, unlike its multi-drug export homologs, possesses a 4 component organization. In accordance with other CBA transporters, CusA, CusB and CusC serve as Resistance, Nodulation and Cell Division (RND), Membrane Fusion protein (MFP) and Outer Membrane Factor (OMF) proteins, respectively. An additional fourth

component, CusF, found only in putative copper/silver resistance systems, is located in the periplasm.

Earlier studies on related CBA transport systems had shown a “closed bridge” export from the cytoplasm to the extracellular space with no periplasmic intermediates, as mediated by the channel formation of three proteins (Koronakis et al., 1989; Thanabalu et al., 1998; Thanassi and Hultgren, 2000). Recent biochemical and structural studies have revealed uptake also from the periplasm (Murakami et al., 2002; Zgurskaya and Nikaido, 2000). The periplasmic component, MFP in these studies, has been proposed to function mostly as an adaptor protein, holding the inner and outer membrane components in place and thus facilitating the efflux process. No direct involvement of MFPs in the periplasmic uptake has been reported. Genetic studies on the CusCFBA system suggest periplasmic copper transport (Grass and Rensing, 2001; Outten et al., 2001). Participation of the periplasmic components CusB and CusF in copper transport was demonstrated by a decrease in the Minimum Inhibitory Concentration (MIC) of copper in the absence of either component (Franke et al., 2003). This indicated that CusB, and likely MFPs in other CBA systems, have an active role in the efflux process. Furthermore, CusF exists as a single polypeptide with CusB in some homologous systems, which points at plausible involvement of CusF in metal extrusion.

### **1.5 Significance: From metal transport systems to multi-drug exporters**

Studies on the bacterial Cus system will not only enhance our understanding of copper regulation/ resistance in bacteria, but may also aid in better understanding of efflux mediated by CBA type multi-drug exporters. There is a growing concern that metal contamination functions as a selective agent in the proliferation of antibiotic resistance. This hypothesis has been tested in a number of different studies. For example, mercury has been used in dental amalgams since the 19<sup>th</sup> century. It is slowly released from the amalgams and retained in the body. A recent report on bacteria isolates from patients with amalgam fillings showed that the bacteria were resistant both to mercury and antibiotics (Pike et al., 2002). In another study, the antibiotic sensitivity of bacteria taken from ash settling basins (ASB) of coal-fired power plants was investigated. Coal-fired power plants are a major source of global metal pollution, accounting for 10-60% of the anthropogenic emissions of different transition and heavy metals. The bacteria isolated from ASBs of these plants were found to be more antibiotic-resistant (Stepanauskas et al., 2005), thus substantiating the co-selection phenomena.

## 1.6 Dissertation Outline

This dissertation is a biochemical study of CusB and its interactions with CusF, aiming to delineate the efflux mechanism. Fundamental information regarding the role of CusB was sought. The prior body of knowledge regarding this class of proteins suggested that they played a relatively passive role in stabilizing the efflux complex. The work in this dissertation sought to determine whether additional functions are present.

In Chapter 2, biochemical characterization of CusB defining its active involvement in the efflux process is presented. It is shown that CusB binds substrates Ag(I) and Cu(I) in a trigonal geometry with methionine ligands and undergoes a conformational change upon binding. The particular residues that form the binding site are determined using sequence alignments and mutagenesis studies. Importantly, metal binding by CusB is also shown to be essential for metal resistance.

In Chapter 3, the chaperone nature of CusF is revealed. Interaction studies between CusF and CusB using isothermal titration calorimetry (ITC) and X-ray absorption spectroscopy (XAS) are presented. Through ITC, it is shown that CusF and CusB interact only in the presence of metal ion and that the interaction between the two proteins is highly specific. Metal transfer between CusF and CusB is demonstrated using a novel XAS approach, which showed that Cu(I) can be reversibly transferred between CusF and CusB, with an approximately 50% end distribution between the two proteins.

Chapter 4 discusses structural characterization of interactions between CusF and CusB using NMR spectroscopy. Chemical shift assignments of Ag(I)-CusF in the

presence of CusB determined the residues in CusF that were significantly affected by the presence of CusB. It is shown that the residues most affected and likely to be involved in interaction with CusB are the ones that are present on the metal binding face of CusF. This is the same face that other proteins with the same fold as CusF (OB fold) use to interact with their respective partners.

In chapter 5, various constructs of CusB that were designed in order to improve upon the recombinant protein yields, and to make the protein more amenable for structural studies, are discussed. Strategies taken in the direction of designing those constructs, and results from initial experiments that were performed to test the system, are presented.

Chapter 6 is a summary of the experiments presented in earlier chapters. It also discusses approaches that may be taken in future to further the understanding of the system.

## CHAPTER 2

### **SUBSTRATE-LINKED CONFORMATIONAL CHANGE IN THE PERIPLASMIC COMPONENT OF A CU(I)/AG(I) EFFLUX SYSTEM**

In this chapter, I report our results from the biochemical characterization of the periplasmic component CusB and discuss the novelty of our findings in relation to findings reported in literature on homologous CBA systems. I have described the resistance, nodulation, division (RND) component of CBA systems in greater detail to differentiate the drug export from metal efflux class and discuss our results with reference to information garnered from drug exporter's studies. The contents of this chapter were published in the Journal of Biological Chemistry with contributions from Wenbo Liu, Ninian J. Blackburn, Christopher Rensing and Megan M. McEvoy (Bagai et al., 2007). Mutants were generated by Wenbo Liu and EXAFS data were collected by Ninian J. Blackburn.

#### **2.1 ABSTRACT**

Gram-negative bacteria utilize dual-membrane RND-type efflux systems to export a variety of substrates. These systems contain an essential periplasmic component that is important for assembly of the protein complex. We show here that the periplasmic protein CusB from the Cus copper/silver efflux system has a critical role in Cu(I) and Ag(I) binding. Isothermal titration calorimetry experiments demonstrate that one Ag(I)

ion is bound per CusB molecule with high affinity. X-ray absorption spectroscopy data indicate that the metal environment is an all-sulfur three-coordinate environment. Candidates for the metal-coordinating residues were identified from sequence analysis, which showed four conserved methionine residues. Mutations of three of these methionine residues to isoleucine resulted in significant effects on CusB metal binding *in vitro*. Cells containing these CusB variants also show a decrease in their ability to grow on copper containing plates, indicating an important functional role for metal binding by CusB. Gel filtration chromatography demonstrates that upon binding metal, CusB undergoes a conformational change to a more compact structure. Based on these structural and functional effects of metal binding, we propose that the periplasmic component of RND-type efflux systems plays an active role in export through substrate-linked conformational changes.

## 2.2 INTRODUCTION

Efflux systems of the resistance nodulation division (RND) family are key players in the intrinsic and acquired antibiotic resistance of gram-negative bacteria (Poole and Srikumar, 2001). These systems confer resistance to otherwise lethal concentrations of drugs and metal ions, and also mediate efflux of bacterial products such as siderophores, peptides, and quorum sensing signals (Piddock, 2006; Yang et al., 2006). With antibiotic-resistant pathogens representing a growing threat to human health, understanding these efflux systems is of significant importance.

RND-type efflux systems form a transenvelope complex comprised of three fundamental components: an energy-utilizing inner membrane protein (Tseng et al., 1999), an outer membrane factor and a periplasmic component (Dinh et al., 1994). The inner membrane components are proton-substrate antiporters of the RND protein superfamily, which are sub-classified on the basis of their exported substrate (Tseng et al., 1999). Members of the heavy metal efflux (HME) sub-family of RND transport systems are highly substrate specific, with the ability to differentiate between monovalent and divalent ions (Tseng et al., 1999). In contrast, the hydrophobe/amphiphile efflux (HAE) sub-family of RND protein systems has significantly broader substrate recognition. Members of the HAE-RND systems transport a wide range of structurally unrelated molecules including antibiotics, dyes, detergents, bile salts, organic solvents and antimicrobial peptides (Poole, 2004).

Insights into the functions of the three fundamental components of RND efflux systems have been gathered from studies of a variety of RND systems. By far, the most information at the structural and biochemical levels is known for the inner and outer membrane proteins. The overall picture that has emerged is that the inner and outer membrane proteins form a channel that spans the periplasmic space (Eswaran et al., 2004; Touze et al., 2004). The substrate is taken up from either the inner membrane, cytoplasm, or periplasm, depending on the properties of the substrate and the particular efflux system (Zgurskaya and Nikaido, 2000). The RND protein drives substrate export through the channel formed by the outer membrane protein utilizing the proton gradient across the inner membrane. Though the periplasmic component is an essential part of RND efflux systems (Franke et al., 2003), the role it plays in the efflux process is much less clear.

Several functions have been postulated for the periplasmic component. It is often termed an adaptor protein, which may have a function in bridging the inner and outer membrane components. This role is supported by biochemical experiments that have shown a direct interaction between this component and the inner and outer membrane proteins (Touze et al., 2004). More recent studies suggest that the periplasmic component could contribute to the regulation of the open and closed states of the outer membrane protein. Evidence for this function of the periplasmic adaptor protein is given by the observation of conformational variants in the crystal structure of the periplasmic protein AcrA from the AcrAB-TolC HAE-RND efflux system (Mikolosko et al., 2006) and observation of direct interactions between the coiled regions of the periplasmic protein and outer membrane protein (Lobedanz et al., 2007). However, the periplasmic

protein likely has a further functional role, since even a constitutively open mutant of an outer membrane protein requires the periplasmic component (Augustus et al., 2004). In a reconstituted system without the outer membrane protein, the periplasmic adaptor AcrA is essential to the function of the RND pump AcrD (Aires and Nikaido, 2005), which further supports the hypothesis that the periplasmic proteins can play active roles in substrate capture and extrusion.

CusCFBA, the Cu(I) and Ag(I) efflux system from *E. coli*, consists of CusB, the periplasmic protein, CusA, the inner membrane proton/substrate antiporter of the HME-RND family and CusC, the outer membrane protein (Franke et al., 2001; Franke et al., 2003; Munson et al., 2000). In addition to the three fundamental proteins, the Cus system has a fourth component, the small periplasmic metal-binding protein CusF, which has homologs only in putative monovalent metal ion resistance systems (Franke et al., 2003). In addition to conferring Ag(I) resistance (Franke et al., 2001), the CusCFBA system has been shown to be important for copper resistance primarily under anaerobic conditions, suggesting that its other physiologically relevant substrate is Cu(I) (Outten et al., 2001). Copper and silver belong to the same group of the periodic table, therefore Cu(I) and Ag(I) have similar coordination chemistries and can be treated interchangeably in many cases (Solioz, 2002). However, silver is predominantly found in the Ag(I) oxidation state under both aerobic and anaerobic conditions, whereas Cu(I) only predominates under anaerobic conditions.

To address the role of the periplasmic component, we examined CusB from the CusCFBA system as a representative of the periplasmic proteins of RND efflux systems.

## 2.3 MATERIALS AND METHODS

**2.3.1 Protein expression and purification.** Genomic DNA from *E. coli* strain W3110 was used to amplify the *cusB* gene. The primers used for the PCR reaction contained unique restriction sites at the 5' end (*EcoRI*) and 3' end (*XhoI*). After restriction enzyme digestion of the PCR product, it was ligated into the pASK-IBA3 (IBA, Germany) vector. The result was a construct that contained the full-length *cusB* gene followed by region encoding a short cloning artifact (LEVDLQGDHGL) and a C-terminal Strep affinity tag (SAWSHPQFEK).

The *cusB*-containing plasmid was transformed into *E. coli* BL21 ( $\lambda$ DE3). Cells were grown in LB media containing 100  $\mu$ g/mL ampicillin at 37 °C until they reached an O.D.<sub>600</sub> of 0.6-1.0, then induced with 200  $\mu$ g/L of anhydrotetracycline (AHT) and grown at 30 °C for another 6-8 hours. Cells were harvested by centrifugation and frozen at -20 °C.

Cell pellets were resuspended in 50 mL of 100 mM Tris (pH 8.0), 150 mM NaCl per liter of cell culture. Protease inhibitors (leupeptin (final concentration 2  $\mu$ g/mL), pepstatin (final concentration 2  $\mu$ g/mL), and PMSF (final concentration 0.5 mM)) and DNaseI (approximately 150 units) were added, then cells were lysed by a French Press. 3-((3-Cholamidopropyl)dimethylammonio)-1-propanesulfonate (CHAPS) (0.1% w/v) (MP Biomedicals) was added to the lysate, then cells were pelleted by centrifugation at 31000Xg. The supernatant was loaded onto *Strep*-Tactin-resin (IBA, Germany) affinity column. After washing the column with 100 mM Tris (pH 8.0), 150 mM NaCl buffer,

protein was eluted using the same buffer, plus 2.5 mM desthiobiotin. The fractions were dialyzed vs. 50 mM Tris (pH 9.0) buffer and loaded onto a MonoQ 10/100 GL anion exchange column (Amersham) equilibrated with the same buffer. CusB was eluted from the column by a linear gradient of 0-300 mM NaCl in 50 mM Tris (pH 9.0). Aliquots of the fractions were run on SDS polyacrylamide gels and stained with Coomassie to determine purity. CusB protein was also verified by Western blot analysis using horseradish peroxidase-conjugated antibody specific to the *Strep*-tag (IBA, Germany). The N-terminal sequence of CusB was confirmed by sequencing. Fractions >95% pure were pooled and dialyzed in appropriate buffer and concentrated using Amicon concentrators with a 5 kDa molecular weight cut-off. Protein concentrations were determined using the BCA assay (Pierce Biotechnology) for all the experiments except EXAFS for which the Bradford assay (Bradford, 1976) (Biorad) was used.

**2.3.2 Isothermal titration calorimetry.** ITC measurements were performed on a Microcal VP-ITC Microcalorimeter (Northampton, MA, USA), typically at 25 °C. The titrant solution was made by mixing appropriate amount of stock metal solution (90 mM AgNO<sub>3</sub> in nanopure Milli-Q water) with buffer retained from the final dialysis of the protein sample. CusB was extensively dialyzed in 50 mM cacodylate (pH 7.0). Both protein and titrant were thoroughly degassed in a ThermoVac apparatus (Microcal). For a titration experiment, approximately 1.7 mL of 22 μM CusB was placed in a reaction cell and injected over 20 seconds with 10 μL 300 μM AgNO<sub>3</sub> solution with a 5-minute interval between each injection. The titrations of the CusB mutants M21I, M36I, M38I

and M283I were carried out as described for wild-type CusB, using protein concentrations of 18.0, 19.0, 20.0 and 24.7  $\mu\text{M}$ , respectively. In order to ensure adequate mixing of the titrand and the titrant, the reaction cell was continuously stirred at 300 rpm. A total of 25 injections were made. The heat due to dilution, mechanical effects and other non-specific effects were accounted for by averaging the last three points of titration and subtracting that value from all data points (Jelesarov and Bosshard, 1999; Kittleson et al., 2006). Data were fitted using a single-site binding model in the Origin software package (MicroCal). The software uses a non-linear least-squares algorithm and the concentrations of the titrant and the titrand to fit the enthalpy change per injection to an equilibrium binding equation. The binding enthalpy change  $\Delta H$ , association constant  $K_a$ , and the binding stoichiometry  $n$  were permitted to float during the least-squares minimization process and taken as the best-fit values.

**2.3.3.1 X-ray absorption spectroscopy.** Samples for EXAFS were prepared in an anaerobic chamber. CusB was first dialyzed in 20 mM 3-(N-Morpholino)-propanesulfonic acid (MOPS), pH 7.0. Ascorbate solution buffered at pH 7.0 was then added to argon-purged protein at a final concentration of 50 mM.  $\text{CuCl}_2$  was added such that the ratio of CusB to Cu(I) was 1:1. The protein was further dialyzed against 20 mM MOPS, 10 mM ascorbate, pH 7.0, to remove unbound copper. The final concentration of protein was determined using the Bradford assay (Bradford, 1976). 80  $\mu\text{L}$  of CusB-Cu(I) was mixed with 20  $\mu\text{L}$  of ethylene glycol, transferred to EXAFS vials, then flash frozen in liquid nitrogen.

**2.2.3.2 Collection and analysis of XAS data.** Cu K-edge (8.9 keV) extended X-ray absorption fine structure (EXAFS) and X-ray absorption near edge structure (XANES) data were collected at the Stanford Synchrotron Radiation Laboratory operating at 3 GeV with currents between 100 and 50 mA. All samples were measured on beam line 9-3 using a Si(220) monochromator and a Rh-coated mirror upstream of the monochromator with a 13 KeV energy cutoff to reject harmonics. A second Rh mirror downstream of the monochromator was used to focus the beam. Data were collected in fluorescence mode using a high-count-rate Canberra 30-element Ge array detector with maximum count rates below 120 kHz. A 6 $\mu$  Z-1 Ni oxide filter and Soller slit assembly were placed in front of the detector to reduce the elastic scatter peak. Six scans of a sample containing only sample buffer were collected, averaged, and subtracted from the averaged data for the protein samples to remove Z-1 K $\beta$  fluorescence and produce a flat pre-edge baseline. The samples (80  $\mu$ L) were measured as aqueous glasses (>20% ethylene glycol) at 10 K. Energy calibration was achieved by reference to the first inflection point of a copper foil (8980.3 eV) placed between the second and third ionization chamber. Data reduction and background subtraction were performed using the program modules of EXAFSPAK (George, 1990). Data from each detector channel were inspected for glitches or drop-outs before inclusion in the final average. Spectral simulation was carried out using the program EXCURVE 9.2 (Binsted et al., 1998; Binsted and Hasnain, 1996; Gurman et al., 1984; Gurman et al., 1986) as described previously (Blackburn et al., 2000).

**2.3.4 Site-directed mutagenesis and growth inhibition studies of *CusB*.** The QuikChange site-directed mutagenesis protocol (Stratagene, La Jolla, Calif.) was used to alter the individual methionines to isoleucines in *CusB*. Plasmid pASK3 containing the *cusB* gene was used as a template. Primer pairs used to introduce the point mutations were antiparallel and overlapping. PCR products were treated with *DpnI* to digest the *dam*-methylated template plasmid. The correct mutations were verified by DNA sequence analysis. The purified PCR product containing the point mutation was transformed into EC950 ( $\Delta cueO$   $\Delta cusB$ ) strain (Franke et al., 2003) of *E. coli*. Wild-type *cusB* and an empty pASK3 vector (without the *cusB* gene) were also transformed into EC950 to use as controls in the growth inhibition studies.

For growth inhibition experiments, mutants, wild type and the cells containing empty vector were grown overnight in LB medium. Cells were diluted 1:100 in fresh media and grown at 37 °C until they reached an  $A_{600}$  of approximately 0.5. At this point, the cells were subjected to two different protocols. For one set, cells were induced for *CusB* expression at the same time as they were exposed to copper by streaking the cells directly on LB-agar plates containing 100  $\mu$ g/mL ampicillin, 50  $\mu$ g/L AHT and varying concentrations of  $CuCl_2$  (0.0, 0.5, 0.75, 1.0 and 1.5 mM). For the second set, the cells were induced to express *CusB* before subjecting them to metal stress. The cells at an  $A_{600}$  of 0.5 were induced with 50  $\mu$ g/L AHT and grown at 30 °C until they reached an  $A_{600}$  of approximately 1.0. At this point, cells were streaked on LB-agar plates containing 100  $\mu$ g/mL ampicillin and varying concentrations of  $CuCl_2$  (0.0, 0.5, 1.0, 1.25 and 1.5 mM), but no AHT. All plates were incubated at 30 °C for approximately 18 hrs.

**2.3.5 Analytical ultracentrifugation.** Sedimentation equilibrium analysis was performed in a Beckman Optima XL-1 analytical ultracentrifuge using an An-60Ti rotor and an absorbance optical system. A six-channel equilibrium centerpiece equipped with sapphire windows was used to run three sample-solvent pairs simultaneously. Sample and solvent volumes were 110  $\mu\text{L}$  and 125  $\mu\text{L}$  respectively. Data were collected at 4 °C at speeds of 15000, 20000 and 25000 rpm on samples at three concentrations ranging from 5  $\mu\text{M}$  to 14  $\mu\text{M}$  for apo-CusB and 5  $\mu\text{M}$  to 14  $\mu\text{M}$  CusB with 10 to 28  $\mu\text{M}$   $\text{AgNO}_3$  for CusB-Ag(I). Samples were allowed to equilibrate for 12 hrs at each speed, after which five replicate scans were taken every 4 hrs in a step size of 0.005 cm. These scans, spaced 4 hrs. apart, were overlaid in order to determine if equilibrium had been established. Final equilibrium scans were then performed in a step size of 0.001 cm and absorbance was monitored at 280 nm and 255 nm. Fifteen replicate scans were taken and averaged at every radial increment.

The SEDNTERP program (Laue et al., 1992) was used to calculate the partial specific volume (0.7318 mL/g) and the buffer density (1.00605 g/mL) at 4 °C. The baseline offset was constrained to approximately 0.04 for all the datasets. The distribution of single ideal species and monomer-dimer/monomer-trimer equilibrium species was analyzed according to equations described by McRorie et al (McRorie and Voelker, 1993). All fits were done by non-linear least squares analysis of the primary data using the General curve fit function of Kaleidagraph version 3.51 (Synergy Software).

**2.3.6 Size exclusion chromatography.** Size exclusion chromatography was performed using a Superdex 200 10/300GL analytical column (Amersham Pharmacia Biotech) on an Akta Prime System (Amersham Pharmacia Biotech). 60-70  $\mu$ L of protein at a concentration of 180  $\mu$ M was loaded onto the column pre-equilibrated with 50 mM sodium phosphate, pH 7.0. The column was run at a flow rate of 0.4 mL/min and absorbance was measured at 280 nm. Fractions of 500  $\mu$ L were collected. For Ag(I)-CusB, AgNO<sub>3</sub> dissolved in water was added to the protein at two-fold molar excess. The size exclusion column was calibrated with the following globular protein markers (molecular mass and retention volumes are reported): thyroglobulin (669 kDa, 9.7 mL), ferritin (440 kDa, 11.2 mL), catalase (232 kDa, 13.0 mL), aldolase (158 kDa, 13.5 mL), albumin (67 kDa, 14.4 mL), ovalbumin (43 kDa, 15.3 mL), chymotrypsinogenA (25 kDa, 17.1 mL), ribonuclease (13.7 kDa, 17.7 mL).

## 2.4 RESULTS

**2.4.1 Calorimetric titration indicates Ag(I) binding by CusB.** To investigate whether CusB could play a role in substrate binding, we employed isothermal titration calorimetry (ITC) to study the binding of Ag(I) by CusB *in vitro*. ITC detects changes in the heat absorbed or released during a binding event (i.e. the binding enthalpy change). The titration of Ag(I) into the solution of apo-CusB showed a change in binding enthalpy that was not seen in the control titrations without CusB protein, clearly indicating a binding event (Figure 2.1). The large exothermic peaks eventually diminished into just the heat of dilution after approximately 11 injections. A single-site binding model was used to fit the data, yielding a  $K_a$  value of  $4.04 \times 10^7 \text{ M}^{-1}$  (corresponding to a  $K_d$  of 24.7 nM) and a stoichiometry of Ag(I) to CusB of  $0.72 \pm 0.01$ . The dissociation constant should be treated as an approximate value as it is at the lower limits of measurement by ITC. This affinity is similar to that measured for the periplasmic copper and silver binding protein CusF from the Cus system (Kittleson et al., 2006), and clearly demonstrates that CusB is a metal binding protein.

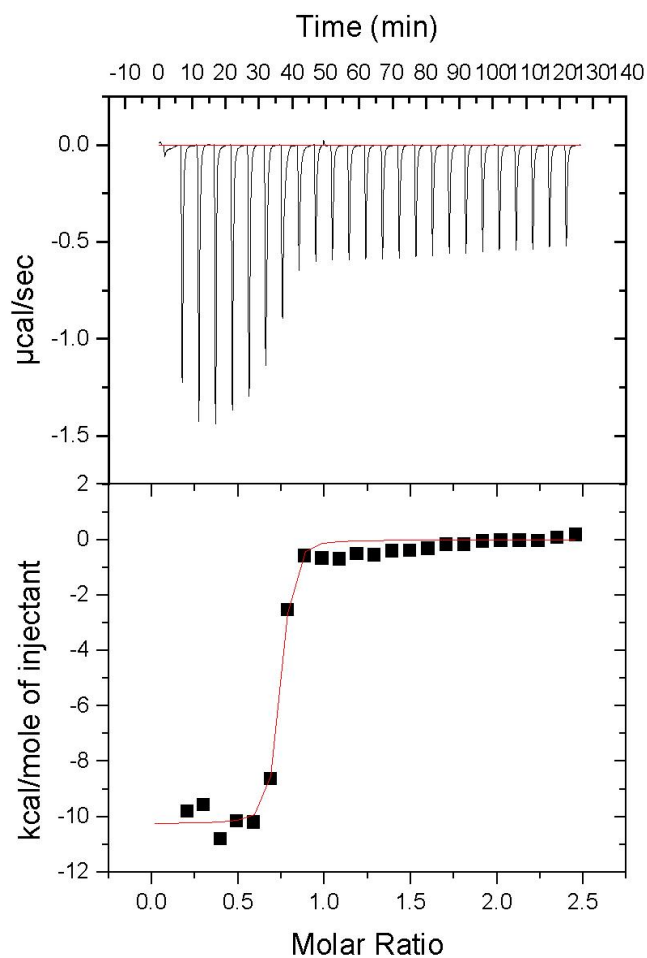


**FIGURE 2.1** ITC data for titration of 22  $\mu\text{M}$  CusB with 300  $\mu\text{M}$   $\text{AgNO}_3$  at 25  $^\circ\text{C}$ . Both solutions were made in 50 mM cacodylate (pH 7.0). *Top*, raw data. *Bottom*, plot of integrated heats versus  $\text{Ag(I)}/\text{CusB}$  ratio. The solid line represents the best fit for a one-site binding model.

**2.4.2 EXAFS spectroscopy of CusB-Cu(I).** In order to identify the potential metal ligands in CusB, we performed X-ray absorption spectroscopy (XAS) of CusB bound to Cu(I). XAS data were collected on two independent samples of copper-loaded CusB and gave identical results within experimental error. The absorption edge region of the spectrum (Figure. 2.2, inset) shows a weak feature at 8983.7 eV with intensity equal to 0.62 of the normalized edge height. The position and intensity of this peak is characteristic of Cu(I) bound to the protein, in a 3-coordinate environment (Pickering et al., 1993; Ralle et al., 2003). Figure 2.2 shows the Fourier transform and extended X-ray absorption fine structure (EXAFS) for a representative sample. The spectrum consists of intense oscillations extending beyond  $k=12.8 \text{ \AA}^{-1}$ , the energy cutoff used to avoid background errors due to small amounts of contaminating Zn in the sample. The first shell of the phase-corrected FT maximizes at  $\sim 2.3 \text{ \AA}$  (characteristic of Cu(I)-thioether or thiolate coordination). The best fit to the data was obtained with 3 Cu-S scattering interactions with Cu-S bond length of  $2.287 \text{ \AA}$  and a Debye Waller factor (DW,  $2\sigma^2$ ) of  $0.011 \text{ \AA}^2$  ( $F = 0.43$ ). We also tested fits that utilized 2 and 4 Cu-S interactions. These gave similar Cu-S bond lengths but had uniformly worse F values (0.70 and 0.56, respectively). Since the simulated bond lengths remained close to those expected for 3-coordination, this analysis confirmed the 3-coordinate assignment. A fit using 2 Cu-S and 1 Cu-O/N interaction had a more acceptable F value (0.51), with 2 Cu-S at  $2.300 \text{ \AA}$  ( $2\sigma^2 = 0.006 \text{ \AA}^2$ ) and Cu-O/N at  $2.050 \text{ \AA}$  ( $2\sigma^2 = 0.017 \text{ \AA}^2$ ), but the large DW term for the single low-Z copper scatterer suggested this latter model was less reasonable than the 3 Cu-S fit. However, the 3S fit also has a high DW for the Cu-S shell suggesting some

heterogeneity in the Cu-S distances. Splitting these distances did not lead to improvements in the F value. We conclude that the most reasonable model to fit the data is 3 slightly inequivalent Cu-S interactions at an average distance of 2.29 Å from the central Cu(I) atom.

Since CusB does not contain any cysteine residues, the sulfur –containing species in CusB that coordinate Cu(I) are methionine residues. The unusually long Cu-S bond length of 2.29 Å is in agreement with this conclusion, since 3-coordinate Cu-cysteinate ligated sites typically exhibit Cu-S bond lengths in the 2.23-2.28 Å range (Pickering et al., 1993; Ralle et al., 2003). Here the weaker donor properties of the thioether ligand appears to lead to lengthening of the Cu-S(met) bonds. Methionines are commonly used in periplasmic proteins for metal coordination because the oxidizing environment of the periplasm renders cysteine less effective. However, few good models exist for 3-coordinate methionine-coordinated Cu(I), and the CusB site represents the first such structure to be described for a metalloprotein.

**2.4.3 Assignment of the metal-chelating ligands.** To identify candidates for the 3 metal-coordinating methionines detected from the EXAFS data, the conservation of the methionines in CusB was examined. From a BLAST search with the mature CusB sequence, the top 51 sequences (considering only one sequence from each genus) were selected for alignment. The alignment, generated with ClustalW using the default parameters, shows that of the 9 methionines in the mature sequence of CusB, 4 methionines (M21, M36, M38 and M283) are well-conserved in these proteins (Appendix

B). Methionine is always found at position 21, with one exception where it is histidine. Position 36 is always a methionine, except for one occurrence where it is an aspartate. Position 38 is always conserved as a methionine. Position 283 is usually found as methionine (47 out of 52 sequences) but is also found as a leucine, threonine, or alanine. Furthermore, in more extensive alignments (data not shown) methionines 21, 36 and 38 are primarily conserved in the periplasmic proteins of putative monovalent metal resistance systems, while M283 is conserved among periplasmic proteins exporting a variety of substrates. The other methionine positions, 162, 199, 213, 296, and 370, show much greater variability in the homologs and do not consistently have the appropriate properties for metal coordination. These positions are usually occupied by hydrophobic residues. Therefore, of the methionines in CusB, three of the four well-conserved methionines are likely candidates for the metal-coordinating methionines.

**2.4.4 *Ag(I)* affinity of conserved methionine mutants in vitro.** To identify which three of the four methionines are involved in metal binding, ITC was used to determine the ability of the four individual CusB mutants M21I, M36I, M38I and M283I to bind Ag(I) *in vitro* (Figure 2.3A-D). CusB M21I showed a 10-fold reduction in the binding affinity for Ag(I) as compared to wild-type CusB, with dissociation constant of 0.2  $\mu$ M. CusB M36I and M38I showed no specific binding to Ag(I). The affinity of CusB M283I for Ag(I) was same as wild-type, with a dissociation constant of 20 nM. Thus, the most significant effects in metal binding affinity are seen for CusB variants M36I and M38I, with a more modest decrease in affinity seen for CusB M21I.

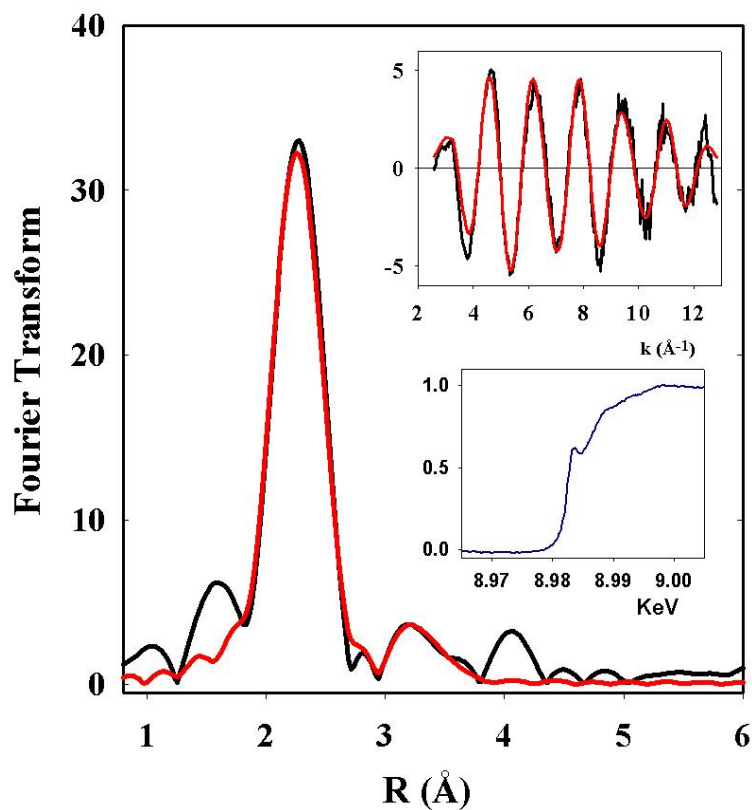


**FIGURE 2.2** EXAFS data for CusB-Cu(I). Experimental (black) and simulated (red) Fourier transforms and EXAFS (top inset) for CusB-Cu(I). X-ray absorption edge intensity of 8983 eV is diagnostic of 3-coordinate geometry (bottom inset).

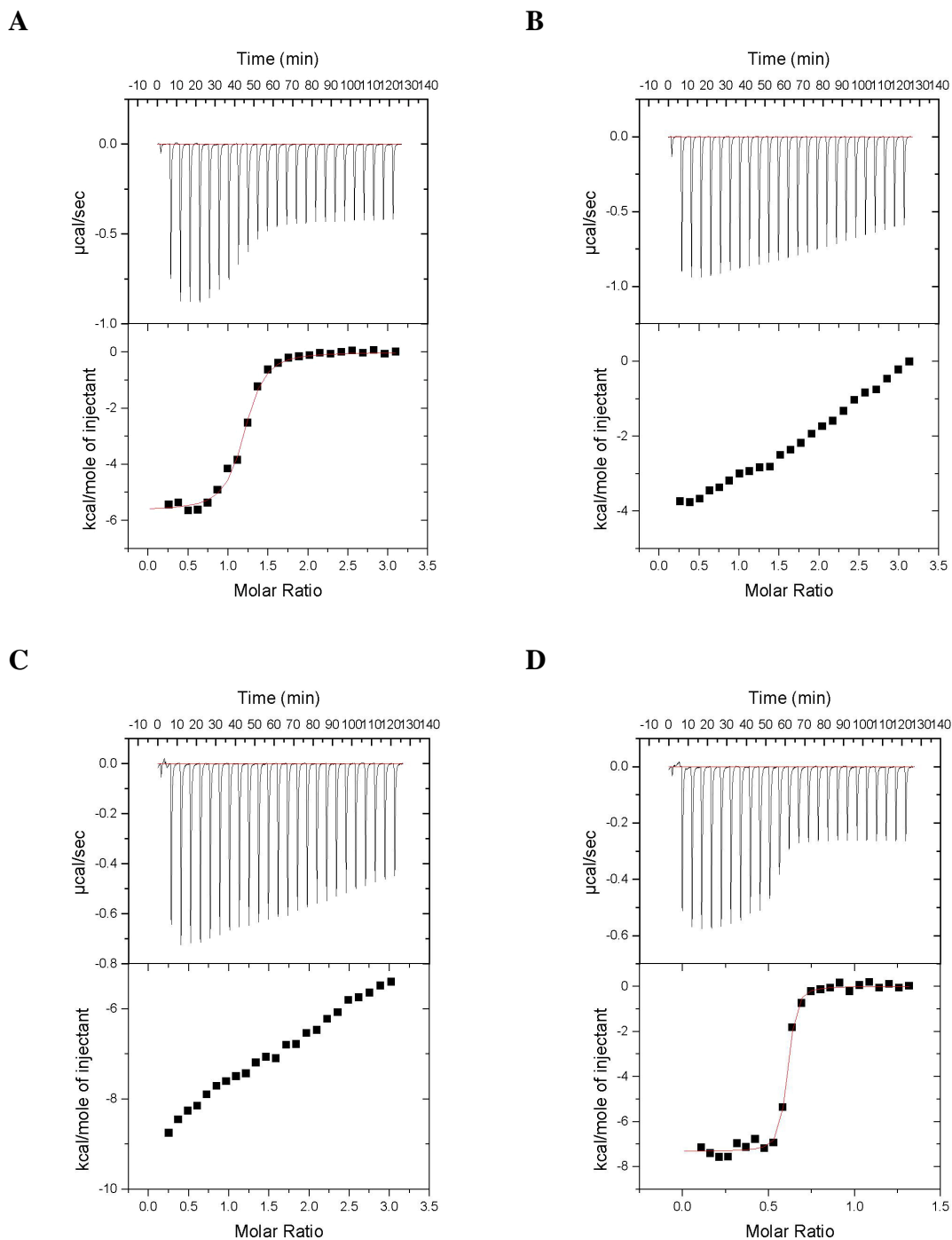


**FIGURE 2.3** ITC data for titration of CusB variants with  $\text{AgNO}_3$ . Experimental conditions were similar to those described for wild-type CusB. *Top*, raw data. *Bottom*, plot of integrated heats versus  $\text{Ag(I)}/\text{CusB}$  ratio. The solid line represents the best fit for a one-site binding model. CusB (A) M21I; (B) M36I; (C) M38I; and (D) M283I.

**2.4.5 Conserved methionines are crucial for metal resistance.** To test whether metal binding by CusB plays a functional role in metal resistance, we examined the ability of *E. coli* cells containing the individual CusB variants M21I, M36I, M38I and M283I to survive under elevated concentrations of copper. Cells containing each of the CusB variants were compared with wild-type CusB for their growth ability in copper-rich environments (Table 2.1), in a background where the chromosomal copies of *cusB* and the multicopper oxidase *cueO* have been deleted. The latter deletion has been shown previously to be required to observe a copper-sensitive phenotype under aerobic conditions (Franke et al., 2001; Franke et al., 2003). Cells were either pre-induced to express CusB before subjecting them to copper stress, (set ‘a’, Table 2.1), or were induced for CusB expression at the same time as they were exposed to the copper-containing media (set ‘b’, Table 2.1) as described in the Experimental Procedures. The results obtained from these two sets of experiments are similar. Cells containing wild-type CusB or each of the variants grow normally up to 0.5 mM CuCl<sub>2</sub> concentration. When CusB expression was induced before the cells were subjected to metal stress (set ‘a’), all the cells expressing CusB variants showed copper sensitivity with mucoid colonies by 1.0 mM CuCl<sub>2</sub> concentration. For the cells that were not pre-induced to express CusB (set ‘b’), at 1.0 mM CuCl<sub>2</sub> the cells with CusB variants M21I, M36I, and M38I did not show growth, cells with the CusB M283I variation showed diminished growth, and the cells with wild-type CusB were not inhibited by these concentrations of copper. Although the mutation of M283 lowered the resistance of cells compared to the wild type, the CusB M283 variant could survive higher copper concentrations compared

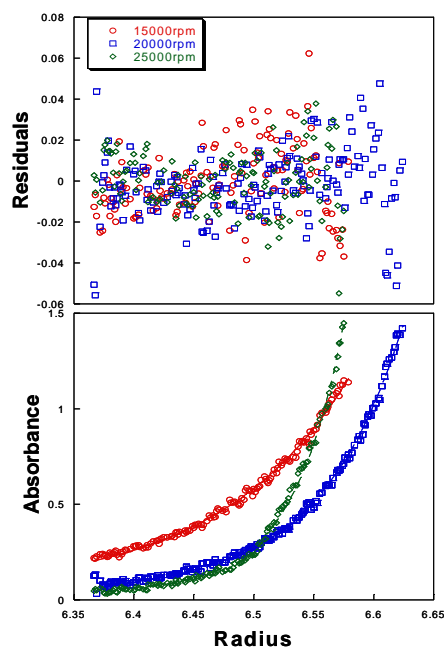
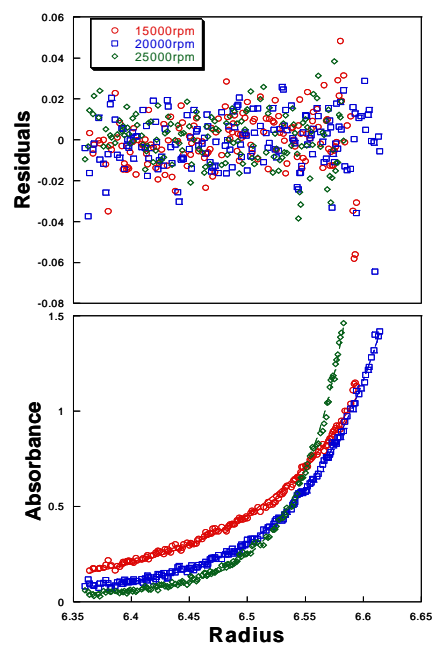
to the other three variants. The mutations of CusB methionines 21, 36 and 38 to isoleucine decreased the tolerance of the cells to copper comparable to the *cusB* deletion, suggesting that these methionines play an essential role in metal resistance.

**2.4.6 *CusB is monomeric in solution.*** The periplasmic proteins clearly function in the cell as part of a multimeric protein complex, though it is not known whether the periplasmic protein itself forms a higher order species. To determine the oligomeric state of CusB *in vitro* in the presence and absence of substrate, we performed sedimentation equilibrium analysis. From this technique the molecular mass of the protein species can be determined in a shape-independent manner. Data from three different concentrations of protein, 5  $\mu\text{M}$ , 9  $\mu\text{M}$ , and 14  $\mu\text{M}$ , with and without Ag(I), were fit well with a single ideal species model at all speeds, with residuals in the acceptable range (Data for 9  $\mu\text{M}$  protein concentration shown in Figure 2.4. Data for 5  $\mu\text{M}$  and 14  $\mu\text{M}$  protein concentrations are not shown). From these experiments, the molecular masses of apo-CusB and CusB-Ag(I) were predicted to be ~43 kDa, consistent with the calculated value of 43.8 kDa. These results indicate that CusB is monomeric in solution, similar to the isolated periplasmic proteins from the HAE family of RND efflux systems (Higgins et al., 2004; Zgurskaya and Nikaido, 1999a). Additionally, these data show that the oligomeric state of CusB does not change in the absence and presence of metal.

**TABLE 2.1** Growth behavior of *CusB* wild-type and variants on agar plates containing various concentrations of  $\text{CuCl}_2$

	$\text{CuCl}_2$ (mM)											
	0.0		0.5		0.75		1.0		1.25		1.5	
	a	b	a	b	a	b	a	b	a	b	a	b
complementing gene <i>in trans</i>	++	++	++	++	++	++	++	++	++	++	++	++
Wild type <i>cusB</i>	++	++	++	++	++	++	++	++	++	++	++	++
<i>cusB</i> (M21I)	++	++	++	++	++	++	++	++	++	++	++	++
<i>cusB</i> (M36I)	++	++	++	++	++	++	++	++	++	++	++	++
<i>cusB</i> (M38I)	++	++	++	++	++	++	++	++	++	++	++	++
<i>cusB</i> (M283I)	++	++	++	++	++	++	++	++	++	++	++	++
no <i>cusB</i> (pASK-IBA3)	++	++	++	++	++	++	++	++	++	++	++	++

++, wild-type growth; +, inhibited growth; ++m, growth with mucoid appearance; +m, inhibited growth with mucoid appearance; 0, no growth; n/d, not determined

**A****B**

**FIGURE 2.4** Sedimentation equilibrium analysis of (A) apo-CusB and (B) CusB-Ag(I). *Bottom panels* show data points and curve fits for protein at a concentration of approximately 9  $\mu\text{M}$  ( $A_{280}=0.43$ ) at three different speeds of ( $\circ$ ) 15000, ( $\square$ ) 20000 and ( $\diamond$ ) 25000 rpm with scans at 280 nm. *Top panels* show the residuals left when subtracting the calculated values from the measured points.

**2.4.7 *Ag(I) binding causes a conformational change.*** The structural properties of CusB in the apo- and Ag(I)-bound states were further analyzed using analytical gel filtration chromatography. Elution volumes from a gel filtration column can determine the relative molecular weight of a species as compared to globular calibration proteins. However, unlike sedimentation equilibrium where molecular weight determination is independent of protein shape, analytical gel filtration retention volumes, and in turn the molecular weight calculation, can be significantly affected by the shape of the protein. Based on homology to two periplasmic proteins from the HAE family of RND systems for which structures have been determined (Akama et al., 2004b; Higgins et al., 2004; Mikolosko et al., 2006), CusB is expected to have a non-globular, elongated structure. Figure 2.5 shows the elution profiles of CusB in both the apo and Ag(I)-loaded forms. As expected, both apo and metal-bound CusB elute from the column with less volume than expected for a 43 kDa globular protein, which likely reflects an elongated shape. However, there is a marked difference in the elution volumes between apo-CusB and CusB-Ag(I). The apo-protein elutes from the column at a retention volume of 14.1 mL whereas CusB-Ag(I) elutes at a retention volume of 14.6 mL. As the analytical ultracentrifugation data clearly indicate that apo-CusB and CusB-Ag(I) are monomeric, the change in elution volume is indicative of a conformational change. The decrease in retention volume of CusB-Ag(I) compared to apo-CusB suggests that CusB undergoes a conformational change upon binding silver to a more globular state.

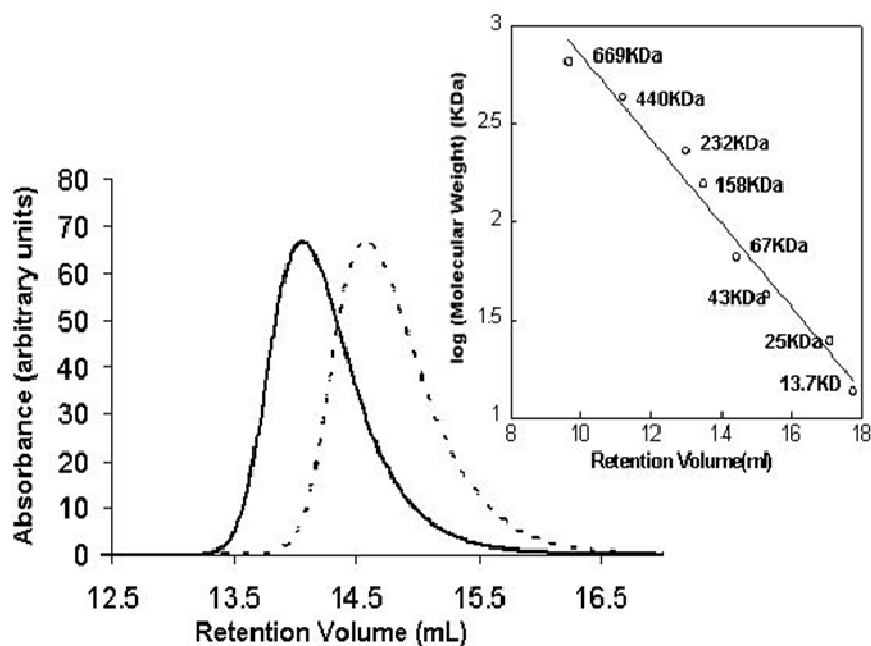


**FIGURE 2.5** Analytical gel filtration on a Superdex 200 10/300GL analytical column of apo- and Ag(I)-bound CusB in 50 mM sodium phosphate, pH 7.0. Solid line represents the apo-CusB, which eluted at approximately 14.1 mL and the dashed line represents CusB-Ag(I) which eluted at approximately 14.6 mL. Absorbance values were normalized. Inset plot shows the relative retention volumes of protein molecular weight standards.

## 2.5 DISCUSSION

We have demonstrated that the periplasmic protein CusB is a metal binding protein and have identified the three residues that are most likely to play a role in metal coordination. Furthermore, we have shown that defects in metal binding result in a loss of metal resistance *in vivo*, suggesting that CusB metal binding plays an important role in metal resistance in this system. Substrate binding by a periplasmic protein has not been previously demonstrated in an RND efflux system. In two distantly related non-RND tripartite export systems where the inner membrane protein belongs to either the major facilitator superfamily (MFS) or the ATP-binding cassette (ABC) superfamily, the periplasmic portions of these systems have been shown to bind substrate (Borges-Walmsley et al., 2003; Thanabalu et al., 1998). However, in RND efflux systems, the only reported substrate binding site is in the inner membrane protein (Murakami et al., 2006).

Substrate binding by CusB suggests that it could have a direct role in substrate efflux and that it does not simply serve as a passive anchor required to link the inner and the outer membrane components. It is possible that the substrate bound by CusB is subsequently exported from the cell. Studies from several other systems have demonstrated that substrates that originate in the periplasm can be exported. Genetic evidence suggests that in the case of Cu(I) and Ag(I) transport in *E. coli*, the inner membrane P-type ATPase CopA is likely responsible for transport across the inner membrane, and that the CusCFBA system does not serve a redundant function to CopA

(Grass and Rensing, 2001). Thus, the most likely origin of substrate transported by CusCFBA is from the periplasm. Uptake of a metal substrate from the periplasm is supported by studies of the divalent metal export system CzcCBA from *Cupriavidus* (formerly *Ralstonia*) *metallidurans*. In this case an additional system that transports Co(II) from the cytoplasm to the periplasm was absolutely required for CzcCBA function, implying that CzcCBA takes up its substrate from the periplasm (Munkelt et al., 2004). In addition, CzcCBA was rendered ineffective in the absence of CadA and ZntA P-type ATPases, which translocate Cd(II) and Zn(II) from the cytoplasm to the periplasm (Munkelt et al., 2004). Other systems similarly suggest a periplasmic mode of drug entry (Aires and Nikaido, 2005; Nikaido et al., 1998).

We have demonstrated that substrate binding is linked to a conformational change to a more compact state. Conformational changes in periplasmic proteins from other systems have been previously proposed. Four conformations of AcrA were captured in the asymmetric unit of the AcrA crystal which differed in the position of the  $\alpha$ -helical domain with respect to the lipoyl domain (Mikolosko et al., 2006). Additionally, using EPR spectroscopy, AcrA was reported to undergo a conformational rearrangement triggered by pH changes (Ip et al., 2003). Molecular dynamics simulations also suggest inter-domain motions of the periplasmic protein MexA (Vaccaro et al., 2006). In all these studies, the suggested consequence of the conformational flexibility is in the association of the three components and the opening or closing of the inner and outer membrane proteins of the tripartite complex.

From these studies, we conclude that the periplasmic protein CusB of the CusCFBA complex has a substrate-linked role beyond that of a scaffolding protein bridging the inner and outer membrane components. It is possible that metal binding to CusB induces a conformational change to open the outer membrane protein channel, or CusB may hand off metal to the inner membrane complex for export. In previous studies of RND efflux systems, substrate binding has only been reported for the inner membrane protein. It is possible that in the Cu(I)/Ag(I) efflux system, where a very specific substrate is exported, substrate selection by the periplasmic component could provide the needed specificity.

## CHAPTER 3

### **DIRECT METAL TRANSFER BETWEEN THE PERIPLASMIC COMPONENTS OF THE CUSCFBA CU(I)/AG(I) EFFLUX SYSTEM ESTABLISHES A ROLE FOR CUSF AS A METALLOCHAPERONE**

In this chapter, I report our results from the interaction studies between the periplasmic components CusB and CusF of the CusCFBA system. I collected and analyzed the data in this chapter, with assistance from Ninian Blackburn in the XAS data collection at SSRL.

#### **3.1 ABSTRACT**

The potential toxicity of excess intracellular copper has led to mechanisms to carefully regulate copper concentrations. In *E. coli*, a tripartite system consisting of CusCBA is expected to span the inner and outer membrane to pump Cu(I) and Ag(I) from the periplasm to the extracellular space. The fourth component of this system, CusF, is a small periplasmic metal binding protein. We show here using isothermal titration calorimetry (ITC) that the interaction of CusF and CusB is metal-dependent, and only occurs when one of the proteins is in the metal-bound state and the other is in the apo state. In the absence of metal, or if both proteins are occupied with metal, no interactions are detected. Metal transfer between CusF and CusB was demonstrated using X-ray

absorption spectroscopy (XAS). As both CusF and CusB use methionine residues for metal coordination, the metal sites of CusF and CusB were distinguished in the XAS experiments by incorporation of selenomethionine into CusF. The results of the XAS experiments on CusF/CusB/Cu(I) samples show that Cu(I) can be reversibly transferred between CusF and CusB with an approximately 50% end distribution between the two proteins. The demonstration of direct transfer of metal between CusF and CusB is consistent with the role of CusF as a metallochaperone, and thus CusF is the first copper chaperone to be reported for proteins involved in metal efflux.

### 3.2 INTRODUCTION

Transition metals are a necessary component of living cells. Due to their redox capability, they participate in numerous enzymatic processes (Nelson, 1999). As important as they are, their ability to undergo redox transition deems them commensurably toxic when present in excess of the required concentration. Additionally, the strong bonds that transition metals form with functional groups such as thiolates and imidazolium nitrogens in proteins can account for some of their toxicity (Wong et al., 2004). Thus, the dual nature of transition metals continually challenges cells to maintain a delicate concentration balance within the cellular milieu.

To aid in the homeostatic balance of essential but toxic metals, cells have evolved a complex network of metal trafficking pathways (Luk et al., 2003). Much of the current state of knowledge regarding these pathways has emerged from studies on copper. Copper exists as a cofactor in more than 30 enzymes in a human body (Lu et al., 1999). Copper has high affinity for ligands commonly present in proteins, and thus could potentially displace other metal cofactors from their natural ligands. In addition, the redox cycling between Cu(I) and Cu(II) can catalyze the production of highly toxic hydroxyl radicals, which can damage lipids, proteins, DNA and other biomolecules (Harrison et al., 2000). An effective means of preventing the cytotoxic effects of copper is to keep it complexed (Singleton and Le Brun, 2007). Free Cu(I) ion has indeed been reported to be very low ( $10^{-18}$  M in an unstressed yeast cell) implying that there is no free metal ion pool inside the cell (Rae et al., 1999).

Until recently, it was not known how copper enzymes obtained their essential cofactors in this apparent vacuum of free copper (Field et al., 2002). With the discovery of Menkes (Davies, 1993; Hamer, 1993), Wilson (Bull and Cox, 1994; Solioz and Vulpe, 1996) and Lou Gehrig's (Corson et al., 1998) diseases, the investigation of the molecular bases of copper metabolism gained greater attention. The molecular details of intracellular trafficking began to emerge with the discovery of copper handling accessory proteins, called copper chaperones (Culotta et al., 1997; Pufahl et al., 1997) or metallochaperones (Rosenzweig, 2001). They are defined as proteins that escort the metal to specific copper-requiring targets in the cell (Pufahl et al., 1997). Not only do they protect the metal ion from the housekeeping scavenging molecules such as glutathione and metallothioneins but also protect the cell from the reactive nature of the metal ion (Elam et al., 2002). Although several copper chaperones have been identified in eukaryotes (O'Halloran and Culotta, 2000), all of them target proteins that inevitably require copper for their activity. No copper chaperones participating in efflux systems have been reported to date. Copper carriers that are identified in some other copper resistance systems have only been postulated to act as chaperones with no clear demonstration of the chaperone function (Djoko et al., 2007; Hussain et al., 2007). Recently a chaperone was identified in the detoxification pump of metalloid arsenite in *E. coli* (Lin et al., 2006).

The CusCFBA system is a Cu(I)/Ag(I) efflux system that is expected to form a complex spanning the inner and outer membranes of *E. coli*. It is thought to pump Cu(I) and Ag(I) from the periplasmic space to the extracellular space, using the proton gradient

across the inner membrane as an energy source. The CusCFBA efflux system consists of CusA, the inner membrane proton/substrate transporter of the resistance-nodulation-division (RND)-type family, CusC, the outer membrane protein, and two periplasmic proteins, CusB and CusF. CusB is a member of the periplasmic adaptor protein or membrane fusion protein (MFP) family, which likely stabilizes the CusCBA complex, and metal binding by this protein serves an essential role in Cus-mediated resistance (Bagai et al., 2007; Franke et al., 2003). The fourth component, CusF, is a small periplasmic metal binding protein (Franke et al., 2003; Kittleson et al., 2006) of unknown function. While CusC, CusB and CusA are homologous to the three components of well-characterized multidrug resistance systems, e.g. AcrAB-TolC, CusF has homologs only in putative monovalent metal resistance systems. It has been postulated that CusF could act as a metallochaperone to deliver metal to the Cus system for removal from the periplasm, or it could potentially serve a role as a metal dependent regulator of the CusCBA complex (Loftin et al., 2005).

Here, we demonstrate that CusF and CusB directly interact *in vitro* in a metal-dependent fashion using ITC analysis. XAS was used to determine the Cu(I) environment in samples containing CusF, CusB and Cu(I). These experiments show that Cu(I) can be transferred between CusF and CusB regardless of whether CusF or CusB was originally in the metal-bound form. An increase in the Cu-Se bond length in CusF was observed in CusF/CusB/Cu(I) mixtures. Direct metal transfer between the two proteins was demonstrated by ITC experiments conducted between proteins of the Cus system and a homologous silver binding protein, SilF. The results of these experiments

are consistent with a role for CusF as a metallochaperone for the CusCFBA Cu(I)/Ag(I) efflux system.

### 3.3 MATERIALS AND METHODS

**3.3.1 Protein expression and purification.** The expression and purification of CusF and CusB in *Escherichia coli* was performed as described earlier (Bagai et al., 2007; Loftin et al., 2005). For EXAFS studies, selenomethionine-labeled CusF (SeM-CusF) was produced from *E. coli* BL21 ( $\lambda$ DE3) cells containing the pASKIBA3/*cusF* plasmid grown in the M9 minimal medium supplemented with L-selenomethionine, leucine, isoleucine and valine at a concentration of 50 mg/L and lysine, phenylalanine and threonine at a concentration of 100 mg/L (Doublié, 1997). All the buffers used for the purification of SeM-CusF contained 10 mM dithiothreitol.

**3.3.2 Isothermal titration calorimetry.** ITC measurements were performed on a Microcal VP-ITC Microcalorimeter (Northampton, MA, USA), typically at 25 °C. Both apo and Ag(I) bound forms of CusB, CusF and SilF were extensively dialyzed in 50 mM cacodylate, pH 7.0. The titrand and the titrant were thoroughly degassed in a ThermoVac apparatus (Microcal). For a titration experiment, approximately 1.5 mL of titrand protein was placed in a reaction cell and injected with titrant protein over 20 seconds. The first injection was 2  $\mu$ L, and all subsequent injections were 10  $\mu$ L. A total of 25 injections were made with a 5-minute interval between each injection. In order to ensure adequate mixing of the two proteins, the reaction cell was continuously stirred at 300 rpm. The heat due to dilution, mechanical effects and other non-specific effects were accounted for by averaging the last three points of titration and subtracting that value from all data

points (Kittleson et al., 2006). In order to investigate the metal dependence of interaction, a series of four different experiments were conducted. These included the titrations of apo-CusF into apo-CusB, Ag(I) bound CusF (Ag(I)-CusF) into apo-CusB, Ag(I)-CusF into Ag(I)-CusB and Ag(I)-CusB into apo-CusF. For the first experiment, approximately 20  $\mu\text{M}$  apo-CusB was titrated with 375  $\mu\text{M}$  apo-CusF. 375  $\mu\text{M}$  Ag(I)-CusF was used in second and third titration experiments. The concentrations of apo and Ag(I)-bound CusB were 24.0  $\mu\text{M}$  and 23.0  $\mu\text{M}$  respectively. For Ag(I)-CusB into apo-CusF titration, 142  $\mu\text{M}$  Ag(I)-CusB was injected into 17  $\mu\text{M}$  apo-CusF. To determine the affinity of SilF for Ag(I), 36  $\mu\text{M}$  apo-SilF was titrated with 300  $\mu\text{M}$   $\text{AgNO}_3$  in 50 mM cacodylate, pH 7.0. Interaction of either CusF or CusB with SilF was tested by titrating 21  $\mu\text{M}$  apo-CusB with 170  $\mu\text{M}$  Ag(I)-SilF, 29  $\mu\text{M}$  apo-CusF with 170  $\mu\text{M}$  Ag(I)-SilF and 30  $\mu\text{M}$  apo-SilF with 275  $\mu\text{M}$  Ag(I)-CusF in 50 mM cacodylate, pH 7.0. As controls, each protein was titrated into buffer, or buffer was titrated into each protein to determine the heat changes due to protein dilution. A single-site binding model was fitted to the data using the Origin software package (MicroCal). The software uses a non-linear least-squares algorithm and the concentrations of the titrant and the titrand to fit the enthalpy change per injection to an equilibrium binding equation. The binding enthalpy change  $\Delta H$ , association constant  $K_a$ , and the binding stoichiometry  $n$  were permitted to float during the least-squares minimization process and taken as the best-fit values.

**3.3.3.1 Extended X-ray absorption fine structure spectroscopy (EXAFS).** Samples for EXAFS were prepared in an anaerobic chamber. CusB and SeM-CusF were first

dialyzed outside in 20 mM N-(2-Acetamido)-2-aminoethanesulfonic Acid (ACES), pH 7.0. Proteins were then argon purged and transferred to the anaerobic chamber. Ascorbate solution buffered at pH 7.0, made inside an anaerobic chamber was added to the argon-purged proteins to a final concentration of 50 mM.  $\text{CuCl}_2$  was then added such that the final copper concentration was 25% in excess of the protein concentration. The proteins were dialyzed against 20 mM ACES, 10 mM ascorbate, pH 7.0, to remove unbound copper. The final concentration of protein was determined using the Bradford assay (Bradford, 1976) (Biorad). For EXAFS sample preparation, proteins were mixed with 20-30% ethylene glycol, transferred to EXAFS vials and flash frozen in liquid nitrogen. EXAFS experiments were conducted on four different samples. These were SeM-CusF in apo- and Cu(I)-bound forms, at concentrations of 380  $\mu\text{M}$  and 200  $\mu\text{M}$ , respectively, Cu(I)-SeM-CusF mixed with apo-CusB and Cu(I)-CusB mixed with the apo-SeM-CusF. In the samples containing Cu(I)-SeM-CusF and apo-CusB, the final concentrations of both proteins were 110  $\mu\text{M}$ . In order to measure the kinetics of the metal transfer reaction, the mixtures of CusF and CusB were allowed to incubate before adding ethylene glycol and flash freezing for either 4, 14 or 34 minutes. For the sample containing Cu(I) bound CusB and apo-SeM-CusF, the final concentration of apo-SeM-CusF was 85  $\mu\text{M}$  and that of Cu(I)-CusB was 125  $\mu\text{M}$ .

**3.3.3.2 EXAFS data collection and analysis.** Cu K-edge (8.980 KeV) and Se K-edge (12.658 KeV) extended X-ray absorption fine structure (EXAFS) data for CusF and CusB were collected at the Stanford Synchrotron Radiation Laboratory operating at 3 GeV with

currents between 100 and 50 mA. All samples were measured on beam line 9-3 by use of a Si(220) monochromator and a Rh-coated mirror upstream of the monochromator with a 13 KeV (Cu) or 15 KeV (Se) energy cutoff to reject harmonics. A second Rh mirror downstream of the monochromator was used to focus the beam. Data were collected in fluorescence mode on a high-count-rate Canberra 30-element Ge array detector with maximum count rates below 120 KHz. A 6  $\mu$  Z-1 metal oxide (Ni, As) filter and Soller slit assembly were placed in front of the detector to reduce the elastic scatter peak. Four to six scans of a sample containing only sample buffer (50 mM sodium phosphate, pH 7.2) were collected at each absorption edge, averaged, and subtracted from the averaged data for the protein samples to remove Z-1  $K_{\beta}$  fluorescence and produce a flat pre-edge baseline. This procedure allowed data with an excellent signal-to-noise ratio to be collected down to 100  $\mu$ M total copper in the sample. The samples (80  $\mu$ L) were measured as aqueous glasses (>20% ethylene glycol) at 10-15 K. Energy calibration was achieved by reference to the first inflection point of a copper metal foil (8980.3 eV) for Cu K-edges and a selenium metal foil (12658.0 eV) for Se K-edges, placed between the second and third ionization chamber. Data reduction and background subtraction were performed with the program modules of EXAFSPAK (George, 1990). Data from each detector channel were inspected for glitches or drop-outs before inclusion in the final average. Spectral simulation was carried out with the program EXCURVE 9.2 (Binsted et al., 1998; Binsted and Hasnain, 1996; Gurman et al., 1984; Gurman et al., 1986) as previously described (Blackburn et al., 2000).

## 3.4 RESULTS

**3.4.1 *CusF and CusB interact only in the presence of metals.*** To determine if CusF and CusB are interacting partners in the metal efflux process mediated by the CusCFBA system, we looked for evidence of an interaction between the two proteins *in vitro* using isothermal titration calorimetry (ITC). ITC detects changes in the heat absorbed/released during a binding event (i.e. the binding enthalpy change). The titration of Ag(I)-CusF into the solution of apo-CusB (Figure 3.1(A)) and the reverse titration of Ag(I)-CusB into apo-CusF (Figure 3.1(B)) showed similar changes in enthalpy. This enthalpy change was not observed in the control titrations of Ag(I)-CusF into buffer or buffer into apo-CusB (data not shown). Additionally, no change in the heat absorbed or released was detected upon titration of apo-CusF into apo-CusB (Figure 3.1(C)) demonstrating that the observed binding depended on the presence of metal ion. Furthermore, titration of Ag(I)-CusF into Ag(I)-CusB also showed no change in enthalpy (Figure 3.1(D)), indicating that an enthalpy change for this system requires one of the two proteins to exist in the apo-form. In the above experiments, the enthalpy changes could be due to direct protein-protein interactions, or could be due to metal release from one protein accompanied by binding by the other, or a combination of these. To account for the macroscopic enthalpy changes and discern the molecular basis of the reaction in our system, X-ray absorption spectroscopy (XAS) studies were conducted.

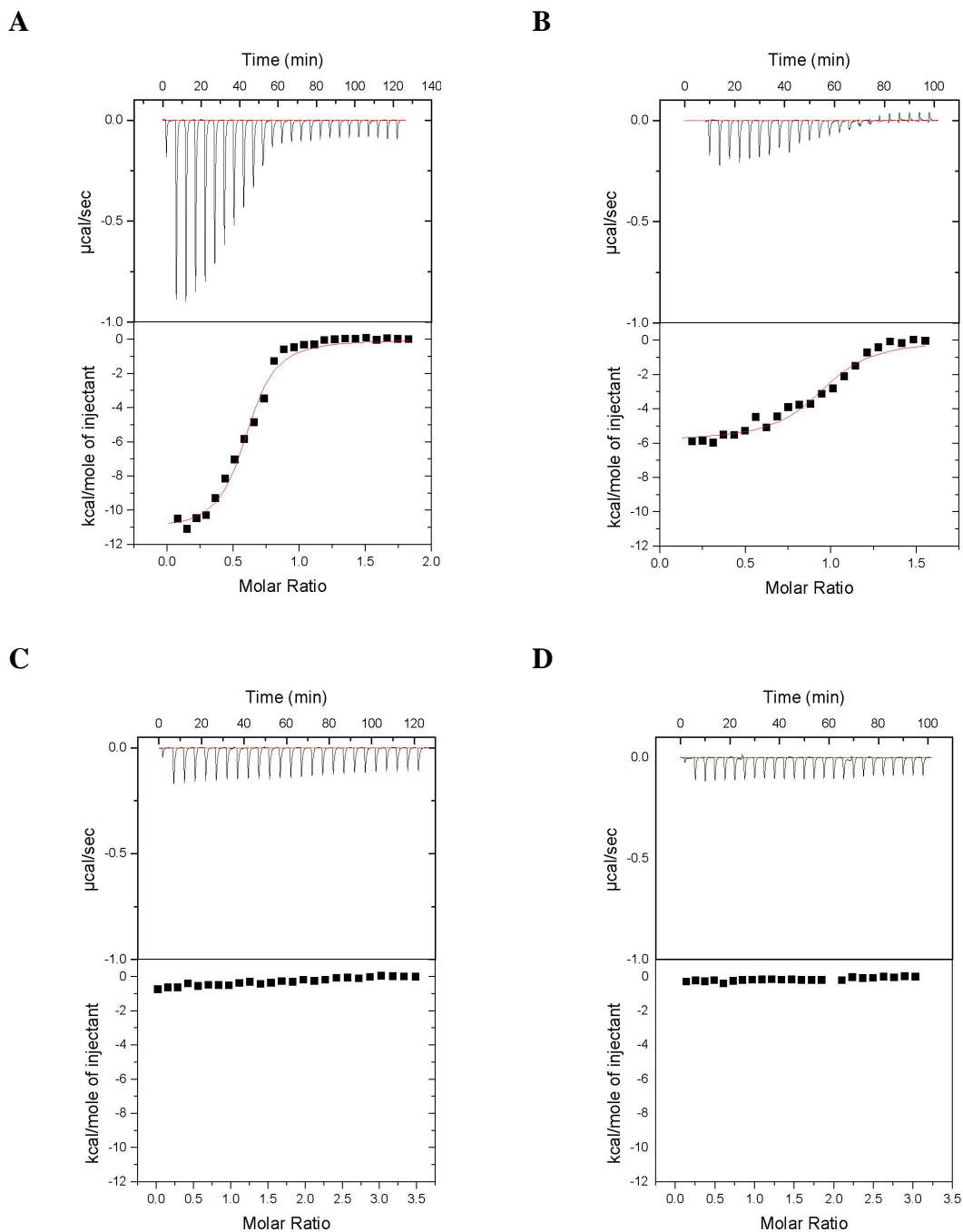


**FIGURE 3.1** ITC data for titration of (A) 375  $\mu\text{M}$  Ag(I)-CusF into 24  $\mu\text{M}$  apo-CusB; (B) 142  $\mu\text{M}$  Ag(I)-CusB into 17  $\mu\text{M}$  apo-CusF; (C) 375  $\mu\text{M}$  apo-CusF into 20  $\mu\text{M}$  apo-CusB; (D) 375  $\mu\text{M}$  Ag(I)-CusF into 23  $\mu\text{M}$  Ag(I)-CusB in 50 mM cacodylate, pH 7.0. *Top*, raw data. *Bottom*, plot of integrated heats versus titrant/titrant ratio. The solid line represents the best fit for a one-site binding model.

**3.4.2 EXAFS analysis of Selenomethionine-labeled CusF.** The metal environments of the individual CusF and CusB proteins have been previously determined (Bagai et al., 2007; Loftin et al., 2007). Both proteins have 3-coordinate sites, with CusF having 2 sulfur ligands from methionines and 1 nitrogen ligand from a histidine (Loftin et al., 2007) and CusB having 3 sulfur ligands from methionines (Bagai et al., 2007). To determine the ligand environment of Cu(I) in samples containing both CusB and CusF, XAS analysis was performed. XAS is a spectroscopic technique that provides both electronic structure and atomic resolution molecular structure information, acting as a bridge between molecular and electronic structure techniques. To distinguish the ligands arising from the methionines of one protein from the other, cells expressing CusF were grown in the minimal medium supplemented with selenomethionine, such that selenomethionine (SeM) was incorporated into CusF in place of methionine. An additional advantage to SeM labeling is that the binding site can be probed prior to metal binding via Se XAS, enabling tracking of the movement of metal ion in the protein mixtures.

Figure 3.2(A) shows the Fourier Transform (FT) and Extended X-ray Absorption Fine Structure (EXAFS) for apo-SeM-CusF from data measured at the Se edge. The spectrum consists of a sharp intense FT peak around 2 Å corresponding to the methyl and methylene C atoms covalently bonded to SeM. This spectrum is typical for an unligated SeM side chain with the Se-C distance of 1.955 Å. However, additional features are present in the FT around 3 Å. The 3 Å feature is well-fit by a Se-Se interaction and suggests that each of the two Se atoms in the copper binding site experiences scattering off the neighboring Se at 2.84 Å.

The Se EXAFS spectrum changes dramatically for Cu(I)-SeM-CusF. While Se-C scattering is still observed at 1.964 Å, a new intense and well-resolved feature is observed in the FT corresponding to a Se-Cu interaction at 2.407 Å (Figure 3.2(B)). Because CusF contains four Met ligands and only two of these are ligands to Cu(I), the shell occupancy of Se-Cu scattering is expected to be 0.5 Se-Cu interactions per total Se in the protein. Simulations using this value of  $N_{\text{Se-Cu}}$  result in a Debye-Waller (DW) factor of 0.005 Å<sup>2</sup>, which is entirely appropriate for a first-shell Se ligand to Cu(I). Of additional interest is the shoulder observed on the high-R side of the Se-Cu peak around 3 Å. Like apo-protein, this feature can be simulated by a Se-Se interaction at 2.85 Å, which implies that the relative position of the Se atoms in the metal binding site does not change when Cu(I) binds, and that the site is therefore pre-formed for metal binding.

The metal binding site was further studied using Cu EXAFS. Figure 3.2(C) shows experimental and simulated data for the Cu EXAFS of Cu(I)-SeM-CusF. Again, since Cu(I) is expected to be coordinated by one N (H36) and two SeM (M47, M49) (Loftin et al., 2007), one might expect a similar pattern of transform peaks as for the Se edge. In actuality, the Cu EXAFS shows an unresolved first-shell peak in the transform which can nevertheless be simulated by 2 Cu-Se and 1 Cu-His (including multiple scattering from outer-shell C $\beta$ , and C $\gamma$ /N $\delta$  atoms of the imidazole ring from the nearby tryptophan). As expected, the Cu-Se distance was found to be identical to that determined from the Se EXAFS (2.406 Å), although curiously the Cu-Se DW factor was higher (0.009 vs. 0.005 Å<sup>2</sup>). When the Cu-Se DW factor was set equal to its value determined from the Se EXAFS, the Cu-Se coordination number fell to 1.4. No easy

explanation exists for the discrepancy since incomplete Se labeling and/or substoichiometric Cu site occupancy should result in lower shell occupancy at the Cu edge. Nevertheless, the combination of Se and Cu EXAFS led to a consistent and unambiguous structural description of the metal binding site with Cu(I) bound by 1 His and 2 SeM ligands at 2.01 and 2.41 Å, respectively.

**3.4.3 Transfer of Cu(I) from CusF to CusB measured by EXAFS.** The addition of apo-CusB to a Cu(I)-SeM-CusF sample caused significant changes in the Se and Cu EXAFS spectra. Figures 3.3(A) and 3.3(B) show the changes at the Cu and Se edges, respectively, for a sample of Cu(I)-loaded SeM-CusF incubated with apo-CusB for 30 minutes before being transferred to the EXAFS cell and frozen. The most dramatic effects are seen in the FT of the Se EXAFS (Figure 3.3(B), 3.3(C)) where a significant decrease in the intensity of the Se-Cu peak is observed, while the intensity of the Se-C peak remains unchanged. Since CusF, but not CusB, is Se-labeled, the decrease in Se-Cu measured by Se EXAFS is the result of loss of Cu(I) specifically from the CusF binding site. For Se EXAFS analysis, the Se-Cu coordination number was allowed to vary, while its DW factor was held constant at  $0.005 \text{ Å}^2$ . Small variations in metrical parameters ( $R_{\text{Se-C}}$ ,  $R_{\text{Se-Cu}}$ ,  $R_{\text{Se-Se}}$ ) were permitted. The analysis led to excellent fits with 50 percent reduction in Se-Cu shell occupancy, a small increase ( $\sim 0.02 \text{ Å}$ ) in the Se-Cu bond length, but no difference in Se-C or Se-Se interactions. This result is entirely consistent with transfer of Cu(I) out of the Se environment and demonstrates the utility of SeM substitution coupled to Se-XAS analysis in observing metal transfer reactivity.

Analysis of the Cu EXAFS provided an additional probe of metal transfer. In previous work, we have reported that CusB binds Cu(I) in an all-S environment, with coordination to 3 methionine residues with Cu-S bond lengths of 2.28 -2.30 Å (Bagai et al., 2007). Copper transfer from CusF to CusB should therefore be accompanied by loss of Cu-N and Cu-Se (the ligands to CusF) and replacement by the Cu-S (Met) environment of CusB. Knowledge of the binding site environment of both donor and acceptor protein allowed us to set constraints on the coordination number as follows:

$$N_{\text{Cu-N}} = 0.5 * N_{\text{Cu-Se}}$$

$$N_{\text{Cu-S}} = 3 - 1.5 * N_{\text{Cu-Se}}$$

The data were analyzed by imposing these constraints, and allowing only the  $N_{\text{Cu-Se}}$  to vary. As before, small variations in distances were permitted. The result of these simulations is that the Cu-Se coordination number dropped by 50 percent, exactly equivalent to the change observed at the Se edge, while an appropriate increase in Cu-S at 2.288 Å was observed (Table 3.1). The Cu edge data are thus consistent with Cu(I) transfer into the all-S environment of the CusB protein, with a Cu-S distance equal to that obtained previously from studies on the fully reconstituted Cu(I)-CusB protein.

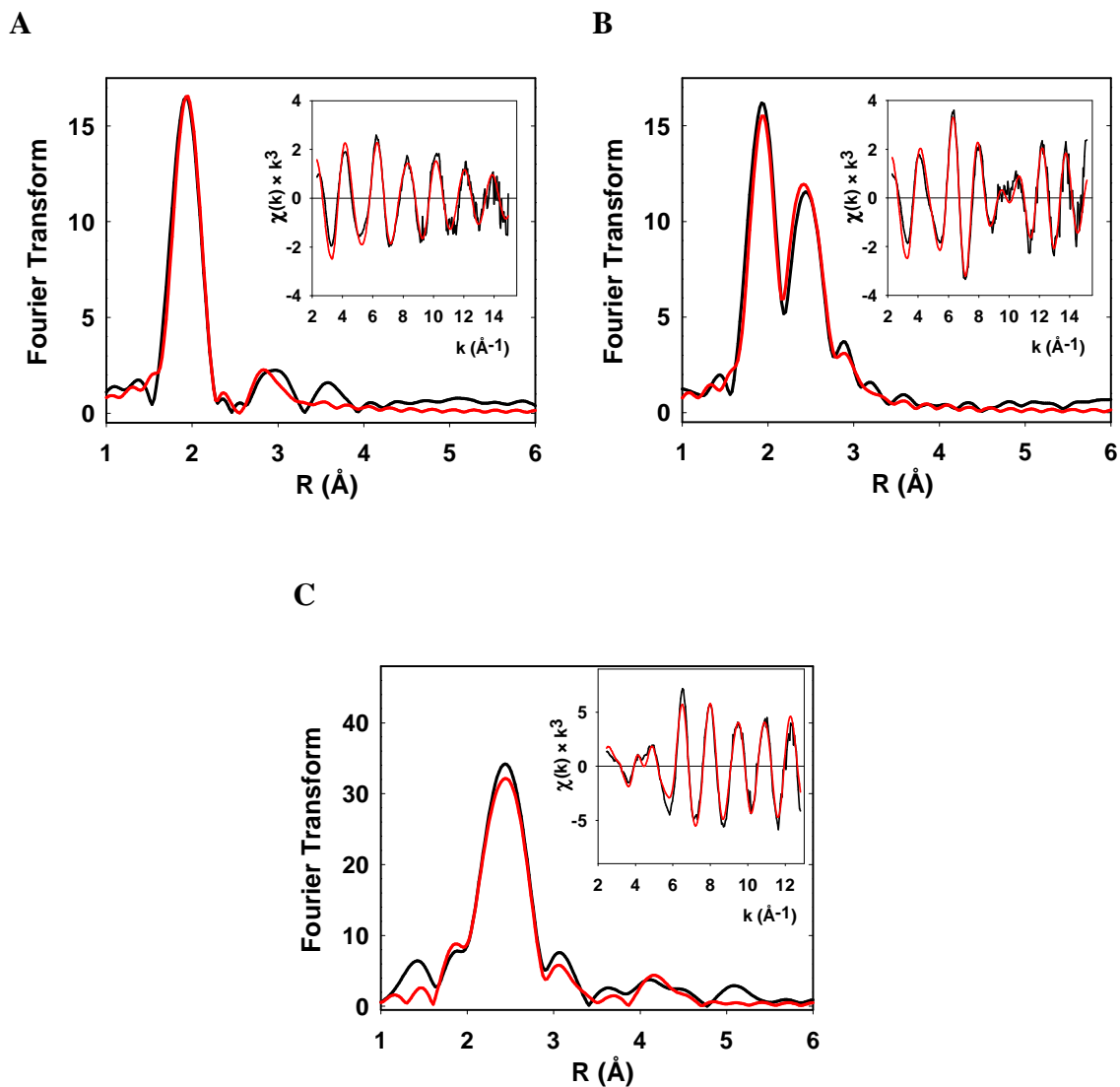


**FIGURE 3.2**(A) Se EXAFS of apo-SeM-CusF; (B) Se EXAFS of Cu(I)-loaded SeM-CusF; (C) Cu EXAFS of Cu(I)-loaded SeM-CusF. Experimental (black trace) versus simulated (red trace) Fourier transform and EXAFS (inset) using metrical parameters listed in Table 3.1.

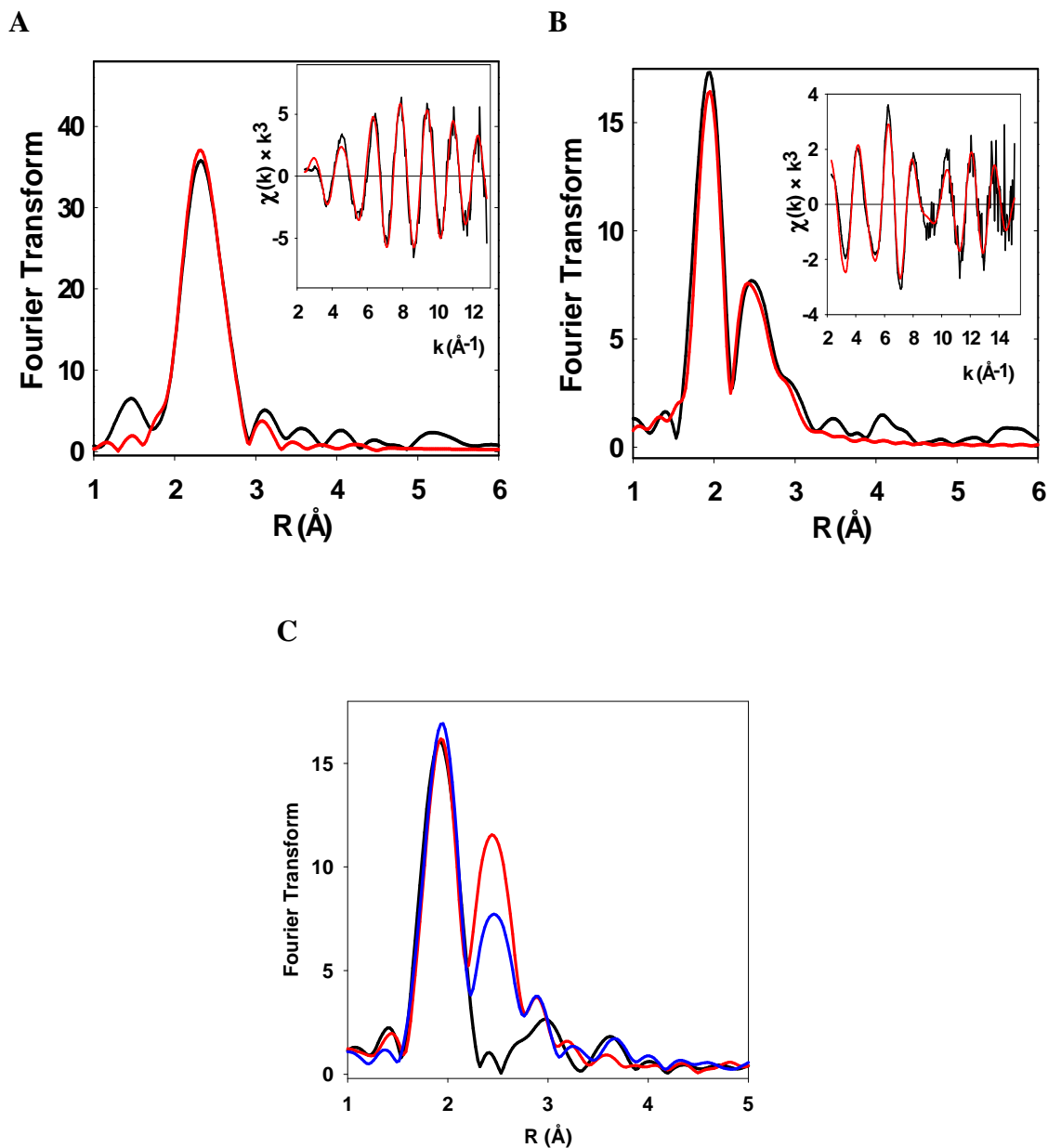


**FIGURE 3.3**(A) Cu EXAFS of Cu(I)-SeM-CusF mixed with apo-CusB and frozen after 34 minutes; (B) Se EXAFS of Cu(I)-SeM-CusF mixed with apo-CusB and frozen after 34 minutes. Experimental (black traces) versus simulated (red traces) FT and EXAFS (inset) using metrical parameters listed in Table 3.1; (C) Comparison of Se edge FT of SeM-CusF. Black: apo- protein, red: Cu(I)-loaded, blue: after transfer to CusB at 4 minutes.

<b>TABLE 3.1</b> Fits obtained to the EXAFS of CusF by curve-fitting using the program EXCURVE 9.2													
Sample/Fit	F <sup>a</sup>	C-N(His) <sup>b</sup>			Cu-Se			Cu-S					
		No <sup>c</sup>	R (Å) <sup>d</sup>	DW (Å <sup>2</sup> )	No <sup>c</sup>	R (Å) <sup>d</sup>	DW (Å <sup>2</sup> )	No <sup>c</sup>	R (Å) <sup>d</sup>	DW (Å <sup>2</sup> )			
<b>Cu-edge</b>													
Cu(I)-CusF	0.364	1	2.007	0.003	2.0	2.406	0.009						4.75
4 mins	0.336	0.48	2.053	0.003	0.96	2.425	0.005	1.57	2.288	0.009			5.07
14 mins	2.33	0.57	2.091	0.002	1.14	2.443	0.004	1.29	2.292	0.003			7.81
34 mins	0.444	0.49	2.079	0.003	0.99	2.422	0.005	1.52	2.276	0.010			5.32
<b>Se-edge</b>		Se-C(met)			Se-Cu			Se-Se					
apo-CusF	0.518	2.0	1.955	0.004				1.0	2.837	0.036			5.58
Cu(I)-CusF	0.545	2.0	1.964	0.005	0.5	2.407	0.005	1.0	2.848	0.030			5.98

4 mins		0.522		2.0	1.966	0.005		0.30	2.415	0.005		1.0	2.835	0.030	6.13
14 mins		0.548		2.0	1.963	0.006		0.26	2.433	0.004		1.0	2.836	0.029	5.62
34 mins		0.675		2.0	1.962	0.004		0.29	2.433	0.005		1.0	2.830	0.032	5.62
<b>Cu(I)-CusB + apo-SemCusF Se-edge</b>															
		0.880		2	1.964	0.005		0.3	2.433	0.005		1	2.85	0.029	5.98
<sup>a</sup> F is a least-squares fitting parameter defined as $F^2 = \frac{1}{N} \sum_{i=1}^N k^6 (Data - Model)^2$															
<sup>b</sup> Fits modeled histidine coordination by an imidazole ring, which included single and multiple scattering contributions from the second shell (C2/C5) and third shell (C3/N4) atoms respectively. The Cu-N-C <sub>x</sub> angles were as follows: Cu-N-C2 126°, Cu-N-C3 126°, Cu-N-N4 163°, Cu-N-C5 163°.															
<sup>c</sup> Coordination numbers are generally considered accurate to ± 25%															
<sup>d</sup> In any one fit, the statistical error in bond-lengths is ±0.005 Å. However, when errors due to imperfect background subtraction, phase-shift calculations, and noise in the data are compounded, the actual error is probably closer to ±0.02 Å.															

**3.4.4 Kinetics of transfer measured by EXAFS.** The ability to directly observe metal transfer out of CusF allowed us to begin to examine the kinetics of the metal transfer process. Such data have not been available in studies of interaction of metallochaperones with their acceptor proteins, since it is generally difficult to observe transfer without separation of donor and acceptor. NMR methods that have been used to examine mixtures (Achila et al., 2006; Banci et al., 2006) cannot utilize frozen solutions, such that the kinetic information is limited to determining exchange rates for systems at equilibrium. The ability to freeze the solution at various time points after mixing followed by Se-XAS analysis of the extent of transfer provides a powerful extra dimension to the present approach. Therefore, in addition to the sample described above, which was incubated for 34 minutes before freezing, two additional samples, incubated for 4 and 14 minutes before freezing, were made. In both cases, the extent of transfer was close to 50 percent, and the Se data were identical to the 34 minute sample (Figure 3.4 (A), (B) and (C)). This result indicates that metal transfer is relatively rapid and proceeds to an end point of equal Cu(I) distribution between donor and acceptor in less than 4 minutes.

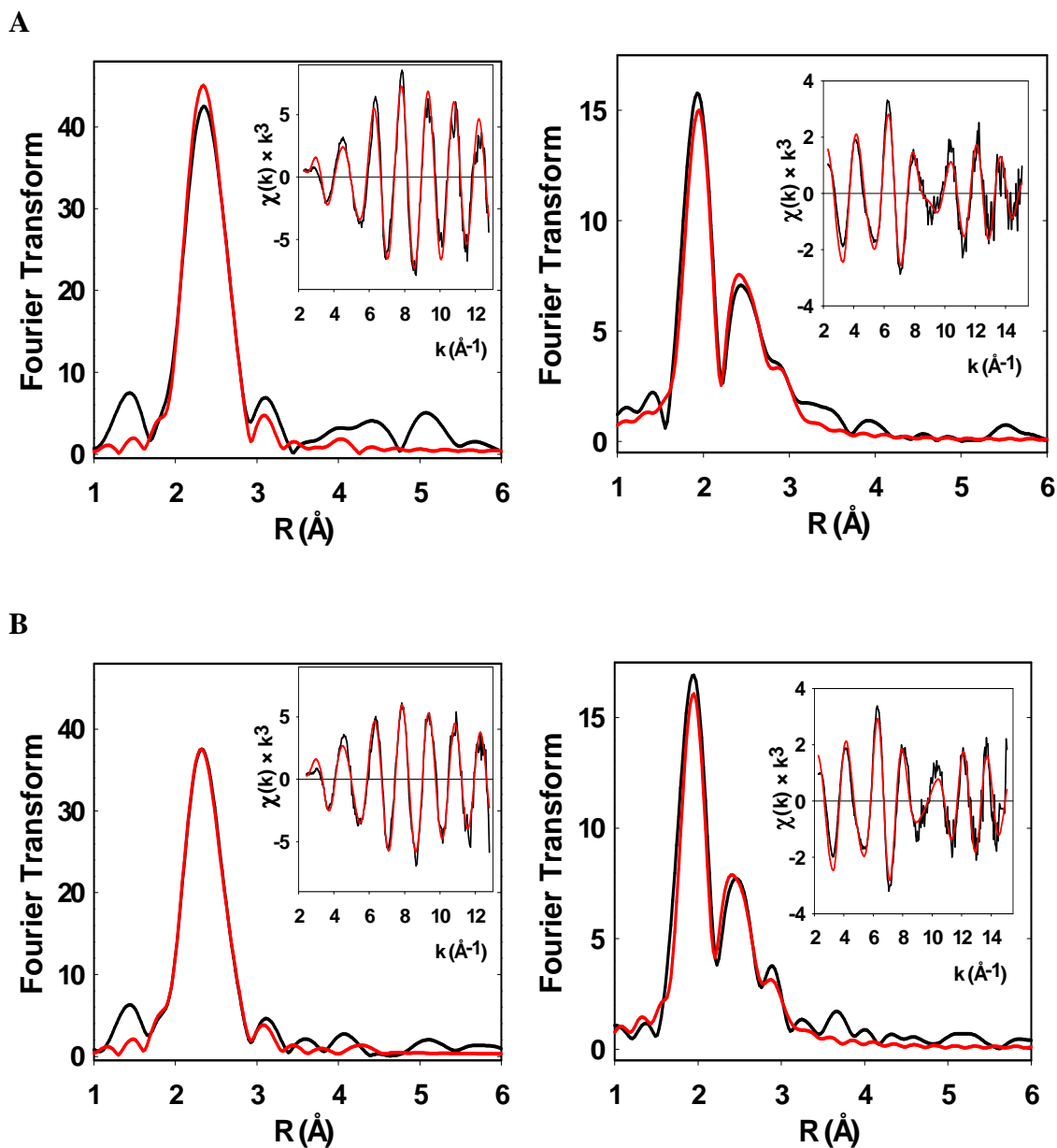


**FIGURE 3.4** Cu (LEFT) and Se (RIGHT) EXAFS of Cu(I)-loaded SeM-CusF mixed with apo-CusB, and **(A)** frozen after 14 minutes; **(B)** frozen after 4 minutes. Experimental (black traces) versus simulated (red traces) FT and EXAFS (inset) using metrical parameters listed in Table 3.1.

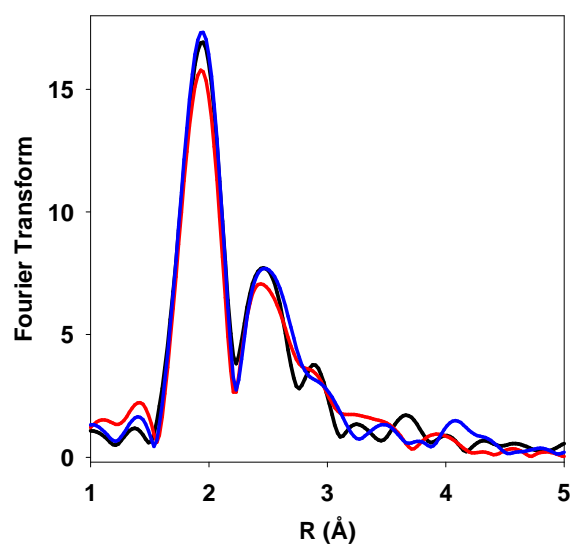


**FIGURE 3.4(C)** Comparison of transfer data from Cu(I)-SeM-CusF to apo-CusB at 4 (black), 14 (red), and 34 minute (blue) time points.

**3.4.5 *Metal transfer is reversible.*** To examine whether metal transfer can directly occur in the reverse direction from CusB to CusF, we monitored the Cu and Se EXAFS of a sample of Cu(I)-CusB mixed with apo-SeM-CusF. The spectra show the loss of the Cu(I)-S environment of CusB and replacement by the Cu(I)-Se environment of SeM-CusF (Figure 3.5). Notably, we again observed an increase in Cu(I)-Se bond length of 0.02Å and approximately 50 percent distribution of Cu(I) between the CusB and CusF proteins. Therefore, Cu(I) transfer between CusF and CusB is reversible, and proceeds to an equivalent end-point regardless of which protein is pre-loaded with Cu(I).

**3.4.6 *Metal transfer occurs directly between proteins of the Cus system.*** Metal equilibration between CusF and CusB, as demonstrated by XAS could be a thermodynamic consequence of their similar affinities for Cu(I)/Ag(I). Thus, metal distribution could result from metal being released by one protein to be taken up by another. In order to determine whether the metal transfer was caused by specific protein-protein interactions or by a simple thermodynamic distribution between the two proteins, we investigated the binding reaction between apo-CusB and a CusF homolog, SilF. SilF, with 51% identity to CusF, is a component of a homologous SilCFBA system present in *Salmonella typhimurium*. SilF binds Ag(I) with a  $K_d$  of 35 nM, similar to the affinity of CusF for Ag(I) (Figure 3.6(A)).

Ag(I)-SilF was titrated into apo-CusB to determine whether it could functionally substitute for CusF. If similar binding isotherms are obtained, it could imply that the proteins were coming together just for the redistribution of metal ion, considering their

similar affinities for Ag(I) and that no true interaction was being monitored. However, we did not see any significant change in binding enthalpy for this titration (Figure 3.6(B)). Furthermore, titration of Ag(I)-SilF into apo-CusF (Figure 3.6(C)) and reverse titration of Ag(I)-CusF into apo-SilF (Figure 3.6(D)) didn't show any enthalpy changes either. This clearly indicates direct metal transfer through protein-protein interactions between CusF and CusB.

It also established that metal transfer is specific amongst the components of heavy metal efflux systems. In addition, it suggested that the metal is not being released into the solution from one protein to be taken up by another rather it is a direct metal exchange between CusF and CusB.

#### ***3.4.7 CusF and CusB found as a single polypeptide in the putative efflux systems.***

BLAST search of the non-redundant protein database using CusF from *E. coli* as the query sequence returned some hits where putative MFP component was present at the N-terminus of CusF homologs. Appendix C shows a ClustalW sequence alignment of CusF and homologous proteins identified from the BLAST search. The existence of CusF as a single polypeptide with CusB in other systems substantiates our proposition that the two proteins interact to mediate metal extrusion.

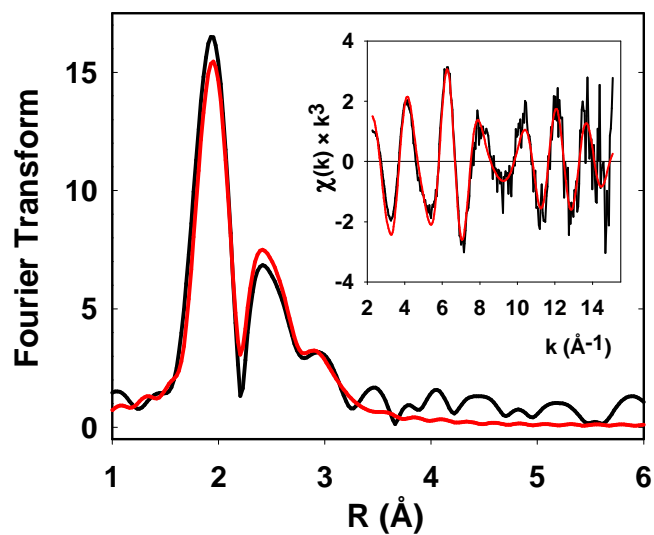


**FIGURE 3.5** Reverse transfer from Cu(I)-CusB to apo-SeM-CusF measured at the Se edge. Experimental (black traces) versus simulated (red traces) FT and EXAFS (inset) using metrical parameters listed in Table 3.1.

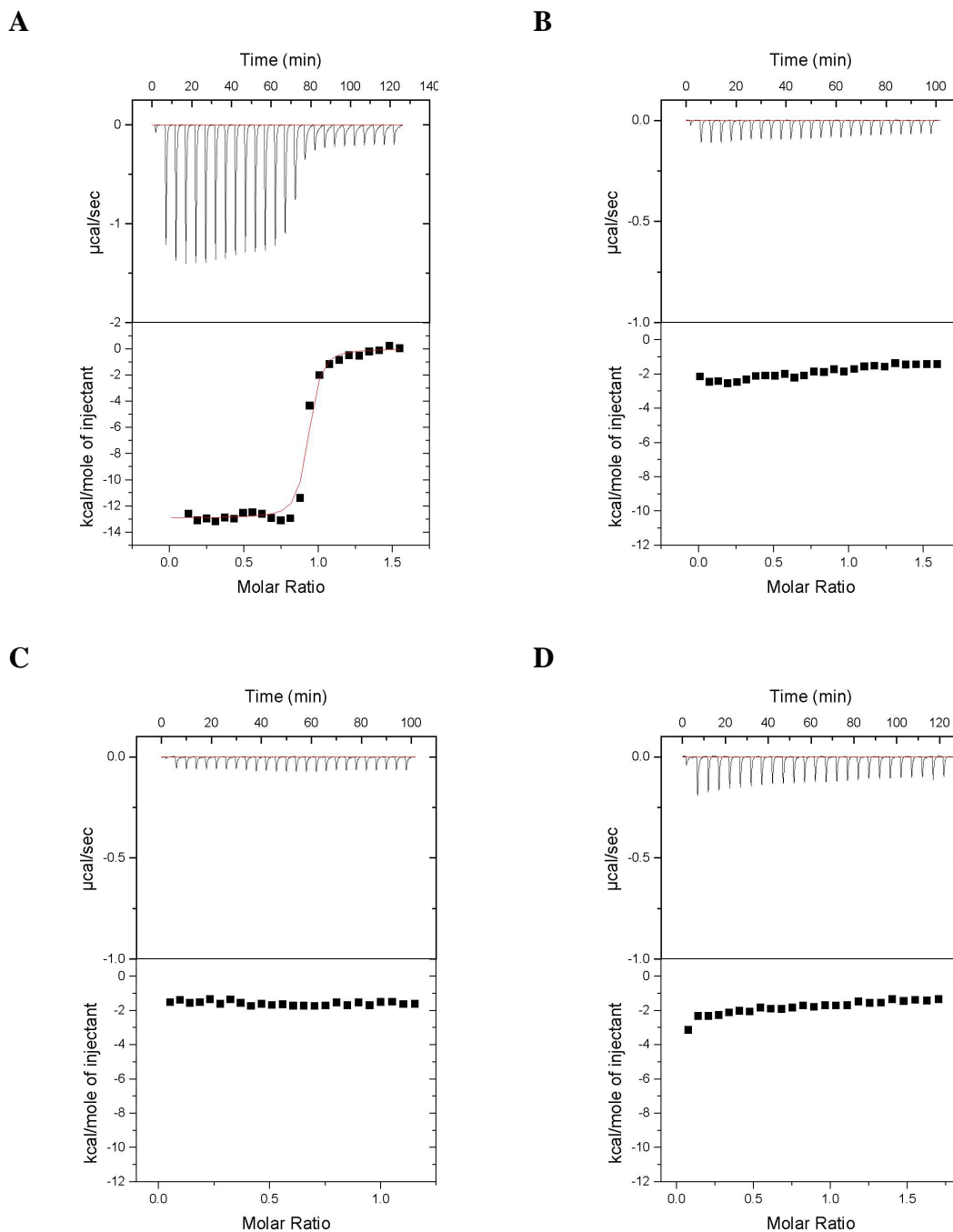


**FIGURE 3.6** ITC data for titration of (A) 36  $\mu\text{M}$  apo-SilF with 300  $\mu\text{M}$   $\text{AgNO}_3$ ; (B) 21  $\mu\text{M}$  apo-CusB with 170  $\mu\text{M}$  Ag(I)-SilF; (C) 29  $\mu\text{M}$  apo-CusF with 170  $\mu\text{M}$  Ag(I)-SilF; (D) 30  $\mu\text{M}$  apo-SilF with 275  $\mu\text{M}$  Ag(I)-CusF in 50 mM cacodylate, pH 7.0. *Top*, raw data. *Bottom*, plot of integrated heats versus titrant/titrant ratio. The solid line represents the best fit for a one-site binding model.

### 3.5 DISCUSSION

We have demonstrated that CusF and CusB interact *in vitro* when either of the two proteins have Ag(I)/Cu(I) bound, but do not interact if both are present as apo-proteins or if both have a bound metal. We have also shown that metal transfer results from specific interaction between proteins in the Cus system such that a replacement of CusF with a homolog SilF failed to reveal a binding enthalpy change upon titration into CusB during ITC analysis. Earlier studies have also noted high specificity in metallochaperone systems. For example, domain I of CCS, an Atx1 homolog, was found to be non-interchangeable with Atx1 in an *in vivo* study (Schmidt et al., 1999). Furthermore, absence of the binding enthalpy change between either CusB and Ag(I)-SilF or CusF and Ag(I)-SilF suggested that we are monitoring a true interaction with a direct metal exchange between CusF and CusB, and not a simple metal distribution process, considering similar affinities of CusB, CusF and SilF for Ag(I).

To discern the structural environment of the metal ion in the reaction mixture, consisting of one protein in the apo and another in a metallated form, XAS analysis was performed. A novel Selenium K-edge EXAFS approach was used to probe the binding site in CusF. Many metallochaperones and metal transporters use S-ligation to coordinate metal ions. This is particularly true for copper transport systems, where cysteine or methionine coordination is used to stabilize the Cu(I) oxidation state. The strong Cu-S scattering observed in the X-ray absorption spectra of these systems has provided valuable structural information on the coordination environment of these

otherwise “spectroscopically silent” Cu(I) environments. Due to its increased scattering power, selenium substitution can provide a convenient XAS probe for both characterization of the metal center and for monitoring the transfer process from donor to acceptor protein. While substitution of selenocysteine (SeC) at the active sites of copper proteins is complicated by the fact that t-RNA-mediated SeC incorporation utilizes complex molecular machinery involving additional SECIS RNA elements that often preclude the use of simple cloning techniques, selenomethionine (SeM) substitution does not suffer from this complexity and has been widely used to enrich proteins with the “heavier” scatterer Se for MAD phasing of protein crystallography density maps. Here we have reported on the use of SeM substitution to characterize the Met-rich sites of CusF and CusB.

Data collection at Se edge for SeM-CusF not only allowed us to examine changes in the CusF binding site upon binding of Cu(I), but also enabled us to monitor the change in Cu(I) environment in the presence of apo-CusB. The data showed unambiguously that on mixing, copper transferred out of the Se environment of CusF into the S-environment of CusB. The small but reproducible increase in Cu-Se bond length when SeM-CusF is mixed with CusB is noteworthy, and suggests that the average Se-Cu environment is different in the mixtures than in an isolated Cu(I)-SeM-CusF. This could imply that when CusF and CusB interact, the Cu which remains in the Se site of CusF is structurally perturbed, and may point to a small population of CusF-CusB complexes where the observed bond length is the average of CusF-Cu(I) and CusF-Cu(I)-CusB adducts. Earlier studies have shown a formation of transient adduct in the transfer of copper ion in

Atx1-Ccc2 (Arnesano et al., 2001; Banci et al., 2006) and HAH1-WLN4 systems, respectively (Achila et al., 2006). Although, the Cu(I) location within protein complexes is modeled using NMR in these studies, this is the first time it has been observed directly in context of the ligands.

Furthermore, the strength of the technique also helped us to establish the reversibility of this process inferred from a 50% equilibrium distribution of copper between both proteins. This is an important finding which implies that CusB has the potential to lose Cu(I). It is significant in the light of the fact that CusCFBA is an efflux system and CusB should be able to transfer Cu(I) to other components of the machinery to mediate its expulsion. The reversibility of reaction has also been shown earlier using indirect methods for transporters like Ccc2 and Wilson's protein (WND) and their cognate chaperones (Huffman and O'Halloran, 2000; Yatsunyk and Rosenzweig, 2007). Kinetic analysis demonstrated that the transfer process is relatively rapid in the forward direction and equilibrium is established within 4 minutes of mixing Cu(I)-CusF and apo-CusB, which is also in line with the results reported for other systems (Huffman and O'Halloran, 2000; Yatsunyk and Rosenzweig, 2007). From Table 3.1 it is evident that the increase in Cu-Se appears greatest at longer time periods, which suggests another plausible scenario for the increased bond length. The longer bond length might be attributed to slower back transfer of Cu(I) from CusB to CusF. As shown in Figure 3.7, the transfer of Cu(I) from CusF to CusB likely involves 3 intermediates, a tetragonal complex consisting of 3 ligands from CusF and 1 from CusB, another adduct with both proteins contributing 2 ligands each and a third tetragonal complex consisting of 3

ligands from CusB and 1 from CusF, respectively. As the metal ion is completely transferred into the trigonal environment of CusB from tetragonal complex, CusB likely undergoes a conformational change (Bagai et al., 2007). This conformational change may sterically inhibit the correct orientation of CusB and CusF for the back transfer to happen. This in turn may increase the activation energy barrier, thus making the reaction kinetically difficult. In an attempt to remove Cu(I) from CusB *in vitro*, ligands in CusF likely undergo structural perturbation, manifesting an increased bond length. Additionally, the conformational change in CusB probably regulates the opening of CusA, CusC channel to mediate Cu(I) efflux by these two proteins.

These findings point at CusF being the copper chaperone of the CusCFBA system. We propose here that CusF sequesters Cu(I)/Ag(I) in the periplasm and is required for the full resistance of the CusCBA components, as suggested earlier (Franke et al., 2003). The sequestered Cu(I) is then carried and handed off to CusB for eventual extrusion from the cell. In this process, CusF likely enhances the metal uptake of the CusCBA machinery by interacting with CusB in the right orientation such that the probability of “effective” collisions between metal ion and CusB is increased and the rate-limiting activation energy barrier is lowered. The specificity and selectivity of interaction with rapid forward transfer are typical properties of copper chaperones. We speculate that the transfer of copper from CusF to CusB is also kinetically controlled, as suggested in Atx1-Ccc2 (Huffman and O'Halloran, 2000) and other systems (Yatsunyk and Rosenzweig, 2007). In the presence of a shallow thermodynamic gradient, as concluded from similar binding affinities of CusF and CusB for Ag(I), the rapid transfer mediated by specific

recognition, which lowers the activation barrier, seems to be the most reasonable explanation. Additionally, the presence of CusF and CusB as one polypeptide in other efflux systems may imply that CusF and CusB worked together as one protein in certain systems and were separated in this system to plausibly allow independent regulation of the two modules of MFPs to enhance the efficiency of copper detoxification.

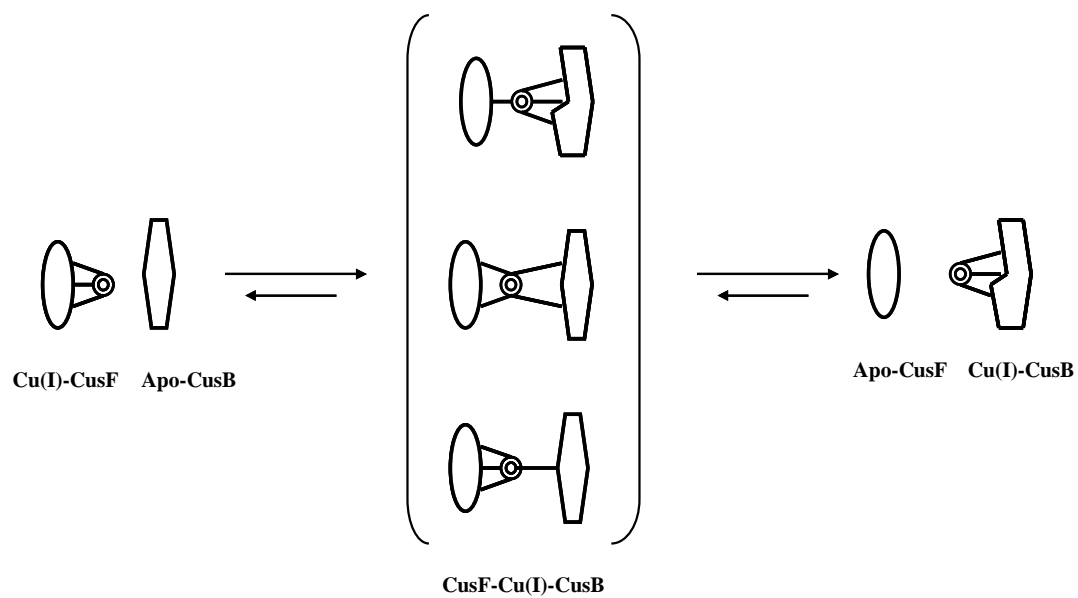


**FIGURE 3.7** Model for Cu(I) exchange between CusF and CusB.

## CHAPTER 4

### THE CUSB BINDING INTERFACE ON CUSF OVERLAPS WITH THE METAL SITE

In this chapter, the structural features of CusF and CusB interactions are investigated by NMR spectra. I performed all the work described in this chapter.

#### 4.1 INTRODUCTION

Copper homeostasis has become an area of intense research in the last few years due to the toxic nature of this redox-active metal. While copper uptake and efflux processes are not well understood, protein-protein interactions have been shown to be an integral component of copper sequestration and transfer processes in both eukaryotes (Arnesano et al., 2001; Horng et al., 2004; Lamb et al., 2001) and prokaryotes (Banci et al., 2003; Cobine et al., 2002). Copper chaperones responsible for delivering copper to various essential enzymes interact specifically with their respective partners (Lu et al., 1999; Strausak et al., 2003), although not essentially in a metal-dependent fashion (Benitez et al., 2008; Casareno et al., 1998; Schmidt et al., 2000).

CusB and CusF are periplasmic components of the CusCFBA Cu(I)/Ag(I) efflux system present in the cell envelope of *Escherichia coli*. While CusB is a homolog of the adaptor component (Bagai et al., 2007) of CBA-type multidrug exporters (Nikaido and Zgurskaya, 2001) present in gram-negative bacteria, CusF homologs are found only in

putative copper/silver transport systems. CusA is a resistance-nodulation-division (RND)-type component located in the inner membrane, which facilitates metal export by coupling it with proton import, and CusC is an outer membrane protein (Franke et al., 2003). We have shown previously that CusF is likely a metallochaperone of the Cus system, which escorts metal ions to the periplasmic adaptor protein, CusB, for their subsequent extrusion from the cell. Here, we have taken a structural approach to investigate interactions between these two components of the CusCFBA efflux machinery.

Through NMR chemical shift perturbation experiments, we show that CusF and CusB interact only in the presence of metal ion and that the interaction is specific between the two proteins. Chemical shift perturbation is a powerful method to decipher protein-protein/protein-ligand contacts. It relies on the observation that although the NMR chemical shifts are primarily determined by covalent structure, the shifts can be further influenced by non-covalent interactions with the environment. The formation of a protein complex results in new non-covalent contacts for atoms in the binding interface and hence in chemical shift variations (Wuthrich, 2000).

Furthermore, chemical shift assignments of CusF-Ag(I)/CusB were used to determine the residues in CusF-Ag(I) that are significantly affected by CusB binding. Mapping of these residues on the CusF structure (Loftin et al., 2007) illustrates that only one face of the CusF  $\beta$ -barrel, which is formed by strands  $\beta$ 1-  $\beta$ 3, is involved in the interaction.

## 4.2 MATERIALS AND METHODS

**4.2.1 Protein expression and purification.** The expression and purification of CusB in *Escherichia coli* was performed as described previously (Bagai et al., 2007). For preparation of uniformly  $^{15}\text{N}$ -labeled CusF, *E. coli* BL21 ( $\lambda\text{DE3}$ ) strain containing *cusF* in pASK-IBA3 was grown in M9 minimal media (Sambrook et al., 1989) containing 1.0 g/liter  $^{15}\text{NH}_4\text{Cl}$  (Cambridge Isotopes Laboratories) as the sole source of nitrogen. Cells were grown in 20 mL of Luria Bertani (LB) media overnight, then centrifuged and transferred to 1 L of M9 media and grown at 37 °C until they reached an O.D.<sub>600</sub> of 0.6-1.0, then induced with 200  $\mu\text{g/L}$  of anhydrotetracycline (AHT). Growth was continued at 30 °C for 8-10 hrs. For  $^{13}\text{C}$  and  $^2\text{H}$  labeling, the procedure was slightly modified. From the glycerol stock of cells maintained at -80 °C, 3.0 mL of LB media was inoculated. Cells were grown for approximately 3 hours at 37 °C after which they were transferred to 50 mL of M9 media made in  $\text{H}_2\text{O}$  and containing 0.15 g  $^{13}\text{C}$  glucose and 0.05 g  $^{15}\text{NH}_4\text{Cl}$  (Gardner and Kay, 1998) at concentrations of 3.0 g/L and 1.0 g/L, respectively. The cells were grown for another 7 hours to an  $A_{600}$  of approximately 1.5, then gently pelleted and transferred to 200 mL of M9 media made in  $^2\text{H}_2\text{O}$  and containing  $^{13}\text{C}$  glucose and  $^{15}\text{NH}_4\text{Cl}$  at the concentrations stated above. The culture was grown for approximately 20 minutes before transferring to 800 mL of M9 ( $^2\text{H}_2\text{O}$ ) at 37 °C. At O.D.<sub>600</sub> of 0.2, cells were induced with AHT at a final concentration of 200  $\mu\text{g/L}$  and the temperature was reduced to 28 °C. Cells were grown for another 12 hours before being harvested by

centrifugation. The purification of CusF was performed as described previously (Loftin et al., 2005).

**4.2.2 NMR spectroscopy.** For NMR samples, both  $^2\text{H}$ ,  $^{15}\text{N}$ ,  $^{13}\text{C}$ -CusF and CusB were dialyzed against 50 mM cacodylate, pH 7.0.  $\text{AgNO}_3$  was added to CusB and the labeled-CusF proteins separately at a concentration ratio of 2:1 each. The proteins were then redialysed in the same buffer to remove unbound  $\text{Ag(I)}$ . CusF and CusB were separately concentrated using Amicon concentrators with a 5 kDa molecular weight cut-off. Protein concentrations were determined using the BCA assay (Pierce Biotechnology).  $^1\text{H}$ - $^{15}\text{N}$  Heteronuclear Single Quantum Coherence (HSQC) (Bodenhausen and Ruben, 1980) experiments with a Transverse relaxation optimized spectroscopy (TROSY) option (Riek et al., 2000) were performed at 298 K on a 600 MHz Varian Inova instrument equipped with a four channel pulsed-field gradient triple-resonance probe. Data were collected on four different samples. Spectra were obtained for (i) 150  $\mu\text{M}$  apo-CusF; (ii) 150  $\mu\text{M}$   $\text{Ag(I)}$ -CusF; (iii) 170  $\mu\text{M}$   $\text{Ag(I)}$ -CusF mixed 1:1 with apo-CusB and; (iv) 160  $\mu\text{M}$  apo-CusF mixed 1:1 with  $\text{Ag(I)}$ -CusB. All samples contained 10%  $^2\text{H}_2\text{O}$  and 0.02%  $\text{NaN}_3$ . 256 increments of 2048 complex data points were collected for each experiment. Spectral widths of 7.2 kHz and 1.82 kHz were used in the  $^1\text{H}$  and  $^{15}\text{N}$  dimensions respectively. Spectra were processed with NMRPIPE (Delaglio et al., 1995) and analyzed with NMRView (Johnson and Blevins, 1994). Control HSQCs of CusF in the presence of either CueO or Bovine serum albumin (BSA) were collected in a similar manner except that the CusF used for the experiments was labeled only with  $^{15}\text{N}$ .  $^{15}\text{N}$ -

CusF was mixed 1:1 with either CueO or BSA and  $\text{AgNO}_3$  was added to the mixture at twice the concentration of the proteins. To determine the backbone assignments of CusF-Ag(I)/CusB, a three-dimensional HNCA (Bax and Ikura, 1991) spectrum was acquired on 170  $\mu\text{M}$  Ag(I)-CusF mixed with apo-CusB in a ratio of 1:1. The standard HSQC and HNCA pulse sequences from Varian Biopack were used to acquire the spectra.

## 4.3 RESULTS

### 4.3.1 *Chemical shift changes reveal metal-dependent interactions between CusF and CusB.*

Results obtained from previous CusF/CusB interaction studies strongly suggest a direct interaction between the two proteins in the presence of Ag(I)/Cu(I) (Chapter 3). To investigate the structural effect in CusF due to CusB binding *in vitro*,  $^1\text{H}$ - $^{15}\text{N}$  HSQC spectra of Ag(I)-containing and apo forms of CusF were collected in the presence of apo and Ag(I)-bound CusB. Since resonances in HSQC correspond to the amide groups of all amino acids in the polypeptide backbone except proline, it provides an effective measure to probe effects of environmental changes on each amino acid in the observed protein without having to mutate individual residues. The HSQC spectrum of apo-CusF mixed 1:1 with apo-CusB showed no change in the chemical shifts when compared with the spectrum of apo-CusF alone (Figure 4.1(A)), indicating no interaction in the absence of metal. However, the HSQC spectrum for apo-CusF mixed 1:1 with Ag(I)-CusB showed significant changes compared to the spectrum of apo-CusF alone (Figure 4.1(B)), indicating that the two proteins interact in the presence of metal ion. A few residues were noted to undergo substantial line broadening such that they could not be detected. Furthermore, the HSQC spectrum of Ag(I)-CusF mixed 1:1 with apo-CusB revealed similar chemical shift changes in comparison to the spectrum for Ag(I)-CusF alone (Figure 4.1(C)). This result indicates that when either CusF or CusB has metal bound to it, the two proteins interact in a similar fashion. The similarity of the HSQC spectra of Ag(I)-CusF mixed with apo-CusB and apo-CusF mixed with Ag(I)-CusB clearly points at

identical interaction between the two proteins regardless of which of the two contained metal before mixing with the apo-form of the other (Figure 4.1 (D)).

Our previous results have shown that in mixtures of CusF and CusB and Ag(I), the metal distributes approximately equally between the two proteins (Chapter 3). If the spectral changes in CusF upon the addition of CusB were simply due to redistribution of metal between both proteins, the CusF HSQC spectra in the presence of CusB and Ag(I) would be expected to be the same as the NMR spectrum of CusF with 0.5 equivalents of Ag(I). However, a comparison of these spectra show that the Ag(I)/CusF/CusB spectra are not the same as the spectrum of CusF containing 0.5 equivalents of Ag(I) (Figure 4.1 (E)). Though the positions of some of the resonances in the Ag(I)/CusF/CusB spectra are similar to those of CusF with 0.5 equivalents of Ag(I), other resonances have positions distinct from those in the spectra of either the apo-CusF, CusF-Ag(I), or CusF with 0.5 equivalents of Ag(I). This result indicates that there are additional effects of CusB on CusF in addition to those caused by the presence or absence of metal.

No change in the chemical shifts of Ag(I)-CusF was seen when either CueO (Figure 4.1 (F)), a periplasmic multicopper oxidase involved also in copper homeostasis in *E. coli* or Bovine serum albumin (Figure 4.1(G)) were added to the NMR sample, suggesting that CusF interacts specifically with CusB.

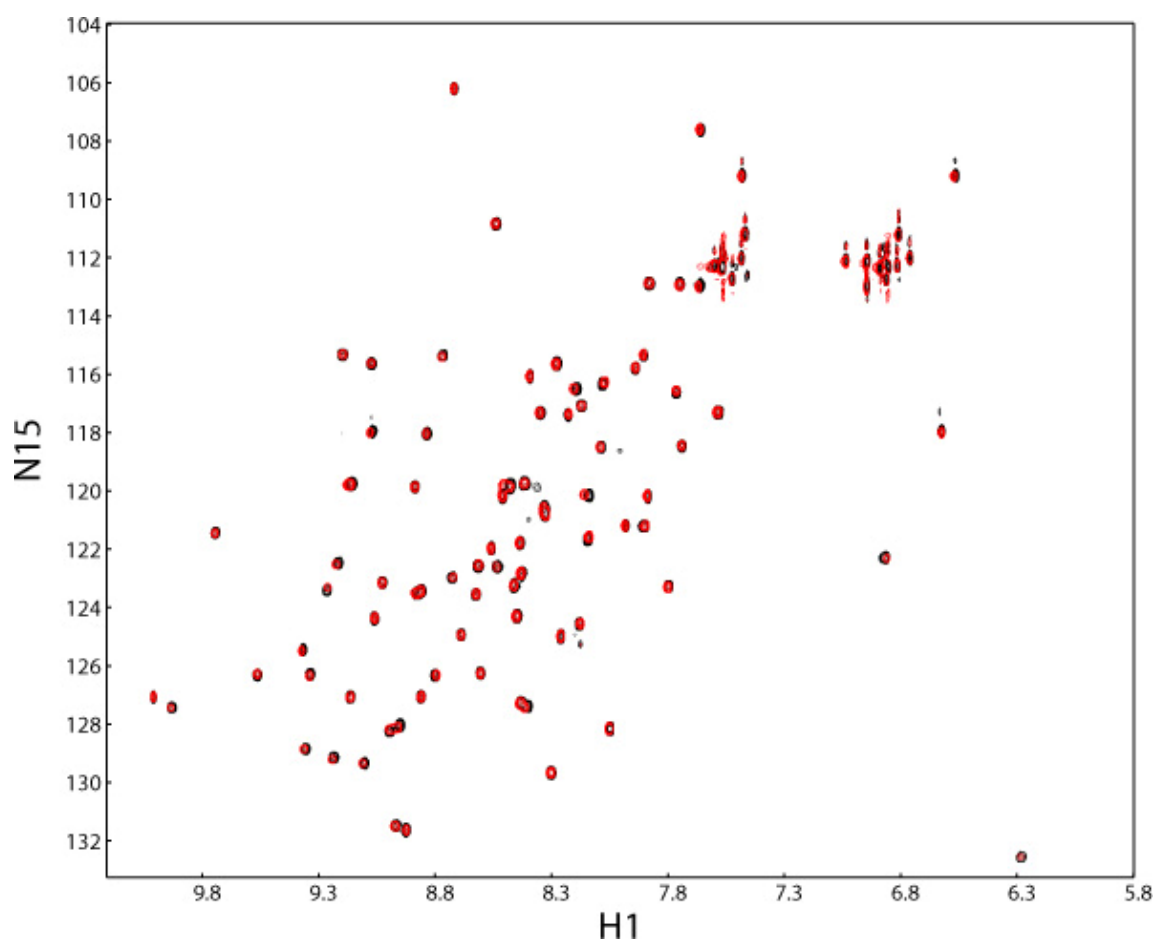


**FIGURE 4.1(A)**  $^1\text{H}$ - $^{15}\text{N}$  HSQC spectral overlay. Apo-CusF (black) and apo-CusF mixed 1:1 with apo-CusB (red).

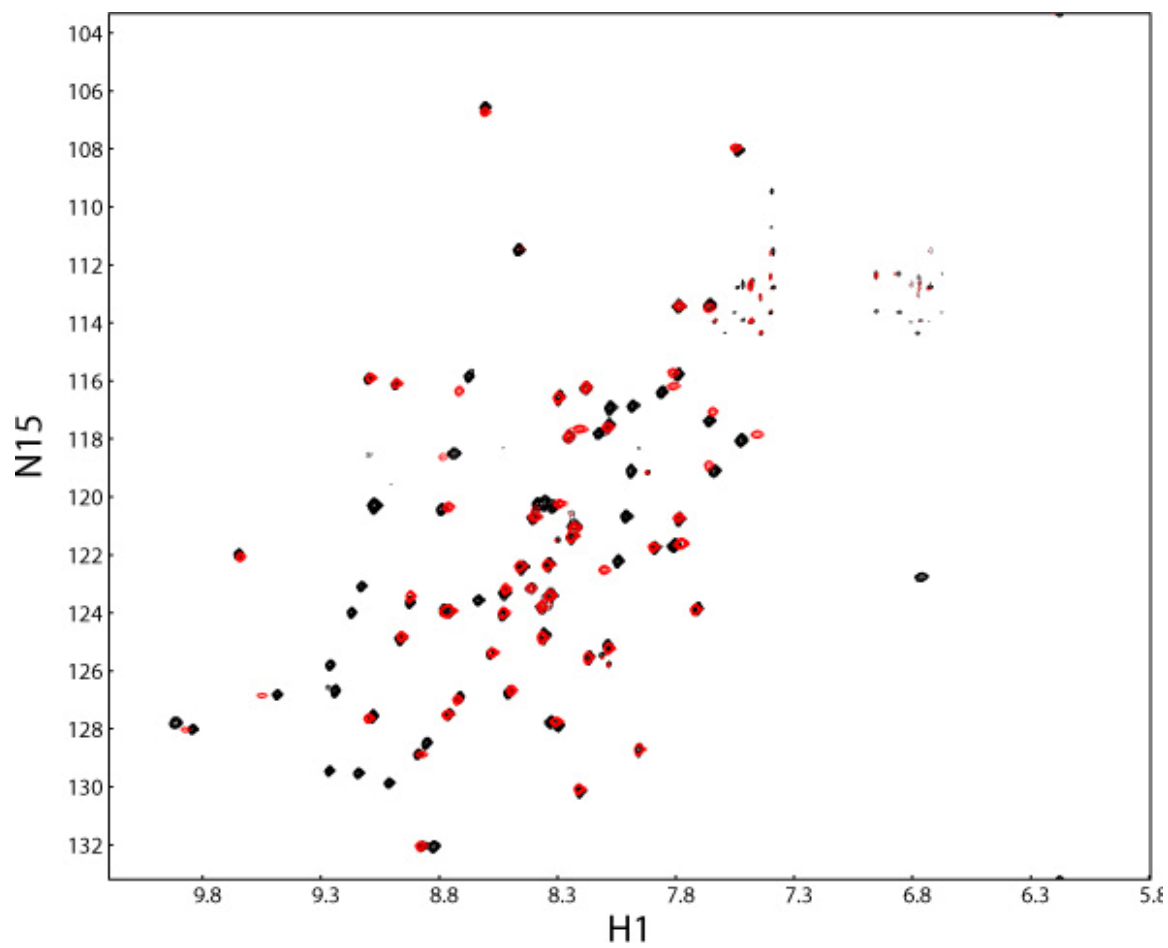


**FIGURE 4.1(B)**  $^1\text{H}$ - $^{15}\text{N}$  HSQC spectral overlay. Apo-CusF (black) and apo-CusF mixed 1:1 with Ag(I)-CusB (red).

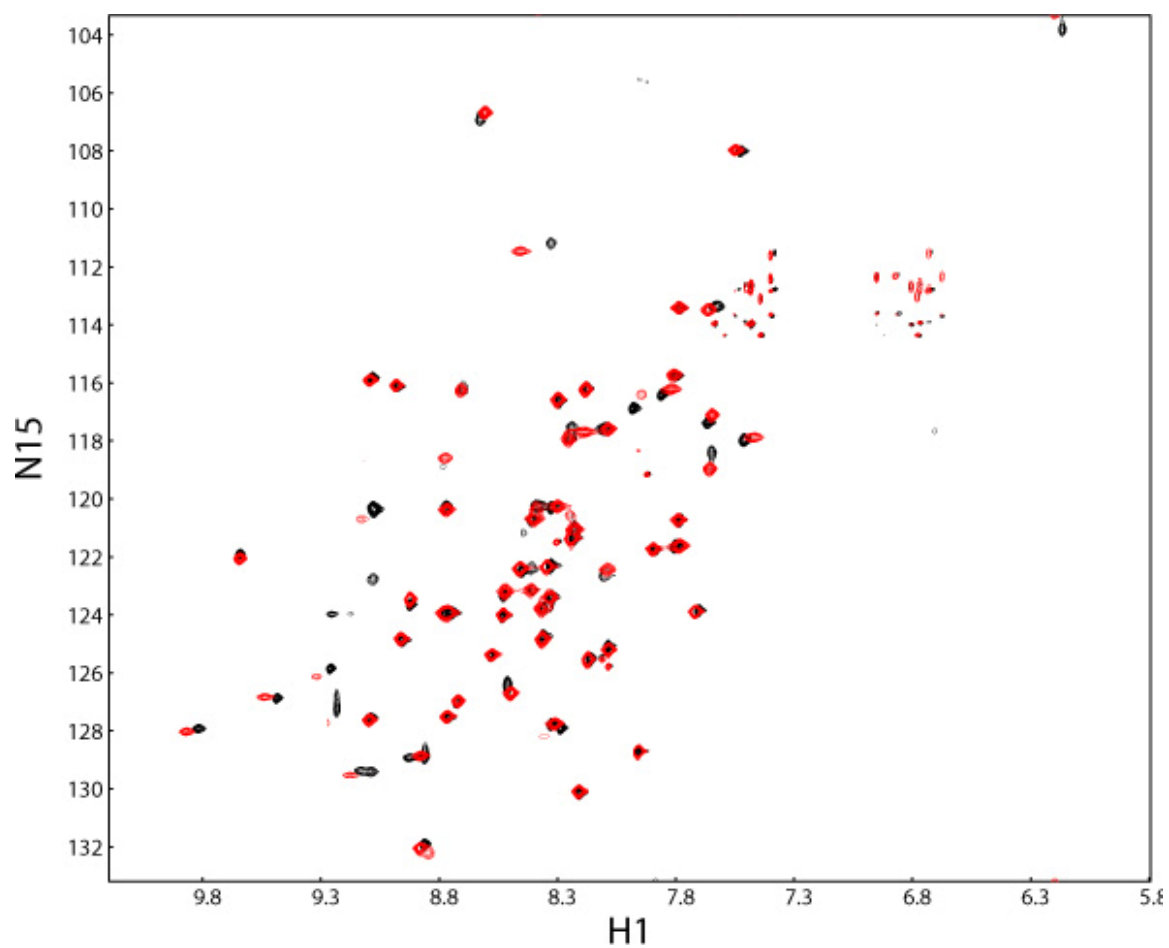


**FIGURE 4.1(C)**  $^1\text{H}$ - $^{15}\text{N}$  HSQC spectral overlay. Ag(I)-CusF (black) and Ag(I)-CusF mixed 1:1 with apo-CusB (red).

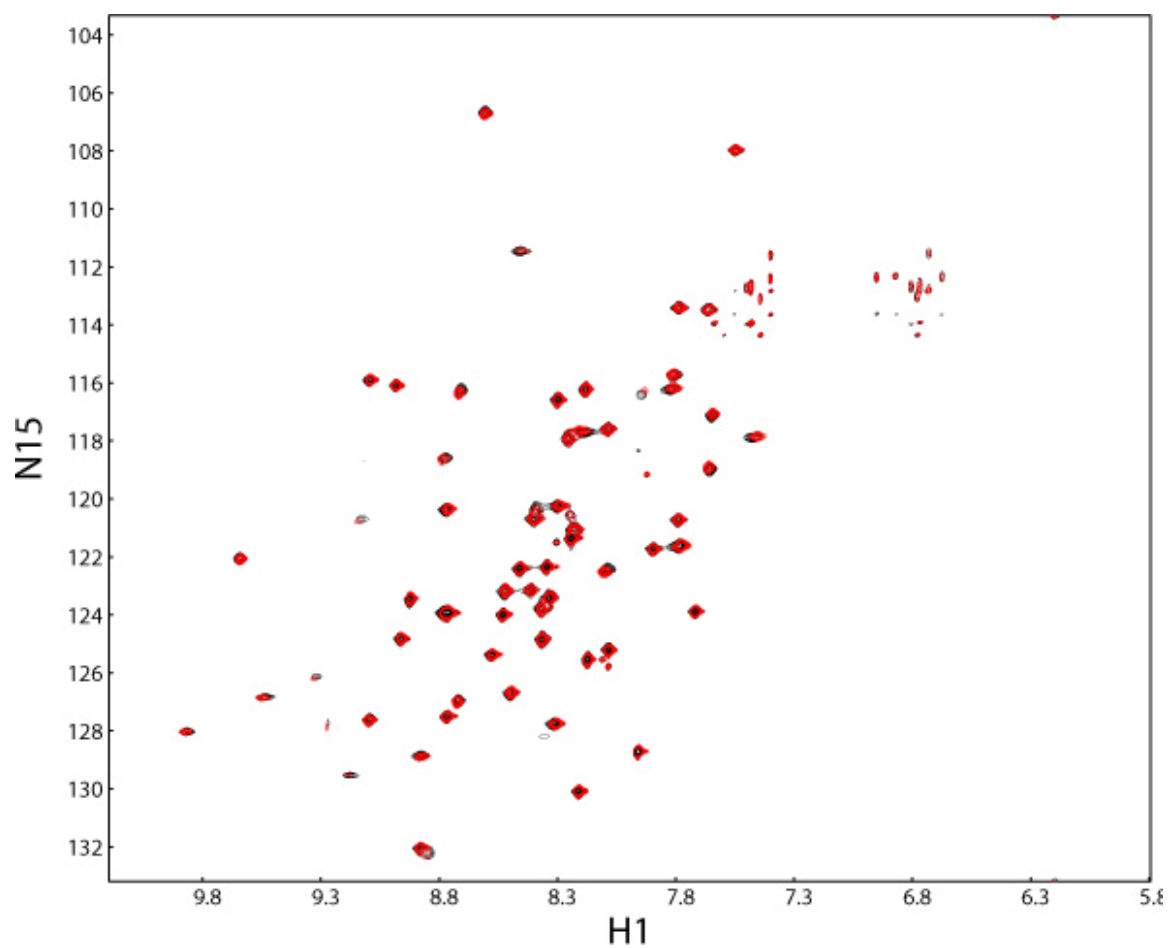


**FIGURE 4.1(D)**  $^1\text{H}$ - $^{15}\text{N}$  HSQC spectral overlay. Apo-CusF mixed 1:1 with Ag(I)-CusB (black) and Ag(I)-CusF mixed 1:1 with apo-CusB (red).

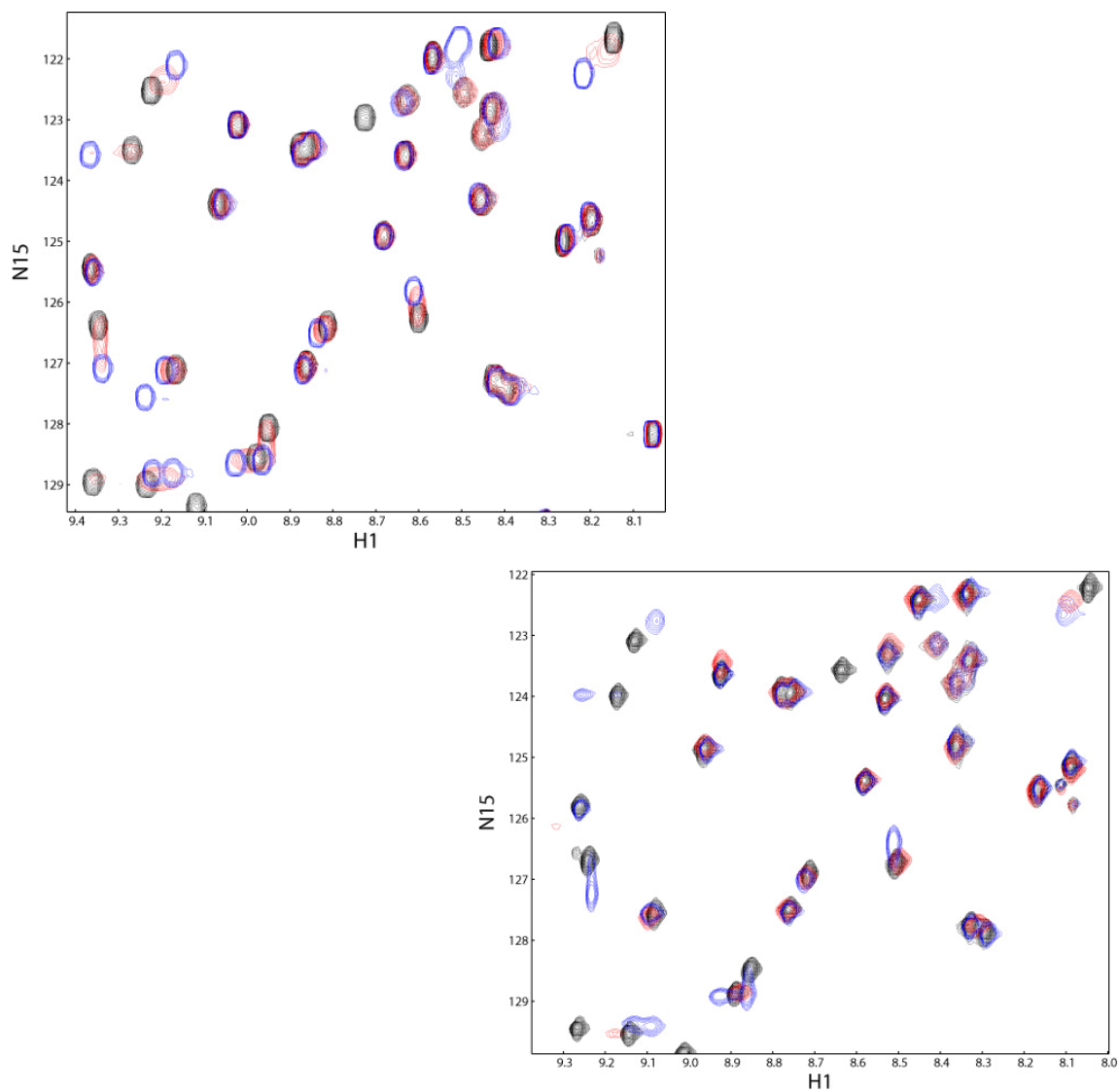


**FIGURE 4.1(E)**  $^1\text{H}$ - $^{15}\text{N}$  HSQC spectral overlay expansions. **(TOP)** Apo-CusF (black) and apo-CusF mixed 1:0.5 with Ag(I) (red) and 1:1 with Ag(I) (blue); **(BOTTOM)** Apo-CusF (black) and Ag(I)-CusF mixed 1:1 with apo-CusB (red) and Ag(I)-CusF (blue).

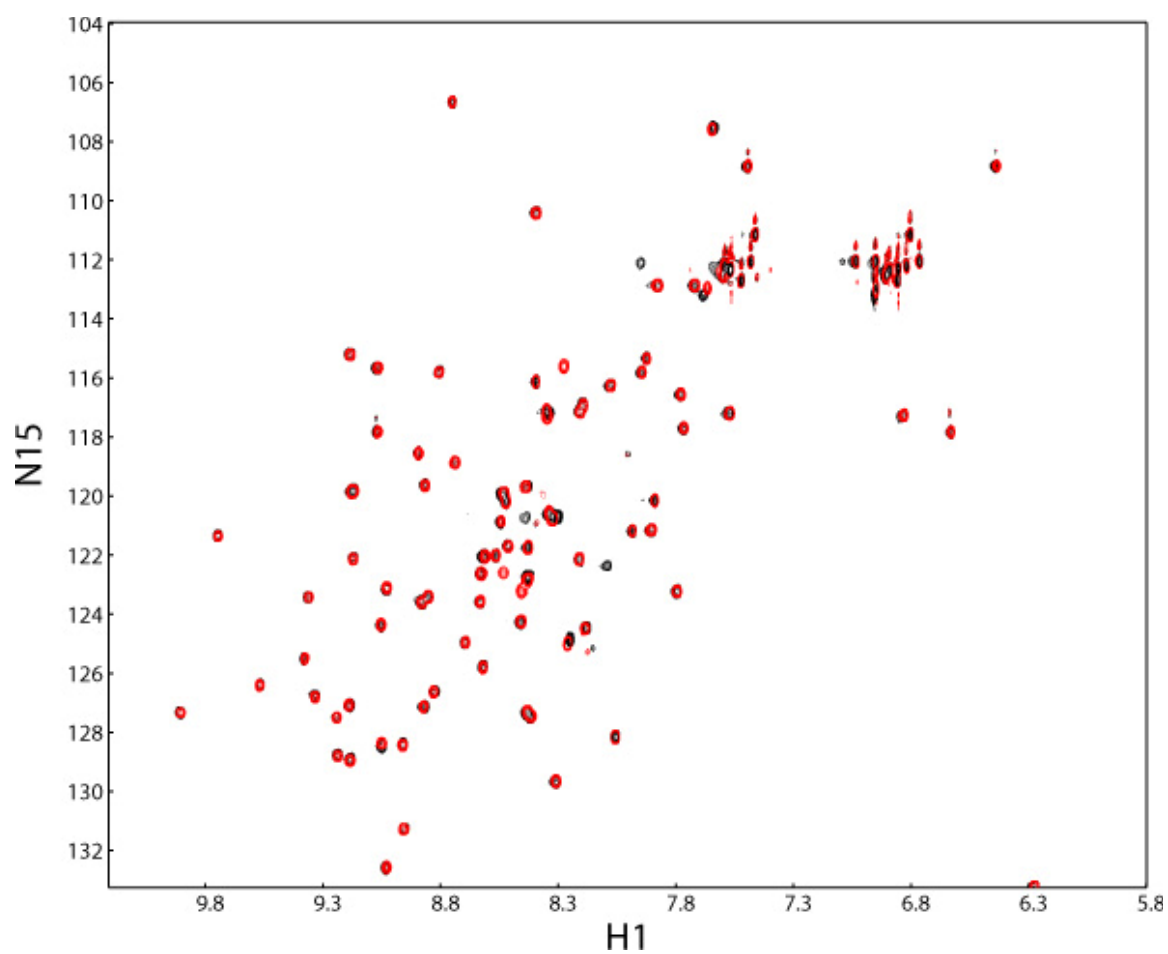


**FIGURE 4.1(F)**  $^1\text{H}$ - $^{15}\text{N}$  HSQC spectral overlay. Apo-CusF (black) and apo-CusF mixed with apo-CueO and Ag(I) at a ratio of 1:1:2 (red).

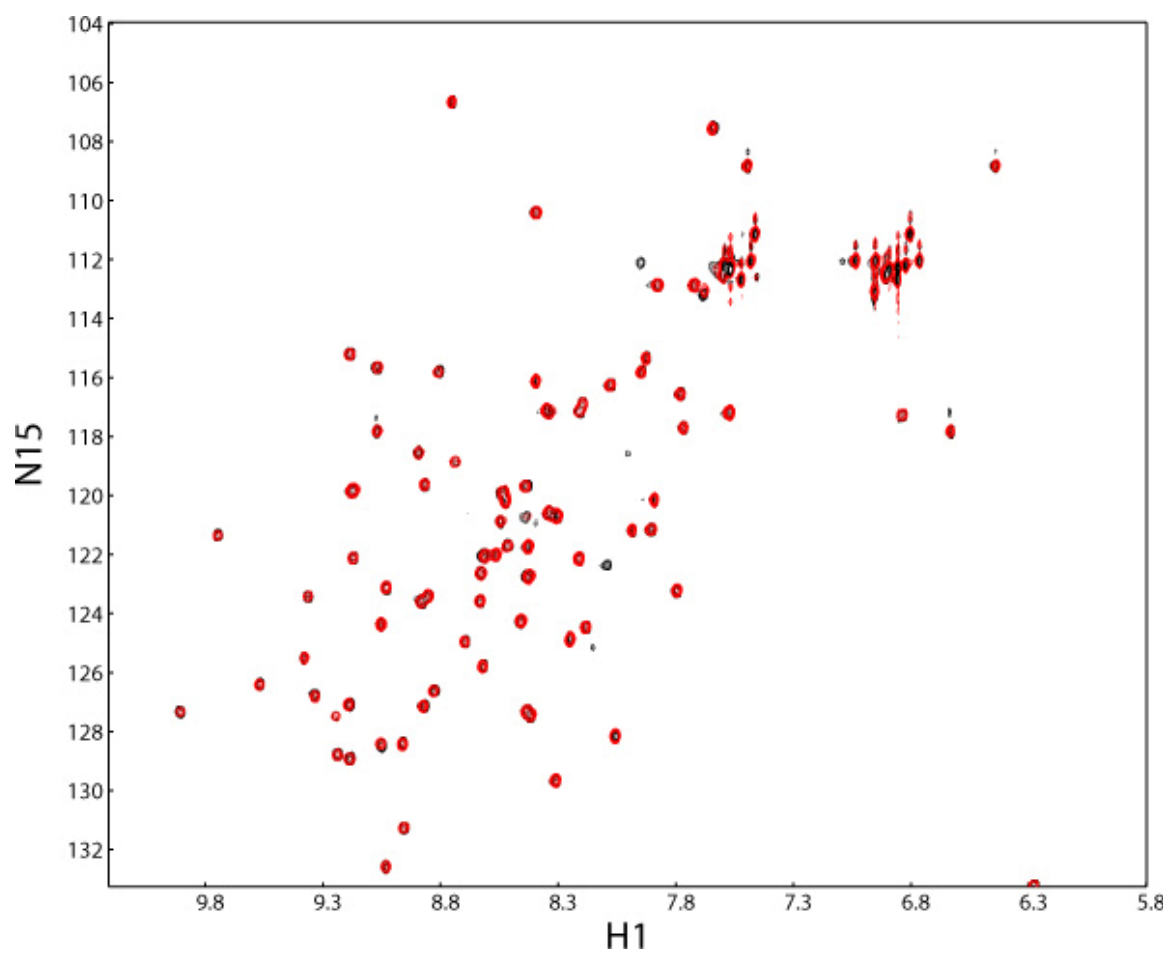


**FIGURE 4.1(G)**  $^1\text{H}$ - $^{15}\text{N}$  HSQC spectral overlay. Apo-CusF (black) and apo-CusF mixed with apo-BSA and Ag(I) at a ratio of 1:1:2 (red).

**4.3.2 Identification of the CusF residues involved in interaction with CusB.** To determine the magnitude of the chemical shift changes caused by CusB binding, we performed the  $^1\text{H}^{\text{N}}$ ,  $^{15}\text{N}$  and  $^{13}\text{Ca}$  assignments of the CusF-Ag(I)/CusB by following sequential connectivities observed in the HNCA spectra (Appendix D). HNCA correlates an amide proton with the  $\text{Ca}$  ( $\text{Ca}^i$ ) atom of its own amino acid and with that of the preceding ( $\text{Ca}^{i-1}$ ) residue. Using this, 70 of the 79 assignable  $^1\text{H}^{\text{N}}$ - $^{15}\text{N}$  resonances were determined. The unassigned residues include I32, H36, M47, R50, F51, Q74 and Q75, which are broadened beyond detection, and I39 and N77, which are not observed in either the Ag(I) bound (Kittleson et al., 2006) or apo forms of CusF (Loftin et al., 2005).

Changes in chemical shifts observed upon addition of apo-CusB to Ag(I)-CusF were calculated as weighted average of the changes in  $^1\text{H}^{\text{N}}$  and  $^{15}\text{N}$  dimensions of CusF-Ag(I)/CusB compared with the Ag(I)-CusF spectrum using  $\Delta_{\text{av}} = ((\Delta\delta_{\text{NH}}^2 + \Delta\delta_{\text{N}}^2/25)/2)^{1/2}$ , where  $\Delta_{\text{av}}$  is the combined chemical shift and  $\Delta\delta_{\text{NH}}$  and  $\Delta\delta_{\text{N}}$  are the chemical shift changes in the  $^1\text{H}^{\text{N}}$  and  $^{15}\text{N}$  dimensions respectively (Figure 4.2). This analysis shows that apart from resonances which could not be observed due to line broadening, the CusF residues that were most significantly affected by the addition of CusB are T48, W44, D37, A40 and T19, in decreasing order. Other residues manifested smaller, but still significant chemical shift changes, including V42, N43, K31, I34, K23, T52, I53, T54 and L81.

Because Ag(I) is expected to distribute approximately equally between the two proteins, the spectra are a reflection of both metal occupancy and protein-protein interactions. Upon comparison with the apo-CusF spectrum, the resonances for residues A18, T19, S29 and F72 in the Ag(I)-CusF plus apo-CusB spectrum were found in

identical positions to those of the apo-CusF spectrum. Resonances for A41, E46, N43, D66, L78, F70, H35 and M49 are found along the trajectory between the resonance positions of apo-CusF and Ag(I)-CusF. However, most residues, including Q14, V21, K23, I25, K30, K31, I34, D37, W44, T52, I53, T54, S60, K63, Q74, L80, L81, I84 and V86 have chemical shifts distinct from those in the spectra of CusF with Ag(I) either fully-bound or at substoichiometric concentrations. These residues reflect the additional effects of the presence of CusB.

The chemical shift comparisons were used to map the interaction site of CusB on the CusF structure. The residues whose resonances had chemical shift differences greater than 0.05 ppm were mapped on the CusF structure (Figure 4.3 (B)). The resonances that were broadened beyond detection can also be considered to be affected by CusB, though the magnitude of the effect is unknown (Figure 4.3 (A)). The residues from both of these classes of effects map to a distinct face on the Ag(I)-CusF structure (Figure 4.3 (C)). The CusB interaction face on CusF as identified by these chemical shift perturbations is on the same face that forms the metal binding site (Figure 4.3 (B)). This face consists primarily of an anti-parallel  $\beta$ -sheet formed by strands  $\beta$ 1-  $\beta$ 3.

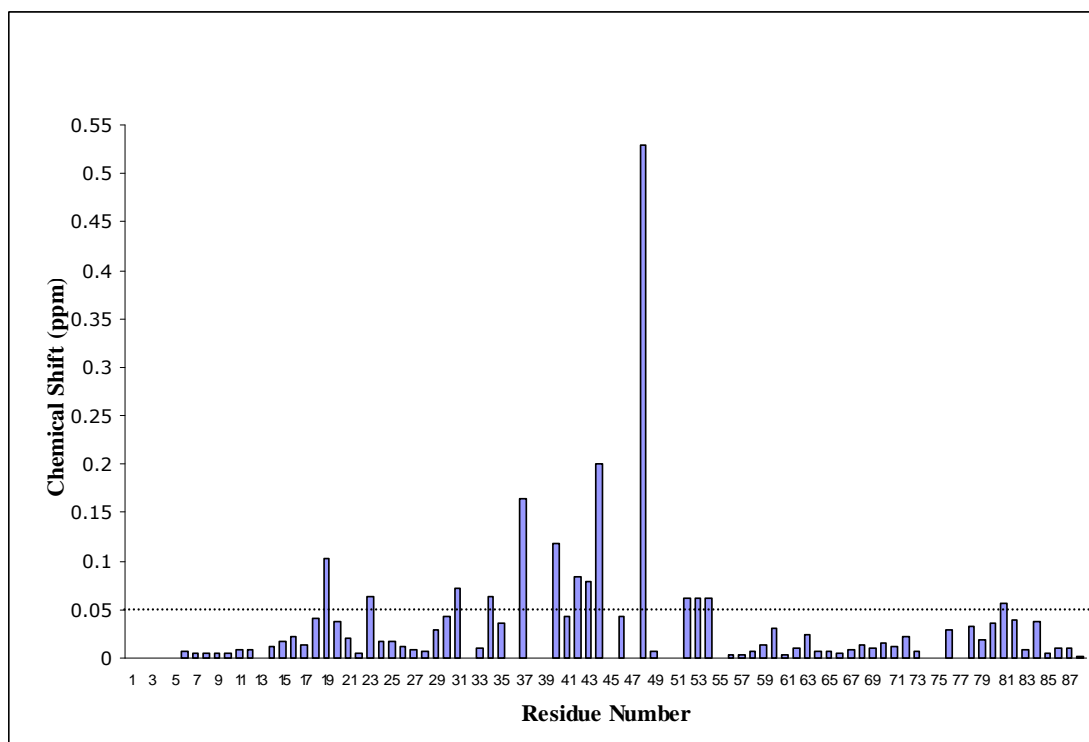


**FIGURE 4.2** Combined  $^1\text{H}$  and  $^{15}\text{N}$  chemical shifts in parts per million between Ag(I)/CusF/CusB and Ag(I)-CusF as a function of CusF residue number.

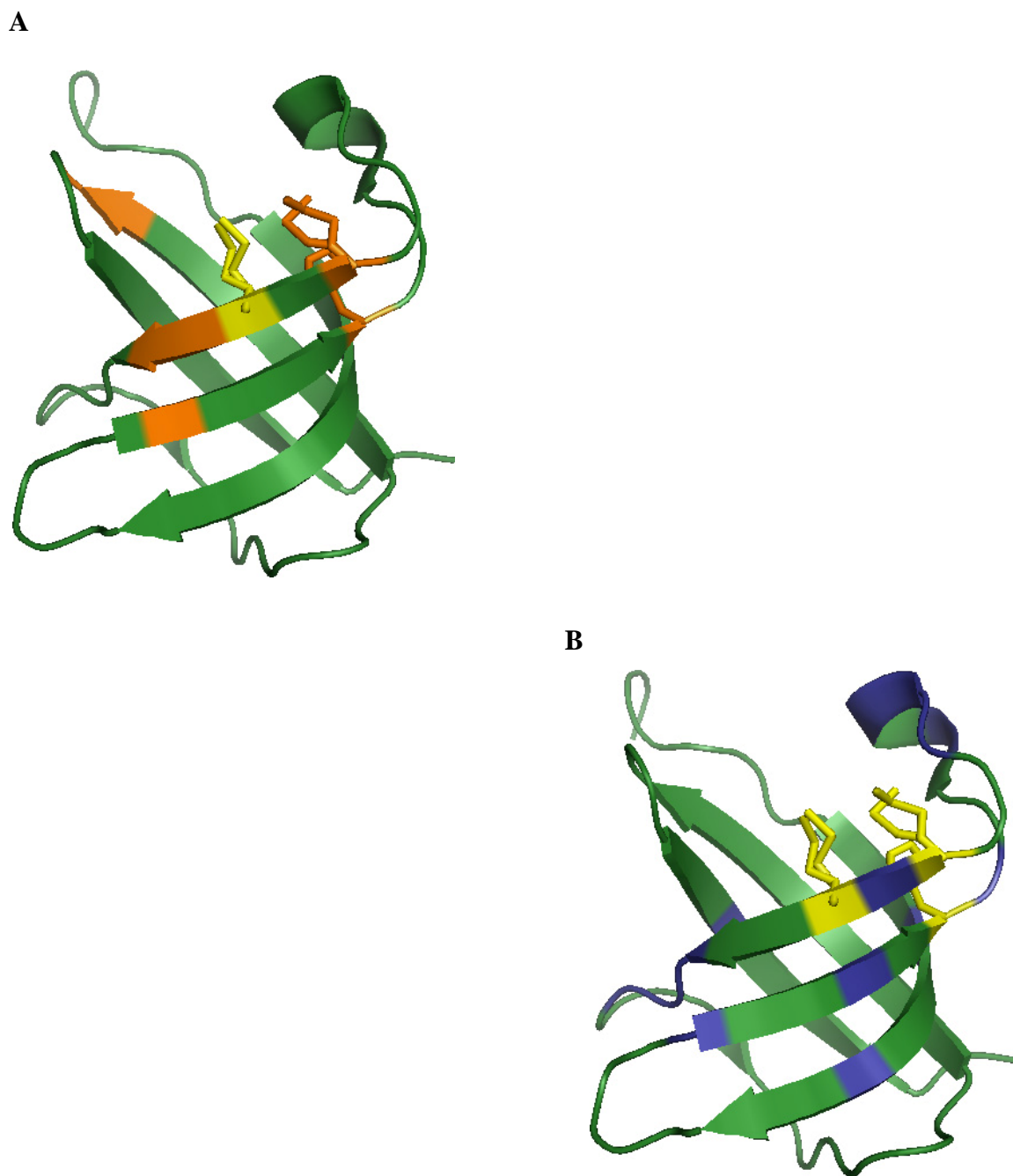


**FIGURE 4.3** Cartoon representation of CusF, showing **(A)** residues (orange) that were broadened beyond detection and; **(B)** residues (blue) that showed significant chemical shift variations, in Ag(I)/CusF/CusB<sup>1</sup>H-<sup>15</sup>N HSQC spectrum. Residues colored in yellow form the Ag(I) binding site in CusF (PDB ID: 2QCP) (Loftin et al., 2007).

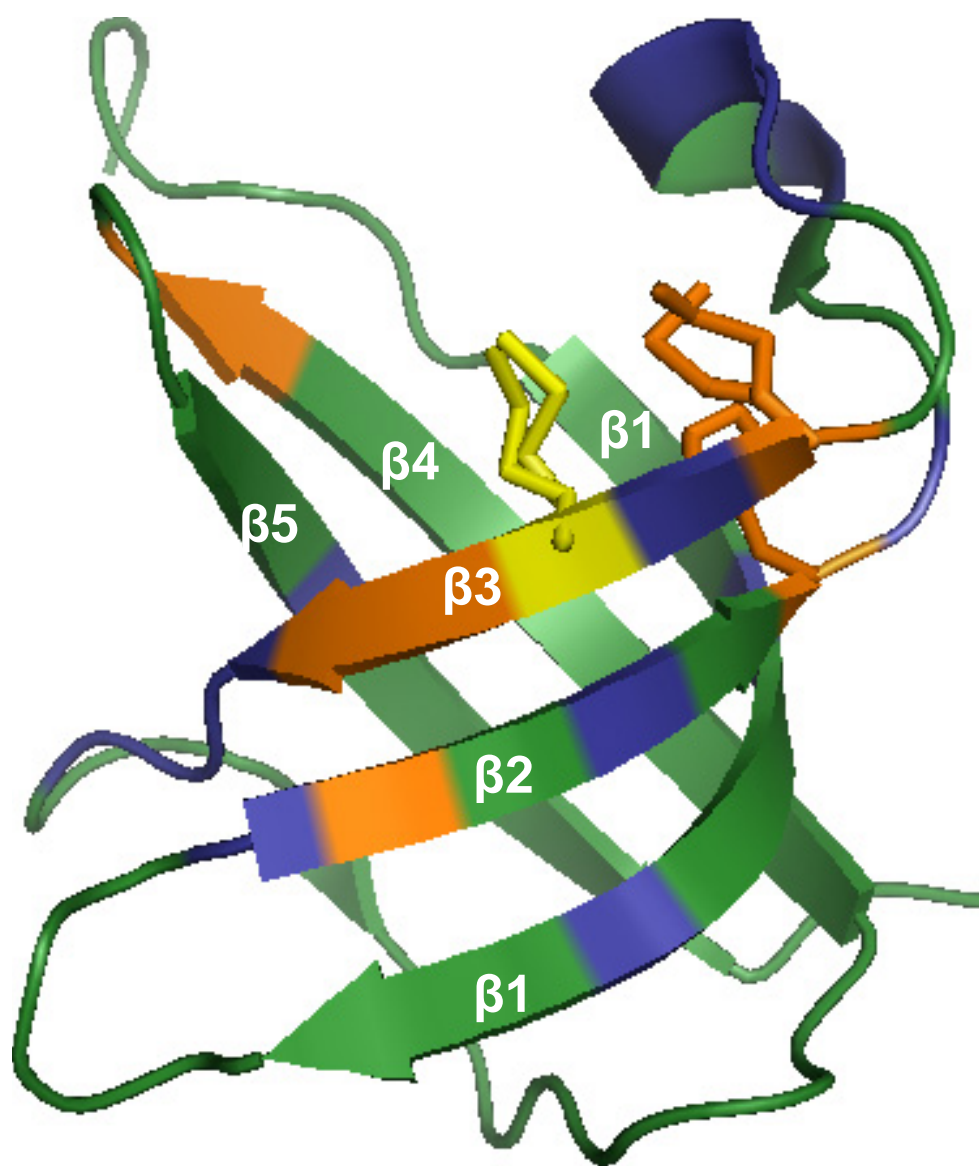


**FIGURE 4.3(C)** Cartoon representation of Ag(I)-CusF showing both effects combined. Residues colored orange are broadened beyond detection; those colored blue show significant variations in the chemical shifts (PDB ID: 2QCP) (Loftin et al., 2007).

## 4.4 DISCUSSION

From these results, it is clear that the interaction between CusF and CusB is specific between the two proteins and depends on the presence of the metal ion. Metal-dependent interaction has been reported previously for chaperone Atx1 and its partner Ccc2 (Banci et al., 2006). Comparison of the Ag(I)-CusF/CusB spectrum with the apo-CusF and Ag(I)-CusF spectra shows that most resonances manifest some amount of change, however small. In addition, Ag(I)-CusF and CusB appear to be in the fast exchange regime on the NMR time scale. Exchange regimes on the NMR time scale (magnitude of the chemical shift difference ( $\Delta\delta$ )), are broadly classified as slow, fast and intermediate regimes; regime being related to the equilibrium dissociation constant (Chowdhry and Harding, 2001). If the complex dissociation is very fast, that is the rate of equilibration ( $1/\tau$ ) is faster than the chemical shift separation ( $1/\tau \gg \Delta\delta$ ), only a single set of resonances whose chemical shifts are the fractionally weighted average of free and bound chemical shifts are observed. In this case, the resonances of the nuclei that are perturbed move in a continuous fashion during titration and are easily traceable. However, in slow ( $1/\tau \ll \Delta\delta$ ) exchange regime, one observes one set of resonances for the free and another for the bound forms of protein (Zuiderweg, 2002). Since we observe only one set of resonances for Ag(I)/CusF/CusB samples, it is reasonable to conclude that they are in fast exchange.

Mapping of the chemical shift variations on the CusF structure demonstrates that CusB binds CusF on the same face as that used to bind the metal ion, which makes sense

because metal is important for the interaction. This is also the face that other proteins with the same fold as CusF, that is the OB fold (Loftin et al., 2005), use for ligand binding (Agrawal and Kishan, 2003). Proteins belonging to the OB fold family have mostly been found to bind either oligosaccharides or oligonucleotides (Murzin, 1993; Murzin et al., 1995) and hence the name 'OB' (oligonucleotide/oligosaccharide binding). Those with a nucleotide binding function are reported to possess one or more patches of aromatic and basic amino acids, which are used for stacking interactions with nucleotides and electrostatic interactions with the phosphate backbone, respectively (Agrawal and Kishan, 2003). Others in the OB-fold family, though they may have diverse function including protein-protein interaction, have also been found to use a particular face of the domain for interaction.

A close look at the residues in CusF affected by CusB binding reveals that two-thirds of these residues are either basic, aromatic or polar uncharged. It is thus plausible that CusF also interacts with CusB via electrostatic/hydrophilic interactions. Electrostatic interactions have been previously showed to be the prime recognition feature in other copper chaperone/acceptor systems like Atx1-Ccc2 (Arnesano et al., 2001; Banci et al., 2001), Cox17-Sco1 (Abajian and Rosenzweig, 2006; Abajian et al., 2004; Horng et al., 2004), and CopZ-BsCopA (Banci et al., 2003). Although CusF possesses a distinct fold compared to those reported for the known copper chaperones and a unique motif that forms a tri-coordinate metal binding site as opposed to bi-coordinate observed in others (Lamb et al., 2001; Wernimont et al., 2000), it likely still shares the chemistry that

governs binding and metal transfer in all these chaperones. A better understanding at the molecular level requires structural characterization of CusB and its complex with CusF.

## CHAPTER 5

### BIOCHEMICAL CHARACTERIZATION OF FULL-LENGTH AND TRUNCATED CUSB CONSTRUCTS

In this chapter, the various constructs are discussed that were designed to either improve the yields of CusB or produce CusB amenable for structural studies. Short constructs consisting of only one domain of CusB were generated, which may be suitable for characterization by either NMR or crystallography. I performed all the work described in this chapter.

#### 5.1 INTRODUCTION

CusB is a periplasmic adaptor component of the CBA-type copper efflux CusCFBA system present in *Escherichia coli*. The three components CusC, CusB and CusA represent the outer membrane factor, the periplasmic adaptor/membrane fusion protein and the inner membrane resistance-nodulation-division (RND) type proton/substrate antiporter, respectively. The Cus system and members of the putative metal efflux CBA systems are homologous to the multi-drug export CBA systems such as AcrAB-TolC and MexAB-OprM. The drug exporting class of CBA systems has been found to be the major cause of intrinsic and acquired resistance in gram-negative bacteria (Poole, 2001). The proteins in this class export a wide variety of toxic molecules

including antibiotics, dyes, detergents, bile salts, organic solvents and antimicrobial peptides (Poole, 2004). CusC, CusB and CusA have amino acid identities of 25%, 25% and 21% with TolC, AcrA and AcrB, components of the drug-export AcrAB-TolC system, with significant BLAST expect values of 0.013, 9e-23 and 3e-49, respectively. Due to the increased emergence of antibiotic resistance, the drug transport CBA systems have been intensively investigated, both at the structural and biochemical levels.

Through X-ray crystal structure studies, the outer membrane components (Akama et al., 2004a; Koronakis et al., 2000) and the inner membrane components (Murakami et al., 2002) have been shown to exist as trimers and are proposed to form a drug extrusion channel as the periplasmic domains of TolC and AcrB dock with each other (Murakami et al., 2006). In contrast, the periplasmic adaptor component AcrA from AcrAB-TolC system and MexA from MexAB-OprM system crystallized as a dimer of dimers (Mikolosko et al., 2006) and tridecamers (Akama et al., 2004b; Higgins et al., 2004), respectively, in the asymmetric unit. The stoichiometry observed for the adaptor component in these structures appears physiologically improbable since it doesn't allow a reasonable docking of the adaptor component with the other two proteins. For the three components to interact in the transport process, they are expected to closely fit with each other. Additionally, the periplasmic adaptor structures from the multidrug resistance systems are missing a significant fraction (approximately 2/3) of the polypeptide chain. In the case of MexA, 28 residues at the N-terminus and 101 at the C-terminus were disordered in the crystal (Akama et al., 2004b) and for AcrA, a 28 kDa stable core, which

was missing 44 residues at the N-terminus and 90 at the C-terminus, was crystallized (Mikolosko et al., 2006).

To obtain a better picture of the periplasmic component of CBA systems and to delineate the molecular details of copper regulation in the Cus system, we attempted structural characterization of CusB through X-ray crystallography and NMR spectroscopy. As both of these techniques require large amounts of purified, stable proteins, the first step towards successful structural characterization is to produce suitable protein. This chapter describes the generation of several overexpression systems, as well as purification and initial characterization of CusB from these systems.

## 5.2 MATERIALS AND METHODS

**5.2.1 *CusB* crystallization and NMR sample preparation.** For crystallization, CusB was purified as described previously (Bagai et al., 2007). However, instead of combining the fractions that contained full-length CusB from MonoQ separation, the fractions that contained a truncated form of protein, which is produced from the full-length protein as a natural consequence of purification, were combined. The truncated version is shortened by 34 residues at the N-terminus and elutes at a higher concentration of NaCl (approximately 130 mM) as opposed to the full-length CusB, which elutes at approximately 50 mM NaCl during the gradient separation on a MonoQ anion exchange column (Amersham). The protein was dialysed against 10 mM Tris-NO<sub>3</sub>, pH 7.0 and concentrated using a 5 kDa cut-off Amicon (Millipore) concentrator to a final concentration of 14.0 mg/mL. The concentration was determined using the BCA assay (Pierce). This protein was sent to the Hauptman-Woodward Medical Research Institute (700 Ellicott Street, Buffalo, NY 14203, USA) for screening of crystallization conditions.

For NMR analysis, CusB was made in M9 minimal media (Sambrook et al., 1989). The cells containing *cusB* on an expression plasmid pASK3 were grown and protein was expressed similar to that described for <sup>15</sup>N-CusF preparation in chapter 4. <sup>15</sup>N-CusB was purified as described previously (Bagai et al, 2007). The protein was dialyzed against 50 mM phosphate, pH 7.0 and concentrated to a final concentration of 200 μM. <sup>2</sup>H<sub>2</sub>O was added to a final concentration of 10%. <sup>1</sup>H-<sup>15</sup>N HSQC (Bodenhausen and Ruben, 1980) experiments were performed at 298 K on a Varian Inova 600 MHz spectrometer. 128

increments of 2048 complex data points were collected. Spectral widths of 7.2 kHz and 1.82 kHz were used in  $^1\text{H}$  and  $^{15}\text{N}$  dimensions respectively. Spectra were processed with NMRPIPE (Delaglio et al., 1995) and analyzed using NMRView (Johnson and Blevins, 1994). Additional spectra were collected using the TROSY (Riek et al., 2000) option of HSQC as supplied by Varian BioPACK.

**5.2.2 Full-length *cusB* (residues 1-379) cloning in pET22b (*CusB*-His) and protein expression.** Genomic DNA from *E. coli* strain W3110 was used to amplify the *cusB* gene. The primers used for the PCR reaction (forward primer, AAACATATGAAAAAATCGCGCTTATTATCGG; reverse primer, AAAC TCGAGGCTGCCGCGCGGCACCAGATGCGCATGGGTAGCACTTTC) contained unique restriction sites at the 5' end (*NdeI*) and 3' end (*XhoI*). The reverse primer also contained a sequence for a thrombin cleavage site. After restriction enzyme digestion of the PCR product, it was ligated into the pET22b (Novagen) vector. The sequence for this and all the other constructs were confirmed by DNA sequencing. The resulting construct contained the full-length *cusB* gene followed by a region encoding thrombin cleavage site (LVPRGS) and a C-terminal His affinity tag (HHHHHH).

For protein expression, *cusB*-containing plasmid was transformed into *E. coli* BL21 ( $\lambda$ DE3). Cells were grown in LB media containing 100  $\mu\text{g/mL}$  ampicillin at 37 °C until they reached an O.D.<sub>600</sub> of 0.6-1.0, then induced with 0.5 mM isopropyl-beta-D-thiogalactopyranoside (IPTG) and grown at 30 °C for another 5 hours. Cells were harvested by centrifugation and frozen at -20 °C.

Cell pellets were resuspended in 40 mL of 50 mM phosphate, 300 mM NaCl, pH 7.5. Protease inhibitors (leupeptin (final concentration 2  $\mu$ g/mL), pepstatin (final concentration 2  $\mu$ g/mL), and PMSF (final concentration 0.5 mM)) and DNaseI (approximately 150 units) were added and cells were lysed by a French Press. Lysate was divided in two halves and 3-((3-Cholamidopropyl) dimethylammonio)-1-propanesulfonate (CHAPS) (0.1% w/v) (MP Biomedicals) was added to one half. Cells were then pelleted by centrifugation at 31000Xg. To determine the levels of expression, samples from both supernatants and pellets obtained from centrifugation were run on SDS-PAGE and stained with Coomassie. CusB-His protein was also verified by Western blot analysis using horseradish peroxidase-conjugated antibody specific to the *His*-tag (Novagen).

**5.2.3 *CusB* N-terminal domain (residues 11-260) (*CusB*-NTD) cloning in *pET28b* and protein purification.** *cusB*-pASK3 (Bagai et al., 2007) was used to amplify the N-terminal domain (NTD) of CusB. The primers used for the PCR reaction (forward primer, AAAAAAAACATATGGAACGTAAAATCTTATTCTGGTAC; reverse primer, AAAAGGATCCTCAATCCACGCCAGGTAGCAGCG) contained unique restriction sites at the 5' end (*NdeI*) and 3' end (*BamHI*). After restriction enzyme digestion of the PCR product, it was ligated into the pET28b (Novagen) vector.

For protein expression, the *cusB*-pET28b construct was transformed into *E. coli* BL21 ( $\lambda$ DE3). Cells were grown at 37 °C in LB media containing 40  $\mu$ g/mL kanamycin until they reached an O.D.<sub>600</sub> of 0.5. At this point, the culture was split into two halves

and tested for induction with different IPTG concentrations. One half was induced with 0.5 mM and the other was induced with 0.05 mM IPTG, respectively. Cell growth was continued at 30 °C for another 5 hours. Cells were harvested by centrifugation and frozen at -20 °C. To determine protein content in the soluble fraction of the CusB-NTD construct, cells were processed in a similar fashion as described above for full-length CusB. SDS-PAGE analysis was done on supernatant and pellet resulting from centrifugation of the cell lysate. The protein was found in the pellets. However, since the pI of this truncated form of protein, as determined using the ProtParam tool in ExPasy (<http://ca.expasy.org/tools/protparam.html>), was 7.2, the protein may have precipitated due to use of a buffer with the pH close to the pI of the protein. However, re-processing the cells in 50 mM Tris, pH 9.0 also resulted in precipitation.

Because the majority of the CusB-NTD was found in inclusion bodies, efforts were made to develop a purification protocol for the protein in inclusion bodies. For protein extraction from inclusion bodies, cells were grown in 4 L of LB media and harvested as above. A total of 27 grams of cell pellet was obtained. The pellet was re-suspended in 140 mL of 100 mM Tris pH 9.0, 10% sucrose using approximately 5 mL of buffer for every gram of cells. After adding suitable concentrations of protease inhibitors, DNase and lysozyme, cells were subjected to sonication. Lysed cells were centrifuged at 31,000Xg. The resulting pellet was weighed and stored at -20 °C until ready to use. A total of 6.0 grams of pellet was obtained. The pellet was re-suspended in the wash buffer (50 mM Tris pH 9.0, 30 mM NaCl and 1 mM EDTA) containing 1% Triton X-100. After readjusting the pH, which had dropped slightly upon Triton addition, the pellet was

gently homogenized using a cold glass homogenizer and then centrifuged at 26000Xg for 30 minutes. The pellet obtained in this step was similarly re-suspended, homogenized and centrifuged again to further clarify the supernatant. Finally, the pellet resulting from the 2 wash steps above was re-suspended in the wash buffer but without detergent. Further homogenization and centrifugation resulted in a pellet that weighed approximately 1.5 grams. This pellet was re-suspended in 10 mL of denaturation buffer (50 mM Tris pH 9.0, 6 M GuHCl) and stirred for approximately 30 minutes before ultracentrifugation at 200,000Xg. The supernatant from centrifugation, which contained the CusB protein, was slowly added to the renaturation buffer (50 mM Tris pH 9.0, 800 mM NaCl, 1 mM EDTA). The protein was stirred in this buffer overnight and was then dialyzed against buffers of gradually decreasing salt concentration from 800 mM NaCl to 400 mM NaCl and then 200 mM NaCl. The slow reduction of the salt concentration prevented the refolding protein from falling out of solution. Finally, the protein was dialyzed against 50 mM Tris pH 9.0.

**5.2.4 *CusB C-terminal domain (residues 260-379) (CusB-His-CTD-Strep) cloning in pET28b, protein purification and CD structure characterization.*** *cusB*-pASK3 (Bagai et al., 2007) was used to amplify the C-terminal domain (CTD) of CusB. The primers used for the PCR reaction (forward primer; AAAAAAACATATGGATGCCGCGACCCGCACG; reverse primer, TTCACAGGTCAAGCTTATTATTTTTC) contained unique restriction sites at the 5' end (*NdeI*) and 3' end (*HindIII*). After restriction enzyme digestion of the PCR product,

it was ligated into the pET28b (Novagen) vector. The resulting construct consists of a His affinity tag and thrombin cleavage site at the N-terminus followed by the gene sequence corresponding to residues 260-379 in CusB and a Strep tag at the C-terminus (CusB-His-CTD-Strep).

For expression and purification, *cusB His-CTD-Strep*-pET28b construct was transformed into *E. coli* BL21 ( $\lambda$ DE3) cells. Cells were grown in LB media containing 40  $\mu$ g/mL kanamycin at 37 °C until they reached an O.D.<sub>600</sub> of 0.5, then induced with 0.1 mM IPTG and allowed to grow for another 7 hours at 25 °C. Cells were harvested by centrifugation for 30 minutes. Cell pellets were then resuspended in 20 mM phosphate, pH 7.0 containing 10 mM imidazole. After adding the protease inhibitors cocktail at concentrations as stated above, cells were lysed by French Press and then pelleted by centrifugation at 31,000Xg for 45 minutes.

The supernatant was loaded at 0.5 mL/min. on an 80 mL Ni Sepharose High Performance (Amersham) column equilibrated with 20 mM phosphate, pH 7.0 containing 10 mM imidazole. The column was washed with the same buffer at 0.5 mL/min until the absorbance signal at 280 nm stabilized. A gradient of 10-500 mM imidazole was run at 5 mL/min and 7 mL fractions were collected. The elution was monitored at 280 nm and individual fractions were analyzed using SDS-PAGE. CusB-His-CTD-Strep containing fractions were combined and concentrated using an Amicon filtration unit with a 10 kDa filter. Protein was dialyzed against 50 mM phosphate, pH 7.0 for Circular Dichroism (CD) structure determination.

CD spectra were obtained using a Jasco J-715 spectropolarimeter. The value of extinction coefficient used ( $\epsilon_{280} = 1,500 \text{ M}^{-1} \text{ cm}^{-1}$ ), was obtained from Pace *et al* (Pace *et al.*, 1995). The constant parameters used for the experiment are: (i) Resolution: 0.1 nm; (ii) Band width: 1.0 nm; (iii) Sensitivity: 20 mdeg; (iv) Response: 2 sec; (v) Speed: 20 nm/min; (vi) Accumulations: 5; and (vii) Temperature: 25 °C. Far UV CD spectra were obtained using protein concentrations of approximately 60  $\mu\text{M}$  in a 0.1 cm circular cell thermostatically controlled at 25 °C.

**5.2.5 *CusB* CTD (residues 260-379) cloning in pET29a (*CusB*-CTD-Strep), protein purification and NMR characterization.** The region encoding the C-terminal domain of *cusB* was sub-cloned from the pET28b construct using NdeI and HindIII restriction enzymes, and ligated to the pET29a (Novagen) vector. The resulting construct consists only of Strep-affinity tag at the C-terminus of CusB-CTD (CusB-CTD-Strep).

For protein expression and purification, cells were grown, harvested and processed in a similar manner to that described above. 100 mM Tris, 150 mM NaCl, pH 8.0 (Tris-NaCl) was used to re-suspend the pelleted cells. The supernatant resulting from French pressing and centrifugation was loaded onto the Strep affinity column. After washing the column with approximately 100 mL Tris-NaCl buffer, protein was eluted using Tris-NaCl buffer containing 2.5 mM desthiobiotin. SDS-PAGE was used to determine the fractions that contained the protein of the right molecular weight. These fractions were combined and protein was concentrated using a 5 kDa cut-off Amicon concentrator (Millipore). Unlike the CusB-His-CTD-Strep protein, the protein purified

from this construct (CusB-CTD-Strep) was soluble under the conditions tested allowing the potential for NMR analysis. For NMR analysis, CusB-CTD-Strep was  $^{15}\text{N}$ -labeled.

For the preparation of uniformly  $^{15}\text{N}$ -labeled protein, *E. coli* BL21 ( $\lambda$ DE3) strain containing pET29a-*cusB-CTD-Strep* was grown in M9 minimal media (Sambrook et al., 1989) containing 1.0 g/L  $^{15}\text{NH}_4\text{Cl}$  (Cambridge Isotopes Laboratories) as the sole nitrogen source.  $^{15}\text{N}$ -CusB-CTD-Strep was expressed and purified as described above, dialyzed against 50 mM MOPS, pH 7.0 and concentrated to 400  $\mu\text{M}$ .  $^2\text{H}_2\text{O}$  was added to a final concentration of 10%.  $^1\text{H}$ - $^{15}\text{N}$  HSQC (Bodenhausen and Ruben, 1980) experiments were performed at 298 K on a Varian Inova 600 MHz spectrometer. 128 increments of 2048 complex data points were collected. Spectral widths of 7.2 kHz and 1.82 kHz were used in  $^1\text{H}$  and  $^{15}\text{N}$  dimensions respectively. Spectra were processed with NMRPIPE (Delaglio et al., 1995) and analyzed using NMRView (Johnson and Blevins, 1994).

**5.2.6 *CusB* (residues 1-260) cloned in pASK3.** The region encoding residues 1-260 of CusB was sub-cloned from the *cusB-pASK3* construct (Bagai et al., 2007). The primers used for the PCR reaction (forward primer; AAAAAAGAATTCATGAAAAAATCGCGCTTATTATCG; reverse primer, AAAAAACTCGAGATCCACGCCAGGTAGCAGCG) contained unique restriction sites at the 5' end (*EcoRI*) and 3' end (*XhoI*). After restriction enzyme digestion of the PCR product, it was ligated into the pASK3 (IBA, Germany) vector. The expressed protein will have residues 1-260 of CusB followed by the Strep tag (CusB-NTD-Strep).

## 5.3 RESULTS

**5.3.1 *CusB* crystallization and NMR characterization.** Full-length CusB, during the process of purification, is partially cleaved at the N-terminus, resulting in a truncated protein which lacks 34 residues at the N-terminus. Crystallization was attempted for this truncated form of CusB. This truncated version of CusB at a concentration of 14 mg/mL was submitted to Hauptman Woodward Institute for crystal screening. Crystals were observed in 2 of the 1530 conditions tested (Figure 5.1 (A)). The two conditions that showed crystals in the screens are (i) 100 mM  $\text{NaH}_2\text{PO}_4 \cdot \text{H}_2\text{O}$ , 100 mM CAPS, pH 10.0, 20% (v/v) PEG 400 and; (ii) 100 mM  $\text{Mg}(\text{NO}_3)_2 \cdot 6\text{H}_2\text{O}$ , 100 mM TAPS, pH 9.0, 40% (v/v) PEG 400.

Reproduction of the crystals in-house was only successful for one of the two conditions, when slight modifications were made. The crystal growth was observed in 150 mM  $\text{NaH}_2\text{PO}_4 \cdot \text{H}_2\text{O}$ , 50 mM CAPS, pH 10.0, 10% (v/v) PEG 400. These crystals were very small (approximately 60  $\mu\text{m}$  on the longest edge) and not suitable for diffraction. A fresh drop of protein in the mother liquor was seeded with one of these crystals but no increase in the crystal size was observed. SDS-PAGE analysis of the protein drops revealed that CusB degrades to the lower molecular weight species within a week of setting up the plate (Figure 5.1(B)).

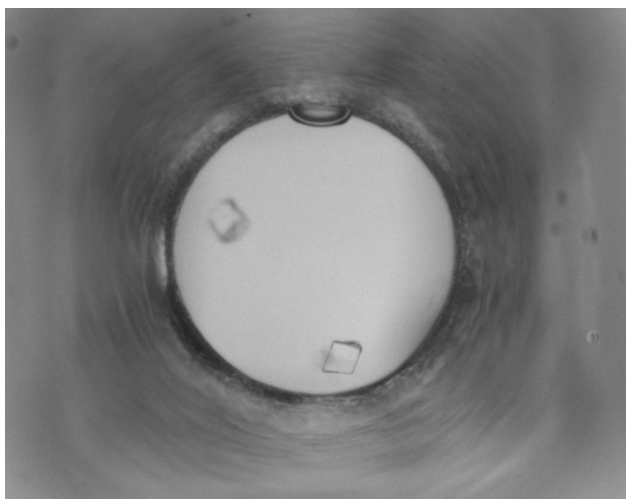


**FIGURE 5.1 (A)** Crystal screening results; (TOP) 100 mM  $\text{NaH}_2\text{PO}_4 \cdot \text{H}_2\text{O}$ , 100 mM CAPS, pH 10.0, 20% (v/v) PEG 400 and; (BOTTOM) 100 mM  $\text{Mg}(\text{NO}_3)_2 \cdot 6\text{H}_2\text{O}$ , 100 mM TAPS, pH 9.0, 40% (v/v) PEG 400.

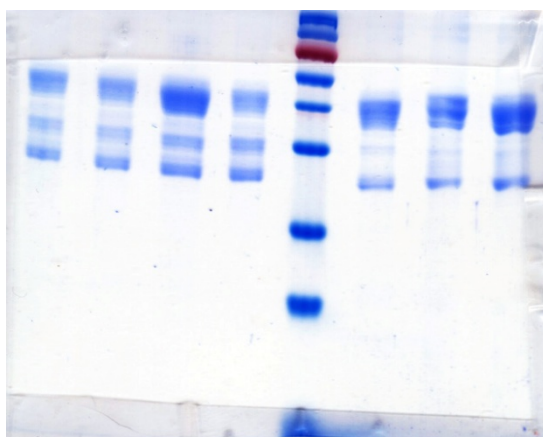
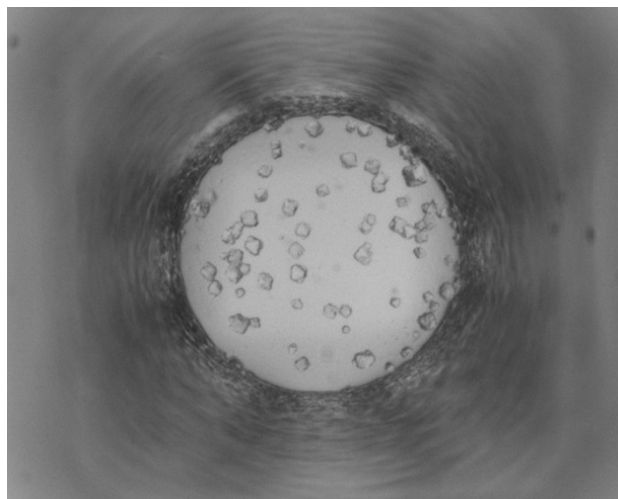


**FIGURE 5.1(B)** CusB drops from crystallization plates run on SDS-PAGE after 1 week of setting up the plate in 150 mM  $\text{NaH}_2\text{PO}_4 \cdot \text{H}_2\text{O}$ , 50 mM CAPS, pH 10.0, 10% (v/v) PEG 40.

Initial attempts at NMR characterization of the full-length CusB resulted in a spectrum ( $^1\text{H}$ - $^{15}\text{N}$  HSQC) with very few peaks collapsed in the centre of the spectral window (Figure 5.2). No change in the spectrum occurred when the HSQC experiment was performed using a Transverse Relaxation- Optimized Spectroscopy (TROSY) pulse sequence (data not shown). The TROSY technique can improve spectral resolution as it suppresses transverse nuclear spin relaxation which is the direct cause of deterioration of NMR spectra of large molecular structures (Riek et al., 2000). This result suggested that the concentration of protein was not high enough to result in a significant signal/noise ratio for all the residues in the protein or it was unfolded or partially aggregated at NMR concentrations.

To improve upon CusB yields and also to obtain a construct amenable for structural studies using NMR or X-ray crystallography techniques, *cusB* was re-cloned either as full-length or a partial sequence in different vectors. To decide the beginning and end of the partial sequences, the CusB sequence was aligned and compared with the sequence of MexA. MexA is a homologous periplasmic adaptor protein from the xenobiotic-exporting MexAB-OprM CBA system, whose crystal structure is available (Akama et al., 2004b). CusB and MexA sequences were submitted to the Protein Disorder Predictor (PONDR) program (Romero et al., 1997) to determine the disordered regions in the two proteins. Additionally, the disordered regions predicted for MexA in the N- and C- terminal regions were compared with the regions that could not be seen in the MexA electron density map. Since the regions that could not be seen in the electron density matched with the ones that were predicted to be disordered by PONDR, the CusB

sequence that was more likely to be disordered as predicted by PONDR was not included in the cloned sequences.

### **5.3.2 Expression of full-length CusB (residues 1-379) cloned in pET22b (CusB-His).**

*cusB* cloning in pET22b resulted in a construct that contained the full-length *cusB* gene followed by a region encoding thrombin cleavage site (LVPRGS) and a C-terminal His affinity tag (HHHHHH) (Figure 5.3(A)).

CusB-His was efficiently expressed from this construct; however most of the expressed protein went into inclusion bodies. This was concluded after comparing the amount of protein present in supernatant versus pellet obtained after cell lysis and centrifugation. (Figure 5.4) shows SDS-PAGE revealing the status of protein in cell pellet versus supernatant. Not only did most of the protein go into inclusion bodies, but it also degraded to a lower molecular weight species.

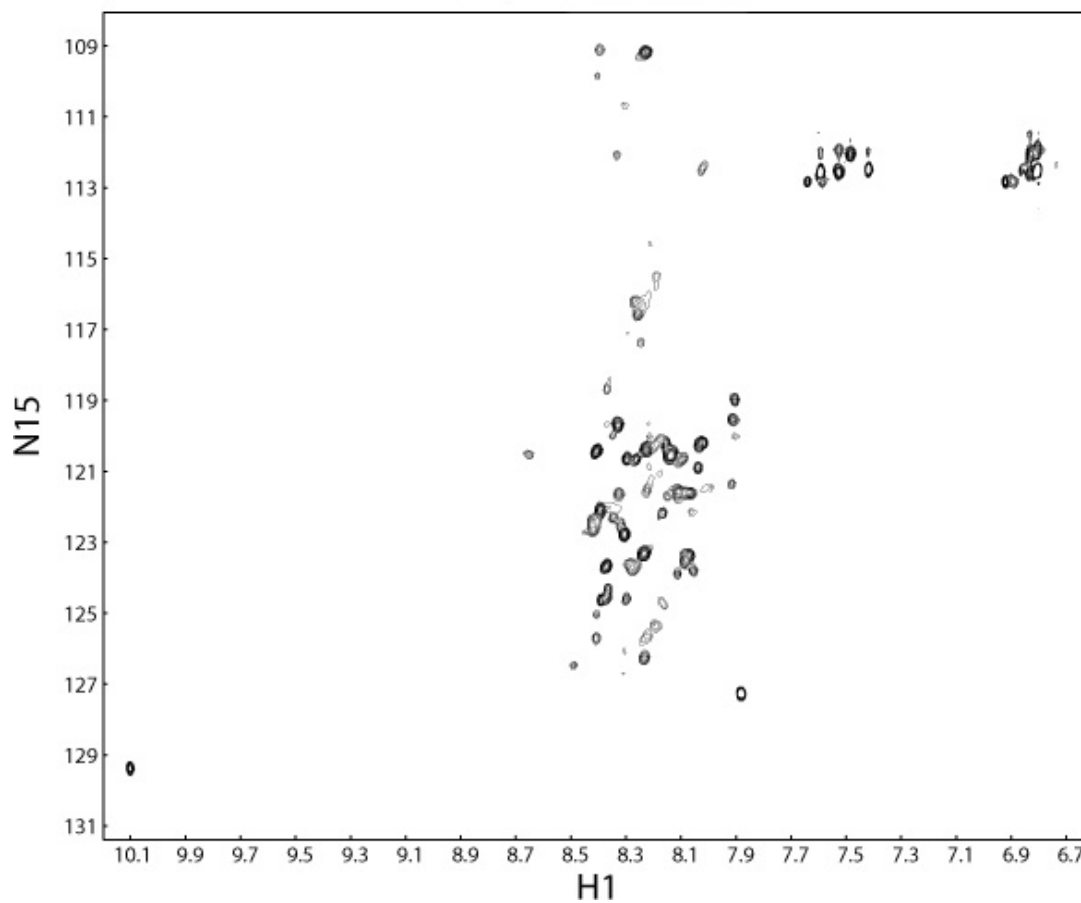


**FIGURE 5.2**  $^1\text{H}$ - $^{15}\text{N}$  HSQC collected at 600 MHz for 200  $\mu\text{M}$  full-length CusB in 50 mM phosphate, pH 7.0.

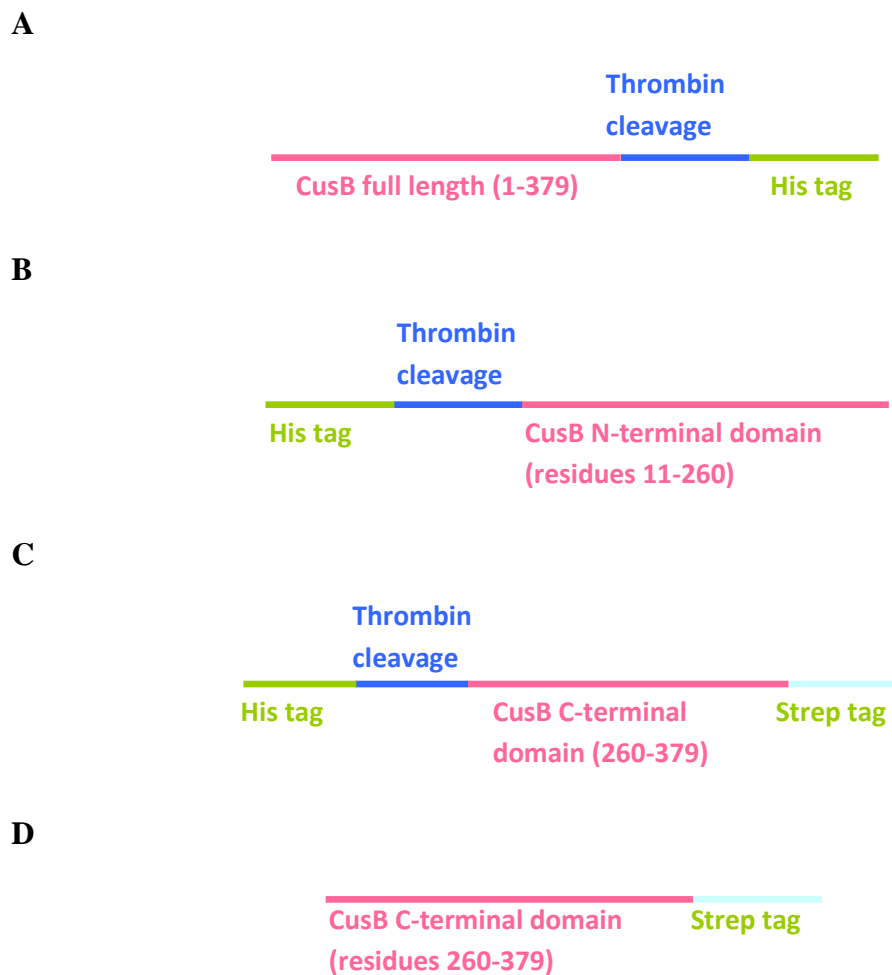


**FIGURE 5.3** Schematic of various CusB constructs. **(A)** CusB full-length in pET22b (CusB-His); **(B)** CusB N-terminal domain (residues 11-260) in pET28b (CusB-His-NTD); **(C)** CusB C-terminal domain (residues 260-379) in pET28b (CusB-His-CTD-Strep); **(D)** CusB C-terminal domain (residues 260-379) in pET29a (CusB-CTD-Strep).

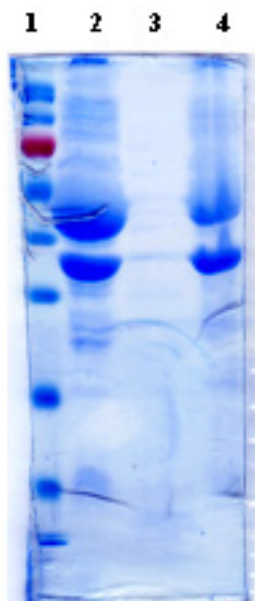


**FIGURE 5.4** SDS-PAGE for CusB-His expressed from *cusB*-pET22b construct. Lanes: (1) Marker; (2) Pellet from lysate mixed with detergent; (3) Supernatant; (4) Pellet from lysate without detergent.

**5.3.3 *CusB* N-terminal domain (residues 11-260) (*CusB*-NTD) in *pET28b*, protein purification and characterization.** In the full-length *CusB*, the first 10 residues following a signal peptide sequence of 24 residues were predicted to be disordered by the PONDR program (Figure 5.5). Additionally, the C-terminal end of *CusB* is likely to be disordered. One-third of homolog MexA C-terminal was not observed in the electron density map (Akama et al., 2004b). By comparison of the *CusB* sequence with that of MexA, a construct lacking the C-terminal third of *CusB* was made.

Furthermore, JPRED secondary structure prediction for *CusB* was done in order to avoid cutting off the sequence in the middle of a well-formed secondary structure. Based on these observations, the region encoding *CusB* residues 11-260 were cloned into the *pET28b* expression vector. At the 5' end of *cusB*, is a gene sequence for His affinity tag followed by a thrombin cleavage site (Figure 5.3(B)).

Upon expression, the *CusB*-NTD was found in inclusion bodies with both 0.5 mM and 0.05 mM IPTG. The protein was extracted and purified from inclusion bodies using the protocol described in the methods section. However, the protein could not be concentrated to more than 60  $\mu$ M because it precipitated on the concentrator membrane. Buffers of different pH and salt concentrations did not help in solubilization of the protein. This construct was not pursued further.

```

                                PONDR Protein Disorder Predictor

    Developed by P.  Romero, X.  Li, A.K.  Dunker,Z.  Obradovic, E.  Garner.

                                VL3 Predictor

                                DEPP Predictor
    Developed by P.  Radivojac

                                VSL1 Predictor
    Developed by K.  Peng and Z.  Obradovic

=====VLXNNP STATISTICS=====
Predicted residues: 379                      Number Disordered Regions: 6
Number residues disordered: 120              Longest Disordered Region: 41
Overall percent disordered: 31.66           Average Prediction Score:0.3280

Predicted disorder segment (1)-(10)         Average Strength= 0.8704
Predicted disorder segment (42)-(64)        Average Strength= 0.7512
Predicted disorder segment (136)-(159)      Average Strength= 0.6955
Predicted disorder segment (270)-(276)      Average Strength= 0.5749
Predicted disorder segment (294)-(308)      Average Strength= 0.6701
Predicted disorder segment (339)-(379)      Average Strength= 0.7066

=====PREDICTOROUTPUT=====

                "D" = Disordered                " " = Ordered

1      EPPAEKTSTA ERKILFWYDP MYPNTRFDKP GKSPFMDMDL VPKYADEESS
VLXT   DDDDDDDDDD                                DDDDDDDDDD

51     ASGVRIDPTQ TQNLGVKTAT VTRGPLTFAQ SFPANVSYNE YQYAIQARA
VLXT   DDDDDDDDDD DDDD

```

101	AGFIDKVYPL TVGDKVQKGT PLLDLTIPDW VEAQSEYLLL RETGGTATQT
VLXT	DDDDD DDDDDDDDDD
151	EGILERLRLA GMPEADIRRL IATQKIQTRF TLKAPIDGVI TAFDLRAGMN
VLXT	DDDDDDDDDD
201	IAKDNVVAKI QGMDPVWVTA AIPESIAWLK KDAQFTLTIV PARPKTLTI
VLXT	
251	RKWTLLPGVD AATRTLQLRL EVDNADEALK PGMNAWLQLN TASEPMLLIP
VLXT	D DDDDDD DDDDDDD
301	SQALIDTGSE QRVITVDADG RFVPKRVAVF QASQGVTLR SGLAEGEKVV
VLXT	DDDDDDDD DD DDDDDDDDD
351	SSGLFLIDSE ANISGALERM RSESATHAH
VLXT	DDDDDDDDDD DDDDDDDDD DDDDDDDDD

**FIGURE 5.5** Disordered regions in processed full-length CusB as predicted by PONDR.

**5.3.4 *CusB C-terminal domain (residues 260-379) (CusB-His-CTD-Strep) cloning in pET28b, protein purification and CD structure characterization.*** This construct was designed to facilitate structural characterization of the C-terminal part of CusB, which in the case of homologous MFPs has eluded structure determination (Akama et al., 2004b; Mikolosko et al., 2006). It consists of a Histidine affinity tag and a thrombin cleavage site at the N-terminus followed by the gene sequence corresponding to residues 260-379 in CusB and Strep tag at the C-terminus (Figure 5.3 (C)).

CusB-His-CTD-Strep was purified using the His affinity column as described in the methods section. The protein could not be concentrated above approximately 60  $\mu\text{M}$  due to protein precipitation. Though this concentration is not suitable for NMR or crystallographic studies, the protein could be used for secondary structure prediction studies using Far-UV CD spectroscopy. From the spectrum, CusB-His-CTD-Strep may have a slight  $\alpha$ -helical character but it mostly exists as a random coil (Figure 5.6).

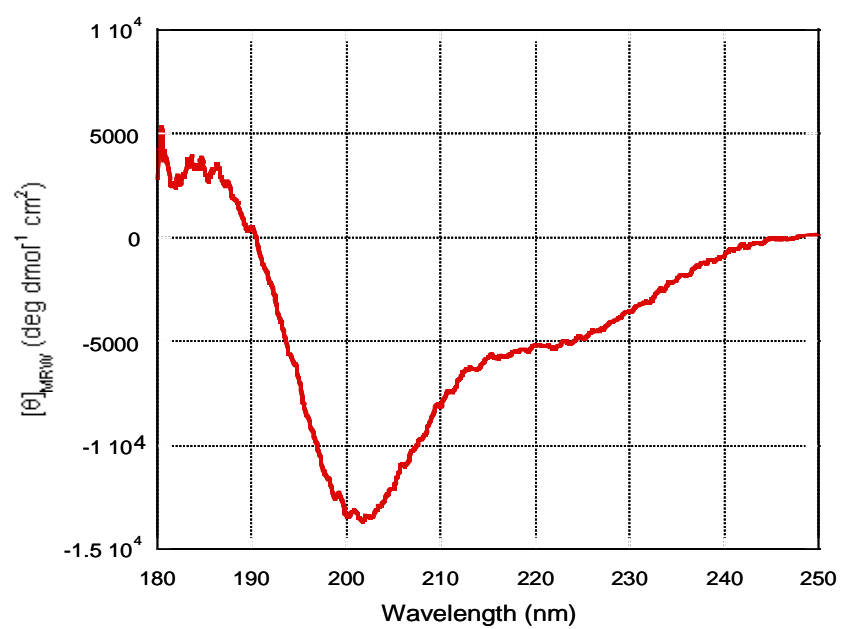


**FIGURE 5.6** Far UV-CD spectra for 60  $\mu\text{M}$  CusB-His-CTD-Strep.

**5.3.5 *CusB* CTD (residues 260-379) cloning in pET29a, *CusB*-CTD-Strep purification and NMR characterization.** This construct consisted of a Strep-affinity tag at the C-terminus of CusB-CTD-Strep (Figure 5.3D). Considering that His tag could partly be responsible for the solubility problems faced with the CusB-His-CTD-Strep construct, CusB-CTD-Strep without a His tag was designed.

CusB-CTD-Strep could be concentrated to 400  $\mu$ M concentration. The  $^1\text{H}$ - $^{15}\text{N}$  HSQC spectrum didn't show any peaks (Figure 5.7), likely due to protein aggregation.

**5.3.6 *CusB* (residues 1-260) expression in pASK3.** pASK3 expression vector has a tet promoter as opposed to the lac promoter in pET vectors. Since expression from the tet promoter is substantially reduced compared to that of the lac promoter, this construct was designed to test whether controlled expression and having a signal peptide sequence, which targets the protein to the periplasm, would prevent the protein from going into inclusion bodies. Due to time constraints, whether this construct is effective in producing soluble protein has not yet been determined.

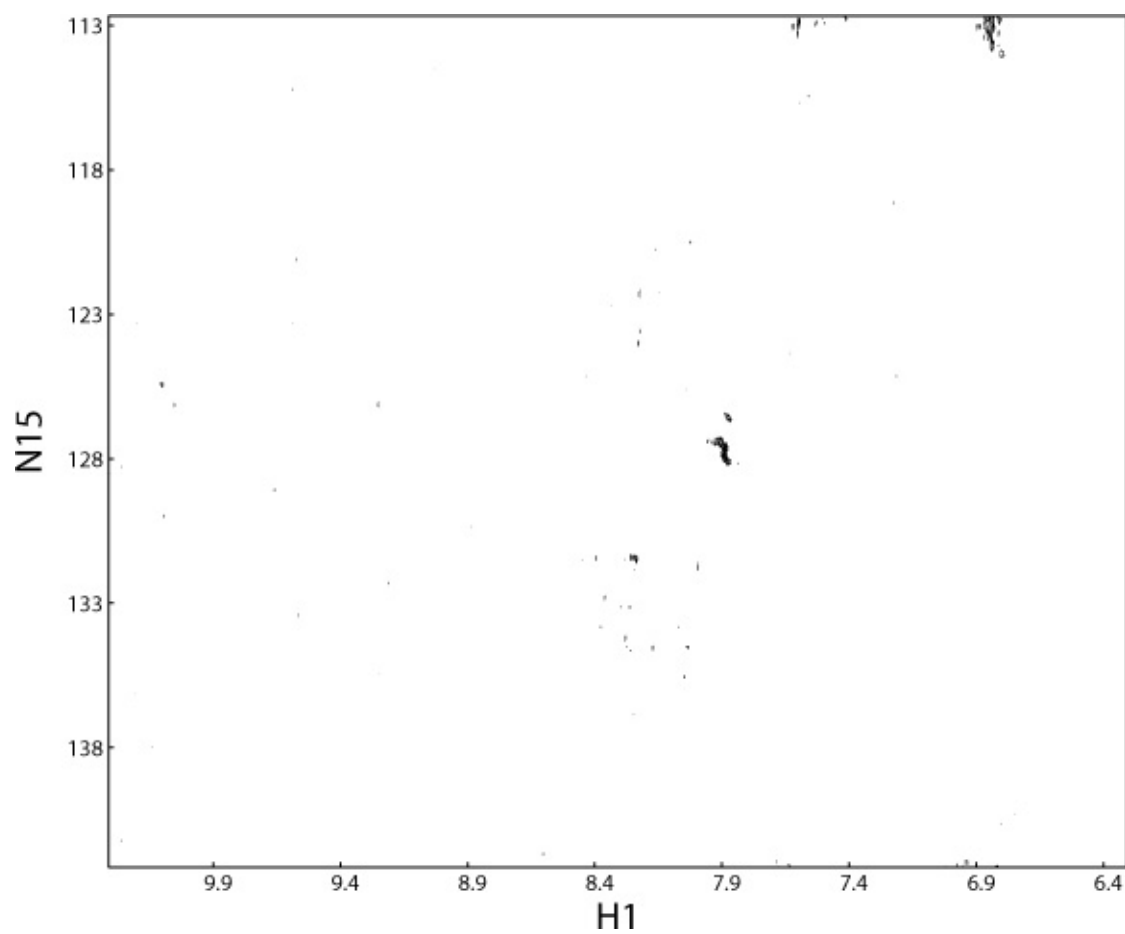


**FIGURE 5.7**  $^1\text{H}$ - $^{15}\text{N}$  HSQC of 400  $\mu\text{M}$  CusB-CTD-Strep in 50 mM MOPS, pH 7.0.

## 5.4 SUMMARY

The following table summarizes the results obtained from testing various CusB constructs that were generated to either improve the yield of CusB or produce CusB suitable for structural studies.

<b>Construct</b>	<b>Affinity tag</b>	<b>Result</b>
CusB(full-length)-pET22b <b>CusB-His</b>	C-terminal His	Protein insoluble
CusB (N-terminal domain; residues 11-260)-pET28b <b>CusB-NTD</b>	N-terminal His	Insoluble
CusB (C-terminal domain; residues 260-379)-pET28b <b>CusB-His-CTD-Strep</b>	N-terminal His and C-terminal Strep tags	Purified using His-affinity column. Far UV-CD suggests that CusB-His-CTD-Strep is mostly a random coil.
CusB (C-terminal domain; residues 260-379)-pET29a <b>CusB-CTD-Strep</b>	C-terminal Strep tag	$^1\text{H}$ - $^{15}\text{N}$ HSQC at 400 $\mu\text{M}$ protein concentration shows no peaks
CusB (N-terminal domain; residues 1-260)-pASK3 <b>CusB-NTD-Strep</b>	C-terminal Step tag	Not tested

## CHAPTER 6

### GENERAL CONCLUSIONS AND FUTURE DIRECTIONS

The work in this dissertation was a biochemical investigation of the periplasmic adaptor/membrane fusion component, CusB and its interactions with CusF of the CBA type copper efflux system present in *E. coli*. The periplasmic component is the least understood of the 3 components studied in homologous CBA type multidrug exporters. The periplasmic component was originally termed a Membrane Fusion Protein (MFP) due to homology with the paramyxoviral membrane fusion proteins (Dinh et al., 1994) and reports citing a function for the periplasmic component in fusing the inner and outer membranes (Zgurskaya and Nikaido, 1999b). More recently it was termed periplasmic adaptor protein based on studies showing its interaction with the inner and outer membrane components (Touze et al., 2004). Thus, it has mostly been postulated to act as a bridge between the inner and the outer membrane proteins with no direct evidence of its active involvement in the efflux process. To better define the role of MFPs in CBA type metal transporters and understand the molecular details of copper regulation demonstrated by Cus system, the study of CusB was undertaken.

Experiments described in chapter 2 indicate the likelihood of CusB's active role in the efflux mechanism. Isothermal titration calorimetry (ITC) experiments demonstrated that CusB binds Ag(I) with high affinity (Figure 2.1). X-ray absorption spectroscopy data (XAS) indicated that the metal environment in CusB is an all-sulfur

three-coordinate environment (Figure 2.2). Candidates for the metal-coordinating residues were identified from sequence analysis, which showed four conserved methionine residues, at positions 21, 36, 38 and 283 (Appendix B). Mutations of three of these methionine residues to isoleucine resulted in significant effects on CusB metal binding *in vitro*. Methionine 36 and 38 mutants showed no specific binding to Ag(I) and the binding affinity decreased 10 fold for the M21I mutant (Figure 2.3). Cells containing these CusB variants also showed a decrease in their ability to grow on copper containing plates, indicating an important functional role for metal binding by CusB (Table 2.1). Furthermore, gel filtration chromatography demonstrated that upon binding metal, CusB undergoes a conformational change to a more compact structure (Figure 2.5). Based on these structural and functional effects of metal binding, it was concluded that the periplasmic component of CBA efflux systems plays an active role in export through substrate-linked conformational changes.

Chapter 3 further substantiates the importance of periplasmic component CusB in the metal export and establishes the role of a fourth component, CusF, uniquely present in the Cus system, as a metallochaperone. Using ITC, it was shown that CusB interacts with CusF in a metal-dependent fashion; the interaction occurs only when one of the proteins is in the metal-bound state and the other is in the apo- state. In the absence of metal, or if both proteins are occupied with metal, no interactions were detected (Figure 3.1). Metal transfer between CusF and CusB was demonstrated using XAS. As both CusF and CusB use methionine residues for metal coordination, the metal sites of CusF and CusB were distinguished in the XAS experiments by incorporation of

selenomethionine into CusF. The results of the XAS experiments on CusF/CusB/Cu(I) samples showed that Cu(I) can be reversibly transferred between CusF and CusB with an approximately 50% end distribution between the two proteins (Figure 3.3, 3.4, 3.5; Table 3.1). It also indicated the possibility of transient adduct formation between CusF and CusB. Furthermore, CusB was shown not to interact with a CusF homolog, SilF which has 51% identity to CusF (Figure 3.6) and binds Ag(I) with a comparable affinity, indicating that the interaction is specific for the proteins in the Cus system. It also proved that there is a direct exchange of metal rather than metal being released into the solution by one protein to be taken up by another. These findings further pointed at a non-passive function of CusB in metal extrusion driven by the CusCFBA system and a copper chaperone role for CusF.

However, these results do not rule out the possibility of CusB being regulated by CusF for the metal transport. In the future, the regulatory function of CusF can be tested by generating CusF mutants that are unable to bind metal, although retain the wild-type structure and investigating their interactions with Ag(I)-CusB. If the mutants interacted with Ag(I)-CusB, it would mean that CusF likely facilitates metal extrusion by CusB, upon sensing metal in the environment. A stronger argument would be made if mutants of CusB are identified that are unable to bind metals though interact with Ag(I)-CusF.

In the future, the functional role of the conformational change in CusB upon metal binding should be investigated. It is likely that the demonstrated conformational change in CusB upon metal binding could have a regulatory role. It is thought that the helical hairpin region of CusB interacts with the helical region of the outer membrane protein

CusC, and thus propagated conformational changes through CusB may influence the opening of the CusC channel.

Additionally, the presence of CusF and CusB as one polypeptide in other efflux systems (Appendix C) implied that CusF and CusB work together as one protein in certain systems. In the Cus system of *E. coli*, perhaps they were separated to allow their independent regulation to enhance the efficiency of metal detoxification. Future experiments could test the effects of a CusB-CusF fusion protein in efficiently supporting metal resistance.

Chapter 4 discusses the structural characterization of interactions between CusF and CusB using NMR spectroscopy. Using HNCA spectra, resonances from Ag(I)-CusF in the presence of CusB were assigned (Appendix D). This revealed the residues in CusF that are significantly affected by the CusB binding (Figure 4.2). Mapping of the residues showing chemical shift variations on the CusF structure demonstrated that the CusB binding face of CusF overlaps with the metal binding site (Figure 4.3). This is also the face which is used by other proteins in the OB fold family to interact with their respective partners. From the nature of residues affected in CusF, it was concluded that electrostatic interactions are likely responsible for binding and specificity in CusF and CusB. For a better molecular characterization, CusB structure and the structure of its complex with CusF need to be solved.

From the HSQC spectrum obtained for the Ag(I)-CusF/CusB, it is clear that the two proteins are in fast exchange on the NMR time scale. The EXAFS data suggests the formation of transient adduct. This may be further verified by performing chemical shift

perturbation experiments at lower temperatures. As the rate of exchange would slow down, it may result in broadening of other peaks or a set of 2 peaks corresponding to two populations.

Determination of the structure of CusB is essential for the better understanding of copper regulation in the Cus system and MFPs in general. In chapter 5, various constructs that were designed to either improve the yields of CusB or produce CusB amenable for structural studies are discussed. While promising initial crystals have been produced, the conditions need refinement to obtain better crystals. Additionally, expression systems that produce more soluble protein could aid in achieving this goal.

The studies described in this dissertation have enhanced our understanding of the mechanism of metal efflux by CBA type transport systems. This work could have far reaching implications in our understanding not only of metal resistance systems, but the broader family of multidrug resistance systems as well. With growing concerns of the overuse of antibiotics and the selection for superbugs, studies like these will have serious impacts on human health.

## APPENDIX A

### ABBREVIATIONS

ABC	ATP-binding cassette superfamily
ACES	N-(2-Acetamido)-2-aminoethanesulfonic Acid
AHT	Anhydrotetracycline
AUC	Analytical ultracentrifugation
BLAST	Basic local alignment and search tool
CAPS	N-Cyclohexyl-3-aminopropanesulfonic acid
CD	Circular dichroism
CHAPS	3-((3-Cholamidopropyl)dimethylammonio)-1-propanesulfonate
DW	Debye-Waller
EXAFS	Extended X-ray absorption fine structure
FT	Fourier transform
HAE	Hydrophobe/amphiphile efflux
HME	Heavy metal efflux
HNCA	Hydrogen, nitrogen, carbon alpha
HSQC	Heteronuclear single quantum coherence
HW	Haber-Weiss
ITC	Isothermal titration calorimetry
JPRED	Secondary structure prediction server
MFP	Membrane fusion protein
MFS	Major facilitator superfamily
MOPS	3-(N-Morpholino)-propanesulfonic acid
NMR	Nuclear magnetic resonance spectroscopy
OMF	Outer membrane factor
PMSF	Phenyl methyl sulfonyl fluoride
PONDR	Protein disorder predictor
RND	Resistance, nodulation and cell division
SDS-PAGE	Sodium-dodecyl-sulfate- polyacrylamide gel electrophoresis
SEC	Size exclusion chromatography
TROSY	Transverse relaxation optimised spectroscopy
TAPS	N-Tris (hydroxymethyl) methyl-3-aminopropanesulfonic acid
XAS	X-ray absorption spectroscopy

## APPENDIX B

ClustalW sequence alignment of the mature, processed form of CusB and homologous proteins identified from a BLAST search of the non-redundant protein database using CusB from *Escherichia coli* as the query sequence. Only the top scoring sequence from each genus was selected for alignment to lower redundancy and generate a representative set. The positions of the nine methionines are indicated in bold text, and residue numbers are indicated above the sequence for methionines 21, 36, 38, and 283. The sequences are:

CusB NP\_415106.1 (*Escherichia coli* K12), YP\_309529.1 (*Shigella sonnei* Ss046), SILB\_SALTY (*Salmonella typhimurium*), YP\_863814.1 (*Shewanella* sp. ANA-3), NP\_941216.1 (*Serratia marcescens*), NP\_943483.1 (*Klebsiella pneumoniae*), ZP\_01039342.1 (*Erythrobacter* sp. NAP1), ZP\_01303698.1 (*Sphingomonas* sp. SKA58), YP\_617588.1 (*Sphingopyxis alaskensis* RB2256), ZP\_01419030.1 (*Caulobacter* sp. K31), YP\_348127.1 (*Pseudomonas fluorescens* PfO-1), YP\_315092.1 (*Thiobacillus denitrificans* ATCC 25259), YP\_693077.1 (*Alcanivorax borkumensis* SK2), YP\_001109837.1 (*Burkholderia vietnamiensis* G4), YP\_001098869.1 (*Hermineimonas arsenicoxydans*), YP\_001085940.1 (*Acinetobacter baumannii* ATCC 17978), YP\_973527.1 (*Polaromonas naphthalenivorans* CJ2), ZP\_01580136.1 (*Delftia acidovorans* SPH-1), YP\_001020823.1 (*Methylobium petroleiphilum* PM1), ZP\_01663246.1 (*Ralstonia pickettii* 12J), YP\_001007785.1 (*Yersinia enterocolitica* subsp.), YP\_049490.1 (*Erwinia carotovora* subsp. atroseptica SCRI1043), YP\_529403.1 (*Saccharophagus degradans* 2-40), ZP\_01109853.1 (*Alteromonas macleodii* 'Deep ecotype'), ZP\_01042144.1 (*Idiomarina baltica* OS145), YP\_957429.1 (*Marinobacter aquaeolei* VT8), ZP\_01075516.1 (*Marinomonas* sp. MED121), YP\_271496.1 (*Colwellia psychrerythraea* 34H), YP\_338846.1 (*Pseudoalteromonas haloplanktis* TAC125), ZP\_01611244.1 (*Alteromonadales bacterium* TW-7), ZP\_01307321.1 (*Oceanobacter* sp. RED65), ZP\_01261191.1 (*Vibrio alginolyticus* 12G01), ZP\_01219559.1 (*Photobacterium profundum* 3TCK), YP\_942789.1 (*Psychromonas ingrahamii* 37), YP\_001142727.1 (*Aeromonas salmonicida* subsp. *salmonicida* A449), ZP\_01166302.1 (*Oceanospirillum* sp. MED92), YP\_434211.1 (*Hahella chejuensis* KCTC 2396), YP\_001251512.1 (*Legionella pneumophila* str. Corby), YP\_742228.1 (*Alkalilimnicola ehrlichei* MLHE-1), YP\_755411.1 (*Maricaulis maris* MCS10), YP\_846551.1 (*Syntrophobacter fumaroxidans* MPOB), YP\_357128.1 (*Pelobacter carbinolicus* DSM 2380), YP\_343544.1 (*Nitrosococcus oceani* ATCC 19707), ZP\_01451725.1 (*Mariprofundus ferrooxydans* PV-1), ZP\_01200378.1 (*Xanthobacter autotrophicus* Py2), YP\_319729.1 (*Nitrobacter winogradskyi* Nb-255), YP\_666000.1 (*Mesorhizobium* sp. BNC1), YP\_114681.1 (*Methylococcus capsulatus* str. Bath), ZP\_01018326.1 (*Parvularcula bermudensis* HTCC2503), YP\_760400.1 (*Hyphomonas neptunium* ATCC 15444)

Escherichia	-----	
Shigella	-----	
Salmonella	-----	
Shewanella	-----	
Serratia	-----	
Klebsiella	-----	
Erythrobacter	-----	
Sphingomonas	-----	
Sphingopyxis	-----	
Caulobacter	-----	
Pseudomonas	-----	
Thiobacillus	-----	
Alcanivorax	-----	
Burkholderia	-----	
Herminiimonas	-----	
Acinetobacter	-----	
Polaromonas	-----	
Delftia	-----	
Methylibium	-----	
Ralstonia	-----	
Yersinia	-----	
Erwinia	-----	
Saccharophagus	-----	
Alteromonas	-----	
Idiomarina	-----	
Marinobacter	-----	
Marinomonas	-----	
Colwellia	-----	
Pseudoalteromonas	-----	
Alteromonadales	-----	
Oceanobacter	-----	
Photobacterium	-----	
Vibrio	-----	
Psychromonas	-----	
Aeromonas	-----	
Oceanospirillum	-----	
Hahella	-----	
Legionella	-----	
Alkalilimnicola	-----	
Maricaulis	-----	
Syntrophobacter	MKPLNNKEPGERLSQPGTTTRTGKKRGRVLILLLVIGAFAGGFYTARNPAIVG-----	53
Pelobacter	MTPLKK-----RFFFILLFVFLSVGGVWYGVHRAGSLA-----	33
Nitrosococcus	-----	
Mariprofundus	-----	
Xanthobacter	-----MKRTVLRGLTLVALVAAGAGGYWAGHRGIVIPGASTLFG	39
Nitrobacter	-----MKPLALMGLALAAILAAGAGGYWAGVRNLPITGLREWLG	39
Mesorhizobium	-----MPSDTWLRVP---WLESAGILP-----	20
Methylococcus	-----MKPSVRPILLFLLAGTGLGGYWLGRK-----	27
Parvularcula	-----	
Hyphomonas	-----MNRRLLLTVATSAALLAACSDASGVRSQGSSAGAG	36

Escherichia	-----EP-----	2
Shigella	-----MKKIALIIGSMIAGGIIISAAGFTWFAKAE-----	30
Salmonella	-----MASLKIKYAAIIISLLIAGGLISVTAWQYLNSSQK-----	35
Shewanella	-----MASLKIKYAAIIISLLIAGGLISVTAWQYVNSSQK-----	35
Serratia	-----MASLKIKYAAIIISLLIAGGLISVTAWQYVNSAQK-----	35
Klebsiella	-----	
Erythrobacter	-----MNSVLERFTQRQLFAAGLGIALVSLAAGYGLHMLGG-----	37
Sphingomonas	-----MGAAWDRLSRPQKSWMMAGTVALISLAAGYGLSQLGE-----	37
Sphingopyxis	-----MKHALSARARLLLLAAAAIALVGGAVGYGVASLS-----	33
Caulobacter	-----MSRATTLSPRS-LIAGAAISLLAAAGGYGLGQWR-----	34
Pseudomonas	-----MNRKQWN-----GVWLAGLALAVGVGGYGLAYQRM-----	31
Thiobacillus	-----MNRQTIKKTIVLGFVVVALLAAGVAAGLWWAGRY-----	35
Alcanivorax	-----MNIKRNALIGLAASLLLLAGIYLGRIYVTPSQS-----	32
Burkholderia	-----MNRKPLARAVLTVFAGAAALLGAGYFAGTRHAATGT-----	35
Herminiimonas	-----MKFKSTSTLKAIIILVIGAGLVFGGYWLGTRQSMKG-----	36
Acinetobacter	-----	
Polaromonas	-----MNKKYLLFALLAAGVLGATGY-VLYALGAKQAGTMPAAPMN---MP	42
Delftia	-----MKTKNLVMAIVAAGVLGAAGY-GLYTLGMRHGADMPATPSNPSGMA	45
Methylobium	-----MNTRQILWTVGAVSALALGGY-ALYQLGMQRG---MGHSATG---PA	40
Ralstonia	-----MN-RTIFARIAASLVASLGMGATYYLGVRQG-----	31
Yersinia	-----MKKYFSLTLVAVAVISG-IAGYLLGKPAS-----	28
Erwinia	-----MLSLMTLAILLSAGGVGYLVGKQQT-----	24
Saccharophagus	-----MKNVVLGGVVGFGALGAGALWALTSLITDRGQI-----	32
Alteromonas	-----MSTIKALVIGGVAGGIMTALAFTFLIPSSSTANN-----	35
Idiomarina	-----MKTVTKSLISLAVGFAVGAGTIGYVMQSTEVSDRS-----	35
Marinobacter	-----MANLVRPLGFVLLGGLAGAVATYWFATDTHALSSA-----	35
Marinomonas	-----MKPFLKNSLIIGVSLSIGAVSALTAYTYFQPLNAIDSSL-----	39
Colwellia	-----MTINKNTNDSVERPVVKVRHITLTGIIILGLVFGVITITLVVTSFLPSTTSV-----	50
Pseudoalteromonas	-----MNTNLKLLIAAVVGGGVLTALVLSLMPASNTDI-----	32
Alteromonadales	-----MNTNLKLFIAAIVGAGLWAGFTQIIADE-----	28
Oceanobacter	-----MVKKFLAALILLLVGALLGWQVAPLFSSAES-----	31
Photobacterium	-----MNKTFSAVITLAIGGALGY-----FAATTFSQNNVDQ-----	33
Vibrio	-----MKTLQVATIALIVGGALGFGANHFLTGSTHDMSAMGG-----	37
Psychromonas	-----MRYFLVLIVGLFLG-----IVATKNQQINSLFS-----	28
Aeromonas	-----MSHKSSQKLLVSALLLALGAGGGYWAAKQTGDGATAK-----	37
Oceanospirillum	-----MNKGFIAVIALSVGAAAGYWAPKQSAESSAEMGG-----	35
Hahella	-----MRLVISIIFIVAFAVAGWFASRHPALTGLMGEMDMA-----	36
Legionella	-----MNKKLLLIIVISIIILGVFLGRWTTNIIITGKASQEATN-----	37
Alkalilimnicola	-----MKFVS-LFIALLIGFGLGAGALWFHQGGTAGQGGG-----	34
Maricaulis	-----MTLKSyllGAALVGAGLTVGFFSASFLNADGSGSSD-----	36
Syntrophobacter	-----EIEKLAGSKGEAESKDVIYCPMPHPQIRSDKPGTCPICNMNEKMEKAPAGEQAA---108	
Pelobacter	-----EHASHD-VEGTQIARQQYTCGMHPMIIITDEPGDCPICGMALTPVKSGTTGQMCAA---87	
Nitrosococcus	-----MSKQTAMVIVLAFLLAALIG---VGGGYWYATYWAPKTAAPVS---40	
Mariprofundus	-----MNKNLLGISAAVAIGLAGGYFIFGGQQGEKDDRSKASARAD---43	
Xanthobacter	-----TTTVAAEPPPSGSGSVIYYKAPDGRFPVYSAAPGRTADDRPFLPVRASEEVSFEETP---94	
Nitrobacter	VEATFAAAEPAGTGAVIYYQDPDGKPAYSATPRKTADGRAFRVRASEDVSFEKQ---95	
Mesorhizobium	-----ASAGPAQSGPVIYYRDPDGQPFYSAPVKKKTANGRDFLAVHADEDVSFEKPG---72	
Methylococcus	-----TAPPPS-----	33
Parvularcula	-----MHPHYISTDPDGTCPICGMDL---21	
Hyphomonas	-----TSTDAQASYTCMHPHYISTDAGGSCPICGMDL---70	

	21	
Escherichia	----PAEKTSTA-----	ERKILFWYDPMYPNTRFDKPG 31
Shigella	----PAEKTSTA-----	ERKILFWYDPMYPNTRFDKPG 59
Salmonella	----TVPAEQKAP-----	EKKVLFWYDPMKPDTKFDKPG 65
Shewanella	----TVQTEQKAP-----	EKKVLFWYDPMKPDTKFDKPG 65
Serratia	----TEKTEQKAP-----	ERKVLFWYDPMKPDTKFDKPG 65
Klebsiella	-----	MLFWYDPMKPDTKFDKPG 18
Erythrobacter	---ESSGAGSA-----	TDTC---EDVLYWYDPMVPGQRFDEPG 70
Sphingomonas	---GQGGASDAGG-----	SATEC---EEVLYWYDPMVPGQHFDKPG 72
Sphingopyxis	-----GTGPAAE-----	RTEGD---RKVLYWYDPMYPNQHFDEPG 65
Caulobacter	-----KAPVPAA-----	GDAPG---RKVLYWYDPMVPAQRFDKPG 66
Pseudomonas	---NGVAASAPAP-----	APSTE---PKALYWYDPMYPQKQFDKPG 66
Thiobacillus	---TDTQDTHTAA-----	PAQHG---RTVLYWYDPMVPGQKFDKPG 70
Alcanivorax	---SISMAMDSGE-----	TNSKADE---KEVLYWYDPMYPQKQHFDEPG 69
Burkholderia	---AVASTGAASP-----	GGKIDPKTGRKVLWHDPMVNPQHFDKPG 74
Herminiimonas	-----ASTSAAAS-----	TERVDPKTGRKILYWHDPMPVGNKFDKPG 73
Acinetobacter	-----	MKPEQHFDKPG 11
Polaromonas	ADAGASPTAGPQS-MAEGEEATRRHISAGLKAGDTPVTGSKILYRDPMPVASKFDKPA	101
Delftia	SPQAATPAVAAPA-NESGEDATRRHIAAGLKAGDVPANGKKILYNDPMVPANKFDKPG	104
Methylobium	DPASPSPAEDPTSSIAAGEAATRRHIKAGIKAGDVPATGKPVLYHDPMPVPGKRFDAPA	100
Ralstonia	--QRSAPTQAAAS--AQAADAP-----	LKAGDIDPKTGRKILYWDPMAPGQRFDEPG 80
Yersinia	---HATSTVAASP-----	EVTAENS---RKVLYWYDPMSPGQRFDEPG 65
Erwinia	---PHSPS-----	TAEPE---RSVLYWYDPMVDPKRFDEPG 54
Saccharophagus	-----	NEAAE---AKPLYWVAPMDPNYRRDKPG 57
Alteromonas	-----	EQNEE---KQPLYWVAPMDPNYRRDEPG 60
Idiomarina	-----	SGNAE---KEPLYWVAPMDPNYRRDKPG 60
Marinobacter	-----	EQTSSDSKEPLYWVAPMDPNFKSDKPG 62
Marinomonas	-----	AEMAIDE--PLYWVAPMDPNYRRDKPG 64
Colwellia	-----	SDSSKEENKPLYWVAPMDANFRDQPG 77
Pseudoalteromonas	-----	KASTEKQPLYWVAPMDSNYRRDEPG 57
Alteromonadales	-----	KPAVKQPLYWVAPMDSNYRRDAPG 52
Oceanobacter	-----	EASSSNEPLYWVAPMDPNYRRDAPG 56
Photobacterium	-----	ETATSSEKQPLYWVAPMDPNYQRDKPG 60
Vibrio	-----	ESAASS--NDPLYWVAPMDPNYKRDKPG 63
Psychromonas	-----	ATQKTAEPEVLYWVAPMDANYQRDKPG 55
Aeromonas	-----	EKTPLYWVNPMDPRDKRDGPA 58
Oceanospirillum	-----	ESQPLYWVAPMDPNFKRDKPG 56
Hahella	-----	AAESGGEKQPLYWVAPMDPNYRRDKPG 63
Legionella	-----	KKPLYWIDPMEMPIHYPGPG 57
Alkalilimnicola	-----	SSEREVLYYQHFNPTIRSDRPG 57
Maricaulis	-----	STEPRLVYQAPMDPSFRSDTPG 59
Syntrophobacter	-----	KEQTSAGKPLEQRKILYWTDAMNPSFRSDKPG 141
Pelobacter	-----	DVPQGDK--PKGERKIKYWVAPMDPTYIRDEPG 118
Nitrosococcus	-----	ETPAK-----KPLFYRSPMNPEITSPVPA 64
Mariprofundus	-----	GPCAGGA-----QPLMWRNPMNPSVTSPAPA 69
Xanthobacter	-----	RAEAEKPAAGSGERRILYRNPMGLPDTSPVPR 126
Nitrobacter	-----	PTTAEATGQPGARRVLYRNPMGLPDTSPTPK 127
Mesorhizobium	-----	NKEVAAAPANGGAKRVLYRNPMGLPDTSPTPK 105
Methylococcus	-----	PAPETAAARRPLFYRNPMNPQVTSPVPA 61
Parvularcula	-----	VPADKTQETSSAGEILYKHPMGKPDTPSPVPK 54
Hyphomonas	-----	VPVSGTTASAG-RGDILYKHPMGQPDTPSPVPK 102

\*

	36 38	
Escherichia	KSPFMDMDLVPKYADE--ESS-----	50
Shigella	KSPFMDMDLVPKYADE--ESS-----	78
Salmonella	KSPFMDMDLVPKYADESGDKS-----	86
Shewanella	KSPFMDMDLVPKYADESGDKS-----	86
Serratia	KSPFMDMDLVPKYADDSGDKS-----	86
Klebsiella	KSPFMDMDLVPKYADESGDKS-----	39
Erythrobacter	KSPFMDMMLVPKCAGEAA-----	88
Sphingomonas	KSPFMDMQLVPKCAGEAA-----	90
Sphingopyxis	KSPFMDMELVPKYADEATS-----	84
Caulobacter	KSPFMDMQLVPRYADEAASA---A-----	87
Pseudomonas	KSPFMDMQLVPRYASGEEG-----	85
Thiobacillus	KSPFMDMDLVPKYADEGGD-----	89
Alcanivorax	PSPFMDMELVPRYANGGDDS---D-----	90
Burkholderia	KSPFMDMQLEPVYADE----GES-----	93
Herminiimonas	KSPFMDMQLVPVYADE-----GSD-----	92
Acinetobacter	KSPFMDMQLVPKYADENTAMTDES-----	35
Polaromonas	KSPFMDMMLVPVY-AAGQAD-----	120
Delftia	KSPFMDMMSPVY-ADGDAD-----	123
Methylobium	KSPFMDMMLVPVYGGAGGED-----	120
Ralstonia	KSPFMDMPLAPVY-ENGAGG-----	99
Yersinia	KSPFMDMELVPRYAGETVE-----	84
Erwinia	KSPFMDMELAPRYADDVQE-----	73
Saccharophagus	KSP-MGMDLIPVYNNDASSGAAG-----	79
Alteromonas	KSP-MGMDLIPVYE-ESSSGDAGPG-----	83
Idiomarina	KSP-MGMDLIPVYGDAAESSSPG-----	82
Marinobacter	KSP-MGMDLIPVYEGGGQADDTAG-----	85
Marinomonas	QSP-MGMDLIPVYANEAN-QDSGAG-----	87
Colwellia	QSP-MGMDLIPVYGSQNNTIDEAG-----	101
Pseudoalteromonas	LSP-MGMDLVPFYDEAPGSSNLDGP-----	82
Alteromonadales	LSP-MGMDLVPVYDEVGNSESEK-----	74
Oceanobacter	KSP-MGMDLVPVYEESSAEDSPG-----	78
Photobacterium	KSP-MGMDLIPFYEESQSGKKDPA-----	84
Vibrio	KSP-MGMDLIPVYAEEDLSG-EQDAP-----	86
Psychromonas	KSP-MGMDLVPVYAEKSAEAEKAEPKILYWVAPMDANYQRDKPGKSPMGMDLVPVFEEAG	114
Aeromonas	KDN-MGMDLIPVYEEQKSG--SPG-----	79
Oceanospirillum	LSP-MGMDLVPVYPEDLAGGDSPG-----	79
Hahella	KSP-MGMDLVPVYEEDAQGNDDGG-----	87
Legionella	KSR-MGMELVPVYPDDNQEKGEKA-----	80
Alkalilimnicola	KDE-MGMDYIPIYAGDEGRDDDP-----	79
Maricaulis	KSP-MGMDLIPVYEGEE-ADPDG-----	80
Syntrophobacter	KAP-DGMDLVPVYEEEDRPGAGLPP-----	165
Pelobacter	KSP-MGMDLVPVYEDQAPSGA-----	138
Nitrosococcus	KDA-MGMDYVPVYADEEGSGKA-PA-----	87
Mariprofundus	KDS-MGMDYIPVCADEGAGG---PA-----	90
Xanthobacter	KDS-MGMDYIPVYDG-----EAEDG-----	145
Nitrobacter	KDS-MGMDYIPVYEG-----EDDGG-----	146
Mesorhizobium	KDS-MGMDYIPIYEG-----EDEDG-----	124
Methylococcus	KDD-MGMDYVPVYAEGLTPSAGSGE-----	85
Parvularcula	KDS-MGMDYIPVYAD-----DTGS-----	72
Hyphomonas	KDF-MGMDYIPVYAD-----EAAE-----	120

. \* \*



Escherichia	VYPLTVGDKVQKGTPLLDLTIPDWVEAQSEYLLLRRETGG-----TATQTEGI	153
Shigella	VYPLTVGDKVQKGTPLLDLTIPDWVEAQSEYLLLRRETGG-----TATQTEGI	181
Salmonella	VYPLTIGDHVKKGTPPLIDITIPDWVEAQSEFLLLSGTGG-----TPTQIKGV	189
Shewanella	VYPLTTGDHVKKGTPPLIDITIPDWVEAQSEFLLLSGTGG-----TPTQIKGV	189
Serratia	VYPMTIGDHVKKGTPPLIDITIPDWVEAQSEFLLLSSTGG-----TSTQIKGV	189
Klebsiella	VYPLTIGDHVKKGTPPLIDITIPDWVEAQSEFLLLSGTGG-----TPTQIKGV	142
Erythrobacter	TYGLAQDDVVRGAPIVDILVPDWGGAQREYIAVLDTG-----DQALADAM	190
Sphingomonas	TYGRAPDDVVRGAPLADILVPEWGAQQEYLAFLNSG-----DELAQAM	192
Sphingopyxis	TYGRAPDDVIEAGAPLVDLLVPDWGGAQAEFLAVLRTG-----DRALASAA	186
Caulobacter	VYGHAPGDIVAAGAPIADLLNPDWAGAQT EYLA VRRIG-----DPRLTAAA	189
Pseudomonas	VYARAPGDVLTAGTALADILVPEWTAQSEFLALRRSG-----DADLIAAA	187
Thiobacillus	VARLAPNDVVRSGAPLIADILVPEWAAVQQEYLAALKALG-----DPSLEGAA	191
Alcanivorax	VWPLAEGDTISSGQPLMQLRVPAPWTGAQHEWLAVLGSG-----NNELIVAG	192
Burkholderia	LYANAPMQRIAKGAPVASLFVPEWLAPQEEYLA LKRGGM-----DATLLEAS	196
Herminiimonas	LYARSPMQRIKGEAIIASIFVPDWIAPQEEYLA LKRGG-----NTELMAAA	194
Acinetobacter	VYGHAVGDMVTEGSPLIADILVPEWTAQTEFLAVLRTG-----DKSLIQAS	137
Polaromonas	LHVRATLDRVRKGQPLLDLYVPEWAAQEEFLAVKRMQGS-----LASLVDGA	225
Delftia	LHVRATLDPVAKGQPLVSLYVPDWIAAQEEFLSVRRMKGTD-----LGGLVDGA	228
Methylibium	LHVRATLDRVRAGQPFADIIYVPEWAAQEEYLA VKRFAKDD-----AG-LAAAA	224
Ralstonia	AYAKTTLDPVKRGQPLIVYVPEWAAQEEYLA VSR TANAL-----QGDLRSAA	204
Yersinia	LYVRANQQPVTKNQPLAQWLIPDWSAAQQEYLAIRKLG-----DDALTAAA	186
Erwinia	LTVNALQQQVKKGETLATLWNPTWAAAQREYLA VRQLD-----DEILTQSA	175
Saccharophagus	LYVKSAGDPVQKGQPLYSLSYSPELVSAQEELILALNTGN-----TKLVKSV	179
Alteromonas	LHVKASGEYVKKGEPLYSLSYSPELVNAQEELLLAMRRNN-----KDLIVAA	183
Idiomarina	LFVKAVGNSVKAGEPLYSIYSPEMVNAQEELVLASQSGN-----QVLIDAA	182
Marinobacter	LFVKAGEGPEVQKQPLYTLYSPTLVNAQEELLLAMNRGN-----QKLVEAA	185
Marinomonas	AYIKASGEKITQGGPLYRLYSPALVNAQEYLFALGRKD-----KSLIKGA	187
Colwellia	LYINAIIGDPVTKGQPLVDFLYSPELVNAQEELLLALDRKN-----AVLVQGA	201
Pseudoalteromonas	LYIKAAGDSVEHGEPLYTLYSPQLVNAQEELLLALNRNN-----QVLIRAA	183
Alteromonadales	LYVKAQGDKVSAGEPLYTLYSPQLVNAQEELLLAVNRNN-----NVLIRAA	175
Oceanobacter	LHVKAVGNPVEKNQPLYDLYSPELVNAQEELLLALKSNN-----ASLLEAS	178
Photobacterium	LNINAIGEKVQKGDVLFDFLYSPELVNAQEELLLNAKRIG-----AVLVQGA	185
Vibrio	LYINAVGEKVKKGDVLFDTLYSPELVKAQEELLLNAYRTGR-----KGLVKGA	187
Psychromonas	LYVKSVEGVEKQALFDLYSPELVKAQESLFNAINLNR-----SNLITSS	220
Aeromonas	LAIKSEGQKVAKGSLLYEIIYAPDLVNAQHEYLLALNTTNP-----LLLLRAA	180
Oceanospirillum	LAVNTEGEAVEKGQQLLYEIIYSPELVNAQEYLLAALQSGN-----RYLRRAS	179
Hahella	LNKSSGDPVSKGQKLYEIIYSPALVNAQEYLLAALRGAN-----KILLKAS	186
Legionella	LVVKAVGDSVKKGQQLLYYSPQLVTAQEYLLIALEGNN-----QSLITAS	180
Alkalilimnicola	LRVRTTGERVTAGEVLFRLYSPALVSAQDELLQTLR--R-----NGNAGPA	178
Maricaulis	LPVAAVGDDVVSAGDLLFRMYSPEIATAQAEYLLQALRIGR-----DTLTSAS	180
Syntrophobacter	VFVDFTGKLVKKGQPLISIIYSPELVSTQMELLLARKSKETFAGSVFDEAASGANVLYEST	280
Pelobacter	LYVDETGQMVKNQPLALYSPKLVSAQQEYLLALNRDALKNSSFEEIAAGGDRLLTAA	252
Nitrosococcus	LFVDKTGAKVQKDEMLLSLYSPQLVATQQEYLLALNRNRETLEMSYPDIRQGAELVQST	202
Mariprofundus	LFVDKTGESVKENTMLLSFYAPELVATQEYLLALANWEQLKASQYKDIRREGAKRLDSS	205
Xanthobacter	VANVTTGERVVKGQALARLYAPDIAAAGAQQYITDL-----NGGVRGASAGGG	247
Nitrobacter	VANVTTGDRVTGQVLVRLYSPDIAAAGALFLSDL-----NIGGRDGAIGGA	248
Mesorhizobium	VASVTTGDRIAKGQALLQLYSPEVAVAGAQLLTVL-----NGSGLSDGLGGA	226
Methylococcus	LDVNTTGQVPVPGEVLLLEAYSPELVSTQEYRIAG-----SGAASRALREGA	187
Parvularcula	LAVNAEGDTPRPGSLLYRIYSPDLIAAQKDYLNFS-----RIG-NEARIASV	172
Hyphomonas	LTVRAEGDLVRPGALLYRVYSPDLIAAQKDYLNAF-----AIG-NDKRIAAV	221

: . \*

Escherichia	LERLRLAGMPEADIRRLIATQKIQTRFTTLKAPIDGVITAFDLRAGMNIKDNVVAQIQGM	213
Shigella	LERLRLAGMPEADIRRLIATQKIQTRFTTLKAPIDGVITAFDLRAGMNIKDNVVAQIQGM	241
Salmonella	LERLRLAGMPEEDIQRLRSTRTIQTRFTIKAPIDGVITAFDLRTGMNISKDKVVAQIQGM	249
Shewanella	LERLRLAGMPEEDIQRLRSTRSIQTRFTIKAPIDGVITAFDLRTGMNISKDKVVAQIQGM	249
Serratia	LERLRLAGMPEEDIQRLRSTRSIQTRFTIKAPIDGVITAFDLRTGMNISKDKVVAQIQGM	249
Klebsiella	LERLRLAGMPEEDIQRLRSTRTIQTRFTIKAPIDGVITAFDLRTGMNISKDKVVAQIQGM	202
Erythrobacter	RQRMRLGMDAMIASVERTRRRAQNTITVTAPVGGAVTMLGVRSGMTVMMEGQTLAEITGF	250
Sphingomonas	RERMRLGMPGLISSVGRNGRPQSTITVTAPIGGAITS LGVRPGMTVMAGQTLAEITGF	252
Sphingopyxis	RQRLVLLGMPQSTIAAVERSGRQNRVITINSPIGGTIKSLGVRQGM SVMAGQTLAEVNGL	246
Caulobacter	RSRLVLGMSPELIAAVERSGRVQPISTVRAPIGGVIQTL DVVRAGMSLTSGQTLAQISGL	249
Pseudomonas	RQRLRLTGMPASLIAQVERSGKVQSELTVTSPLGGVLQALDVVRAGMTVASGETLARVNGL	247
Thiobacillus	RERMRLSGMPESLIRDVAARGKIRNRIAITAPRGGVIQELDVVRAGMTVMGQTLARINGI	251
Alcanivorax	RERLLSLGMPASLIRSIERQQRKPLETWTVTAPHDGVIRSLNARAGMTLSAGAPVAEIQSL	252
Burkholderia	RARMRLSIPDGI IASLDRTGKAQTHVLLTSPESGVVSELNVRDGMVAPGQTLAKIAGL	256
Herminiimonas	RQRMRAMSIPDGLINQADRTGQSQQHFTLTSPVTGVITELSVRDGMVAPGMTIAKVAGL	254
Acinetobacter	RQRLQLLGI PQNVIHQVARTRRVQNTITLQAPISGFIDSLVRNGMALANGMTLAKIAGL	197
Polaromonas	RQRMRLAGMSDEQIRQVEASGKSQARFTITAPLGGVVVELMAREGMTVMAGTTLFRINGL	285
Delftia	RQRMRLQVGMDDAQIALVERSGQTQPRITLSAPLGGVAVEVLAREGMTVAPGATLFRINSL	288
Methylobium	RQRLLLAGMSEAQVVRVDAASTVQPRITLVAPSSGVVAELVAREGMTVSPGMMLARINGL	284
Ralstonia	LLRMRLQAGMTEAQIRLVESGKVPQRLAISIDGVI TEVGVDRGMVAPGMTLFRINSL	264
Yersinia	RQRLQLQFMPEEVIRSVEKSGQPQTRVTLRSPANGYVVKLDIRAGSQVTATQSLFELASL	246
Erwinia	RQRLALLFMPEAII RQVERSGKPDRIAITAPVDGYVVKLEVRQGVQLNPAQSLFELASL	235
Saccharophagus	ESRLKALHFPFAKEIAELTHTRKVQAVMFPSPQNGVVDNLNIREGFYVTPGTTLSIGITL	239
Alteromonas	RSRLNALQVPEDVVETLTTRKNVQQTTFAPQTFGVVDNLNIREGFYVTPGTTLSIGITL	243
Idiomarina	EERLRALQVSESEIKKLKETRKIQKTITVKAKQSGVLDRLTVREGAFVTPSMNLTIAQL	242
Marinobacter	TERLAALNV PASLISRLRQSRDIQRTMTVYAPRSGVIENLVNREGGMF IKPGDRVLSIAAL	245
Marinomonas	KERLLALNFPPEIEKRLTRTLKVQSVTFFAPSDGVADYLNMDVGMF IKPGMELLSIASL	247
Colwellia	ENRLIALQIPRKAINALKKDKKVLNVTFFAPQNGVVESELVVRQGFYVVKPETMMLSIIDL	261
Pseudoalteromonas	KARLKS LNISDDFVERLQSKSQVMQNTITFYAIQSGVVEELNVREGGFYVNP GTTMMSIGKL	243
Alteromonadales	KARLES LNVS AEIERLQKNKQIMQNTITFYARQSGIVDELNVREGGFYVVKPGTSMMSIAQL	235
Oceanobacter	LDNLRALNFPQATIQALRKDKTVKQTVTFRAPQSGVLENLQIREGFYFVGP SKTLMISIVNL	238
Photobacterium	KERLSSLGV DNNQINAILRKGKSFKNIAIKAPADGVIT ALNVRTGAYLSPAQNVISGGSL	245
Vibrio	TERLVTLGVDRAQIKSITRRGKASQTIEIKAPADGVIASLVNREGGGLSPAQAVISAGPL	247
Psychromonas	KARLQALGVNQDQIENI IRNKKVLQNTITVFAPQKGTISELKLNEGAFISPSTVVITAVNL	280
Aeromonas	EGKLKSLQVPADQIAALKRNRQVRETIGIYAPSSGVVSELKVREGQYVEPAAALFNISTL	240
Oceanospirillum	ESKLKSLGADSEIF EKLKSGKQSFNRLPVYAPQSGYVSQNLNVRQGMF IKPASKLMRIGPL	239
Hahella	RERLLALGLNNAQISRLEKRLVDQRISVYAEQSGVVDALMVREGGMF IKPATEIMSIGGL	246
Legionella	YKRLQALHISEQQIEDIKKGHSNQLVAVYAPQDGIVAALNIREGM RVTPDVEIMSLVDL	240
Alkalilimnicola	RERLRALGMPADAIRQVEQQGRALNLVPVKAPQDGVVQALNVAEGM FVQPGTEVMSIADL	238
Maricaulis	RSRLMALGVTRDQISRIARTGNAGELVEVRAGQDGVVIAVAVREGSHVRPGTQLMTISDL	240
Syntrophobacter	RERFRLWNIPDAQVREIEKRGKPSMTLSSPAGGFVNNRNAYPGQRITPETEISYIVDL	340
Pelobacter	RQRLRYWDISERQISRLEKTGKVHKTTLTYAPSKGVVTM KMAMPQQFIKAGQELFQISDI	312
Nitrosococcus	RERLQLLDVPEHQIRELEQA EKIYNLHIHSPFHGVVLQIGVREGQYVTPQTELYTLADL	262
Mariprofundus	LDRLRFFDVPEHQIRALQRTHKVLKNMHIHAPAAGIVTKIGVRD GARVTPATELYQIADL	265
Xanthobacter	RQRLLENLGVPAEIAEIERTRKVPLSMTWRAPRDGVVLERNVAVDGMRAEPGAVLFRIADI	307
Nitrobacter	RQRLLENLGVPEEIAEIERTRKVPLSITWRAPRDGVVLERNVVEGMKAAPGDVLFRLADI	308
Mesorhizobium	RQRLLENLGVPSGAIAEIERTRKVPLSMTWRAPRDGIVLQRNAVEGMKAAPGDILFRLADV	286
Methylococcus	IQRLRNWNVPESWLRRFEASGEIQRRVPFASPVNGIVLEKNAVQGMRFMPGDTLFRVADL	247
Parvularcula	RQRLRSLGMQNAIDRLTETRQVIERVPVYAEAGGTVAELQVRNGDYVVKPGTPILRLQSY	232
Hyphomonas	RQRLRSLGMQDAAINRVAETRAVIERVPVYAEAGGTVAAL EVREGDYVVKPGTPILRLQSY	281

. : . : \* \* \*

Escherichia	DPVWVTAAIPESIAWLVKDASQFTLTVPARPKTLTIRKWTLLPGVDAATRTLQRLLEVD	273
Shigella	DPVWVTAAIPESIAWLVKDASQFTLTVPARPKTLTIRKWTLLPGVDAATRTLQRLLEVD	301
Salmonella	DPVWISAAVPESIAYLKDTSQFEISVPAYPDKTFHVEKWNILPSVDQTTRTLQVRLQVT	309
Shewanella	DPVWISAAVPESIAYLKDTSQFEISVPAYPDKTFHVEKWNILPSVDQTTRTLQVRLQVS	309
Serratia	DPVWISAAVPESIAYLKDTSQFEISVPAYPDKTFHVEKWNILPSVDQTTRTLQVRLQVS	309
Klebsiella	DPVWISAAVPESIAYLKDTSQFEISVPAYPDKTFHVEKWNILPSVDQTTRTLQVRLQVS	262
Erythrobacter	TPIWLEASVPEVQAANVRQGPISATLAAYPDQRFAGRIVAILPSADAASRTITVRAELP	310
Sphingomonas	SPIWLEAAVPERQAATVRVQGPVSATLTAFPEERFSGPIIAILPSAQDASRTITVRAQLP	312
Sphingopyxis	GTVWLDAAVPEAMAGRLRPDMPVTATLAAYPGESFAGRIRAILPQAESRTITARVEIP	306
Caulobacter	SSVWLILSAPEAQAGLIKIGQAVSAQLAAFPGETFNGRVSAILPSAQVDSRTLQVRVELA	309
Pseudomonas	NSVWLAVAVPESQTSVAVGQAVEARLPAPFGRVFNGTVSAILPDTNPDSTRLVRVELT	307
Thiobacillus	GTVWLDVAVPEARAGSVIRGQAAEHFAAFPGEVPQGRVTALLPALDDTARTTLKVRLELP	311
Alcanivorax	NPVWVEIAVPERQLGQVSSGNAVDVTVQGVKPALREGQVADILPLVDQSSRTVPVRVTL	312
Burkholderia	SKLWLIVEIPEALALGVQPGMTVDATFAGDPTQHFNGRREILPGISTTSRTTLQARLEID	316
Herminiimonas	NKVWLVAEVPEALSNVVRSGMTVEATFSGDANRKYSGKVEILPGISTATRTLQARLELD	314
Acinetobacter	NPIWLEAAVPEKQIAGIKRGLPVSVEANFAAFS-QKVTGKVIDILPDLTTSRTTLKVRLELP	256
Polaromonas	STVWANAEPESQAALVRPGAKVQASSPAAPGMTFDGKVQAILPEVNSATRTLKARLELD	345
Delftia	STVWANAEPESQAALLRPAGAKVQARSAPAGSSFDGKVQAILPEVNPSTRTLKARMELA	348
Methylibium	AAVWANAELPESQAALVRPGSQVEARSPPGVGAVFRGTVQALLPEVNATRTLKARVQFA	344
Ralstonia	STVWVLAEPESQASAIRPGQAVTATATAIAGHALTGKVDAILPDMNANTRTLKVRLELQ	324
Yersinia	DPVWIVMDYPQSQASLVRIGSEVTATTASWPGESFHGKVSSELLPNMDLATRTLKARITLE	306
Erwinia	NPVWVDVDYPEAAQALTLIGSDISATSSAWPGKTFHGNISELLPVLDSSTRTLKARVVL	295
Saccharophagus	DEVWVVAEVEFERQASLVQVQGPVTMYLDYLPNKQWAGKVDYVYPSLDAKTRTARVRLRFK	299
Alteromonas	DEVWVDAEVEFERQTAQIVEGLPVTMTLDLPGKTWQGVVDYVYPTLEQSTRTLKVRLELFA	303
Idiomarina	DKIWIWIAEVEFERQLNQVEVGNDVQMNLEYAPGKEWQGVVDYVYPSLNPKTRTGQVRIHFD	302
Marinobacter	DEVWVLI GEVFESQLSAVEAGNRVQMTLDYMPGREWRGSDYVYPEVNPSTRTLKVRLEL	305
Marinomonas	DEVWVEAEVFEKQTSLIKEGLAVQMSLDYLPKGSWLGVVDYVYPTLDASRTLKVRLEL	307
Colwellia	NQVWVKAIEVFERDVFVKVIGDSASMRDLDFLPKQWLKGVHVEHVMPLNPKTRTLKVRLEL	321
Pseudoalteromonas	DEVWVEAQVFERQAEELIKIGQPVSMTLDYLSGQSWQGVVDYIYPTLDAKNRTLKVRLEL	303
Alteromonadales	DEVWVEAEI FERQSSLSISVGLPVTMTLDYFPGKIWQGVVDYIYPALDAKNRTLKVRLEL	295
Oceanobacter	DKVWVEAEV FQS QSLHWLKQGLAVSVALHGFDDK-LNGQVDYIYQNLNMQNRTRGRVIRVLN	297
Photobacterium	DNIWVDAEVEFERQSTWIIQSGIAADMTLGLALPGKHWQGKIDYVYPI LDPNTRTLKVRLEL	305
Vibrio	DNVWVDAEVEFERQAHWMKAGSQATMTLDAIPGNEWQGVVDYVYPI LDPKTRTLKVRLEL	307
Psychromonas	DTVWVDVEVFAAQVSLVKLGDLASMTLDYFPGQKWEGQVDFIYPEMNASNRTLKVRLEL	340
Aeromonas	QQVWVSAEVEFERQAAQLKVGDPVTMTLDYAPGRSWQGRVDYLYPTLDAATRTLKVRLEL	300
Oceanospirillum	QQIWATAELFERQAGQVSVGDQAEMLDLDFLPKGSWRGKVDYIYPALDQKTRTLKVRLEL	299
Hahella	EQVWVIAEVEFERQAGVWKAGQPVVMQVAAAPGRTWEGKVDYLYPVLDAKTRTLKVRLEL	306
Legionella	ANVWVIAQIFEEQANWVKIGDQAEARISAFPGKQWKGRVEYIYPRLEPMTRTVKVRLEL	300
Alkalilimnicola	SRIWVIADLFEHQSDAVREGLDAEVHFFPRPGETLVGSGVYIYPTLASPTRTIRARITLD	298
Maricaulis	SSVWILVDVFEDDALMVSQGDVHIRSTSDPSRTWHGEVEYVYPTVDPQSRVSVPRIRSS	300
Syntrophobacter	STIWALAEVYEVPLIKLGQDATMTLSYVPGKTYKGVYIYPEVDKTRTLKVRMEFP	400
Pelobacter	SKVWVYADIYELPWETQAEVILPFVGGQSLKANIDYIYPYVEPQTRTVKARIVFD	372
Nitrosococcus	CQVWVYVDIYELPWVQAGDEAEMRVTAIPGQVPHGTVAIYIYPLEKQTRTVQLRLEFD	322
Mariprofundus	SRVWVLADLYEYIIPWVKVGSASLSIASMPGRTFTGKITIYIYPYLDPKTRTNKVRLEFD	325
Xanthobacter	STLWVLADVPEHDLAAVRIGASASVRVRGRPGVAFNGQVSLVYPQVSEVTRTARVRIEIA	367
Nitrobacter	STIWVLADVPEFDLAAVRIGAPVTVRVRSPLGRSFEGRVSLIYYPQVGEATRTARVRIEIA	368
Mesorhizobium	STVWVADVPEYQLAAVKLGAAATIRLRGRPGQSFTGHVALIYYPQVATDTRTTKVRLEIP	346
Methylococcus	STVWVIASIFEQDLGHVRVGTARIGFKAYPDRSFDGRVAYVYPTVTDVARTARVRIELA	307
Parvularcula	ADVWVIASVPESDLPLVQAGMPAELDFPSAPDAPGKGQVDYIYPTIDPKTRTADVRIEVD	292
Hyphomonas	AGVWIMAAVPEPDLSTLIETGFPVRLSFPSPAEPAGTGVIDYIYPTIDPKTRTAQVRIEID	341

: \*

:

: \*

\*:

:

283

Escherichia	NADEALKPGMNAWLQNTA--SEPMLLIPSQLIDTGSEQRVITVDADGRFVPKRVAVFQ	331
Shigella	NADEALKPGMNAWLQNTA--SEPMLLIPSQLIDTGNEQRVITVDADGRFVPKRVAVFQ	359
Salmonella	NKDEFLKPGMNAYLKLNTQ--SQEMLLIPSQLAVIDTGKEQRVITVDDEGKFVPKQIHVLH	367
Shewanella	NKDEFLKPGMNAYLKLNTK--SQEMLLIPSQLAVIDTGKEQRVITVDDEGKFVPKQIHVLH	367
Serratia	NKDEFLKPGMNAYLKLNTK--SQEMLLIPSQLAVIDTGKEQRVITVDDEGKFVPKQIHVLH	367
Klebsiella	NKDEFLKPGMNAYLKLNTK--SQEMLLIPSQLAVIDTGKEQRVITVDDEGKFVPKQIHVLH	320
Erythrobacter	NPRGRLKPGMFAQVSLSPD-TRR-ALLVPSEAVIRTGRRNLVMLKQDEGAFLPAEVEIGR	368
Sphingomonas	NASGRLKPGMFAQVSLTPD-TRR-ALLVPSEAVIRTGRRITVMVKQDEGFMFAEVRIGR	370
Sphingopyxis	NRGRLRPKGMFATVSFAGE-QRP-ALLVPSEALIRTGKRTLVMMLALDKGRYQPAEVRTGM	364
Caulobacter	NRDGRLRPKGMFATASLGSD-AAP-VLTVPSEAVIRTGRRDLVMLAQGGGRYQAAEVRVGR	367
Pseudomonas	NADGRLRPKMTAQVRLNRS-TGQDSLVPSEAVIRTGKRALVMLAEDAGHYRPVEVRLGQ	366
Thiobacillus	NPGGRLRPGLTAQVSLRGA-GGDSALRVPTAVIRTGRRALVVVAEAGRYRPVEVTLGA	370
Alcanivorax	NDEGDLRPKMSAQVRIHGE-ATQKALAVPTAALLHTGKRSLVMLDEGEGRYRPQAVLPGG	371
Burkholderia	NAGFKLTPGMLMRVRVAGQ-KAVSRLVPSEAVITGKRSVVIVKNGDGRQLPATVTVGN	375
Hermiinimonas	NRDGSLLTPGMLMRVRLNAD-KSVSKLLVPSEAVIANGKQSIIVLVGNNMFPVVTIGR	373
Acinetobacter	NPSGQLKPGMFASVNIINN-PQSS-LVVPEQAVIRTGTRNVVIVGREQGRFPPVVQLGQ	314
Polaromonas	NPGARLVPKGMFVSMHFMGM-QAQKSLVPTEAVIQTGKRITVVLAAEENGWFSFVDPVQPGI	404
Delftia	NPGGRLVPKGMFVTMNFVDM-RPDKTLLVPTEAVIQTGKRITVVLAAEDNGRFRPAEVDAGI	407
Methylobium	NPEDRLVPGLFVTMQFMDM-EAQAAMLVPTEAVIQTGRRVVMVAEEGGRFAPVETGL	403
Ralstonia	NRDRRLLPKMFANVRFGAQ-AGPDKLLVPTEALIRTGTRITVMVDAGNGGFNPVETKGA	383
Yersinia	NPQQQLKPGMYLNVQSTPTDTLEPVLVLPQEAALLMTGSRNTVLLAEGNGHFYKPEVVSAGQ	366
Erwinia	NPQQQLKPGMYLTVQRSHT-QAQPRLAIPQEAALLVSGSQNRVLLSDGSGHFTPRRVTAGA	354
Saccharophagus	NADHLLKPNMFAEVI IHVA-NAENALVIPREAVIRTGSQDRVVLALGDGQFYSVAVELGR	358
Alteromonas	NQDYTLKPNMFAQVTIHS-DNSTNLIVPTEAVIRTGNQNRVVLALGDGKFYSVAIKIGR	362
Idiomarina	NPDGFLKPGMFANLNIKAG-LGDKNLIIPKEALIRMGDSNRVVLALGDGKFYSVNVVGR	361
Marinobacter	NEDGALMPKMFARLEVQGE-RGKRQFLVPRESVIRTGQSDRLVLALAEAGFKSVNVSVGR	364
Marinomonas	NQEQLKPNMFAKINILID-EAAPSLQVPKEAVIRVEQSNRVVLALGDGKFYSINVEIGR	366
Colwellia	NQNGDLRPNMFAQISIAIN-DNEPALQVPKEAVIRTGNQDRVVLALGDGYFYSVAVKIGR	380
Pseudoalteromonas	NEGHLKLPNMFAQVNIHTQ-ANKAQLVVPKEAVIRTGNQNRVVLALGDGKFYSVAVEMGR	362
Alteromonadales	NKDLKLKANMFAQVTIHTN-ASEPQLVVPKEAVIRTQHQRNVVIALGEGRFYSVEVQVQG	354
Oceanobacter	NPQQKIKAGMYADVTFATQ-SSKAVTVVPREAVIRLGDSDNRVVKHVDGQYKSIAMKTGV	356
Photobacterium	NADGALKPNMFANITLIPQ-SNNKVLLVPNQAVIRSAGMSRVVLALGNGKFRSTRVETGR	364
Vibrio	NPDGALKPNMFANIALQPV-TDDAVLTIPKSSVIRSGGMTRVVLAEAGDGKYSARIEVGR	366
Psychromonas	NPTALLKPNMFASVTLIPQ-MKQRTLQIPREAVIYAGNMNRVVLALGEGNFYSVLVNLGL	399
Aeromonas	NPDEFLKPNMFAKVAIRTG-QGEPRLVVPSEAVIRTGSQDRVLALGDGNFYSVAVTLGS	359
Oceanospirillum	NPDLQLKPD MFARIEIETS-ATKPVLPNPASALIKTGSQERIVVDMGEGRYKSVEVTSQG	358
Hahella	NPDLTLKPNMFADLTQAK-VDDQALSIPREAVIRTGSHDRVVLAEAGDGRYPAPVVKLG	365
Legionella	NPDNQLKPNMYASISILVN-PKSNVLSIPLEALIRSPQGDRVIVALGKGRFQVRQVKAGM	359
Alkalilimnicola	NPDGRLKPGMWTDVHIDGE-STEPVLHVPAAEAVIRTGRQDRVVTEEEGRFRVHEVRVGR	357
Maricaulis	NADGALRPETYVNVVAIDTE-PHVQALTIPREAVIRGGQSDRVIIAEAGEGRYPARPVETGM	359
Syntrophobacter	NADFQLKPD MYANVGIE-V-DFGRQVSIQEAVLDSGTEQIVFVALGDGYFEPKRVQVGA	458
Pelobacter	NPGLELKPD MYVNVRIHGM-EVKDALAVPSEAVLNSGEKQTVFVALGDGKFEPKRVKTVG	431
Nitrosococcus	NSDLLLKPEMFANVTIHAS-KQVDVAVVPEAAIVRSQGTREQVFVVRGPGKFEPREVKVGV	381
Mariprofundus	NRDGALKPD MFQDVAIASS-TSKPGIYVPREAVLITGKQAHLFVQVGPGRFEPRTVKTGT	384
Xanthobacter	NPDGVLKPNMYADVAVGTG-DAAPVLAVPDGAVIDTGTRQMVILDRGDGRFEPDVAUGH	426
Nitrobacter	NPDGVLKPNMYAEVEIGTG-DAAPVAVPDSAVIDTGTRQVVIIDRGDGRFEPDVKIGL	427
Mesorhizobium	NPYGTLLPD MYADVEIASG-SGAEVVAVPDNAVIDTGSQVQVIVDKGDGRFEPQVQVQ	405
Methylococcus	NPKQLKPNMYGDTVLAQAA-ETEPVLAVPDSAVLDSGTRQLVLVRLGEGRFEPRPVETGQ	366
Parvularcula	NVSGYLRPGAYADIRLNI--GRPRLSVPSEAILLGSEGARVVIAEGNGRFSGRAVQTGI	350
Hyphomonas	NADGFLRPGAYADIAIDIP--GKSHLSVPSEAVLQDSRGTVIIALGEGRFTGRAVTTGI	399

\* : . : \* : : : . . :

Escherichia	A-SQGVLTALRSGLAEGEKVVSSGFLIDSEANISGALERMR-----	371
Shigella	A-SQGVLTALHSGLAEGEKVVSSGFLIDSEANISGALERMR-----	399
Salmonella	E-SQQQSGIGSGLNEGDTVVSGLFLIDSEANITGALERMRHPEK-----	411
Shewanella	E-SQQQSGIGSGLNEGDTVVSGLFLIDSEANITGALERMRHPEK-----	411
Serratia	E-SQQQSGIGSGLNEGDTVVSGLFLIDSEANITGALERMRHPEK-----	411
Klebsiella	E-SQQQSGIGSGLNEGDTVVSGLFLIDSEANITGALERMRHPEK-----	364
Erythrobacter	E-ANGRTEILAGLAEGEQVVTSGQFLIDSEASLSGIDVRSIDGTMSM-----	414
Sphingomonas	E-AGGRTEVLAGLSAGDQVVTSGQFLIDSEASLTGLDVRPIDQADDA-----	416
Sphingopyxis	E-ADGQTEVLAGLAEGEKVVTSQGFLIDSEASLSAMQARPIAGGSPQ-----	410
Caulobacter	Q-AGGRTEILGGLKAGDQVVASGQFLIDSEASLAGLEPRPLSADEPVNSMPAGPATK----	423
Pseudomonas	E-SDGRTVILEGLAEGQSVVTSGQFLIDSEASLKGIVAEPL-----	407
Thiobacillus	E-SGSDTVILSGLAEGQKVVASGQFLIDSEASLQGIVARGTG-----	411
Alcanivorax	E-LGDQTLILAGLKEEQKVVSQGFLIDSEASLQGIAVQELAMSDETEMMNALHYAEGVV	430
Burkholderia	D-IGNETEVLSSGLNDGDTVVASGQFLIDSEASLSVLPRLLEGSTGAS-----	421
Herminiimonas	D-IGSDTEILNGLSDGQKVVASGQFLIDSEASLKSIVLPKFAGTK-----	416
Acinetobacter	S-DGNKIAVLQGLKAGQKVVTSGQFLIDSEANLQGILDKLNTGQP-----	358
Polaromonas	E-SGGQTEIKRGLQAGQRVVSSQFLIDSEASLKGVEARLNENPKPADATAT-----	455
Delftia	E-SGGQTEIKHGLSAGQRVVSSQFLIDSEASLKGVEARLNSAPSAVAASPP-----	459
Methylobium	E-ISGQTEIKRGLKAGQRVVSSQFLIDSEASLKGVEARLNNQPAPT-----	449
Ralstonia	E-ANGQTEVTDGLSAGQKVVSQFLIDSEASLRGTAQRMASPPAASAP-----	431
Yersinia	T-QDGWVEIKSGLSHGQLVVTSGQFLIDSEASLQSTLPQMADTPEPQ-----	412
Erwinia	S-LGDWVEIIDGLKEGDNVVTSGQFLIDSEASLSALPQFDADTS-----	398
Saccharophagus	M-DDNFVEIILEGLEENERIVTSAQFLIDSESSKTSDFKRM-----HSQNL-----	403
Alteromonas	V-VDEFTEVLEGLIDGDSIVTSGQFLIDSESSISSDFKRM-----PPEES-----	407
Idiomarina	L-GSSRVEILSGLMAGDEIVTSAQFLIDSESSKSSDFKRM-----HDSNTDSESHD----	412
Marinobacter	V-GEKYAEIILDGLMPGDTVVTSAQFLIDSESSKSSDFFRMS-----APQTR-----	409
Marinomonas	T-DKDSIEIVSGLFEGDEVVTSALFLLDSESSKSSDFKRM-----YPPSSVMDM-----	415
Colwellia	F-DRDNIEIISGLSEGEKVVSQFLIDSESSKTSDFKRMHIEEFQSDDFMDE-----	432
Pseudoalteromonas	S-DSKNTAILSGIMADDDVVSAQFLIDSESSKSSDFKRMQ-----APQAVSSVWSEGIVNS	418
Alteromonadales	T-SVDETIILSGVVNDVVTSAQFLIDSESSKLSDFKRM-----MPAADS-----	400
Oceanobacter	S-NEQFIAIEQGLKLGERIVTSAQFLIDSESSKQSDFKRID-----RGSATR-----	402
Photobacterium	E-SGNQIEIVKGLNPNDTIVTSSHFLIDSESSLSADLSRIS-----NRNETKTAVSAPVHDM	420
Vibrio	E-AGEQIEVLQGLKQGDKIVTSSHFMLDSESSQSADLSRINGVEAAAETAWAKGEITDVM	425
Psychromonas	E-NKKSVEVLSGLSEGQEIIVTSAQFLIDSESSISADFGRML-----	439
Aeromonas	Q-FGDKVAIKAGVETGDSIVSSAQFLIDSESAIDSDFQRM-----AVRP-----	403
Oceanospirillum	Q-MNGRVAIEQGLYPQDRVVSAQFMLDSESSISSDFLRMT-----PPKM-----	403
Hahella	E-ADDRVQVLKGLKAGDQVVTSGQFLIDSESKVDVALAALESFSQSAQQDAAP-----	417
Legionella	E-SGDRVEILSGLKVGENVVSGQFLIDSESNLKAGLERLE-----	399
Alkalilimnicola	R-AGDRLEIILEGLQVGARIVTSGQFLIDSESSVTSLARLQAAAEEADDGS-----	406
Maricaulis	E-SDGRIEILAGLAEGEIVVSSQFLIDSEASLQGAALRMSPPGAVDEDAGIQ-----	411
Syntrophobacter	RVGDRFIVVS-GLNPGEQVSSGNFLIDSESRKLSALRGMGSPAHAGHGATGGEAGV---	514
Pelobacter	QDQEGFTEITQGLLEGETVVTSAQFLFDSESKLREAIQKMLEPKTT-----	477
Nitrosococcus	S-AEGFTEILAGLKPGEKVVTSSQFLIDSESKLREATAKMKPEK-----	424
Mariprofundus	S-AEQQVEILDGVKAGELVVSSQFLIDSESSIREAAAKMVEPKTMA-----	430
Xanthobacter	S-GQGFTTEIRAGLAEGDRVVAANFLIDAESNLKAALRGLAPVEAKP-----	472
Nitrobacter	R-GEGLTEIREGIAEGDRVVAANFLIDAESNLKAALRGLTPPEARP-----	473
Mesorhizobium	Q-GGGFTEIRSGIAAGDKIVVAANFLIDAESNLKAALNGMTSAEATP-----	451
Methylococcus	R-VEGYTEIRRGLESEGEVVTRANFLIDSESNLRAAIGGFSTEPAPAPTDSMPGGH---	422
Parvularcula	S-ANGRTEILSGLSEGMVVASGQFLIDSEANLKEGLAKLEAPDASASPETPLSDIPVD	409
Hyphomonas	Q-AKGRTEILSGLTAGDEVVASGQFLIDSEANLREGLAKLQGPAAVTAGPDTPLSELVVD	458

: \* : : \* . \* : : \* :

Escherichia	-----	
Shigella	-----	
Salmonella	-----	
Shewanella	-----	
Serratia	-----	
Klebsiella	-----	
Erythrobacter	-----	
Sphingomonas	-----	
Sphingopyxis	-----	
Caulobacter	-----	
Pseudomonas	-----	
Thiobacillus	-----	
Alcanivorax	EQLNGSKIMLDHGPFKSLSPAMTMRFNLANEQVGKGIS--VGDRVRIGIRDTDKGLIVE	488
Burkholderia	-----	
Herminiimonas	-----	
Acinetobacter	-----	
Polaromonas	-----	
Delftia	-----	
Methylibium	-----	
Ralstonia	-----	
Yersinia	-----	
Erwinia	-----	
Saccharophagus	-----	
Alteromonas	-----	
Idiomarina	-----	
Marinobacter	-----	
Marinomonas	-----	
Colwellia	-----	
Pseudoalteromonas	IMAEHRMVNISHEPIAELDWPSMTMDFTVADDVDFTAFENGQTLHFELTKQADGSYVLTA	478
Alteromonadales	-----	
Oceanobacter	-----	
Photobacterium	ASH-----STEQPAK	430
Vibrio	KDHRMLTINHQPVPPEWDWPGMVNMFTFADGVEMG-----DLKKGQAIEFEMQKTESGQY	479
Psychromonas	-----	
Aeromonas	-----	
Oceanospirillum	-----	
Hahella	-----	
Legionella	-----	
Alkalilimnicola	-----	
Maricaulis	-----	
Syntrophobacter	-----	
Pelobacter	-----	
Nitrosococcus	-----	
Mariprofundus	-----	
Xanthobacter	-----	
Nitrobacter	-----	
Mesorhizobium	-----	
Methylococcus	-----	
Parvularcula	SKA-----	412
Hyphomonas	AAT-----	461

Escherichia	-----SESATHAH-----	379
Shigella	-----SESATNAH-----	407
Salmonella	-----TENSMPAMSEQPVNMHSGH-----	430
Shewanella	-----TESSMPAMSDQPVNRHSGH-----	430
Serratia	-----TESSMPAMSDQPVNMHSGH-----	430
Klebsiella	-----TESSMPAMSDQPVNMHSGH-----	383
Erythrobacter	-----ASEGSPNMRTYTATGRVTKIAGASITLHAPVPALEWPSMVMPFALEDAAL--	465
Sphingomonas	-----STGGEDAPATFGATGTIQQSIANGSVTLRHGPVPRLDWPAMTMTFRTKSAAQ--	467
Sphingopyxis	-----APSKAQGHR---AIGTIEKIEPGSVTLRHGPVPSASWPAMTMRFRLLADPAT--	458
Caulobacter	-SAAPAMKSAPAAKALLQAEGRIEEITADTITLSHGVPVPAIGWPAMTMTFKLDPPTL--	480
Pseudomonas	-----SGGNVSGSQP-----	417
Thiobacillus	-----EAAAAPALHEADGVDDISAEYVTLTHGPFKTLAMPGMTMEFPLARPEL--	461
Alcanivorax	RLEKQVAEQKDTQVNSLHYAEGVIEGLSDGKVKLKHGPFKTLGMPGMTMRFRLLASEQV--	546
Burkholderia	---ASAPASAPAVAAQTYETTGKVEKVTADITFHSQPVVPAALGWGAMTMAFNKPAPDA--	476
Herminiimonas	-----QTMQPVAAQSVYRGIGTVEKVTTPKALTLSHKPIPELEWGAMTMDFNKLRLPEL--	467
Acinetobacter	-----ITSSQTIKRSTYQGLGKVEKVTNQDITISHQAIPELGWGAMTMIFFKQP-VQP--	409
Polaromonas	-----TATAAPRHEGQAKVMAIGKEAITLSHGPIATLKWGAMTMDFKRPAPPD--	503
Delftia	-----VPMASAPRHSGEAKVVGIGKDALTLSHGAIPTLKWGPMTMDFKLDPDGS--	509
Methylobium	-----AANTAQRHSAQGLIESLDRESVTLSHGPIPSVGMGAMTMEFKLPPPNR--	497
Ralstonia	-----AAAAIEHEGVGRIEAVTSEGLTISHGAIPSAHWSAMTMDFAAPPSPG--	477
Yersinia	---VPAVDNTTPAPVDIYSVQGEVNAINGSTITLSHGAIAALKWGAMTMDFLLPPGKL--	467
Erwinia	---ISSTTSATPAAPVGYQTQGVKKAINGNQVTIEHEAVPALNWSPMTMDFTLPSSSL--	453
Saccharophagus	-----LAPVWVEAKVEQVMVMNMVKLTHEPIPEWDWVMTMMFFVDDSID--	449
Alteromonas	-----PTSVFTEVMITDVMPSHNMITAKHGPIPEWDWVMTMDFVVAEHIN--	453
Idiomarina	-----SMSSDAAAQAVWVEATVKNVMPQHSMTVLEHGEISEWDWPAMTMDFDVASDVE--	465
Marinobacter	-----DNGGMN-----HEGMD--	420
Marinomonas	-----SEMDHGS-----MDH-----	425
Colwellia	-----SNNDVSSAMVNGTVTSVMTDHRMVTIDREAIEKWNREPASVDFIVSESDV--	482
Pseudoalteromonas	IHIMKSTVTNSEKNTATVLGTINSIDKAQRANISRGAIEKWGREPARLDFTFADDID--	536
Alteromonadales	-----SNDDNSQ--SATVNGVINTIDAATRIVNISREAIPKWNRPATMNFVLAHPHIE--	451
Oceanobacter	-----LPNASVMGKVNYVDKNSVINISRAAIEKWNRPATMDFVLDPSIPNK	450
Photobacterium	QSTDN-----SAWTTGVIRNVMLDHKMLTIQHSPIPEWQWPAMQDMFMVKDDVD--	479
Vibrio	QIVDYKADNSVIAAEVWLTGDTMLMADFGMITLNLHPVAEWNWDAGEMNFSVGEEVD--	537
Psychromonas	-----ELDKNKQSQPESD-----SIGEDED--	459
Aeromonas	-----AQVWTQGTVQSMDLASRTLMAHPPPIPEWQWPAMEMEFTVAEGVD--	448
Oceanospirillum	-----RIEEVWAAQIRSVQDENRSVVLKHGEIAEWKQPGMVMEVPVDPALD--	450
Hahella	-----GTVWATGTINSVMAGHGMNLNISHDPVKAWNWPMSMDMDFTTVEGLP--	462
Legionella	-----VAAEGRINHVDPEARQVNLDPHEPIAELGWPAMTMDFEVAEDVA--	449
Alkalilimnicola	-----LDQAQGGQGVIVSLMAGHGMIDLEHDPIDELGWPAMSMFLALEGVD--	457
Maricaulis	-----GRGQPPSGIDHSSHQQKNGKTMQREDTAPPRTGVG---	549
Syntrophobacter	-----ESSPSEDHAGHDMPEEDLEALFE-----	500
Pelobacter	-----LGAINAEKQEDAGKHKQRITPK--GSP--	450
Nitrosococcus	-----SPQGSAGQDMEGMNMQGMMDYHVSAGEPNGM	463
Mariprofundus	-----	
Xanthobacter	-----	
Nitrobacter	-----	
Mesorhizobium	-----	
Methylococcus	-----	
Parvularcula	-LAEIDHFTDMALYFHEALRDGYDIDPLFVDPALALVPVLRDRYANTKLAPVMDATQTAL	471
Hyphomonas	-LANIDHFTDMALYFHEALTDNRYRIDARFVDPALFLGETLRARFAQTKLEFVLEAEAAAL	520

Escherichia	-----	
Shigella	-----	
Salmonella	-----	
Shewanella	-----	
Serratia	-----	
Klebsiella	-----	
Erythrobacter	VDG-IEPGDKVEFTFSQHDTGP-RIESIRKTD-----	496
Sphingomonas	MRG-LETGDRVRFTFTQQDAGP-RIESITRAGQ-----	498
Sphingopyxis	VRG-FKPGDKVNFTFDQPAQGP-TVRSITRENGR-----	490
Caulobacter	ARG-LKTGDQAAFGFEQRPDGP-VVRS�HRAEASR-----	513
Pseudomonas	-----	
Thiobacillus	AKG-LKAGDRVRVGARETADGL-VVEKLVKTDKTGGAK-----	497
Alcanivorax	ASD-IAVGDRVRVGKDTDNGL-TVVSLDKQEVAP-----	579
Burkholderia	FPD-VKAGQTVHFVFKQSDDEGY-QLTKVEPVGGVQ-----	509
Herminiimonas	FGE-İKAGQEVFESFKENDDGY-LLETVKPFGGKQ-----	500
Acinetobacter	FTR-IQQGDQVNFSTKVGNYS-VISDISKMSMASMKN-----	445
Polaromonas	LPKNLAVGSQVGFEFMDAEGLPQLTRVTPMALAAPGAAPMAAGEQK-----	552
Delftia	APK-VQVGDRVSFEFFMGADDLPLQLTRVTPMAAGGKP-----	545
Methylibium	LPRGLAVGDRVDFEFYVDPTDGPVTLTLLPPAAPAAAAPGASR-----	542
Ralstonia	LPKRFKPGDRVRFRQLHDDGMAVLSSVEPAGADQGGKP-----	516
Yersinia	SAD-IHVGSEVNFTFTLTEQGAQIRQIQPVKTNSSTDIHGSHL-----	509
Erwinia	PQG-VGIGSTVSFQNMDDSGIHVLHFLPADDPHAG--HGGHP-----	493
Saccharophagus	-MGQFETGLTLHVQIEKDADEDYVITQVHIP-----NGTAPHASGGAK-----	491
Alteromonas	-LATVKGSSSAHIEISKQTDGQYVVTTHII-----DSAQSTQATMSESVWTEVKINSV	506
Idiomarina	-LSQLSTGLSLHAEITQVGKQQYQLTSIHIP-----EQKQVTEQEHND-----	508
Marinobacter	-HGAMNHGAMNHSSMNQDQVEQDTMDHSTMN-----HGGGE-----	455
Marinomonas	-----SQMQMT-----SPMNMS-----EEGNKP-----	443
Colwellia	-MALFTVDAYLMFTFEIREGEFIVSAMAMK-----KMSGSSSHDMAQGEKQ-----	529
Pseudoalteromonas	-LTALAAQQQINFSTSLQQGEFVISHIN-----GEHSTSASGNHTMQLHNAH-----	582
Alteromonadales	-VNSLIKGQTIDFTFSIINDDFVITALN-----NIDAIDHSSMQHTMGEEVK-----	497
Oceanobacter	LINGLHKSQSIHFMFVIDDEFYVTEIHPMESEPADHDNMNHSEMGHGSMNHEDMNH--	508
Photobacterium	-MNQFVGQGSIRFLIEKTAKQYVVADVDQVN-----TDNDTNNAEVAQ-----	523
Vibrio	-LSGFEEGQKVRFLVEKQGS-DYVLKQLVPAT-----TAVEG-----	572
Psychromonas	-LDWLDLGEQSDFLSGNNTSGPVARKVTL-----	488
Aeromonas	-ISKLAEGQTLHLQVIQEGDEYRITTIHQESAKESAP-ATGHAPEQATDEMEGMDHSQH	506
Oceanospirillum	-MNVFANQQ--NLQVLLNGGD--MTDLKLT DYVVPRPKAPGSLPGGAM-----	493
Hahella	-LENVAPGQVRVFEITRSSPSDFQITALDIIS-----AAPSIDAQEAMQTEGAQ-----	510
Legionella	--TPEENEKRIQSTNPKGQKP-----	418
Alkalilimnicola	-LTDLEPGDPVIIHIREREDEEY-VYELTHIERLADPTGETDDAPDHAHTGHDH-----	502
Maricaulis	-LSDFTVGQAVTFELQRNEEGEWRI SAIMARDMDMSPTPSEPEQGDHAGHGHH-----	509
Syntrophobacter	-HAGHSTGGSGVPPGMDTGRSSHDPKSHQAGGK-----	581
Pelobacter	-----	
Nitrosococcus	AKDNHTPHTHSAPEEVR-----	467
Mariprofundus	TKGHMKGEGQDAPNHMDMKQMNGEKMQMSMEGGTDEHK-----	504
Xanthobacter	-----	
Nitrobacter	-----	
Mesorhizobium	-----	
Methylococcus	-----	
Parvularcula	AAAQDATDREDLATQLSDLVEALKPWLEAGAPQHYSEAGLVLYRDATATGRYWLQEAKPA	531
Hyphomonas	RAAKTADDGSALADNLARLMTALEPWLLDGAPVHYREAGLTLFKETGTGRLWLQEGTTPR	580

Escherichia	-----	
Shigella	-----	
Salmonella	-----	
Shewanella	-----	
Serratia	-----	
Klebsiella	-----	
Erythrobacter	-----	
Sphingomonas	-----	
Sphingopyxis	-----	
Caulobacter	-----	
Pseudomonas	-----	
Thiobacillus	-----	
Alcanivorax	-----	
Burkholderia	-----	
Herminiimonas	-----	
Acinetobacter	-----	
Polaromonas	-----	
Delftia	-----	
Methylibium	-----	
Ralstonia	-----	
Yersinia	-----	
Erwinia	-----	
Saccharophagus	-----	
Alteromonas	MDGHRMINVDHPAIKEWDWPAMTMDFNVDNITLSDLASGTLAHIEISKSSSGEYLVSTI	566
Idiomarina	-----	
Marinobacter	-----	
Marinomonas	-----	
Colwellia	-----	
Pseudoalteromonas	-----	
Alteromonadales	-----	
Oceanobacter	-----	
Photobacterium	-----	
Vibrio	-----	
Psychromonas	-----	
Aeromonas	MGAKP-----	511
Oceanospirillum	-----	
Hahella	-----	
Legionella	-----	
Alkalilimnicola	-----	
Maricaulis	-----	
Syntrophobacter	-----	
Pelobacter	-----	
Nitrosococcus	-----	
Mariprofundus	-----	
Xanthobacter	-----	
Nitrobacter	-----	
Mesorhizobium	-----	
Methylococcus	-----	
Parvularcula	NPYSADGAERIDWLNPMAGMSMTTNDGETGADQAPGHSGDSHD-----	574
Hyphomonas	NPYTDGQAEFVAWPDPMAGTQP-----	602

Escherichia	-----	
Shigella	-----	
Salmonella	-----	
Shewanella	-----	
Serratia	-----	
Klebsiella	-----	
Erythrobacter	-----	
Sphingomonas	-----	
Sphingopyxis	-----	
Caulobacter	-----	
Pseudomonas	-----	
Thiobacillus	-----	
Alcanivorax	-----	
Burkholderia	-----	
Herminiimonas	-----	
Acinetobacter	-----	
Polaromonas	-----	
Delftia	-----	
Methylibium	-----	
Ralstonia	-----	
Yersinia	-----	
Erwinia	-----	
Saccharophagus	-----	
Alteromonas	HVVEEASSETSTAVDAVWTQATVNAVMSASNQLSLEHDPIEAWDWPAMTMDFNVANEDL	626
Idiomarina	-----	
Marinobacter	-----	
Marinomonas	-----	
Colwellia	-----	
Pseudoalteromonas	-----	
Alteromonadales	-----	
Oceanobacter	-----	
Photobacterium	-----	
Vibrio	-----	
Psychromonas	-----	
Aeromonas	-----	
Oceanospirillum	-----	
Hahella	-----	
Legionella	-----	
Alkalilimnicola	-----	
Maricaulis	-----	
Syntrophobacter	-----	
Pelobacter	-----	
Nitrosococcus	-----	
Mariprofundus	-----	
Xanthobacter	-----	
Nitrobacter	-----	
Mesorhizobium	-----	
Methylococcus	-----	
Parvularcula	-----	
Hyphomonas	-----	

Escherichia	-----
Shigella	-----
Salmonella	-----
Shewanella	-----
Serratia	-----
Klebsiella	-----
Erythrobacter	-----
Sphingomonas	-----
Sphingopyxis	-----
Caulobacter	-----
Pseudomonas	-----
Thiobacillus	-----
Alcanivorax	-----
Burkholderia	-----
Herminiimonas	-----
Acinetobacter	-----
Polaromonas	-----
Delftia	-----
Methylibium	-----
Ralstonia	-----
Yersinia	-----
Erwinia	-----
Saccharophagus	-----
Alteromonas	SDITAGMRLHIEITKTQDGAYVITTVHIQASDKGTMDSQHEGAHE 672
Idiomarina	-----
Marinobacter	-----
Marinomonas	-----
Colwellia	-----
Pseudoalteromonas	-----
Alteromonadales	-----
Oceanobacter	-----
Photobacterium	-----
Vibrio	-----
Psychromonas	-----
Aeromonas	-----
Oceanospirillum	-----
Hahella	-----
Legionella	-----
Alkalilimnicola	-----
Maricaulis	-----
Syntrophobacter	-----
Pelobacter	-----
Nitrosococcus	-----
Mariprofundus	-----
Xanthobacter	-----
Nitrobacter	-----
Mesorhizobium	-----
Methylococcus	-----
Parvularcula	-----
Hyphomonas	-----

## APPENDIX C

ClustalW sequence alignment of CusF and homologous proteins identified from a BLAST search of the non-redundant protein database using CusF from *Escherichia coli* as the query sequence. Only sequences that are Membrane Fusion Proteins are selected for alignment and generate a representative set. The sequences are:

CusF NP\_286298.1 (*Escherichia coli* O157), ZP\_00829705.1 (*Yersinia frederiksenii* ATCC 33641), ZP\_00823574.1 (*Yersinia bercovieri* ATCC 43970), CzcB family protein ZP\_01039342.1 (*Erythrobacter* sp. NAP1), CzcB family protein ZP\_01864860.1 (*Erythrobacter* sp. SD-21), CzcB family protein YP\_457789.1 (*Erythrobacter litoralis* HTCC2594), CzcB family protein ZP\_01303698.1 (*Sphingomonas* sp. SKA58), Secretion protein HlyD ZP\_01419030.1 (*Caulobacter* sp. K31), Putative membrane fusion protein silB precursor YP\_001633190.1 (*Bordetella petrii*), MFP subunit YP\_985765.1 (*Acidovorax* sp. JS42), Secretion protein HlyD YP\_285471.1 (*Dechloromonas aromatica* RCB), Secretion protein HlyD YP\_521697.1 (*Rhodoferrax ferrireducens* T118), MFP subunit YP\_742228.1 (*Alkalilimnicola ehrlichei* MLHE-1), Membrane-fusion protein YP\_434211.1 (*Hahella chejuensis* KCTC 2396)

```

Yersinia frederiksenii -----MKKLFSLTLVAVAVISGLTGYLLGRPAPHATSASAI 37
Yersinia bercovieri -----MKKQLSLTLVAVAVISGLGGYLLGQPPSTAPAAAATH 37
Erythrobacter sp. SD-21 ----MKAVFERLSRQRSYAAAAGIALVSLGAGYGLSMLG--GGSDGGDA 44
Erythrobacter litoralis ----MNSALERFTPRQRMYAAGLGIALVSLLAGYGLSMLG--SES-GGDA 43
Sphingomonas sp. SKA58 ----MGAAWDRLSRQKSWMMAGTVALISLAAGYGLSQLG--EGQGGASD 44
Erythrobacter sp. NAP1 ----MNSVLERFTQRQLFAAGLGIALVSLAAGYGLHMLG--GESSGAS 44
Caulobacter sp. K31 ----MSRATTLSPRS-LIAGAAAI SLAAAGGYGLGQWR--KAPVPAAG 42
Bordetella petrii ----MKASFT----LGQITLGMVVAATAAGAGYALANRN--VPTSSAVS 40
Acidovorax sp. JS42 MT----TGFKAGVLLAIVAAGLAAGGGYVWGQRQSEAHSG--DQTASPGA 44
Acidovorax sp. JS42 MT----TGFKAGVFLAIVAAGLAAGGGYWMGQRQSEARSG--DQTASQGA 44
Dechloromonas aromatica RCB MTGANPSGMKQGVLAIVAIVAILAGAGGYWAG-HKSTGQTD--AMAQPAAT 47
Rhodoferrax ferrireducens -----MKQGTGLAVAVMAAVIAAGAGYWLGHKGPASQAQGTVSATAAAV 44
Alkalilimnicola ehrlichei -----MKFVS--LFIALLIG--FGLGAGALWFHQG-----GTAG 30
Hahella chejuensis -----MRLVISIIFIVAFAFVAGWFA SRHPALTGLMG-----EMDM 35
Escherichia coli -----

```

```

Yersinia frederiksenii ADTATENSRKVLWYDPMSPGQRFDPKPGKSPFMDMELVPRYAG---ETE 83
Yersinia bercovieri ADATAENSRVLYWYDPMSPGQRFDPKPGKSPFMDMDLVPRYAG---ETT 83
Erythrobacter sp. SD-21 A--ADTGCEEVLYWYDPMVPDQRFDEPGKSPFMDMQLVPKCAGG--DAQA 90
Erythrobacter litoralis A--TDTGCEDVLYWYDPMVPDQRFDEPGKSPFMDMQLVPKCAGG--DAQG 89
Sphingomonas sp. SKA58 AGGSATECEEVLYWYDPMVPGQHFDEPGKSPFMDMQLVPKCAG---EEA 90
Erythrobacter sp. NAP1 A--TDTDCEDVLYWYDPMVPGQRFDEPGKSPFMDMMLVPKCAG---EAA 88
Caulobacter sp. K31 D----APGRKVLYWYDPMVPAQRFDPKPGKSPFMDMQLVPRYADE--AASA 86
Bordetella petrii TAINSKGDRQVLYWYDPMVPTQHFDPKPGKSPFMDMELVPKYAD---EGN 86
Acidovorax sp. JS42 SAVAAKKERKVLFFYRNPMLPDTSPTPKKDP-MGMDYIPVYEGEQUEEAET 93
Acidovorax sp. JS42 SAGPTKKERKVLFFYRNPMLPDTSPTPKKDP-MGMDYIAVYEGEQUEEAET 93
Dechloromonas aromatica RCB SGAPAKKERKLRFFYRNPMLPDTSPVPKKDP-MGMDYIPVYEGEEDDEEPG 96
Rhodoferrax ferrireducens DTGAGSTSRKLLYYRNPMLPDTSPTPKKDP-MGMDYIAVYAGGADEEPA 93
Alkalilimnicola ehrlichei QGGGSS-EREVLYYQHPHNPTIRSDEPRKDE-MGMDYIPIYAGDEGRDD- 77
Hahella chejuensis AAAESGGKQPLVYWVAPMDPNYRRDKPGKSP-MGMDLVVPYEEDAQGQN- 83
Escherichia coli -----

```

```

Yersinia frederiksenii EDGGVTISARQQQNLGVRTAPAE MRTLNYRLAGYGT VVTDERGVQVIAAR 133
Yersinia bercovieri DDGGVTISARQQQNLGVRTAPAE MRALNYRLHGYGT VATDERTLQVIAAR 133
Erythrobacter sp. SD-21 GE-GVSDLSALVNFGIRTAEEYGVLEPETTVTGT LAYNGSEVAIVQPR 139
Erythrobacter litoralis AG-GVSDSTLVNFGIRTAEEYGVLEPEISVTGT LAYNGSEMAIVQPR 138
Sphingomonas sp. SKA58 TA-GVRIDPGLVNFGIRTAEEYGVLEPEITVTGVLAYNERDVAIVQPR 139
Erythrobacter sp. NAP1 EA-GVRIDPGLVNFGIRTAEEYGVLEPEITVTGVLAYNSRDVAIVQPR 137
Caulobacter sp. K31 ASPGVAVDPRGAQTLGLRLARAEMTPLASGLTVPGSIDFNQRLDAIVQTR 136

```

Bordetella petrii	GAQGIMIEPTIQNLGIRIVKVQQGPIPGAIEATASIKLNDRLVLTILQAR	136
Acidovorax sp. JS42	NSNQIRISTEKIQKLGVRTEAVSLRSLDKVVRAAGRIEPDERQTFTIAAK	143
Acidovorax sp. JS42	NSNQIRISTEKIQKLGVRTEAVSLRSLDKVVRAAGRIEPDERQTFTIAAK	143
Dechloromonas aromatica RCB	AANQISISTEKVKQLGVKTEAASLRALDKIVRAAGRIEPDERRTYTIAPK	146
Rhodoferrax ferrireducens	AANQVRISTEKVKQLGVVEAAQLRALDKSVRASGRIEPDERRVYAIAPK	143
Alkalilimnicola ehrlichei	DPDVLRIISPVVQNMVGVRTAEVERGALHRQISTVGFVEVDEAAQSHVHLR	127
Hahella chejuensis	DDGGVTINPTMEHNLGVRVAKVEQGELMLPIHTVGYVAFDEDRLTHVHSR	133
Escherichia coli	-----	

Yersinia frederiksenii	ANGIIIEQLYVRAEQPVTKNQPLAQLWVPDWSAAQQEYLAIRQLGDHPLT	183
Yersinia bercovieri	ANGIIIEQLYVRANQQPVTKNQPLAQLWVPDWSAAQQEYLAIRTLGDSQLT	183
Erythrobacter sp. SD-21	AGGYVQRTYGHAPQDLIARGAPIVDLLVPEWGGAQQEFLAVAATGDAALT	189
Erythrobacter litoralis	AGGYVQRTYGHAPQDLIARGAPIVDILVPEWGGAQNEYLAVAATGDEALT	188
Sphingomonas sp. SKA58	AGGYVQRTYGRAPDDVVGRGAPLADILVPEWGGAQQEYLAVALNSGDEELA	189
Erythrobacter sp. NAP1	AGGYVQRTYGLAQDDVVRRGAPIVDILVDPDWGGAQREYIAVLDTGDQALA	187
Caulobacter sp. K31	TAGFVQRVYGHAPGDIVAAGAPIADLLNPDWAGAQTTEYLAVRRIGDPRLT	186
Bordetella petrii	TTGYVDKVYPLAPGDVLASGTPIAELIVPEWEGAQLEFLALMRSGERSLA	186
Acidovorax sp. JS42	FEGYVERLHVNTGQAVSKGQPLFEVYSPELVSAQREYIAAQQGVDAKLG	193
Acidovorax sp. JS42	FEGYVERLHVNTGQAVSKGQPLFEVYSPELVSAQREYIAAQQGVDAKLD	193
Dechloromonas aromatica RCB	FEGYVERLLVNATGQPVGKGQPLFEVYSPELVSAQREYIAAADGVRSLNA	196
Rhodoferrax ferrireducens	FEGYVERLHVNTGQAVGKGQPLFEVYSPELVSAQREYIAAQQGVATLKD	193
Alkalilimnicola ehrlichei	TEGWIEDLRVTTGERVTAAGEVLFRLYSPALVSAQDELLQTLR--RNGNA	175
Hahella chejuensis	VEGWIEALNVKSSGDPVSKGQKLYEISYSPALVNAQEYLAALRGANKILL	183
Escherichia coli	-----	

Yersinia frederiksenii	A-----AARQLQLQFMPEEVIRSVESKSGQPQTRVILRSPAN	220
Yersinia bercovieri	A-----AARQLQLQFMPEEVIRSVESKSGQPQTRVTLRSPSD	220
Erythrobacter sp. SD-21	N-----AARQLRLGLMPEGVISSVARSGRPQSTITVTAPQS	226
Erythrobacter litoralis	R-----AARERLRLGLMPDSMIASVTRSGRPQTIITVTAPQS	225
Sphingomonas sp. SKA58	Q-----AMRERMRLGLMPDGLISSVGRNRPQSTITVTAPIG	226
Erythrobacter sp. NAP1	D-----AMRQRMRLGLMTDAMIASVERTTRAQNTITVTAPVG	224
Caulobacter sp. K31	A-----AARSRLVLAGMSEPLIAAVERGGVRQPISTVRAPIG	223
Bordetella petrii	R-----AARERMRLGLMPDGLIERTRKAQPTLTIRAPST	223
Acidovorax sp. JS42	ASGEAQRMRELADSSLARLRNWDISDEQVKLAKSGESRRTLTFRSPVT	243
Acidovorax sp. JS42	ASGETQRMRELADSSLARLRNWDISDEQVKTLAKSGDARRTLTFRSPVA	243
Dechloromonas aromatica RCB	AGGEAQSGMKQLADSSLARLRNWDISEQVKALAKSGETKRTLTFRSPVN	246
Rhodoferrax ferrireducens	AGGQAQSGMQQLAGASLQRLRNWDISEAQIKALTQSGATTRTLTFRSPVS	243
Alkalilimnicola ehrlichei	G-----PARERLRALGMPADAIRQVEQQGRALNLVPVKAPQD	212
Hahella chejuensis	K-----ASRERLLALGLNNAQISRLEKRLRLVDQRISVYAEQS	220
Escherichia coli	-----	

Yersinia frederiksenii	GYVNKLDIRAGSQVTATQSLFELASLDPVWIVVDYPQSQASLVISGSGIS	270
Yersinia bercovieri	GYVNKLDIRVGSQVTATQSLFELASLDPVWIVVDYPQSQASLVTLGSTIA	270
Erythrobacter sp. SD-21	GAITSLGVRPGMTVMAGQSLAEISGYSPIWLEAAVPEALAGSARVGQPV	276
Erythrobacter litoralis	GAITSLAVRPGMTVAAGQSLAEISGYSPIWLEAAVPEALAGNARVVGQPV	275
Sphingomonas sp. SKA58	GAITSLGVRPGMTVMAGQTLAEITGFSPWLEAAVPERQAATVRVGQPV	276
Erythrobacter sp. NAP1	GAVTMLGVRSGMTVMEGQTLAEITGFTPIWLEASVPEVQAANVRQGPIS	274
Caulobacter sp. K31	GVIQTLDRVAGMSLTSGQTLAQISGLSSVWLILSAPEAQAGLIKIGQAVS	273
Bordetella petrii	GLLQTLNVRNGMAVSAGTVLAQLNGLDAVWLDAAVPETQARMRPGLEAK	273
Acidovorax sp. JS42	GIITDKKAVQGMRFMPGDMLYQVANLSSVWVIADVFEQDIGLVKLGGKAK	293
Acidovorax sp. JS42	GIITDKKAIQGMRFMPGEMLYQVANLSSVWVIADVFEQDIGLVKSGGKAK	293
Dechloromonas aromatica RCB	GIVTEKKAIQGMRFMPGEALYQIADLSAVWVVAEVFEQDIGLVKSGAKAK	296
Rhodoferrax ferrireducens	GIVMEKKAVQGMRFMPGEALYQIADLSTVWVIADVFEQDIGLVKNGAKAT	293
Alkalilimnicola ehrlichei	GVVQALNVAEGMFVQPGTEVMSIADLSRIWVIADLFEHQSDAVREGDAE	262
Hahella chejuensis	GVVDALMVREGMFIKPAEIMSIGGLEQVWVIAEVFERQAGVWKAGQPVV	270
Escherichia coli	-----	

Yersinia frederiksenii	ATTASWPGETFHHGKVSELLPNMDLTTRTLKARIVLENPQQKLKPGMYLNV	320
Yersinia bercovieri	ATTASWPGETFHHGKISELLPNMELATRTLKARVLENPQQQLKPGMYLSV	320
Erythrobacter sp. SD-21	ATLTAFPGERFAGRIIAILPSAQEASRTITVRAAMPNPGRLKPGMFAQV	326
Erythrobacter litoralis	ATLTAFPGERFAGRIIAILPSAQDASRTITVRAAMPNPGRLKPGMFAQV	325
Sphingomonas sp. SKA58	ATLTAFPEERFSGPIIAILPSAQDASRTITVRAQLPNASGRKLPKMFAQV	326
Erythrobacter sp. NAP1	ATLAAYPDQRFAGRIVAILPSADAASRTITVRAELPNPRGRKLPKMFAQV	324
Caulobacter sp. K31	AQLAFAFPGETFNGRVSAILPSAQVDSRTLQVRVELANRDGRLRPGMFATA	323
Bordetella petrii	VSFPAPFGHTVVGKVSILPEVDAASRTARIRIELQNPDGQLRPGLFAKV	323
Acidovorax sp. JS42	VQINAYPKVQQTQTVSYVYPTLKPETRTVQVRVDLSNTGGLLKPGMFAQV	343

Acidovorax sp. JS42	VQINAYDPKVFQGTVSIVYPTLKPETRTVQVRVDSLNTGGLLKPGMFAQV	343
Dechloromonas aromatica RCB	VKISAYPDKTFEGAVTVYPTLTAATRTVPVRVELANPGLLKPGMFAQV	346
Rhodoferrax ferrireducens	VSINAYPKAFAGRVTVYPTLKAETRTVAVRVELANPGLLKPGMFAQV	343
Alkalilimnicola ehrlichei	VHFFPRPGETLVGSGVYIYPTLASPTRTIRARITLNDPDGRLKPGMWTDV	312
Hahella chejuensis	MQVAAAPGRTWEGKVDLYPVLDAKTRTLRVRLRFPNPDLTLPKPNMFADL	320
Escherichia coli	-----	
Yersinia frederiksenii	QSAQSDNLKPVLAIQPQEALLMTGNRRNVLLAQKGHFKPVEVSAGQTQDG	370
Yersinia bercovieri	QSASADKLQSVLAIPQEALLMSSNRNTVLLAQGEGHFKPVEVSTGQTQEG	370
Erythrobacter sp. SD-21	MIAPE--RREALLPSEAVIRTGERTLVMITQEGGGYRPAEVRIGREAGG	374
Erythrobacter litoralis	MLAPE--RREALLPSEAVIRTGERTLAMIAQGGGGYRPAEVRIGREANG	373
Sphingomonas sp. SKA58	SLTPD--TRALLVPSEAVIRTGRTIIVMVKQDEGGFMPAEVRIGREAGG	374
Erythrobacter sp. NAP1	SLSPD--TRALLVPSEAVIRTGRRNLVMLKQDEGAFLPAEVEIGREANG	372
Caulobacter sp. K31	SLGSD--AAPVLTVPSEAVIRTGRRDLVMLAQGGGRYQAAEVRVGRQAGG	371
Bordetella petrii	EFAHTG-EKAGLLIPSESVIRSGKRNVIIVTDNGRFLPTVEQLNGEADG	372
Acidovorax sp. JS42	ELPTAS-KGSVLTVPVTSVIDSGTRQIVLVQLKEGRFEPDRVKVGARSDD	392
Acidovorax sp. JS42	ELPTAS-KGAVLTVPVTSVIDSGTRQIVLVQLKEGRFEPDRVKVGARSDD	392
Dechloromonas aromatica RCB	ELPVSA-KGSVTVVPVSAVIDSGTRQIVLVQAKEGRYEPREVKLARSDD	395
Rhodoferrax ferrireducens	ELPVTA-KGQVITVPVSAVIDSGTRQIVLIQAPGRFEPREVKLARSDD	392
Alkalilimnicola ehrlichei	HIDGES-TEPVLHVPAEAVIRTGRQDRVVTMEEEGRFRVHEVRVGRAGD	361
Hahella chejuensis	TLQAKV-DDQALSIPEAVIRTGSHDRVLLAEAGDGRYRPAFVKLGVEADD	369
Escherichia coli	-----MKKALQVAMFSLFT-----VIGFNAQA	22
	: . : :	
Yersinia frederiksenii	WVEIKSGLSSGQVVTSGQFLIDSEASLQSAQPQMDMPETP-----	412
Yersinia bercovieri	WVEIKSGLNVGQVVTSGQFLIDSEANLQSAQPQMDPTPAV-----	412
Erythrobacter sp. SD-21	RTEVLAGLAAGEVVTSGQFLIDSEASLAGIDVRSIEDAPT-----	416
Erythrobacter litoralis	RTEVLAGLAAGERVVTSGQFLIDSEASLAGIDVRPVDQAPSG-----	415
Sphingomonas sp. SKA58	RTEVLAGLSAGDQVVTSGQFLIDSEASLTGLDVRPIDQA-----	413
Erythrobacter sp. NAP1	RTEILAGLAAGEQVVTSGQFLIDSEASLSGIDVRSIDGT-----	411
Caulobacter sp. K31	RTEILGGLKAGDQVVASGQFLIDSEASLAGLEPRPLSADEPVNSMPAGPA	421
Bordetella petrii	KTVVAKGLKEGQVVASGQFLIDSEANLRGVLARLATDSS-----	412
Acidovorax sp. JS42	RIEVIIEGVREGEQVVIANFLIDAESNLKAAVGGFGHSSHGAKPDAQG--	440
Acidovorax sp. JS42	RIEVTGEVREGEQVVIANFLIDAESNLKAAVGGFGHSSHGAKSEAQG--	440
Dechloromonas aromatica RCB	YVEVLGDKNGEPVVAANFLIDAESNLKAAVGGFGHAAHGKTPP----	441
Rhodoferrax ferrireducens	HVEVREGVKEGEQVVIANFLIDAESNLKAAVGGFGHAAHGKTPP----	440
Alkalilimnicola ehrlichei	RLEILEGLQVGARIVTSGQFLIDSESSVTVSLARLQ-----AAAEAD--	403
Hahella chejuensis	RVQVLKGLKAGDQVVTSGQFLIDSESKVDVALAALLESFSQSAQQDAA---	416
Escherichia coli	NEHHHETMSEAQPQVIS-----	39
	: . * :	
Yersinia frederiksenii	----DPSMDSATTPVDIYSVQGEVNAINGST--ITLSHGPIAALKWGAM	456
Yersinia bercovieri	----TPPAESAAGSPVDIYSVQGEVKAINGQS--ITLSHGPIAALKWGAM	456
Erythrobacter sp. SD-21	---AGENETQADADEPTTYRATGTIERITARS--ITLRHGPPVPALEWPA	461
Erythrobacter litoralis	---ASEDRGSDDADEPTTYRATGTIERINANS--VTLRHGPPVPALEWPA	460
Sphingomonas sp. SKA58	-----DASTGGEDAPATFGATGTIQSIANGS--VTLRHGPPVPRLDWPA	456
Erythrobacter sp. NAP1	-----MSMASEGSPNMRTYTATGRVTKIAGAS--ITLHNHAPVPALEWPSM	454
Caulobacter sp. K31	TKSAAPAMKSAPAAAKALLQAEGRIEEEITADT--ITLSHGPPVPAIGWPAM	469
Bordetella petrii	---AAATPSAGPTTGASHHKATGTVKITPTD--ITISHGPPVPSIGWPAM	457
Acidovorax sp. JS42	TPDAGKPA-----AASVGHGRGEKVEELDTKNGTVTIAHGPIPTLKWPA	485
Acidovorax sp. JS42	TPDASKP-----AASVGHQGEGRVEESDAKAGTVTIAHGPIPTLKWPA	484
Dechloromonas aromatica RCB	TEGAACKPA-----SAGAGHHAEGKVEEIDTKTGAVSISHGPVDSLKWPA	486
Rhodoferrax ferrireducens	TAVAAPATQAAAPAKAVGHQATGTVGVDLKAGTVSLSHGPIASLKWPA	490
Alkalilimnicola ehrlichei	-----DGSVAAEGRINHVDPPEARQVNLDPHEPIAELGWPA	438
Hahella chejuensis	-----PGTVWATGTINSVMAGHGMNLNISHDPVKAWNWPSP	451
Escherichia coli	-----ATGVVKGFDDLESKKITIHDPPIAANWPEM	69
	* : :. * * : *	
Yersinia frederiksenii	TMDFLPLPGDLSPEIRVGSQVNFFTTSLDEGAQIRHIKPVKTNNSDTHG	506
Yersinia bercovieri	TMDFLPLPTSKLAPPIVGSRVNFFTTSLDEGAQIRHIKPVKTNNSADTHG	506
Erythrobacter sp. SD-21	TMGFATEGPAQVRGFRQGRDRTVFTFVQASTGPRIVSIRKTGQ-----	503
Erythrobacter litoralis	TMGFATEGPEQLRGFARGDRVSFTFVQASTGPRIVSIRKTGQ-----	502
Sphingomonas sp. SKA58	TMTFRTKSAAQMRGLETGDRVRFFTTQQDAGPRIESTIRAGQ-----	498
Erythrobacter sp. NAP1	VMPFALEDAALVDGIEPGDKVEFTFSQHDTPGPRIVSIRKTDR-----	496
Caulobacter sp. K31	TMTFFKLDPTLARGLKTGDQAAFGEQRPDGPPVRSLSHRAEASR-----	513
Bordetella petrii	TMTFFKVIDPGLTRDIKTGEAVAFQFVQEEDSYVVQTIQASGASR-----	501
Acidovorax sp. JS42	SMEFFKVSNSGLLADMKGALVAFEFVERGQGEWVITSVKPVG-----	527

Acidovorax sp. JS42	SMEFKVSNNGLMAGLQPGAAVVFEFVERGQGEWVVTSVKPMG-----	526
Dechloromonas aromatica RCB	TMEFKAANESLLQTLKPGAKVAFEFVERQPGGEWVITAATLLAPNTGASAP	536
Rhodferax ferrireducens	TMEFKTANAALLQALKPGAKVTVEFIERQPGGEWVITSAKPAD-----	532
Alkalilimnicola ehrlichei	TMDFEVAEDVALTDLEPGDPVIIHIREREDEEYVYELTHIERLADPTGET	488
Hahella chejuensis	DMDFTTVEGLPLENVAPGQVRVFEITRSSPSDFQITALDIIISAAPSIDAQ	501
Escherichia coli	TMRFTITPQTKMSGIKTGDKVAFNFVQQGNLSLLQDIKVSQ-----	110
	* * . * . . :	
Yersinia frederiksenii	SHL-----	509
Yersinia bercovieri	GHL-----	509
Erythrobacter sp. SD-21	-----	
Erythrobacter litoralis	-----	
Sphingomonas sp. SKA58	-----	
Erythrobacter sp. NAP1	-----	
Caulobacter sp. K31	-----	
Bordetella petrii	-----	
Acidovorax sp. JS42	NAAANPHAGHN---	538
Acidovorax sp. JS42	KAAATPHADHN---	537
Dechloromonas aromatica RCB	ASAASPHAGH----	546
Rhodferax ferrireducens	-----PHAGQ----	537
Alkalilimnicola ehrlichei	DDAPDHDAHTGHDH	502
Hahella chejuensis	EAMQTEGAQ-----	510
Escherichia coli	-----	

## APPENDIX D

## HNCA assignments of Ag(I)-CusF/apo-CusB spectra

Residue	$\delta_{\text{NH}}$	$\delta_{\text{N}}$	$\delta\text{C}\alpha^{\text{i}}$	$\delta\text{C}\alpha^{\text{i-1}}$
88Q	8.04068	128.1269	55.95192	57.36882
87S	8.84282	122.9705	57.39588	63.07
86V	8.5393	121.5643	63.07316	54.55266
85K	8.65974	124.3768	54.55943	60.51445
84I	7.9026	115.4705	60.52825	53.46595
83D	7.88993	115.0017	53.45918	56.82682
82Q	9.94899	127.1893	56.79122	55.99277
81L	9.3951	125.3143	55.97789	54.38677
80L	9.61768	125.7831	54.36187	57.20887
79S	8.48498	119.6893	57.59637	54.33142
78L	8.1728	121.5643	54.32381	52.98968
77N			NA	
76G			NA	
75Q			B	
74Q			B	
73V	8.7866	115.4705	59.41405	55.97372
72F	9.72575	121.0955	55.98593	51.74459
71N	8.16751	116.8767	51.75296	55.50597
70F	8.85177	119.6893	55.50198	51.05965
69A	8.85898	122.9705	51.08045	58.511
68V	9.17466	115.0017	58.52899	55.85727
67K	8.6106	122.9705	55.75205	55.75205
66D	7.97819	121.0955	55.59249	43.84803
65G	9.06618	115.0017	43.80994	64.95456
64T	8.37837	115.9392	64.96511	54.11689
63K	9.00488	122.5018	54.12352	59.0525
62I	7.79808	122.9705	59.05087	57.48231
61E	8.30971	120.158	57.44827	57.44827
60S	7.55086	117.3455	57.50151	54.43812
59M	8.44682	123.9081	54.46067	55.48421
58K	8.29194	129.0644	55.50365	64.21223
57T	7.87334	119.6893	64.21452	55.87377
56Q	7.86762	112.6579	55.86752	64.31309
55P				
54T	9.21194	119.6893	59.36871	61.07956
53I	8.454	127.1893	61.133	NA
52T	9.181	119.2205	63.565	57.437
51F			B	
50R			B	
49M	8.80321	126.2518	53.69383	62.24991

48T	8.26277	115.4705	62.239	55.124
47M			B	
46E	8.27178	116.8767	56.69308	61.62159
45P				
44W	7.96928	115.0017	51.96832	54.57326
43N	7.73773	118.283	54.55283	59.02036
42V	6.28276	132.8144	59.02288	55.23677
41A	8.85796	117.8142	55.26718	55.26718
40A	8.92561	131.4081	55.36799	59.73818
39I			NA	
38P				
37D	8.328	119.6893	55.983	
36H			B	
35H	8.95728	128.1269	54.76841	59.97712
34I	9.34	127.6581	59.977	62.554
33T	9.17771	126.7206	62.55053	59.67875
32I			B	
31K	8.019	115.4705	53.605	NA
30K	7.72931	116.408	56.86069	58.15383
29S	7.74482	112.6579	58.25966	59.02356
28E	8.48357	119.6893	59.0323	57.0056
27L	9.04383	123.9081	57.01584	52.18662
26D	8.39431	126.7206	52.19548	61.5891
25I	8.60224	122.5018	61.59469	45.89806
24G	7.63005	107.0329	45.89091	54.44378
23K	9.26281	128.5956	54.39915	63.93091
22V	8.84888	126.7206	63.88682	59.80418
21V	8.3804	119.2205	59.81185	46.61472
20G	8.6903	105.6266	46.63033	59.54214
19T	8.53867	110.7829	59.5325	51.20707
18A	8.5789	125.7831	51.26845	56.68988
17S	7.86479	120.6268	56.7041	59.79741
16I	8.96183	131.4081	59.79852	62.07082
15V	8.16498	124.3768	62.07455	55.26845
14Q	8.42738	121.0955	55.27034	62.588
13P				
12Q	8.32442	120.6268	53.44429	52.36914
11A	8.25474	124.3768	52.46899	56.26722
10E	8.41608	122.5018	56.27221	58.36132
9S	8.33686	116.8767	58.36967	55.51459
8M	8.4478	122.9705	55.5168	61.73803
7T	8.26277	115.4705	61.74765	56.50507
6E	8.49275	122.5018	56.47457	55.09266

NA: Not assigned

B: Broadened beyond detection

## REFERENCES

- Abajian, C., and Rosenzweig, A. C. (2006). Crystal structure of yeast Sco1. *J Biol Inorg Chem* 11, 459-466.
- Abajian, C., Yatsunyk, L. A., Ramirez, B. E., and Rosenzweig, A. C. (2004). Yeast cox17 solution structure and copper(I) binding. *J Biol Chem* 279, 53584-53592.
- Achila, D., Banci, L., Bertini, I., Bunce, J., Ciofi-Baffoni, S., and Huffman, D. L. (2006). Structure of human Wilson protein domains 5 and 6 and their interplay with domain 4 and the copper chaperone HAH1 in copper uptake. *Proc Natl Acad Sci U S A* 103, 5729-5734.
- Agrawal, V., and Kishan, K. V. (2003). OB-fold: growing bigger with functional consistency. *Curr Protein Pept Sci* 4, 195-206.
- Ainscough, E. W., and Brodie, A. M. (1976). The role of metal ions in proteins and other biological molecules. *J Chem Educ* 53, 156-158.
- Aires, J. R., and Nikaido, H. (2005). Aminoglycosides are captured from both periplasm and cytoplasm by the AcrD multidrug efflux transporter of *Escherichia coli*. *J Bacteriol* 187, 1923-1929.
- Akama, H., Kanemaki, M., Yoshimura, M., Tsukihara, T., Kashiwagi, T., Yoneyama, H., Narita, S.-i., Nakagawa, A., and Nakae, T. (2004a). Crystal structure of the drug discharge outer membrane protein, OprM, of *Pseudomonas aeruginosa*: dual modes of membrane anchoring and occluded cavity end. *J Biol Chem* 279, 52816-52819.
- Akama, H., Matsuura, T., Kashiwagi, S., Yoneyama, H., Narita, S., Tsukihara, T., Nakagawa, A., and Nakae, T. (2004b). Crystal structure of the membrane fusion protein, MexA, of the multidrug transporter in *Pseudomonas aeruginosa*. *J Biol Chem* 279, 25939-25942.
- Arnesano, F., Banci, L., Bertini, I., Cantini, F., Ciofi-Baffoni, S., Huffman, D. L., and O'Halloran, T. V. (2001). Characterization of the binding interface between the copper chaperone Atx1 and the first cytosolic domain of Ccc2 ATPase. *J Biol Chem* 276, 41365-41376.

Askwith, C., Eide, D., Van Ho, A., Bernard, P. S., Li, L., Davis-Kaplan, S., Sipe, D. M., and Kaplan, J. (1994). The FET3 gene of *S. cerevisiae* encodes a multicopper oxidase required for ferrous iron uptake. *Cell* 76, 403-410.

Augustus, A. M., Celaya, T., Husain, F., Humbard, M., and Misra, R. (2004). Antibiotic-sensitive TolC mutants and their suppressors. *J Bacteriol* 186, 1851-1860.

Bagai, I., Liu, W., Rensing, C., Blackburn, N. J., and McEvoy, M. M. (2007). Substrate-linked conformational change in the periplasmic component of a Cu(I)/Ag(I) efflux system. *J Biol Chem* 282, 35695-35702.

Balamurugan, K., and Schaffner, W. (2006). Copper homeostasis in eukaryotes: Teetering on a tightrope. *Biochim Biophys Acta* 1763, 737-746.

Banci, L., Bertini, I., Cantini, F., Felli, I. C., Gonnelli, L., Hadjiliadis, N., Pierattelli, R., Rosato, A., and Voulgaris, P. (2006). The Atx1-Ccc2 complex is a metal-mediated protein-protein interaction. *Nat Chem Biol* 2, 367-368.

Banci, L., Bertini, I., Ciofi-Baffoni, S., Del Conte, R., and Gonnelli, L. (2003). Understanding copper trafficking in bacteria: interaction between the copper transport protein CopZ and the N-terminal domain of the copper ATPase CopA from *Bacillus subtilis*. *Biochemistry* 42, 1939-1949.

Banci, L., Bertini, I., Ciofi-Baffoni, S., Huffman, D. L., and O'Halloran, T. V. (2001). Solution structure of the yeast copper transporter domain Ccc2a in the apo and Cu(I)-loaded states. *J Biol Chem* 276, 8415-8426.

Barber, R. S., Braude, R., and Mitchell, K. G. (1955). Effect of adding copper to the diet of suckling pigs on creep meal consumption and liveweight gain. *Chem Ind*, 1554-1554.

Bax, A., and Ikura, M. (1991). An efficient 3D NMR technique for correlating the proton and <sup>15</sup>N backbone amide resonances with the alpha-carbon of the preceding residue in uniformly <sup>15</sup>N/<sup>13</sup>C enriched proteins. *J Biomol NMR* 1, 99-104.

Beers, J., Glerum, D. M., and Tzagoloff, A. (1997). Purification, characterization, and localization of yeast Cox17p, a mitochondrial copper shuttle. *J Biol Chem* 272, 33191-33196.

Bender, C. L., and Cooksey, D. A. (1987). Molecular cloning of copper resistance genes from *Pseudomonas syringae* pv tomato. *J Bacteriol* 169, 470-474.

Benitez, J. J., Keller, A. M., Ochieng, P., Yatsunyk, L. A., Huffman, D. L., Rosenzweig, A. C., and Chen, P. (2008). Probing transient copper chaperone-Wilson disease protein interactions at the single-molecule level with nanovesicle trapping. *J Am Chem Soc* 130, 2446-2447.

Binsted, N., Gurman, S. J., and Campbell, J. W. (1998). Daresbury Laboratory (Warrington, England).

Binsted, N., and Hasnain, S. S. (1996). State-of-the-art analysis of whole X-ray absorption spectra. *J Synchrotron Radiat* 3, 185-196.

Blackburn, N. J., Ralle, M., Hassett, R., and Kosman, D. J. (2000). Spectroscopic analysis of the trinuclear cluster in the Fet3 protein from yeast, a multinuclear copper oxidase. *Biochemistry* 39, 2316-2324.

Bodenhausen, G., and Ruben, D. J. (1980). Natural abundance N-15 NMR by enhanced heteronuclear spectroscopy. *Chem Phys Lett* 69, 185-189.

Borges-Walmsley, M. I., Beauchamp, J., Kelly, S. M., Jumel, K., Candlish, D., Harding, S. E., Price, N. C., and Walmsley, A. R. (2003). Identification of oligomerization and drug-binding domains of the membrane fusion protein EmrA. *J Biol Chem* 278, 12903-12912.

Bradford, M. M. (1976). Rapid and sensitive method for quantitation of microgram quantities of protein utilizing principle of protein-dye binding. *Anal Biochem* 72, 248-254.

Brewer, G. J. (2000). Recognition, diagnosis, and management of Wilson's disease. *Proc Soc Exp Biol Med* 223, 39-46.

Brown, N. L., Barrett, S. R., Camakaris, J., Lee, B. T., and Rouch, D. A. (1995). Molecular genetics and transport analysis of the copper-resistance determinant (pco) from *Escherichia coli* plasmid pRJ1004. *Mol Microbiol* 17, 1153-1166.

Brown, N. L., Lee, B. T. O., and Silver, S. (1994). Bacterial transport of and resistance to copper. *Met Ions Biol Syst* 30, 405-434.

Bruins, M. R., Kapil, S., and Oehme, F. W. (2000). Microbial resistance to metals in the environment. *Ecotoxicol Environ Saf* 45, 198-207.

Bull, P. C., and Cox, D. W. (1994). Wilson disease and Menkes disease: new handles on heavy-metal transport. *Trends Genet* 10, 246-252.

Casareno, R. L. B., Waggoner, D., and Gitlin, J. D. (1998). The copper chaperone CCS directly interacts with copper/zinc superoxide dismutase. *J Biol Chem* 273, 23625-23628.

Chowdhry, B. Z., and Harding, S. E. (2001). *Protein-Ligand Interactions: Structure and Spectroscopy: a Practical Approach* (Oxford: Oxford University Press).

Cobine, P. A., George, G. N., Jones, C. E., Wickramasinghe, W. A., Solioz, M., and Dameron, C. T. (2002). Copper transfer from the Cu(I) chaperone, CopZ, to the repressor, Zn(II)CopY: metal coordination environments and protein interactions. *Biochemistry* 41, 5822-5829.

Conry, R. R. (2006). Copper: Inorganic & coordination chemistry, In *Encyclopedia of Inorganic Chemistry*, R. B. King, ed. ([Chichester ; Hoboken, NJ]: Wiley).

Corson, L. B., Strain, J. J., Culotta, V. C., and Cleveland, D. W. (1998). Chaperone-facilitated copper binding is a property common to several classes of familial amyotrophic lateral sclerosis-linked superoxide dismutase mutants. *Proc Natl Acad Sci* 95, 6361-6366.

Culotta, V. C., Howard, W. R., and Liu, X. F. (1994). Crs5 encodes a metallothionein-like protein in *Saccharomyces cerevisiae*. *J Biol Chem* 269, 25295-25302.

Culotta, V. C., Klomp, L. W. J., Strain, J., Casareno, R. L. B., Krems, B., and Gitlin, J. D. (1997). The copper chaperone for superoxide dismutase. *J Biol Chem* 272, 23469-23472.

da Silva, J. J. R. F., and Williams, R. J. P. (1991). *The Biological Chemistry of the Elements: the Inorganic Chemistry of Life* (Oxford [England]: Clarendon Press).

- Dancis, A., Yuan, D. S., Haile, D., Askwith, C., Eide, D., Moehle, C., Kaplan, J., and Klausner, R. D. (1994). Molecular characterization of a copper transport protein in *Saccharomyces cerevisiae* - an unexpected role for copper in iron transport. *Cell* 76, 393-402.
- Davies, K. (1993). Cloning the Menkes disease gene. *Nature* 361, 98-98.
- Deisenhofer, J., and Michel, H. (1992). High-resolution crystal structures of bacterial photosynthetic reaction centers. *New Compr Biochem* 23, 103-120.
- Delaglio, F., Grzesiek, S., Vuister, G. W., Zhu, G., Pfeifer, J., and Bax, A. (1995). NMRPipe - a multidimensional spectral processing system based on Unix Pipes. *J Biomol NMR* 6, 277-293.
- Derome, L., and Gadd, G. M. (1987). Measurement of copper uptake in *Saccharomyces cerevisiae* using a  $\text{Cu}^{2+}$ -selective electrode. *FEMS Microbiol Lett* 43, 283-287.
- Dinh, T., Paulsen, I. T., and Saier, M. H. (1994). A family of extracytoplasmic proteins that allow transport of large molecules across the outer membranes of gram-negative bacteria. *J Bacteriol* 176, 3825-3831.
- Djoko, K. Y., Xiao, Z. G., Huffman, D. L., and Wedd, A. G. (2007). Conserved mechanism of copper binding and transfer. A comparison of the copper-resistance proteins PcoC from *Escherichia coli* and CopC from *Pseudomonas syringae*. *Inorg Chem* 46, 4560-4568.
- Doublet, S. (1997). Preparation of selenomethionyl proteins for phase determination. *Methods Enzymol* 276, 523-530.
- Elam, J. S., Thomas, S. T., Holloway, S. P., Taylor, A. B., and Hart, P. J. (2002). Copper chaperones. *Adv Protein Chem* 60, 151-219.
- Ellis, L. B. M., Hou, B. K., Kang, W. J., and Wackett, L. P. (2003). The University of Minnesota biocatalysis/biodegradation database: post-genomic data mining. *Nucleic Acids Res* 31, 262-265.

Eswaran, J., Koronakis, E., Higgins, M. K., Hughes, C., and Koronakis, V. (2004). Three's company: component structures bring a closer view of tripartite drug efflux pumps. *Curr Opin Struct Biol* 14, 741-747.

Falconi, M., and Desideri, A. (2002). Molecular modeling and dynamics of copper proteins, In *Handbook of Copper Pharmacology and Toxicology*, E. J. Massaro, ed. (Totowa, N.J.: Humana Press), pp. 81-101.

Ferreira, A. M. D., Ciriolo, M. R., Marcocci, L., and Rotilio, G. (1993). Copper(I) transfer into metallothionein mediated by glutathione. *Biochem J* 292, 673-676.

Field, L. S., Luk, E., and Culotta, V. C. (2002). Copper chaperones: Personal escorts for metal ions. *J Bioenerg Biomembr* 34, 373-379.

Fogel, S., and Welch, J. W. (1982). Tandem gene amplification mediates copper resistance in yeast. *Proc Natl Acad Sci U S A* 79, 5342-5346.

Franke, S., Grass, G., and Nies, D. H. (2001). The product of the *ybdE* gene of the *Escherichia coli* chromosome is involved in detoxification of silver ions. *Microbiology-UK* 147, 965-972.

Franke, S., Grass, G., Rensing, C., and Nies, D. H. (2003). Molecular analysis of the copper-transporting efflux system CusCFBA of *Escherichia coli*. *J Bacteriol* 185, 3804-3812.

Freedman, J. H., Ciriolo, M. R., and Peisach, J. (1989). The role of glutathione in copper metabolism and toxicity. *J Biol Chem* 264, 5598-5605.

Fukino, H., Hirai, M., Hsueh, Y. M., Moriyasu, S., and Yamane, Y. (1986). Mechanism of protection by zinc against mercuric-chloride toxicity in rats - effects of zinc and mercury on glutathione metabolism. *J Toxicol Environ Health* 19, 75-89.

Gaetke, L. M., and Chow, C. K. (2003). Copper toxicity, oxidative stress, and antioxidant nutrients. *Toxicology* 189, 147-163.

Gaggelli, E., Kozlowski, H., Valensin, D., and Valensin, G. (2006). Copper homeostasis and neurodegenerative disorders (Alzheimer's, Prion, and Parkinson's diseases and Amyotrophic Lateral Sclerosis). *Chem Rev* 106, 1995-2044.

Gardner, K. H., and Kay, L. E. (1998). The use of  $^2\text{H}$ ,  $^{13}\text{C}$ ,  $^{15}\text{N}$  multidimensional NMR to study the structure and dynamics of proteins. *Annu Rev Biophys Biomol Struct* 27, 357-406.

Georgatsou, E., and Alexandraki, D. (1999). Regulated expression of the *Saccharomyces cerevisiae* Fre1p/Fre2p Fe Cu reductase related genes. *Yeast* 15, 573-584.

George, G. N. (1990). Stanford Synchrotron Radiation Laboratory (Menlo Park, CA).

Glerum, D. M., Shtanko, A., and Tzagoloff, A. (1996). Characterization of *cox17*, a yeast gene involved in copper metabolism and assembly of cytochrome oxidase. *J Biol Chem* 271, 14504-14509.

Grass, G., and Rensing, C. (2001). Genes involved in copper homeostasis in *Escherichia coli*. *J Bacteriol* 183, 2145-2147.

Gurman, S. J., Binsted, N., and Ross, I. (1984). A rapid, exact curved-wave theory for EXAFS calculations. *J Phys C-Solid State Physics* 17, 143-151.

Gurman, S. J., Binsted, N., and Ross, I. (1986). A rapid, exact, curved-wave theory for EXAFS calculations .2. The multiple-scattering contributions. *J Phys C-Solid State Physics* 19, 1845-1861.

Halcrow, M. A., Knowles, P. F., and Phillips, S. E. V. (2001). Cu proteins in transport and activation, In *Handbook on Metalloproteins*, I. Bertini, A. Sigel, and H. Sigel, eds. (New York: Marcel Dekker), pp. xxvii, 1182 p.

Halliwell, B., and Gutteridge, J. M. (1984). Oxygen toxicity, oxygen radicals, transition metals and disease. *Biochem J* 219, 1-14.

Hamer, D. H. (1993). 'Kinky hair' disease sheds light on copper metabolism. *Nat Genet* 3, 3-4.

Harrison, M. D., Jones, C. E., Solioz, M., and Dameron, C. T. (2000). Intracellular copper routing: the role of copper chaperones. *Trends Biochem Sci* 25, 29-32.

Hassett, R., and Kosman, D. J. (1995). Evidence for Cu(II) reduction as a component of copper uptake by *Saccharomyces cerevisiae*. *J Biol Chem* 270, 128-134.

Hellman, N. E., and Gitlin, J. D. (2002). Ceruloplasmin metabolism and function. *Annu Rev Nutr* 22, 439-458.

Higgins, M. K., Bokma, E., Koronakis, E., Hughes, C., and Koronakis, V. (2004). Structure of the periplasmic component of a bacterial drug efflux pump. *Proc Natl Acad Sci U S A* 101, 9994-9999.

Hobman, J. L., Yamamoto, K., and Oshima, T. (2007). Transcriptomic responses of bacterial cells to sublethal metal ion stress, In *Molecular Microbiology of Heavy Metals*, D. H. Nies, and S. Silver, eds. (Berlin, Heidelberg: Springer-Verlag Berlin Heidelberg), pp. 73-115.

Horng, Y. C., Cobine, P. A., Maxfield, A. B., Carr, H. S., and Winge, D. R. (2004). Specific copper transfer from the Cox17 metallochaperone to both Sco1 and Cox11 in the assembly of yeast cytochrome C oxidase. *J Biol Chem* 279, 35334-35340.

Housecroft, C. E., and Sharpe, A. G. (2001). *Inorganic Chemistry*, 1 edn (Spain).

Huffman, D. L., Huyett, J., Outten, F. W., Doan, P. E., Finney, L. A., Hoffman, B. M., and O'Halloran, T. V. (2002). Spectroscopy of Cu(II)-PcoC and the multicopper oxidase function of PcoA, two essential components of *Escherichia coli* pco copper resistance operon. *Biochemistry* 41, 10046-10055.

Huffman, D. L., and O'Halloran, T. V. (2000). Energetics of copper trafficking between the Atx1 metallochaperone and the intracellular copper transporter, Ccc2. *J Biol Chem* 275, 18611-18614.

Hughes, M. N., and Poole, R. K. (1989). *Metals and Micro-organisms* (London: Chapman and Hall).

Hung, I. H., Suzuki, M., Yamaguchi, Y., Yuan, D. S., Klausner, R. D., and Gitlin, J. D. (1997). Biochemical characterization of the Wilson disease protein and functional expression in the yeast *Saccharomyces cerevisiae*. *J Biol Chem* 272, 21461-21466.

Hussain, F., Sedlak, E., and Wittung-Stafshede, P. (2007). Role of copper in folding and stability of cupredoxin-like copper-carrier protein CopC. *Arch Biochem Biophys* 467, 58-66.

Ip, H., Stratton, K., Zgurskaya, H., and Liu, J. (2003). pH-induced conformational changes of AcrA, the membrane fusion protein of *Escherichia coli* multidrug efflux system. *J Biol Chem* 278, 50474-50482.

Jelesarov, I., and Bosshard, H. R. (1999). Isothermal titration calorimetry and differential scanning calorimetry as complementary tools to investigate the energetics of biomolecular recognition. *J Mol Recognit* 12, 3-18.

Johnson, B. A., and Blevins, R. A. (1994). NMRView: a computer program for the visualization and analysis of NMR data. *J Biomol NMR* 4, 603-614.

Kaim, W. (2003). The chemistry and biochemistry of the copper-radical interaction. *Dalton Trans*, 761-768.

Kaim, W., and Rall, J. (1996). Copper - A "modern" bioelement. *Angew Chem Int Ed Engl* 35, 43-60.

Kaim, W., and Schwederski, B. (1994). *Bioinorganic Chemistry: Inorganic Elements in the Chemistry of Life: an Introduction and Guide* (Chichester ; New York: Wiley).

Kampfenkel, K., Kushnir, S., Babiychuk, E., Inze, D., and Vanmontagu, M. (1995). Molecular characterization of a putative *Arabidopsis thaliana* copper transporter and its yeast homolog. *J Biol Chem* 270, 28479-28486.

Kang, Y. J., and Enger, M. D. (1988). Glutathione is involved in the early cadmium cytotoxic response in human-lung carcinoma-cells. *Toxicology* 48, 93-101.

Keilin, D., and Mann, T. (1939). Carbonic anhydrase. *Nature* 144, 442-443.

Kittleson, J. T., Loftin, I. R., Hausrath, A. C., Engelhardt, K. P., Rensing, C., and McEvoy, M. M. (2006). Periplasmic metal-resistance protein CusF exhibits high affinity and specificity for both Cu(I) and Ag(I). *Biochemistry* 45, 11096-11102.

Knight, S. A., Labbe, S., Kwon, L. F., Kosman, D. J., and Thiele, D. J. (1996). A widespread transposable element masks expression of a yeast copper transport gene. *Genes Dev* 10, 1917-1929.

Kobayashi, K., and Ponnamperna, C. (1985). Trace elements in chemical evolution. II: Synthesis of amino acids under simulated primitive earth conditions in the presence of trace elements. *Orig Life Evol Biosph* 16, 57-67.

Koch, K. A., Pena, M. M., and Thiele, D. J. (1997). Copper-binding motifs in catalysis, transport, detoxification and signaling. *Chem Biol* 4, 549-560.

Koronakis, V., Koronakis, E., and Hughes, C. (1989). Isolation and analysis of the C-terminal signal directing export of *Escherichia coli* hemolysin protein across both bacterial membranes. *EMBO J* 8, 595-605.

Koronakis, V., Sharff, A., Koronakis, E., Luisi, B., and Hughes, C. (2000). Crystal structure of the bacterial membrane protein TolC central to multidrug efflux and protein export. *Nature* 405, 914-919.

Kuper, J., Llamas, A., Hecht, H. J., Mendel, R. R., and Schwarz, G. (2004). Structure of the molybdopterin-bound Cnx1G domain links molybdenum and copper metabolism. *Nature* 430, 803-806.

Labbe, S., and Thiele, D. J. (1999). Pipes and wiring: the regulation of copper uptake and distribution in yeast. *Trends Microbiol* 7, 500-505.

Lacerda, C. M., Choe, L. H., and Reardon, K. F. (2007). Metaproteomic analysis of a bacterial community response to cadmium exposure. *J Proteome Res* 6, 1145-1152.

Lamb, A. L., Torres, A. S., O'Halloran, T. V., and Rosenzweig, A. C. (2001). Heterodimeric structure of superoxide dismutase in complex with its metallochaperone. *Nat Struct Biol* 8, 751-755.

Laue, T. M., Shah, B. D., Ridgeway, T. M., and Pelletier, S. L. (1992). Computer-aided interpretation of analytical sedimentation data for proteins, In *Analytical Ultracentrifugation in Biochemistry and Polymer Science*, S. R. Harding, A. J. Rowe, and J. C. Horton, eds. (Cambridge, UK: The Royal Society of Chemistry), pp. 90–125.

Lee, J., Adle, D., and Kim, H. (2006). Molecular mechanisms of copper homeostasis in yeast, In *Molecular Biology of Metal Homeostasis and Detoxification: from Microbes to Man*, M. J. Tamás, and E. Martinoia, eds. (Berlin; New York: Springer), pp. 1-36.

Lee, S. M., Grass, G., Rensing, C., Barrett, S. R., Yates, C. J., Stoyanov, J. V., and Brown, N. L. (2002). The Pco proteins are involved in periplasmic copper handling in *Escherichia coli*. *Biochem Biophys Res Commun* 295, 616-620.

Lin, C. M., and Kosman, D. J. (1990). Copper uptake in wild type and copper metallothionein-deficient *Saccharomyces cerevisiae*. Kinetics and mechanism. *J Biol Chem* 265, 9194-9200.

Lin, S. J., and Culotta, V. C. (1995). The ATX1 gene of *Saccharomyces cerevisiae* encodes a small metal homeostasis factor that protects cells against reactive oxygen toxicity. *Proc Natl Acad Sci U S A* 92, 3784-3788.

Lin, S. J., Pufahl, R. A., Dancis, A., O'Halloran, T. V., and Culotta, V. C. (1997). A role for the *Saccharomyces cerevisiae* ATX1 gene in copper trafficking and iron transport. *J Biol Chem* 272, 9215-9220.

Lin, Y. F., Walmsley, A. R., and Rosen, B. P. (2006). An arsenic metallochaperone for an arsenic detoxification pump. *Proc Natl Acad Sci U S A* 103, 15617-15622.

Lobedanz, S., Bokma, E., Symmons, M. F., Koronakis, E., Hughes, C., and Koronakis, V. (2007). A periplasmic coiled-coil interface underlying TolC recruitment and the assembly of bacterial drug efflux pumps. *Proc Natl Acad Sci U S A* 104, 4612-4617.

Loftin, I. R., Franke, S., Blackburn, N. J., and McEvoy, M. M. (2007). Unusual Cu(I)/Ag(I) coordination of *Escherichia coli* CusF as revealed by atomic resolution crystallography and X-ray absorption spectroscopy. *Protein Sci* 16, 2287-2293.

Loftin, I. R., Franke, S., Roberts, S. A., Weichsel, A., Heroux, A., Montfort, W. R., Rensing, C., and McEvoy, M. M. (2005). A novel copper-binding fold for the periplasmic copper resistance protein CusF. *Biochemistry* 44, 10533-10540.

Lu, Z. H., Cobine, P., Dameron, C. T., and Solioz, M. (1999). How cells handle copper: a view from microbes. *J Trace Elem Exp Med* 12, 347-360.

Luk, E., Jensen, L. T., and Culotta, V. C. (2003). The many highways for intracellular trafficking of metals. *J Biol Inorg Chem* 8, 803-809.

Lutkenhaus, J. F. (1977). Role of a major outer membrane protein in *Escherichia coli*. *J Bacteriol* 131, 631-637.

Lutsenko, S., and Petris, M. J. (2003). Function and regulation of the mammalian copper-transporting ATPases: insights from biochemical and cell biological approaches. *J Membr Biol* 191, 1-12.

Magnani, D., and Solioz, M. (2007). How bacteria handle copper, In *Molecular Microbiology of Heavy Metals*, D. H. Nies, and S. Silver, eds. (Berlin, Heidelberg: Springer-Verlag Berlin Heidelberg), pp. 259-285.

McCord, J. M., and Fridovich, I. (1969). Superoxide dismutase. An enzymic function for erythrocuprein (hemocuprein). *J Biol Chem* 244, 6049-6055.

McRorie, D. K., and Voelker, P. J. (1993). Self-associating systems in the analytical ultracentrifuge, In *Beckman Instruments, Inc. (Fullerton, CA)*, pp. 1-61.

Mellano, M. A., and Cooksey, D. A. (1988a). Induction of the copper resistance operon from *Pseudomonas syringae*. *J Bacteriol* 170, 4399-4401.

Mellano, M. A., and Cooksey, D. A. (1988b). Nucleotide sequence and organization of copper resistance genes from *Pseudomonas syringae* pv. tomato. *J Bacteriol* 170, 2879-2883.

Mikolosko, J., Bobyk, K., Zgurskaya, H. I., and Ghosh, P. (2006). Conformational flexibility in the multidrug efflux system protein AcrA. *Structure* 14, 577-587.

- Mills, S. D., Lim, C. K., and Cooksey, D. A. (1994). Purification and characterization of CopR, a transcriptional activator protein that binds to a conserved domain (cop box) in copper-inducible promoters of *Pseudomonas syringae*. *Mol Gen Genet* 244, 341-351.
- Moller, L. B., and Horn, N. (2002). Copper uptake in eukaryotic cells, In *Handbook of Copper Pharmacology and Toxicology*, E. J. Massaro, ed. (Totowa, N.J.: Humana Press), pp. 189-196.
- Munkelt, D., Grass, G., and Nies, D. H. (2004). The chromosomally encoded cation diffusion facilitator proteins DmeF and FieF from *Wautersia metallidurans* CH34 are transporters of broad metal specificity. *J Bacteriol* 186, 8036-8043.
- Munson, G. P., Lam, D. L., Outten, F. W., and O'Halloran, T. V. (2000). Identification of a copper-responsive two-component system on the chromosome of *Escherichia coli* K-12. *J Bacteriol* 182, 5864-5871.
- Murakami, S., Nakashima, R., Yamashita, E., Matsumoto, T., and Yamaguchi, A. (2006). Crystal structures of a multidrug transporter reveal a functionally rotating mechanism. *Nature* 443, 173-179.
- Murakami, S., Nakashima, R., Yamashita, E., and Yamaguchi, A. (2002). Crystal structure of bacterial multidrug efflux transporter AcrB. *Nature* 419, 587-593.
- Murzin, A. G. (1993). OB(oligonucleotide/oligosaccharide binding)-fold: common structural and functional solution for non-homologous sequences. *EMBO J* 12, 861-867.
- Murzin, A. G., Brenner, S. E., Hubbard, T., and Chothia, C. (1995). SCOP: a structural classification of proteins database for the investigation of sequences and structures. *J Mol Biol* 247, 536-540.
- Nelson, N. (1999). Metal ion transporters and homeostasis. *EMBO J* 18, 4361-4371.
- Nies, D. H. (1999). Microbial heavy-metal resistance. *Appl Microbiol Biotechnol* 51, 730-750.

Nies, D. H. (2003). Efflux-mediated heavy metal resistance in prokaryotes. *FEMS Microbiol Rev* 27, 313-339.

Nikaido, H., Basina, M., Nguyen, V., and Rosenberg, E. Y. (1998). Multidrug efflux pump AcrAB of *Salmonella typhimurium* excretes only those beta-lactam antibiotics containing lipophilic side chains. *J Bacteriol* 180, 4686-4692.

Nikaido, H., and Zgurskaya, H. I. (2001). AcrAB and related multidrug efflux pumps of *Escherichia coli*. *J Mol Microbiol Biotechnol* 3, 215-218.

O'Halloran, T. V., and Culotta, V. C. (2000). Metallochaperones, an intracellular shuttle service for metal ions. *J Biol Chem* 275, 25057-25060.

Ochi, T., Otsuka, F., Takahashi, K., and Ohsawa, M. (1988). Glutathione and metallothioneins as cellular defense against cadmium toxicity in cultured Chinese hamster cells. *Chem Biol Interact* 65, 1-14.

Outten, F. W., Huffman, D. L., Hale, J. A., and O'Halloran, T. V. (2001). The independent cue and cus systems confer copper tolerance during aerobic and anaerobic growth in *Escherichia coli*. *J Biol Chem* 276, 30670-30677.

Pace, C. N., Vajdos, F., Fee, L., Grimsley, G., and Gray, T. (1995). How to measure and predict the molar absorption coefficient of a protein. *Protein Sci* 4, 2411-2423.

Payne, A. S., and Gitlin, J. D. (1998). Functional expression of the Menkes disease protein reveals common biochemical mechanisms among the copper-transporting P-type ATPases. *J Biol Chem* 273, 3765-3770.

Pearson, R. G. (1963). Hard and soft acids and bases. *J Am Chem Soc* 85, 3533-3539.

Perutz, M. F. (1962). Relation between structure and sequence of haemoglobin. *Nature* 194, 914-917.

Pickering, I. J., George, G. N., Dameron, C. T., Kurz, B., Winge, D. R., and Dance, I. G. (1993). X-ray-absorption spectroscopy of cuprous thiolate clusters in proteins and model systems. *J Am Chem Soc* 115, 9498-9505.

Piddock, L. J. (2006). Multidrug-resistance efflux pumps - not just for resistance. *Nat Rev Microbiol* 4, 629-636.

Pike, R., Lucas, V., Stapleton, P., Gilthorpe, M. S., Roberts, G., Rowbury, R., Richards, H., Mullany, P., and Wilson, M. (2002). Prevalence and antibiotic resistance profile of mercury-resistant oral bacteria from children with and without mercury amalgam fillings. *J Antimicrob Chemother* 49, 777-783.

Poole, K. (2001). Multidrug resistance in gram-negative bacteria. *Curr Opin Microbiol* 4, 500-508.

Poole, K. (2004). Efflux-mediated multiresistance in gram-negative bacteria. *Clin Microbiol Infect* 10, 12-26.

Poole, K., and Srikumar, R. (2001). Multidrug efflux in *Pseudomonas aeruginosa*: components, mechanisms and clinical significance. *Curr Top Med Chem* 1, 59-71.

Poulos, T. L. (1999). Helping copper find a home. *Nat Struct Biol* 6, 709-711.

Pufahl, R. A., Singer, C. P., Peariso, K. L., Lin, S. J., Schmidt, P. J., Fahrni, C. J., Culotta, V. C., PennerHahn, J. E., and O'Halloran, T. V. (1997). Metal ion chaperone function of the soluble Cu(I) receptor Atx1. *Science* 278, 853-856.

Rae, T. D., Schmidt, P. J., Pufahl, R. A., Culotta, V. C., and O'Halloran, T. V. (1999). Undetectable intracellular free copper: the requirement of a copper chaperone for superoxide dismutase. *Science* 284, 805-808.

Ralle, M., Lutsenko, S., and Blackburn, N. J. (2003). X-ray absorption spectroscopy of the copper chaperone HAH1 reveals a linear two-coordinate Cu(I) center capable of adduct formation with exogenous thiols and phosphines. *J Biol Chem* 278, 23163-23170.

Rees, E. M., and Thiele, D. J. (2004). From aging to virulence: forging connections through the study of copper homeostasis in eukaryotic microorganisms. *Curr Opin Microbiol* 7, 175-184.

Rensing, C., and Grass, G. (2003). *Escherichia coli* mechanisms of copper homeostasis in a changing environment. *FEMS Microbiol Rev* 27, 197-213.

Riek, R., Pervushin, K., and Wuthrich, K. (2000). TROSY and CRINEPT: NMR with large molecular and supramolecular structures in solution. *Trends Biochem Sci* 25, 462-468.

Roat-Malone, R. M. (2002). *Bioinorganic Chemistry: a Short Course* (Hoboken, N.J.: Wiley-Interscience).

Romero, P., Obradovic, Z., Kissinger, C. R., Villafranca, J. E., and Dunker, A. K. (1997). Identifying disordered regions in proteins from amino acid sequences. *Proc IEEE International Conference on Neural Networks 1*, 90-95.

Rosenzweig, A. C. (2001). Copper delivery by metallochaperone proteins. *Acc Chem Res* 34, 119-128.

Rosenzweig, A. C. (2002). Metallochaperones: bind and deliver. *Chem Biol* 9, 673-677.

Rouch, D., Camakaris, J., Lee, B. T., and Luke, R. K. (1985). Inducible plasmid-mediated copper resistance in *Escherichia coli*. *J Gen Microbiol* 131, 939-943.

Rouch, D. A., and Brown, N. L. (1997). Copper-inducible transcriptional regulation at two promoters in the *Escherichia coli* copper resistance determinant *pco*. *Microbiology* 143 ( Pt 4), 1191-1202.

Sambrook, J., Fritsch, E. F., and Maniatis, T. (1989). *Molecular Cloning: a Laboratory Manual*, 2nd edn (Cold Spring Harbor, N.Y.: Cold Spring Harbor Laboratory Press).

Schmidt, P. J., Kunst, C., and Culotta, V. C. (2000). Copper activation of superoxide dismutase 1 (SOD1) *in vivo*. Role for protein-protein interactions with the copper chaperone for SOD1. *J Biol Chem* 275, 33771-33776.

Schmidt, P. J., Rae, T. D., Pufahl, R. A., Hamma, T., Strain, J., O'Halloran, T. V., and Culotta, V. C. (1999). Multiple protein domains contribute to the action of the copper chaperone for superoxide dismutase. *J Biol Chem* 274, 23719-23725.

Schwarz, G., and Mendel, R. R. (2006). Molybdenum cofactor biosynthesis and molybdenum enzymes. *Annu Rev Plant Biol* 57, 623-647.

Silver, S. (1996). Bacterial resistances to toxic metal ions--a review. *Gene* 179, 9-19.

Silver, S., and Phung le, T. (2005). A bacterial view of the periodic table: genes and proteins for toxic inorganic ions. *J Ind Microbiol Biotechnol* 32, 587-605.

Silver, S., and Phung, L. T. (1996). Bacterial heavy metal resistance: new surprises. *Annu Rev Microbiol* 50, 753-789.

Singhal, R. K., Anderson, M. E., and Meister, A. (1987). Glutathione, a first line of defense against cadmium toxicity. *FASEB J* 1, 220-223.

Singleton, C., and Le Brun, N. E. (2007). Atx1-like chaperones and their cognate P-type ATPases: copper-binding and transfer. *Biometals* 20, 275-289.

Solioz, M. (2002). Role of proteolysis in copper homoeostasis. *Biochem Soc Trans* 30, 688-691.

Solioz, M., and Vulpe, C. (1996). CPx-type ATPases: a class of P-type ATPases that pump heavy metals. *Trends Biochem Sci* 21, 237-241.

Stepanauskas, R., Glenn, T. C., Jagoe, C. H., Tuckfield, R. C., Lindell, A. H., and McArthur, J. V. (2005). Elevated microbial tolerance to metals and antibiotics in metal-contaminated industrial environments. *Environ Sci Technol* 39, 3671-3678.

Stillman, M. J. (1995). Metallothioneins. *Coord Chem Rev* 144, 461-511.

Strausak, D., Howie, M. K., Firth, S. D., Schlicksupp, A., Pipkorn, R., Multhaup, G., and Mercer, J. F. B. (2003). Kinetic analysis of the interaction of the copper chaperone Atox1 with the metal binding sites of the Menkes protein. *J Biol Chem* 278, 20821-20827.

Tetaz, T. J., and Luke, R. K. (1983). Plasmid-controlled resistance to copper in *Escherichia coli*. *J Bacteriol* 154, 1263-1268.

Thanabalu, T., Koronakis, E., Hughes, C., and Koronakis, V. (1998). Substrate-induced assembly of a contiguous channel for protein export from *E.coli*: reversible bridging of an inner-membrane translocase to an outer membrane exit pore. *EMBO J* 17, 6487-6496.

Thanassi, D. G., and Hultgren, S. J. (2000). Multiple pathways allow protein secretion across the bacterial outer membrane. *Curr Opin Cell Biol* 12, 420-430.

Thiele, D. J. (1988). ACE1 regulates expression of the *Saccharomyces cerevisiae* metallothionein gene. *Mol Cell Biol* 8, 2745-2752.

Tietze, F. (1969). Enzymic method for quantitative determination of nanogram amounts of total and oxidized glutathione: applications to mammalian blood and other tissues. *Anal Biochem* 27, 502-522.

Totter, S., Harvie, D. R., and Robinson, N. J. (2005). Understanding how cells allocate metals using metal sensors and metallochaperones. *Acc Chem Res* 38, 775-783.

Totter, S., Harvie, D. R., and Robinson, N. J. (2007). Understanding how cells allocate metals, In *Molecular Microbiology of Heavy Metals*, D. H. Nies, and S. Silver, eds. (Berlin, Heidelberg: Springer-Verlag Berlin Heidelberg), pp. 1-33.

Touze, T., Eswaran, J., Bokma, E., Koronakis, E., Hughes, C., and Koronakis, V. (2004). Interactions underlying assembly of the *Escherichia coli* AcrAB-TolC multidrug efflux system. *Mol Microbiol* 53, 697-706.

Tseng, T. T., Gratwick, K. S., Kollman, J., Park, D., Nies, D. H., Goffeau, A., and Saier, M. H., Jr. (1999). The RND permease superfamily: an ancient, ubiquitous and diverse family that includes human disease and development proteins. *J Mol Microbiol Biotechnol* 1, 107-125.

Turner, J., and Robinson, N. J. (1995). Cyanobacterial metallothioneins: biochemistry and molecular genetics. *J Ind Microbiol* 14, 119-125.

Vaccaro, L., Koronakis, V., and Sansom, M. S. (2006). Flexibility in a drug transport accessory protein: molecular dynamics simulations of MexA. *Biophys J* 91, 558-564.

Wackett, L. P., Dodge, A. G., and Ellis, L. B. (2004). Microbial genomics and the periodic table. *Appl Environ Microbiol* 70, 647-655.

Walker, J. M., Tsivkovskii, R., and Lutsenko, S. (2002). Metallochaperone Atox1 transfers copper to the NH<sub>2</sub>-terminal domain of the Wilson's disease protein and regulates its catalytic activity. *J Biol Chem* 277, 27953-27959.

Wernimont, A. K., Huffman, D. L., Lamb, A. L., O'Halloran, T. V., and Rosenzweig, A. C. (2000). Structural basis for copper transfer by the metallochaperone for the Menkes/Wilson disease proteins. *Nat Struct Biol* 7, 766-771.

Williams, R. J. P., and Abolmaali, B. (1998). *Bioinorganic Chemistry: Trace Element Evolution from Anaerobes to Aerobes* (Berlin ; New York: Springer).

Wong, M. D., Fan, B., and Rosen, B. P. (2004). Bacterial transport ATPases for monovalent, divalent and trivalent soft metal ions, In *Handbook of ATPases: Biochemistry, Cell Biology, Pathophysiology*, Y. Wada, and J. H. Kaplan, eds. (Weinheim: Wiley-VCH.), pp. xxiv, 469 p.

Wuthrich, K. (2000). Protein recognition by NMR. *Nat Struct Biol* 7, 188-189.

Xiao, Z., Loughlin, F., George, G. N., Howlett, G. J., and Wedd, A. G. (2004). C-terminal domain of the membrane copper transporter Ctr1 from *Saccharomyces cerevisiae* binds four Cu(I) ions as a cuprous-thiolate polynuclear cluster: sub-femtomolar Cu(I) affinity of three proteins involved in copper trafficking. *J Am Chem Soc* 126, 3081-3090.

Yang, S., Lopez, C. R., and Zechiedrich, E. L. (2006). Quorum sensing and multidrug transporters in *Escherichia coli*. *Proc Natl Acad Sci U S A* 103, 2386-2391.

Yatsunyk, L. A., and Rosenzweig, A. C. (2007). Cu(I) binding and transfer by the N terminus of the Wilson disease protein. *J Biol Chem* 282, 8622-8631.

Yuan, D. S., Stearman, R., Dancis, A., Dunn, T., Beeler, T., and Klausner, R. D. (1995). The Menkes/Wilson disease gene homologue in yeast provides copper to a ceruloplasmin-like oxidase required for iron uptake. *Proc Natl Acad Sci U S A* 92, 2632-2636.

Zgurskaya, H. I., and Nikaido, H. (1999a). AcrA is a highly asymmetric protein capable of spanning the periplasm. *J Mol Biol* 285, 409-420.

Zgurskaya, H. I., and Nikaido, H. (1999b). Bypassing the periplasm: reconstitution of the AcrAB multidrug efflux pump of *Escherichia coli*. *Proc Natl Acad Sci U S A* 96, 7190-7195.

Zgurskaya, H. I., and Nikaido, H. (2000). Multidrug resistance mechanisms: drug efflux across two membranes. *Mol Microbiol* 37, 219-225.

Zhang, L., Koay, M., Maher, M. J., Xiao, Z., and Wedd, A. G. (2006). Intermolecular transfer of copper ions from the CopC protein of *Pseudomonas syringae*. Crystal structures of fully loaded Cu(I)/Cu(II) forms. *J Am Chem Soc* 128, 5834-5850.

Zuiderweg, E. R. (2002). Mapping protein-protein interactions in solution by NMR spectroscopy. *Biochemistry* 41, 1-7.